ENDOCANNABINOID TURNOVER AND FUNCTION

By

Annie Patel B.Sc.(Hons), M.Sc.

School of Biomedical Sciences
Medical School
Queen's Medical Centre
University of Nottingham

Thesis submitted to the University of Nottingham for the degree of Doctor of Philosophy

September 2009

Abstract

The therapeutic benefits of cannabis have been known for centuries of years. Yet it has only been in the last 40 years that an understanding of the system by which its works in our bodies has begun to be defined. This has in turn led to the discovery and understanding of the endogenous cannabinoid (eCB) system, alongside its main synthesizing and hydrolysing enzymes as well as the endogenous ligands.

The use of synthetic cannabinoid receptor (CBR) ligands for therapeutic use has provided problems regarding the natural endogenous regulatory tone of the eCBs, which in turn has resulted in unwanted side effects. Part of the reason of this is due to synthetic agonists producing the well documented psychotropic effects at CB_1 receptors. Alternative targets for the manipulation of the eCB system for therapeutic benefits have been explored. One remains to be the use of FAAH inhibitors, which in turn potentially increase levels of eCBs in the system, hence potentiating their effects at the CBRs, or at other receptor sites. Therefore we have developed two HTS assays for the identification of potential inhibitors of FAAH and MAGL. They prove to be robust, cheap and facile and provide a clear indication of inhibitable levels of FAAH and MAGL activity. The FAAH assay can be further used to establish concentration-response curves of initial 'hit' compounds. Yet, the HTS MAGL assay requires further characterization for use in construction of concentration-response curves, as they are not assays specific for MAGL acitivity and include hydrolysis of the substrate 4-NPA by non-specific esterases.

Z-factor scores were calculated for both assays, indicating excellent assays, which can potentially be applied to industrial lab robotics for screening of compound libraries.

The effects of CB hydrolysing enzymes leads to an accumulation of various eCB and endocannabinoid-like molecules. One of which is oleoylethanolamine OEA, which has shown to have no affinity for CBRs, yet has been documented to have a peripherally regulated effect on satiety. This led us to investigate the effects of OEA in feeding behaviour and the involvement of the peripherally located nuclear receptor PPARα, in wild-type mice and PPARα knockout mice.

We found OEA to have a transient effect in the reduction of food intake, yet the use of genetic tools and PPARα known agonists and antagonists indicated the involvement of an additive pathway where OEA also exerts effects of satiety.

Therefore further investigation is required to fully determine the actions of OEA in vivo towards feeding behaviour and to define its therapeutic potential as an anti-obesity compound.

Acknowledgments

I would firstly like to thank everybody who I have worked with during my PhD for the great times and friendships I have made, but the greatest of all being with my supervisor Dr Stephen Alexander, who has provided me with the greatest guidance, his utmost support and the worst jokes I have ever heard (!). I am most grateful to both Steve and Professor Dave Kendall for fuelling my enthusiasm for the cannabinoids over the duration of my PhD and the great opportunities they have given me to meet other world-influencing researchers in the field – which has led me directly into the world of cannabinoid medicines as my career. For every bit of this – to them I am forever grateful.

I would also like to thank Dr Michael Garle for his never ending help in the lab, without whom, the lab would never be as great a place as it is! I would also like to thank Professor Fran Ebling for all his help and guidance in my in vivo studies.

Finally, I would like thank my Mum and Dad for their undying love and belief in me. My time in Nottingham, without their support, would never have been so special, so memorable. Last, but not least, I would like to thanks my Fiancé Neil – who joined me in Nottingham to share some of the best years of our lives, full of love, life and laughter. We made memories here – never to be forgotten.

Abbreviations

CBs	Cannabinoids
GC/MS	gas chromatography mass spectrometry
Δ^9-THC	delta-9-tetrahydrocannabinol
CBD	Cannabidiol
THCV	Tetrahydrocannabinovarin
MS	multiple sclerosis
CB	Cannabinoid
GPCRs	G protein-coupled receptors
THC	Tetrahydrocannabinol
CB_1	cannabinoid receptor 1
CB_2	cannabinoid receptor 2
GDP	guanosine 5'-diphosphate
GTP	guanosine 5'-triphosphate
AC	adenylate cyclase
ATP	adenosine triphosphate
cAMP	cyclic adenosine monophosphate
Gαs	Gα stimulatory subunit
Gαi	Gα inhibitory subunit
GTPase	guanosine triphosphatase
CHO	chinese hamster ovary
cDNA	cyclic deoxyribonucleic acid
$CB_1^{-/-}$	cannabinoid receptor 1 knockout
CNS	central nervous system
eCB	Endocannabinoids
mRNA	messenger ribonucleic acid
RT-PCR	real-time polymerase chain reaction
AEA	Anandanmide
2-AG	2-arachidonoylglycerol
MAGs	Monoacylglycerols
FAAs	fatty acid amides
eCBs	Endocannabinoids
FAAH	fatty acid amide hydrolase
eCBL	endocannabinoid-like
Ca^{2+}	Calcium ion
NAPE	N-acyl phosphatidylethanolamine
mGLU	metabotropic glutamate
PLC	phospholipase C

K^+	Potassium
MAPK	mitogen-activated protein kinase
MAGL	monoacylglycerol lipase
AMT	anandamide membrane transporter
ND	not detectable
$FAAH^{-/-}$	fatty acid amide hydrolase knockout
$FAAH^{+/+}$	fatty acid amide hydrolase wild type
NSAIDs	Non-Steroidal anti-inflammatorys
PMFS	Phenylmethanesulphonylfluoride
PG	Prostaglandin
2-OG	2-oleoylglycerol
2-AG	2-acylglycerol
SREBP-1c	sterol response element-binding protein-1c
FFA	free fatty acid
i.p.	Intraperitoneally
OEA	Oleoylethanolamide
CCK	Cholecystokinin
GLP-1	glucagon-like peptide-1
NAPE-PLD	N-acyl phosphatidylethanolamine phospholipase D
GI	gastro-intestinal
EC_{50}	maximal effective concentration
nM	Nanomolar
SEA	Stearoylethanolamide
PPAR-α	peroxisome proliferator-activated α receptor
PPAR-$\alpha^{-/-}$)	peroxisome proliferator-activated α receptor knockout
pmol/g	picomolar per gram
NO	nitric oxide
iNOS	inducible NO synthase
mg/kg	milligrams per kilogram
μM	Micromolar
PKC	protein kinase C

Introduction

1.1 Cannabis

Cannabis, derived from the plant *Cannabis sativa* L., has a long history of use as a medicine, a material and a psychoactive recreational drug. Cannabis contains over 60 individual compounds and is arguably one of the most potentially versatile medicines available, yet due to the stigma associated with its prohibited legal status, knowledge of the pharmacological effects and therapeutic benefits are largely unknown. Research into the pharmacological effects of the cannabinoids (CBs) is ever growing and their therapeutic effects are beginning to be exploited as medicines.

Most CBs are extracted from the leaves and mature unseeded female flowers of the plant and can be smoked or otherwise orally ingested.

Today, government controlled sites of plants all cut from a 'mother plant', are cloned to produce high yields of desired CBs, allowing their extraction and purification and separation by gas chromatography mass spectrometry (GC/MS) (Repetto et al., 1976), for use in medicinal research.

In 1964, delta-9-tetrahydrocannabinol, or Δ^9-THC, the main psychoactive ingredient of cannabis was extracted and isolated by Raphael Mechoulam and his lab (Gaoni Y, 1964). Experimentally, purified Δ^9-THC has been shown to exert essentially the same effects as cannabis preparations. Further investigations lead to the identification of a number of structurally related compounds, including cannabidiol (CBD) and tetrahydrocannabinovarin (THCV) which are also found in high amounts within cannabis but are non-psychoactive (Izzo et al., 2009).

Despite its illegal status and registration as a drug of abuse, cannabis still continues to be (illegally) used medicinally for the relief of chronic symptoms that are not helped by first line treatment drugs. Cannabis is slowly emerging as a potential add-on drug aiding drug action in the treatment of various pathological conditions, such as reduced spasticity in multiple sclerosis, MS (Baker et al., 2000).

Medicinal use of cannabis is currently beginning to be licensed around the world, yet it still remains a controversial and widely debated drug of use. One of the drawbacks towards cannabis-medicine licensing is the undesirable route of smoking administration. Smoking cannabis is, as expected, damaging to your lungs, where daily (?) smoking 3-4 cannabis cigarettes, 'spliffs', has been shown to produce histological effects on lungs comparable to smoking 20 tobacco cigarettes (Johnson et al., 2000). A leading pharmaceutical company in the development of cannabis-based medicines have developed an oromucosal form of delivery allowing production and licensing of the only naturally derived cannabinoid (CB) medicine available for medicinal use to date, Sativex. Sativex is an equal ratio of THC: CBD, used in the treatment of neuropathic pain (Turo et al., 2007), MS (Baker et al., 2000) and is being further investigated for its effects in cancer, diabetes and epilepsy.

In recent decades, funding into the research of cannabis has advanced rapidly, leading to the discovery and understanding of CB receptors and their signalling properties. This has lead to the identification of an entire endogenous CB system, capable of regulating many processes. This chapter continues to describe the receptors, hydrolytic enzymes, ligands and signalling of this system and the potential role of endogenous CB regulation of feeding behaviour.

1.2 Cannabinoid Receptors

There is evidence of the existence of two types of CB receptor, CB_1 and CB_2 receptors. As well as activation by exogenous CBs, humans are known to produce endogenous agonists at the CB receptors, providing both physiological and pharmacological importance. The CB_1 receptor was first cloned in 1990 (Matsuda et al., 1990) and the CB_2 receptor cloned in 1993 (Munro et al., 1993) and have been found to be present in many species including human, rat and mouse (Matsuda, 1997; Matsuda et al., 1997).

The psychotropic effects of cannabis have been known for centuries and their measured effects in humans are similar to other drugs known to act via receptor mediated mechanisms. These effects are dose-dependant yet stronger than those of drugs, such as alcohol (ethanol), which are not thought to be receptor mediated, yet cannabinoids are. This and further evidence suggested the CB_1 and CB_2 receptors were members of the superfamily of G protein-coupled receptors (GPCRs). In its inactive state, a GPCR co-exists with a G-protein made up as a trimer of Gα, Gβ and Gγ subunits. Guanosine 5'-diphosphate (GDP) is bound to the Gα subunit where activation of the receptor induces a number of signal transduction pathways, beginning with the displacement of GDP by guanosine 5'-triphosphate (GTP), causing the Gα subunit to dissociate from the trimer. GPCRs are coupled to secondary messenger systems, such as adenylate cyclase (AC), to which the dissociated Gα binds to either inhibit or stimulate the hydrolysis of adenosine triphosphate (ATP) to the secondary messenger cyclic adenosine monophosphate (cAMP). This is determined by whether the Gα subunit is stimulatory (Gαs) of

inhibitory (Gαi). The receptor returns to its inactive state once guanosine triphosphatase (GTPase) activity inherent in the Gα subunit hydrolyses the bound GTP to GDP. CBs and the related endogenous ligands are known to evoke signalling cascades predominantly through the Gαi protein.

1.2.1 The CB_1 Receptor

Experiments using the radiolabelled synthetic CB compound ^{3}H-CP-55,940 demonstrated a novel binding site in rat brain (Devane et al., 1988) which led to its characterisation as the CB_1 receptor. Functional expression of the receptor was achieved in Chinese hamster ovary (CHO) cells allowing the demonstration, for the first time, that CB_1 receptor activation by either Δ^9-THC or CP-55,940 led to the inhibition of cAMP production in a concentration-dependent manner (Song and Howlett, 1995). Further investigation of the receptor amino acid sequence in cloned rat CB_1 receptor, cyclic deoxyribonucleic acid (cDNA) provided confirmation of CB_1 being a GPCR (Matsuda et al., 1990).

Sequence analysis of different species clones of the CB_1 receptor (e.g. mouse and human) demonstrated 99% and 97% amino acid identity with rat CB_1 receptor protein. CB_1 receptors have also been cloned in diverse vertebrate species, including *Taricha granulose* (newt) (Soderstrom et al., 2000) and *Fugu rubripes* (puffer fish) (Yamaguchi et al., 1996), displaying 84% and 72% homology, respectively, with human CB_1 receptors. This high level of species conservation implies a key physiological role in animals.

The distribution of CB_1 receptors in the brain is heterogeneous (Glass et al., 1997),

and correlate well with evidence for particular pharmacological properties of CB_1 receptor agonists, including the well documented effects of sedation, impaired cognition, motor function and memory, as well as effects on analgesia.

Animal models, commonly mice, have been developed using disruption of the gene encoding the CB_1 receptor to create CB_1 knockout ($CB_1^{-/-}$) mice. Different methods have been used to create $CB_1^{-/-}$ mice, where in the development of the $CB_1^{-/-}$ mouse model (Lędent mice), the first 233 amino acids were removed and in the $C57Bl6^{-/-}$ model (Zimmer mice), the entire protein-coding sequence was removed. This appears to have differences between CB_1-null mice models in locomotor activity and nociceptive responses, which might aid investigations for the actions of the endogenous ligands acting on this receptor. Mice lacking the fatty acid amide hydrolase gene have also been described, and differences between models may lead to identification of agonistic roles of endogenous cannabinoids in various physiological functions.

The CB_1 Receptor tissue distribution and expression

CB_1 receptors appear to mediate most, if not all of the psychoactive effects of Δ^9-THC and related compounds. They are predominantly found in the central nervous system (CNS) and in some peripheral tissues, including immune cells, heart, lung and gastrointestinal tissues. Many of the CB_1 receptors are located in the terminals of central and peripheral nerves, as they are well known to be pre-synaptic receptors involved in the reduction of neurotransmitter release (Pertwee, 2001). They reduce the release of various excitatory and inhibitory neurotransmitters in different parts of the brain and it is this response which allows the CB_1 receptor to modulate pain

perception (Hohmann and Suplita, 2006), emphasizing the important role of this receptor in modulating neurotransmission at specific synapses. The CB_1 receptor is dense in the cerebral cortex, as well as being found in the hippocampus, amygdala and cerebellum (Mackie, 2005), hence its distribution corresponds well to the most prominent behavioral effects of cannabis. In addition, this distribution helps to predict potential neurological and psychological routes where manipulation of the endocannabinoid (eCB) system might be beneficial. While the knowledge of CB_1 localization in the CNS has advanced much in past two decades, further detailed knowledge of the localisation of the precursors for endogenous CBs, the synthesizing and hydrolyzing enzymes, specifically in the areas of CB_1 receptor distribution may allow further development of therapeutic drugs that modify the eCB system.

CB_1 receptor clones have been isolated from over 60 different mammalian species, which all displayed sequence diversity of 0.41-27% (Stincic and Hyson, 2008). In addition to mammals, CB_1 receptor has also been isolated from birds (Alonso-Ferrero et al., 2006), fish (Soderstrom and Johnson, 2001), amphibians (Soderstrom et al., 2000) and as has previously mentioned, invertebrates (Beatrice et al., 2006).

1.2.2 The CB_2 Receptor

The CB_2 receptors are mainly expressed in the periphery, and found in immune cells, consistent with their anti-inflammatory and immunosuppressive properties (Pertwee, 1997) (Pertwee, 2001) (Cabral et al., 2001). Investigation of this receptor led to the understanding that the CB_2, like the CB_1, receptor is negatively coupled to AC activity *via* the $G_{i/o}$ G-protein (Bayewitch et al., 1995); (Shire et al., 1996). However,

homology between the two CB receptors is poor, sharing 44% amino acid identity. Despite this lack of homology, the eCB and Δ^9-THC have strong binding affinities to the CB_2 receptor (Mackie and Stella, 2006). Thus, despite their structural differences, many cannabinoid compounds have displayed comparable affinities for both receptors (Silvestri et al., 2009). Recent studies indicate that CB_2 receptors may regulate cytokine release in health and disease (Arévalo-Martín et al., 2008). Therefore, it could be hypothesised that, as CB_1 receptors modulate neurotransmitter release, a concerted action of both CB receptors may result in the regulation of the release of neurotransmitters and immune mediators.

The CB_2 Receptor tissue distribution and expression

The CB_2 receptor is predominantly found in the immune system, yet recently it was reported that there was expression of CB_2 receptor messenger ribonucleic acid (mRNA) and protein localization on brainstem neurons, the first report of a central expression (Van Sickle et al., 2005). Additionally, real-time polymerase chain reaction (RT-PCR) methods have located CB_2 receptors in the peripheral nervous system (Griffin et al., 1997).

The receptor was initially cloned using a human macrophage cell line HL60 (Munro et al., 1993). Since then, it has been reported in many other species, including mouse (Shire et al., 1996) (Ho and Zhao, 1996), rat (Brown et al., 2002) and puffer fish (Elphick, 2002). Investigation of the distribution of CB_2 receptors showed them to be specifically localized in immune cells including rat peritoneal mast cells (Carayon et al., 1998), mouse splenocytic T-cells (Rao et al., 2004), macrophages (Carlisle et al., 2002), and a murine T-cell line (Carayon et al., 1998). The rank order of CB_2

mRNA levels in the periphery has been suggested to be B-cells > natural killer cells ≫ monocytes > polymorphonuclear neutrophil cells > T8 cells > T4 cells (Galiegue et al., 1995). As GPCRs are known to control cell maturation, proliferation and migration, the CB_2 receptor distribution suggests it is a good candidate for such influences (Cabral et al., 2008).

CB_2 receptor shows less homology between species compared to CB_1 receptors; for example, human and mouse CB_2 receptors share 82% amino acid identity (Shire et al., 1996) and the mouse and rat CB_2 receptor share 93% amino acid identity (Griffin et al., 2000). in comparison, human CB_1 and CB_2 receptors have been shown to share 68% amino acid homology and only 44% identity through the whole protein (Bari et al., 2006) (Pertwee, 1997).

1.3 The Endogenous Cannabinoid System

Once the CB receptors were indentified in the 1990s and found to be activated by Δ^9-THC (Cravatt and Lichtman, 2003), as well as by its endogenous ligands (e.g. AEA), an understanding of the endogenous system began to be established. The endogenous cannabinoid (eCB) system comprises of the two receptors, their endogenous ligands and the proteins for their synthesis and transformation. Reports of the wider actions of both the CBs and the eCB ligands is ever growing, with new activities being identified as well as other pathways of transformation – the understanding of just how far the effects of the eCB system extends is yet to be fully defined. This leads to further complications in modulating the eCB system in whole animals for different therapeutic reasons, as we do not yet understand fully actions of the whole system

and therefore of any endogenous effects (compensatory or synergistic) that occur when an element of the system is modulated (i.e. alternative eCB synthesis routes or hydrolysis enzymes).

1.3.1 Endocannabinoid Receptor Ligands

Anandamide (AEA) was the first lipid constituent isolated (from pig brain) shown to activate CB_1 receptors (Devane and Axelrod, 1994) and is an analogue of arachidonic acid (Devane and Axelrod, 1994). The identification of 2-arachidonoylglycerol (2-AG) as a second eCB strengthened the hypothesis that the G-protein coupled CB receptors recognize lipids as their natural ligands (see **Figure 1.1**) (Cravatt and Lichtman, 2003). AEA exhibits similar affinity to the CB_1 receptor to that of Δ^9-THC and has slightly more affinity to CB_1 receptors than CB_2, as does 2-AG (Hillard et al., 1999) (Felder et al., 1995), acting as a partial agonist at both receptors.

Both AEA and 2-AG belong to two large classes of natural lipids, the fatty acid amides (FAAs) and monoacylglycerols (MAGs), respectively. Several FAAs, in addition to AEA appear to serve as endogenous signalling lipids. Representatives from this group of eCBs are displayed in **Figure 1.1** (Cravatt and Lichtman, 2003).

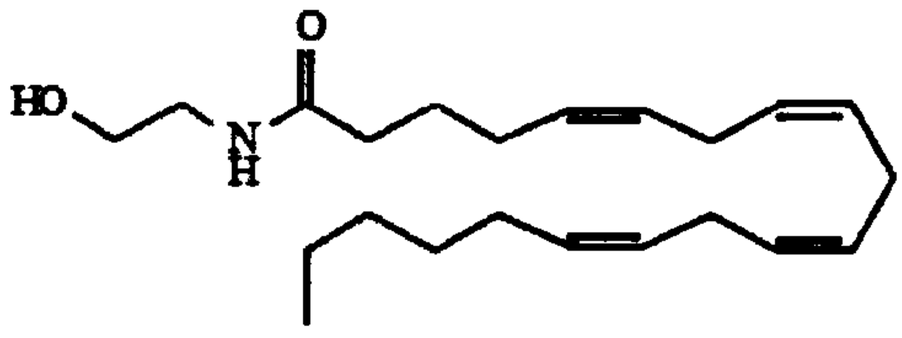

Anandamide

(N-Arachidonoyl-ethanolamine, AEA)

Endogenous ligand for CB1

Substrate for FAAH

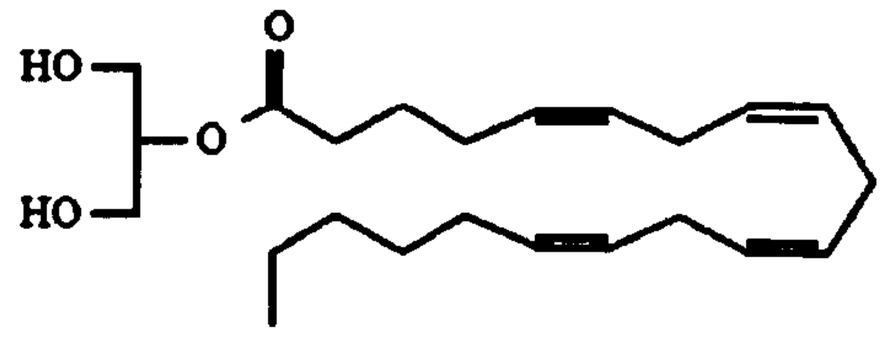

2-Arachidonoyl-glycerol (2-AG)

Endogenous ligand for CB1 and CB2

Substrate for FAAH

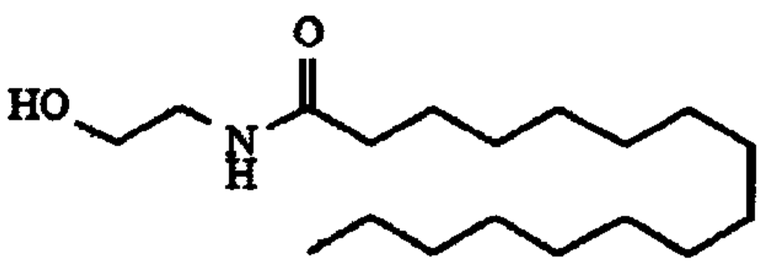

***N*-Palmitoylethanolamine (PEA)**

Endogenous ligand for CBn

Substrate for FAAH

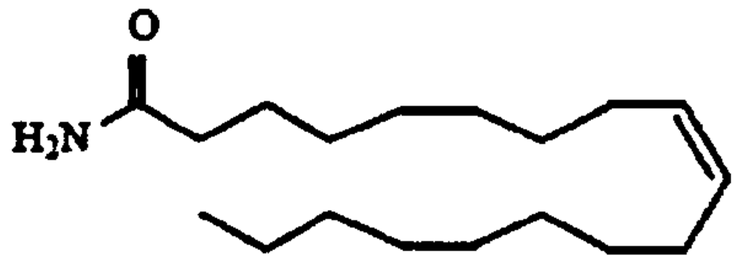

***cis*-9-octadecenoamide**

(Oleamide, ODA)

Substrate for FAAH

Figure 1.1 Chemical structures, and possible molecular targets, of representative members of the four classes of fatty acid derivatives that are substrates for fatty acid amide hydrolase (FAAH) (Cravatt and Lichtman, 2002).

Despite the structural similarities of these endogenous FAA's, many lack affinity at CB receptors, hence are called endocannabinoid-like (eCBL) molecules (e.g. Oleoylethanolamide (OEA), palmitoyl ethanolamine (PEA)). A previously hypothesised role of the eCBL's is described in **section 1.5**, yet it is currently emerging that these eCBL molecules display affinity for various other families of receptors. Despite uncertainty in the physiological roles of many of the eCBL's, these other areas of receptor regulation may, in the future, provide additional routes of therapeutic interest. Many actions of exogenous and endogenous ligands are mediated by the centrally located CB_1 receptors. Actions of the eCBs at this

receptor have been shown to be blocked by use of the selective CB_1 receptor antagonist SR141716A, which, up to recently, has been employed clinically as the therapeutic compound Rimonabant or Acomplia, used for the treatment of obesity. Prolonged use of this agent led to the development of depression and suicidal thoughts in patients, resulting in the drug being removed from the market. The beneficial and protective role of the eCB system is widely known, hence, the outcome of Rimonabant further provided evidence for the necessity and protective mechanisms conducted by the eCBs in the CNS via the CB_1 receptors.

1.3.2 Endocannabinoid Synthesis

eCBs are thought to be primarily synthesised and released at the post-synaptic synaptic membrane and act in a retrograde fashion at CB_1 receptors located on the pre-synaptic membrane, to inhibit or down regulate the release of neurotransmitters (see **Figure 1.2**) (Sipe et al., 2005a).

AEA has been suggested not to be stored in 'resting' cells, but to be synthesised and released 'on demand' (*de novo* synthesis) following physiological stimuli, e.g. nerve depolarization and the subsequent changes in levels of intracellular calcium (De Petrocellis et al., 2004). Depolarisation in post-synaptic neurones opens voltage-dependant calcium ion (Ca^{2+}) channels allowing Ca^{2+} to activate the enzyme responsible for synthesis of eCBs from their lipid precursors (e.g. N-oleoylphosphatidylethanolamine (NAPE)-Phospholipase D for generation of AEA from NAPE. Another route of eCB synthesis is through activation of metabotropic glutamate (mGlu) receptors, which, in turn, activate phospholipase C (PLC) to make

diacylglycerol, which is then broken down by diacylglycerol lipase to form 2-AG.

1.3.3 Endocannabinoid Signalling

After their synthesis, eCBs are free to leave the post-synaptic cell and activate pre-synaptically located CB_1 receptors. As a result of CB_1 receptor activation, pre-synaptic Ca^{2+} influx is inhibited causing a decrease in neurotransmitter release from the pre-synaptic neurone (see **Figure 1.2**).

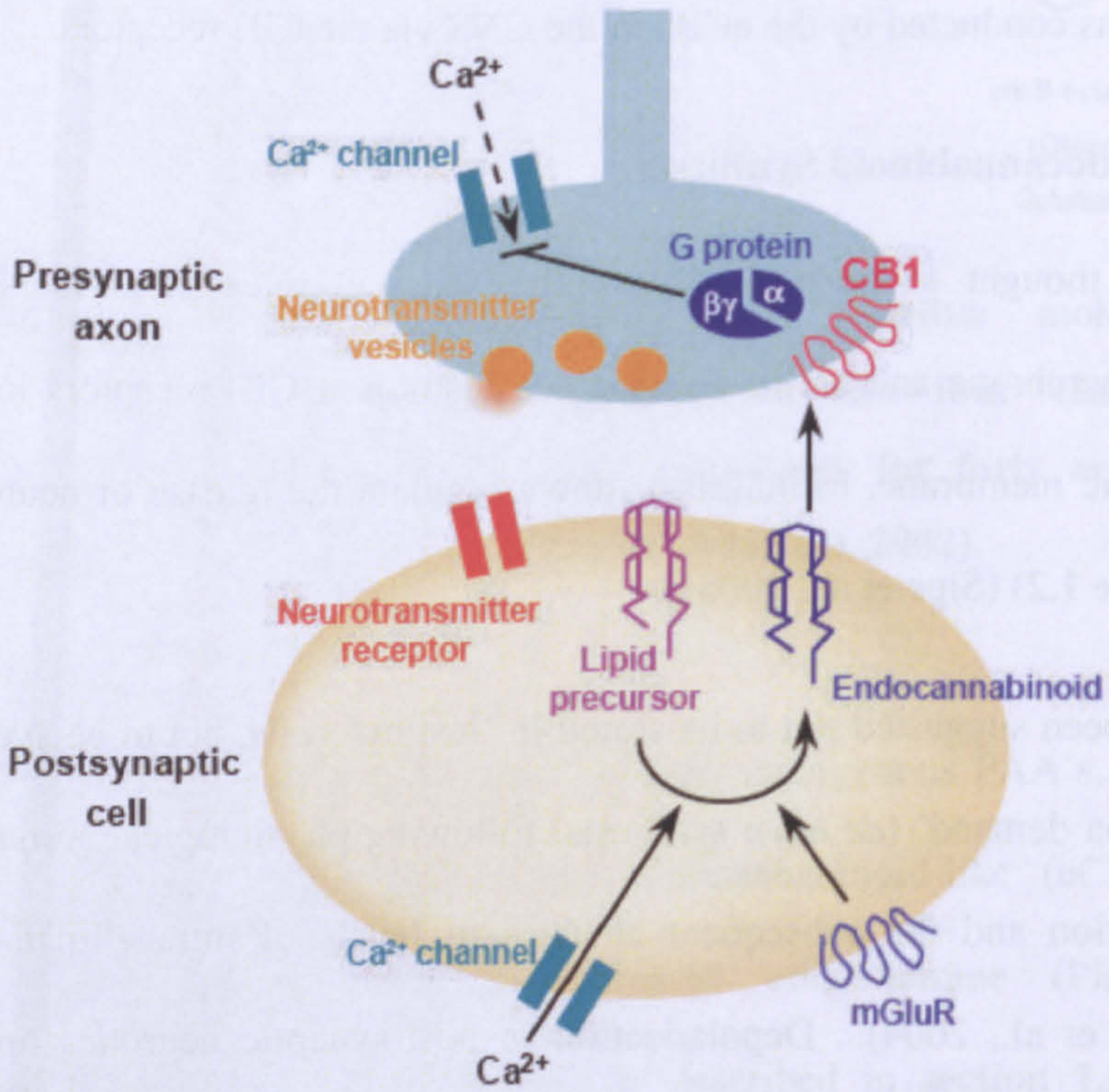

Figure 1.2 Retrograde signalling by endocannabinoids (Sipe et al., 2005a).

These signalling lipids have been shown to be cell and time specific in their production, action and breakdown.

As previously mentioned in section 1.2.1, identification of the CB receptors as

GPCRs negatively coupled to AC, resulting in the inhibition of cAMP production, results in various downstream effects. Their involvement in the regulation of many pathological states is described later in this chapter. However, this appears not to be the only effect produced by these receptors. It has previously been seen in striatum tissue, in the presence of both $G_{i/o}$-coupled D_2 and CB_1 receptors, that CB receptor agonists lead to an accumulation of cAMP through stimulatory G protein (G_s) activation (Glass and Felder, 1997). Using recombinant cell lines – this was not observed in CB_2 receptors (Wade et al., 2004). CB_1 receptors have also been shown to inhibit N/P/Q-type Ca^{2+} channels, following activation (Begg et al., 2001), as well as the activation of inwardly rectifying Potassium (K^{+}) within the CNS (Mackie et al., 1995) (Felder et al., 1995) (Twitchell et al., 1997). Modulation of Ca^{2+} and K^{+} channels primarily affects neuronal signaling resulting in the well known neuromodulatory effects of the CB and eCB compounds (Di Marzo et al., 1998). Although this effect appears to be mediated solely through CB_1 receptors, both CB receptors appear to activate mitogen-activated protein kinase (MAPK), following GPCR $G_{i/o}$-dependant activation (Bouaboula et al., 1997) (Bouaboula et al., 1999). MAPK has the ability to phosphorylate other proteins, causing changes in their activity and therefore causing further downstream effects into cellular processes.

1.4 Endocannabinoid Hydrolysing Enzymes

Any molecule acting as an endogenous regulator of physiological and pathological responses requires mechanisms for its action on specific molecular targets and its rapid inactivation (De Petrocellis et al., 2004). Following eCB synthesis and CB_1

receptor activation, the eCB can be taken up pre-synaptically and broken down; 2-AG hydrolysis occurs by monoacylglycerol lipase (MAGL)-mediated hydrolysis to form AA and glycerol. The mechanism of transport is still to be fully understood. A transporter identified on post-synaptic neurones is reported to carry AEA back into the neurones, the anandamide membrane transporter (AMT), making AEA available to FAAH for hydrolysis into arachidonic acid and ethanolamine (Sipe et al., 2005b). The occurrence of this transporter is controversial, however. It is now understood that the enzymes lipoxygenase and cyclooxygenase, as well as cytochrome P450s, provide alternative routes of transformation of some eCBs, resulting in the production of different metabolites, compared to hydrolysis by FAAH or MAGL (Pertwee and Ross, 2002).

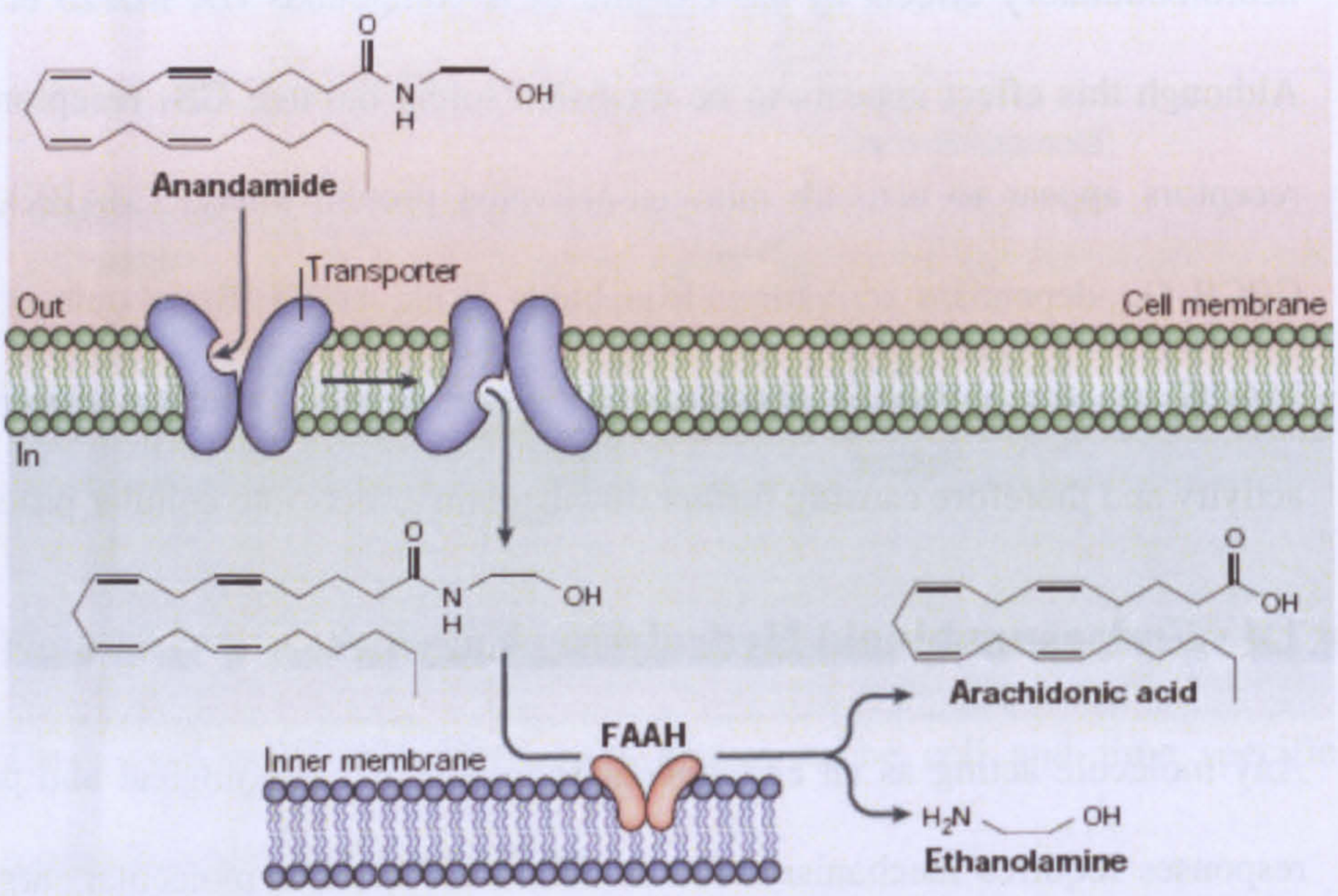

Figure 1.3 Deactivation of endocannabinoids by FAAH in neurons.

The characterisation of the principle metabolic pathways of eCB inactivation provides an important step towards the understanding and modulation of the eCB system. Knowledge of the mechanisms through which the endogenous levels of the eCBs, and hence their state of activation at the CB or other receptors, may have a big impact on the development of new therapeutic drugs (de Lago et al., 2005).

1.4.1 Fatty Acid Amide Hydrolase

As a corollary of the de novo synthesis of endogenous signalling molecules for immediate action, eCBs require rapid hydrolysis after their use, so their actions are not extended. Hence effective metabolism of eCBs is a prerequisite for their action. The principle inactivating (hydrolysing) enzyme of endogenous CB receptor ligands is FAAH, which has been identified as the catabolic enzyme inactivating primarily AEA (see **Figure 1.3**) (Sipe et al., 2005b) as well as many other eCBs and eCBL compounds; for example, the sleep-inducing eCB oleamide, is broken down into oleic acid and ammonia (Fowler et al., 2005). Selective inhibition of FAAH has been shown to produce increased levels of AEA, but not 2-AG, in the brain, suggesting that MAGL is the main hydrolysing enzyme of 2-AG.

FAAH Tissue distribution

FAAH is a dimeric membrane-bound enzyme, found in microsomal and mitochondrial membranes, that degrades neuromodulatory fatty acid amides and esters. It is an enzyme originally purified and cloned from rat liver microsomes, but has also been cloned from three other mammalian species; man, mouse and pig. FAAH catalyzes the hydrolysis of both AEA and 2-AG (De Petrocellis et al., 2004)

(Bisogno et al., 2002), and is found to be optimally active at alkaline pH. Its distribution in the CNS suggests that it is poised to degrade the neuromodulating fatty acid amides at their sites of action and is therefore intimately related to the regulation of the effects evoked (Boger et al., 2000).

Often the major hint of the possible physiological role of proteins can be obtained from the study of its tissue distribution in mammals. There may be undiscovered regions of tissues where FAAH is expressed, as it has sometimes proved difficult to detect. For example, little or no activity was initially observed in the gastrointestinal tract, due to the presence of endogenous inhibitors of the enzyme, such as the mono-acylglycerols, being highly abundant in these tissues (Bisogno et al., 2002). To date, high expression of FAAH has been determined in rat liver, brain and testis, with low levels in the spleen and very low levels in the heart, as shown in **Table 1.1** (Bisogno et al., 2002).

Organs	**Human**	**Rat**	**Mouse**
Pancreas	ooo		++
Brain	ooo	ooo +++++++++	++++
Kidney	oo	oo	
Skeletal Muscle	oo	ND	
Liver	o	ooooo ++++++++++	+++++
Placenta	o		

Heart	ND	ND	ND
Lung	ND	++	ND
Testis		°°° ++++++	+++
Parathyroid gland		°° +++++	
Submaxillary gland		°°°° ++++	
Small intestine		°°°°° +++	
Stomach		°°°° ++	
Spleen		°° ++	+
Cerebellum		++++++	
Esophagus		ND	
Colon		+	

Table 1.1 **Distribution of FAAH activity (+) and mRNA (°, measured by Northern blot) in various organs from the rat, mouse and man. ND, not detectable (Bisogno et al., 2002).**

1.4.2 FAAH activity *in vivo*

FAAH's distribution in the CNS suggests that it is poised to degrade neuromodulating FAAs at their site of action and is therefore intimately related to the regulation of the effects evoked (Cravatt and Lichtman, 2003).

FAAH inhibitors are not currently in use in any therapeutic areas today. Yet, their

potential as a target of eCB system modulation is clearly apparent.

Different transgenic mice have also been developed lacking the CB_1 gene. One model commonly used for FAAH studies has been developed by Cravatt's lab (Cravatt and Lichtman, 2002) (Cravatt et al., 2001) , where the gene encoding FAAH was disrupted by deletion of the promoter region of the gene, producing mice lacking the FAAH enzyme (Cravatt and Lichtman, 2002).

Fatty acid amide hydrolase knockout ($FAAH^{-/-}$) mice were viable, fertile and largely indistinguishable from the wild type ($FAAH^{+/+}$) litter mates in terms their of general cage behaviour, unlike the differences observed with $CB_1^{-/-}$ mice (Cravatt and Lichtman, 2002). $FAAH^{-/-}$ mice were severely impaired in their ability to degrade AEA and responded to normally inactive doses of AEA by producing the typical 'tetrad' of CB_1-dependant behavioural responses which include analgesia, catalepsy, hypolocomotion and hypothermia (Bisogno et al., 2002). These behavioural effects induced by AEA are reminiscent of those elicited by treatment with the exogenous CB Δ^9-THC, suggesting that AEA is indeed acting as an endogenous ligand at CB_1 receptors *in vivo* (Cravatt et al., 2001). This further supports FAAH as a key regulator of AEA signalling *in vivo* (Cravatt and Lichtman, 2002). AEA's behavioural effects in $FAAH^{-/-}$ mice were completely blocked by pre-treatment with the CB receptor antagonist rimonabant, hence this model allows further investigation of FAAH activity *in vivo*.

FAAH distribution in the brain may allow us to correlate its presence with a possible involvement in different physiological processes regulated in those areas (see **Figure**

1.2). For example, although discrepancies are seen between the various methods used to determine FAAH distribution in the brain; all the cases show the hippocampus to have the highest degree of FAAH expression (Bisogno et al., 2002), which is known to be involved in the formation of new memories as well as energy balance and satiety in mammals. The brainstem and hypothalamus are the areas showing the least FAAH expression. Most importantly, FAAH brain regional distribution overlaps to a large extent with that of CB_1 receptors, and in some areas where both CB_1 receptors and FAAH are expressed, they have complementary distribution, hence areas where eCBs act on CB_1 receptors are open to CB_1 and FAAH manipulation through therapeutic agents, depending on eCB function in that area. The low levels of both CB_1 and FAAH in the hypothalamus (the main brain region controlling appetite), compared to other brain regions, may suggest eCB involvement in feeding behaviour to be occurring through unexpected pathways in the brain than initially anticipated (or more peripheral involvement than central), or alternatively, despite the low levels of CB_1 receptors in the hypothalamus, tissue or brain area specific manipulation of FAAH in different areas of the brain may allow us to further determine the involvement of FAAH on feeding behaviour.

1.4.3 Inhibitors of FAAH

There have been many different classes of FAAH inhibitors discovered over years in CB system research. Fowler has reviewed these classes of inhibitors, non-steroidal anti-inflammatorys (NSAIDs): structures of ibuprofen and indomethacin; substrate analogues: phenylmethanesulphonylfluoride (PMSF); organophosphates: PMSF;

carbamates: URB597) (Fowler et al., 2003) available today. A commonly used strategy in the development of enzyme inhibitors is using known substrates as a template. This was a method used in the development of OL-135, which is a reversible FAAH-selective inhibitor (Lichtman et al., 2004) and belongs to a class of α-keto heterocycle inhibitors (Patterson et al., 1996). Further investigation in the use of OL-135 found it to promote CB_1 receptor mediated analgesia in a number of *in vivo* models of pain (Lichtman et al., 2004).

A second group of inhibitors are the organophosphates and organosulfates, which were in fact accidentally discovered during the characterization of FAAH (Deutsch and Chin, 1993) a serine protease inhibitor, PMSF was added to *in vitro* assay samples to prevent degradation of native enzyme preparations and was, in turn, found to inhibit AEA hydrolysis. Other inhibitors belonging to this group of compounds have been developed, yet they all lack selectivity for FAAH and are therefore limited in the potential use as therapeutic modulators of the eCB system (Fowler, 2004).

The third group of FAAH inhibitors, the carbamates, is the most significant developed to date. Until recently, the most potent FAAH inhibitor found in this group, URB597, is a reasonably selective FAAH inhibitor, which upon its first investigations, was found to increase endogenous AEA levels significantly in rats (Kathuria et al., 2003). URB597 is reported to also inhibit other serine hydrolases, aside from FAAH, yet the physiological consequences *in vivo* of this are still undetermined (Lichtman et al., 2004).

The last group of FAAH inhibitors is the group of compounds which exert their

primary actions on cyclooxygenase, the NSAIDs. The well known NSAID ibuprofen was found to inhibit AEA hydrolyzing activity using rat brain (Fowler et al., 1997), as well as indomethacin, which was found to inhibit AEA hydrolyzing activity in mouse uterus tissue (Paria et al., 1996). NSAIDs are known to be anti-inflammaotry through a mechanism which inhibits prostaglandin (PG) synthesis (Vane, 1971), yet their potential action as FAAH inhibitors, which would in turn increase AEA and in turn increasing their anti-inflammatory actions through alternative mechanisms (involving the eCB system) supports the therapeutic potential of the use of FAAH inhibitors.

1.4.4 Monoacylglycerol Lipase

As previously mentioned in section 1.4.1, FAAH inhibition, at concentrations that block AEA hydrolysis, causes elevation of AEA and not 2-AG (Beltramo and Piomelli, 2000). In the case of 2-AG, multiple metabolic pathways are possible, as it is also a substrate for lipoxygenases and cyclooxygenases *in vitro* (Fowler et al., 2005). Further investigations using FAAH knockout mice reported that hydrolysis of a related monoacyl glycerol, 2-oleoylglycerol (2-OG), in brain and liver was preserved, while AEA hydrolysis was not (Lichtman et al., 2002) and it was Dinh *et* al in 2002 (Dinh et al., 2002) that suggested 2-acylglycerol (2-AG), but not AEA was catalysed by MAGL to convert both 2- and 1- monoacylglycerides to fatty acid and glycerol metabolites, further supporting MAGL as the second enzyme of the eCB system.

1.4.5 Inhibitors of MAGL

Until recently there have been no selective inhibitors of MAGL described, but it was Cravatt's group developed the compound named JZL-184 (Long et al., 2009), which displayed highly selective activity at MAGL to elevate 2-AG levels in brain tissue. The testing of several FAAH inhibitors on 2-AG hydrolysing activity using membrane preparations, found that, as expected, selective FAAH inhibitors (URB597) did not affect 2-AG levels, whereas the non-selective inhibitors (PMSF) did (Saario et al., 2004). Yet, now, with the development of JZL184 it is hoped that this provide a good template for the discovery of further selective and highly potent MAGL inhibitors.

1.5 The Entourage Effect

There are several reports that eCBL's, such as OEA and PEA, are potentially endogenous substrates for FAAH acting as reversible inhibitors of the primary cannabinoid hydrolysing enzyme (Mechoulam et al., 1997). Studies suggest that due to the lack of affinity of eCBL's at the CB receptors, their primary role is suggested to be to protect AEA from enzymatic hydrolysis by diverting FAAH activity, leading to an accumulation and potentiation of eCB effects at the CB receptors, 'the entourage effect'. The same has been stated for the protection of 2-AG from hydrolysis by MAGL by the compounds 2-linoleoylglycerol and 2-palmitoylglycerol (Mechoulam et al., 1998).

1.6 Therapeutic Potential Of Endocannabinoid Enzyme Inhibitors

CB receptors and modulators of eCB modulators have various pharmacological effects throughout the body and CBs have been used for their therapeutic advantages in a wide array of disorders for centuries. CB receptor agonists inhibit the release of various excitatory and inhibitory neurotransmitters including glutamate (Shen et al., 1996), dopamine (Burkey et al., 1997), noradrenaline (Schlicker et al., 1997), and acetylcholine (Carta et al., 1998), resulting in acute effects on analgesia, memory and reduced locomotor activity. The eCB system itself has been suggested to be involved in diseases such as multiple sclerosis (Baker et al., 2001) (Baker et al., 2000), and schizophrenia (Leweke et al., 1999). Unfortunately, the unwanted side effects, predominantly observed by activation of centrally located CB_1 receptors have slowed down research into the therapeutic advantages of the eCB system and its ligands and also provide a further challenge in using CB_1 agonists and, as recent evidence attests, CB_1 receptor antagonists (Tarik Ugura, 2008). This in turn has directed much research to turn back towards the effects of peripheral CB_1 receptor activation, modulation of the eCB system using the natural partial CB receptor agonists and eCBs and looking further into novel peripheral receptor targets and mechanisms involving the eCB and eCBL compounds, potentially leading to new therapeutic targets.

1.7 Endocannabinoids In Feeding Behaviour

It is well documented that CB agonist induce the onset of feeding, namely 'the munchies'. This is a central effect, resulting from activation of CB_1 receptors located directly in the brain (Onaivi et al., 2008). It is known to increase the desire for high-calorific foods.

eCBs in recent years, have been linked with leptin, a gut hormone which plays a key part in modulating food intake and body fat. Leptin-deficient mice have been shown to become obese and exhibit increased levels of eCBs in the hypothalamus, whereas administration of leptin decreases feeding behaviour and consequently shows a decrease in levels of AEA and 2-AG in the hypothalamus (Lichtman and Cravatt, 2005), suggesting a dual role of eCBs in regulating body weight through a central orexigenic effect as well as a peripheral role in the regulation of lipogenesis (Lichtman and Cravatt, 2005). The liver is a primary site responsible for eCB-mediated modulation of lipogenesis; hence it links pathways for peripheral lipogenesis and central appetite regulation by an eCB signalling system, primarily in the hypothalamus (Lichtman and Cravatt, 2005). The eCB system in the liver undergoes adaptive changes in response to diet, mice maintained on a high-fat diet developed fatty liver associated with increases in hepatic expression of CB_1 and increased levels of AEA (Lichtman and Cravatt, 2005). This increase in hepatic AEA appears to be a result of decreased FAAH activity, although the level of FAAH activity was unaffected directly by diet. It was suggested that this phenomenon was mediated through elevation of FAAs, like the eCBL's and other endogenous factors,

competing for FAAH hydrolysis (Lichtman and Cravatt, 2005).

CB_1 activation of hepatic cells leads to an increase in hepatic fatty acid synthesis by increasing the expression of lipogenic transcription factor sterol response element-binding protein-1c (SREBP-1c). SREBP1c regulates the expression of genes involved in fatty acid synthesis, including acetyl coenzyme carboxylase-1 and fatty acid synthase. Treatment of mice with a potent CB_1 agonist (HU-210) increases free fatty acid (FFA) synthesis by increasing hepatic levels of SREBP1c and its regulated genes, and this has been shown to be prevented by pretreatment with rimonabant (Lichtman and Cravatt, 2005).

This mechanism provided a target for anti-obesity treatment, leading to the production of rimonabant. In animal studies, rimonabant was found to mediate hypophagia through reduction of the appetitive or preparatory aspects of the motivation to feed, as well as causing reduced food consumption behaviour through the inhibition of the positive feedback processes which are normally associated with food intake (Thornton-Jones et al., 2005). But its lack of success as a therapeutic drug was due to inhibiting the actions of many eCBs at CB_1 receptor, which clearly regulate the beneficial effects of eCB's on regulating mood. Hence, new mechanisms for the effects of eCB's and the eCBL's on non-CB receptors and other receptor groups are being researched.

Obesity has also been found to be associated with a dysregulation of eCBs, where animal models of genetically-induced obesity show long-lasting overstimulation of the eCB system synthesis, leading to a permanent activation of the CB_1 receptor,

which may, in fact, help maintain their obese state (Pagotto et al., 2005). Studies have also shown the up-regulation of CB_1 receptor in obese animals, further supporting a role for the CB_1 receptor in obesity. This group also found that peripheral CB_1 receptor activation stimulates lipogenesis in adipocyte cells and CB_1 receptor antagonists demonstrate increased adiponectin production in adipocyte cells. Adiponectin drives fatty acid oxidation and free FFA clearance. Such findings favour a peripheral CB_1 receptor target as an alternative route of eCB modulation for the treatment of obesity.

1.7.1 OEA and Peripheral Regulation of Feeding

Clearly FAAH regulates the levels of several endogenous FAAs, most of which do not interact with CB receptors, but appear to possess distinct sites of action and functions in the nervous system and periphery. The functions of many of these 'orphan' FAAs and how these activities might be affected by FAAH inhibition is an area of research with possible leads to therapeutic benefits. We know that symptoms of several central and peripheral disorders are due to, or are related to, changes in eCB biosynthetic and degradative pathways, and, subsequently, of pathologically altered activation of either CB_1 or CB_2 cannabinoid receptors, or alternatively differing peripheral receptor activation (de Lago et al., 2005). If it is found that the symptoms of a certain disorder are caused, for example, by altered eCB levels or that eCBs are produced in order to counteract the symptoms or the progress of the disorder, then substances selectively inhibiting eCB hydrolysis may produce beneficial effects by prolonging eCB life-span and enhancing eCB levels (de Lago et

al., 2005).

Studies of peripheral regulation of feeding and appetite have identified that OEA is produced in the small intestine in response to food. It is suggested to activate nerves in the walls of the small intestine, rather than in the brain, to send a signal to parts of the brain (hypothalamus and nucleus accumbens) which control food intake, and so to reduce appetite directly at the satiety centre.

It was hypothesized whether OEA worked in the same manner as gut hormones, being carried in the blood to directly activate their receptors in the brain (e.g. ghrelin, Cholecystokinin (CCK), glucagon-like peptide-1 (GLP-1) to regulate feeding. Studies have, however, shown OEA not to cause changes in circulating gut hormone levels (Proulx et al., 2005). Alongside this, Cravatt's group (Rodriguez de Fonseca et al., 2001) showed that OEA injected directly into the brain, in mice, did not exert orexigenic effects, yet it did when injected i.p., further indicating OEA to be involved in a peripheral receptor mechanism regulating food intake.

The actions of OEA have been investigated primarily in the GI tract. It was Piomelli's group in 2006 that found onset of feeding led to mobilisation of OEA in proximal areas of the small intestine (duodenum) and alongside this, the OEA-generating precursors N-acyl phosphatidylethanolamine (NAPE) and expression of its synthesizing enzyme N-acyl phosphatidylethanolamine phospholipase D (NAPE-PLD) was increased. FAAH activity decreased along with these changes upon feeding, indicating nutrient availability to regulate and control this peripheral effect of feeding (Piomelli et al., 2006). So it can be wondered whether ingested foods

transit through the small intestine and stimulate nutrient-sensing cells, causing the release of bioactive peptides and lipid mediators (such as OEA) or increase the activity of NAPE-PLD, eventually leading to the OEA mediated effects. So, it is possible food intake may also control the mobilization of OEA and act as a lipid derived satiety factor, yet the molecular mechanisms underlying OEA release in the gastro-intestinal (GI) tract are still undefined.

OEA resembles the endogenous lipids that activate the peroxisome proliferator-activated α receptor (PPARα) family of nuclear receptors. These receptors are the target of fibrate drugs used in the treatment of hyperlipidemia (Lo Verme et al., 2005). OEA has been found to have high binding affinity to PPARα, with *in vitro* analysis displaying maximal effective concentration (EC_{50}) values of 120 nanomolar (nM). Such a low activation concentrations suggests levels of OEA in the gut, in response to feeding, are adequate enough to cause full activation of PPARα, as well as this OEA is found to be present in the same areas as PPARα (Fu et al., 2003), further indicating its importance in food regulation.

Activation of PPARα by OEA seems sturucturally selective, as other eCBL's (stearoylethanolamide; SEA) and eCB's (AEA) do not show any effect at this receptor (Stella and Piomelli, 2001). Interestingly, the range of fibrate drugs used to induce antihyperlipidemc effects are actually weak PPARα agonists and demonstrate *in vivo* to have no anorexic effects (Fu et al., 2003).

Direct injection of OEA into the brain failed to evoke a reduction in appetite, while PPARα null ($PPAR\alpha^{-/-}$) mice were still responsive to OEA (Rodriguez de Fonseca et

al., 2001). OEA effects at PPARα receptor suggests a potential therapeutic route toward obesity treatment, possibly through tissue specific modulation of FAAH activity creating an accumulation of OEA in areas of the GI tract, which may have benefits on appetite reduction and lipid lowering, as well as powerful insulin-sensitising agents.

The regulation by feeding of OEA levels in the duodenum and jejunum (Rodriguez de Fonseca et al., 2001) (Fu et al., 2003) implies that OEA may act on PPARα receptors localized within cells of the small intestine. It has been reported that OEA content in rat small intestine rises from 132 ± 18 picomolar per gram (pmol/g) in a fasting state to 329 ± 150 pmol/g after feeding (Rodriguez de Fonseca et al., 2001), where the concentration of OEA found post-feeding is two-fold higher than the EC_{50} of OEA for PPARα (120 nM), suggesting that post-feeding levels of endogenous OEA are high enough for PPARα receptor activation (Fu et al., 2003).

It has been hypothesized that OEA exerts its effects on peripherally located receptors leading to signals sent *via* vagal sensory neurons located in the walls of the small intestine, directly to the hypothalamus to induce satiety (Fu et al., 2003) (Rodriguez de Fonseca et al., 2001), yet the mechanism by which OEA exerts this effects is still undetermined. The chain of molecular events that join PPARα activation to vagal sensory fibre recruitment is unknown, but it has been hypothesized that the message between the receptor and neuron may, at least in part, be through the release of nitric oxide (NO). It has been reported that enterocytes produce large amounts of NO and it may have a role as a peripheral appetite-stimulating signal (Calignano et al., 1993).

We know PPARα represses the expression of inducible NO synthase (iNOS), which is responsible for the production of NO (Fu et al., 2003) (Gaetani et al., 2003)], therefore through the repression of iNOS by PPARα may well contribute to the effects of OEA on satiety. These studies have also shown that OEAs actions are rapid and transient (Gaetani et al., 2003), which contrasts with traditional mechanisms of PPARα activity, associated with gene transcriptional changes. OEAs effects on PPARα may, therefore, provide evidence for the involvement of PPARα receptors in non-transcriptional mechanisms.

1.7.2 GPR119

A recently deorphanised GPCR, GPR119, was suggested to be a close relative of the CB receptors on the basis of amino acid sequence comparisons (Overton et al., 2006). Tissue distribution of GPR119 is still incompletely defined, yet transcripts of human and rodent GPR119 have been found predominantly in intestinal tissues and the pancreas (Lauffer et al., 2008) (Soga et al., 2005) and rodents have also been found to express the receptor in certain brain regions (Overton et al., 2008). Using immunoreactivity methods, GPR119 was found to be localized in the villi in small intestine (Chu et al., 2007). Its has been reported that cells expressing GPR119 at concentrated levels display a constitutive increase in cAMP (Chu et al., 2007), which implies GPR119 to be coupled to a stimulatory G protein (G_s). Due to the high level of homology between GPR119 and the CB receptors, compounds active in the eCB system were first investigated for their actions on GRP119. It was found that OEA showed the highest affinity to GPR119, followed by PEA and SEA, which displayed

weak effects at the receptor, with AEA apparently inactive (Overton et al., 2006). OEA stimulated cAMP production in cell lines expressing GPR119, where cells without GPR119 failed to produce an effect. As previously mentioned, OEA produces hypophagia apparently through activation of PPARα (Fu et al., 2003) (Rodriguez de Fonseca et al., 2001). Like OEA, a synthetic GPR119 agonist suppressed food intake and weight gain *in vivo*, but displayed no effect at the PPARα receptors. Interestingly, OEA displayed equipotent effects in the suppression of food intake in wild-type and GPR119 deficient mice (Lan et al., 2009), which suggests that these GPR119 agonists may work through different mechanisms, or obtain additive effects aside from activity at GPR119. OEA at a dose of 30 milligrams per kilogram (mg/kg), administered i.p., displayed a significant reduction in food intake in free feeding rats, and this effect was shown to last up to 2 hours post-injection, indicating a transient effect at this receptor (Overton et al., 2006). The agonist action of OEA on GPR119, leading to a reduction in appetite, provides a clear therapeutic target for the development of GPR119 agonists for the regulation of appetite and feeding behavior *in vivo*.

1.7.3 $TRPV_1$

TRPV1 is expressed in both nociceptive neurons, where it is involved in the detection of noxious chemicals and thermal stimuli, and in visceral sensory neurons and brain, where it could have a role in food intake control. OEA has been shown to have affinity for and directly activate TRPV1 receptors with an EC_{50} of ~2 micromolar (μM) at room temperature (Ahern, 2003). This effect was seen to be through direct

phosphorylation of TRPV1, as no responses to OEA were observed with TRPV1 receptors lacking critical PKC phosphorylation sites. Hence, if TRPV1 is phosphorylated by the protein kinase C (PKC), it becomes more sensitive to OEA activation and therefore it is thought to work in a PKC-dependent manner, resulting in OEA-induced Ca^{2+} rises that were selective for capsaicin-sensitive cells, in sensory neurons. This effect was inhibited by the TRPV1 antagonist, capsazepine. This provides evidence that TRPV1 represents a potential target for OEA and may contribute to the excitatory satiety signalling action of OEA, where TRPV1 provides access for OEA stimulation of the vagal sensory nerve to signal satiety directly to the hypothalamus.

It has also been found that some effects of OEA mediated by TRPV1 receptor may be a result of OEA acting as an antagonist. It has been hypothesised that, in addition to the actions of OEA at PPARα receptors to cause modulation of food intake and lipid metabolism, circulating OEA could block TRPV1 receptors on neuronal cells. This mechanism would modify the electrical status of the Ca^{2+} channel, inducing small depolarization (Wang et al., 2005). Therefore, the vagal sensory nerves would be excited, directly influencing food intake regulation. To confirm TRPV1 involvement in OEA effects on food intake, normal mice and TRPV1-null mice were injected with OEA (12.5 mg/kg). Short-term feeding was significantly reduced in the control group, but not in the TRPV1-null group, showing the role of this receptor in feeding regulation (Movahed et al., 2005) (Wang et al., 2005), providing further evidence of another possible peripheral route for the hypophagic actions of OEA *in vivo*.

1.7.4 Peroxisome Proliferator-Activated Receptor-alpha (PPARα)

Peroxisome proliferator-activated receptors (PPARs) are a group of nuclear receptors that function as transcription factors and regulate the expression of genes (Michalik *et al,*. 2006), leading to the regulation of metabolism. There are three types of PPAR subtypes which have been identified and named alpha (α), gamma (γ), and delta (δ) (beta) (Berger *et al,*. 2002). PPARs are found to be in most cells in the body, high levels of expression of PPARα are found in the liver, heart, muscle and adipose tissue. PPARβ/δ are also found predominantly in adipose tissue as well as the brain and PPAR γ has three isoforms which are found in almost all tissues of the body.

The function of PPARα is dependent on the binding properties of its ligand and as well as having synthetic agonists, like fenofibrate, it is also activated by endogenous ligands such as free fatty acids and has now led to investigate the ligand binding effects of endogenous cannabinoid ligand OEA. Research into the role of PPARα agonist by the endocannbinoid OEA has indicated a possible site of peripheral regulation of food intake. PPARα is the main target of fibrate drugs, a class of amphipathic carboxylic acids medications currently on the market (clofibrate, gemfibrozil, ciprofibrate, bezafibrate, and fenofibrate) for the treatment of disorders creating high levels of both cholesterols and triglycerides.

Fenofibrate

Fenofibrate is a fibric acid and is a well-established PPARα agonist displaying lipid modifying effects in humans, with all effects mediated by activation of PPARα. The

agonist action of fenofibrate, like other fibrates, produces dyslipidaemic effects by a reduction in low density lipoproteins (LDL) and very low density lipoproteins (VLDL) alongside an increase in high density lipoproteins (HDL) and a reduction in triglyceride levels. In addition, through modulation of the synthesis and catabolism of VLDL fractions, fenofibrate increases the LDL clearance and reduces small and dense LDL, the levels of which are found to be elevated in coronary heart disease (Yang *et al,*. 2009) as well as a beneficial effect in insulin resistance (Wysocki *et al,*. 2004). Fenofibrate has also been used as an add-on therapy to the use of statins as it increases the serum level of statins, therefore, a lower dose of statin is generally necessary in the treatment of hypercholesterolemia and hypertriglyceridemia.

PPARα antagonist GW6471

GW6471 is a PPARα antagonist, yet very little is known of GW6471 pharmacology. It has mainly been used *in vitro* to investigate interruption of PPARα binding and transcriptional activity. GW6471 has only been reported once to being used *in vivo*, using an intraplantar injection as route of administration, not allowing for the observation of potential behavioral effects caused by systemic circulation *in vivo*. The understood rationale of PPARα antagonism does not lead to the need of its investigation. Chronic activation of PPARα would lead to a metabolic shift leading to the utilisation of proteins as an energy source and extensive degradation of proteins can lead to myopathy or rhabdomyolysis (Motojima, 2002). Hence the development of a specific PPARα antagonist and research in this area is limited to date. In this instance, new knowledge of the involvement of the cannabinoid system, in particular

OEA, and its actions and potential effects regulated by PPARα provides GW6471 as a tool for the investigation of mechanism pathways involved in the effects of OEA. Yet results of its use as a pharmacological tool may be limited as its absorption profile *in vivo* is unknown and therefore effective dosing remains an issue.

1.8 Aims and objectives

The aims of this thesis is to develop functional high throughput screening (HTS) assays, which are rapid, cheap and facile, for the identification of potential inhibitors of both the main eCB system hydrolysing enzymes FAAH and MAGL leading to potential eCB system modulation. Where inhibition of these enzymes would lead to an increase in the endogenous tone of eCBs and eCBL molecules, we have investigated the role of eCBL compound OEA, its peripheral role in the regulation of feeding and satiety signaling and whether its response is mediated by PPARα receptors in the periphery. This would therefore provide further information towards targeting FAAH with inhibitors and whether this may be a potential therapeutic target for the beneficial increase of OEA towards regulation of feeding behaviours.

Chapter 2: Characterisation of a novel assay for fatty acid amide hydrolase activity

2.1 Introduction

2.1.1.1 Existing assays for Fatty Acid Amide Hydrolase activity

In recent years, there has been increased interest in the potential therapeutic benefits of FAAH inhibition, which has stimulated research into FAAH activity assay development for novel inhibitor identification. The predominant methods of FAAH assay involve radiochemical and chromatography methods. Radiochemical methods involve incubation of FAAH with a radiolabelled substrate; separation of the radioactive reaction product then allows determination of the FAAH reaction rate. Chromatography methods applied include mini-column chromatography (Desarnaud et al., 1995), thin layer chromatography (Deutsch and Chin, 1993), or reverse-phase high performance liquid chromatography (Marcelis van der et al., 1997) (Maccarrone et al., 1999). An alternative to radiochromatography methods involves the use of anandamide (or related substances) radiolabelled on the ethanolamine section of the compound, allowing measurement of the radioactive cleaved portion of the substrate following FAAH catabolism. An organic solvent is used to stop enzyme activity, at the same time generating two phases, where the ethanolamine hydrolysis product partitions into the aqueous phase, leaving unreacted substrate to remain in the organic phase. The aqueous phase is sampled for activity measurement using scintillation counting, eliminating the use of chromatography (Omeir et al., 1995), essentially,

making it the 'gold standard' for FAAH/assay activity.

Other assays have described the use of non-radioisotopic chromatography methods to determine FAAH activity. One version employed UV absorbance detection (at 204 nm) following separation of arachidonic acid from FAAH substrates by HPLC, which involves extraction of reaction products containing carbon-carbon double bonds, following substrate-enzyme incubation, which are then identified by RP-HPLC as a measure of FAAH activity (Lang et al., 1996). A follow-up assay from the same group used o-phthaldehyde derivatization of the evolved ethanolamine following FAAH-catalysed anandamide hydrolysis, which involves anandamide incubation with FAAH, followed by addition of o-phthaldehyde which separates the reaction product ethanolamide, by binding to it, producing an isoindole derivative, with subsequent HPLC separation and detection at 230 nm (Qin et al., 1998).

Despite their high levels of sensitivity (femtomolar range) for FAAH activity, all of these methods have limitations in their use, by being either expensive due to the use of radiolabelled substrates, time-consuming because of the chromatographic analysis, or both.

Two further methods of FAAH assay appeared to reduce some of the drawbacks mentioned above. One method used oleamide as a FAAH substrate, measuring the reaction product ammonia using ion-specific electrodes (Patterson et al., 1996). A second assay, based on fluorescence ligand displacement, measured arachidonic acid or oleic acid production from anandamide or oleamide hydrolysis, since the fatty acids compete for binding of a fluorescent fatty acid analogue, DAUDA (11-(5-

dimethylamino napthalensulphonoyl)-undecanoic acid), to a fatty acid binding protein (Thumser et al., 1998). However, these methods still have drawbacks. The first method requires large assay volumes (10 mL) to accommodate the size of the electrode. The second assay involves the laborious extraction of the binding protein from rat liver or *E. coli* expressing the recombinant protein. Also, there was significant cross-sensitivity to the substrates anandamide and oleamide, reducing the usefulness of the assay.

FAAH assays using fluorogenic reaction products are attractive for the development of high throughput screening (HTS) methodologies. One such method involved the use of AAMCA (*N*-arachidonoylaminomethylcoumarin) as a novel FAAH substrate (Ramarao et al., 2005). The fluorescent product 2-amino-7-methylcoumarin was measured in a kinetic manner over 1 hour, limiting screening time.

A further development in FAAH activity assays from the labs in Nottingham was the use of a spectrophotometric dual-enzyme assay to measure the rate of ammonia production from oleamide hydrolysis (De Bank et al., 2005) L-Glutamate dehydrogenase catalyses the production of glutamate from the ammonia product and 2-oxoglutarate, using NADH as a co-factor. The oxidation of NADH to NAD^+ can be measured using a UV spectrophotometer due to its high molar extinction coefficient at 340 nm. The reduction in absorbance is directly proportional to the hydrolysis rate of oleamide. Although this assay was amenable to HTS screening, it has the drawbacks of being an indirect assay of FAAH activity, as well as being a 'destructive' assay, where a decline in the parameter measured reflects enzyme

activity. A more useful method measures accumulation of a product to allow viable measurement of low enzyme activities.

2.2 Objectives

Due to the limitations of these existing assays, we aimed to develop a simpler end-point FAAH assay, which would be rapid, cheap and sensitive, as well as being amenable for high throughput screening (HTS). We continued to use oleamide as a FAAH substrate, where oleic acid and ammonia are the resulting reaction products (DeBank *et al.*, 2005), to develop a simple two-step assay. We used the novel approach of derivatising the reaction product ammonia with o-phthaldehyde in the presence of (hydro) sulphite to generate a 1-sulphonatoisoindole fluorescent derivative at alkaline pH (**Scheme 2.1**). Fluorescence can then be detected at wavelengths of ex. 360, em. 490 nm and directly indicates the rate of oleamide hydrolysis by FAAH.

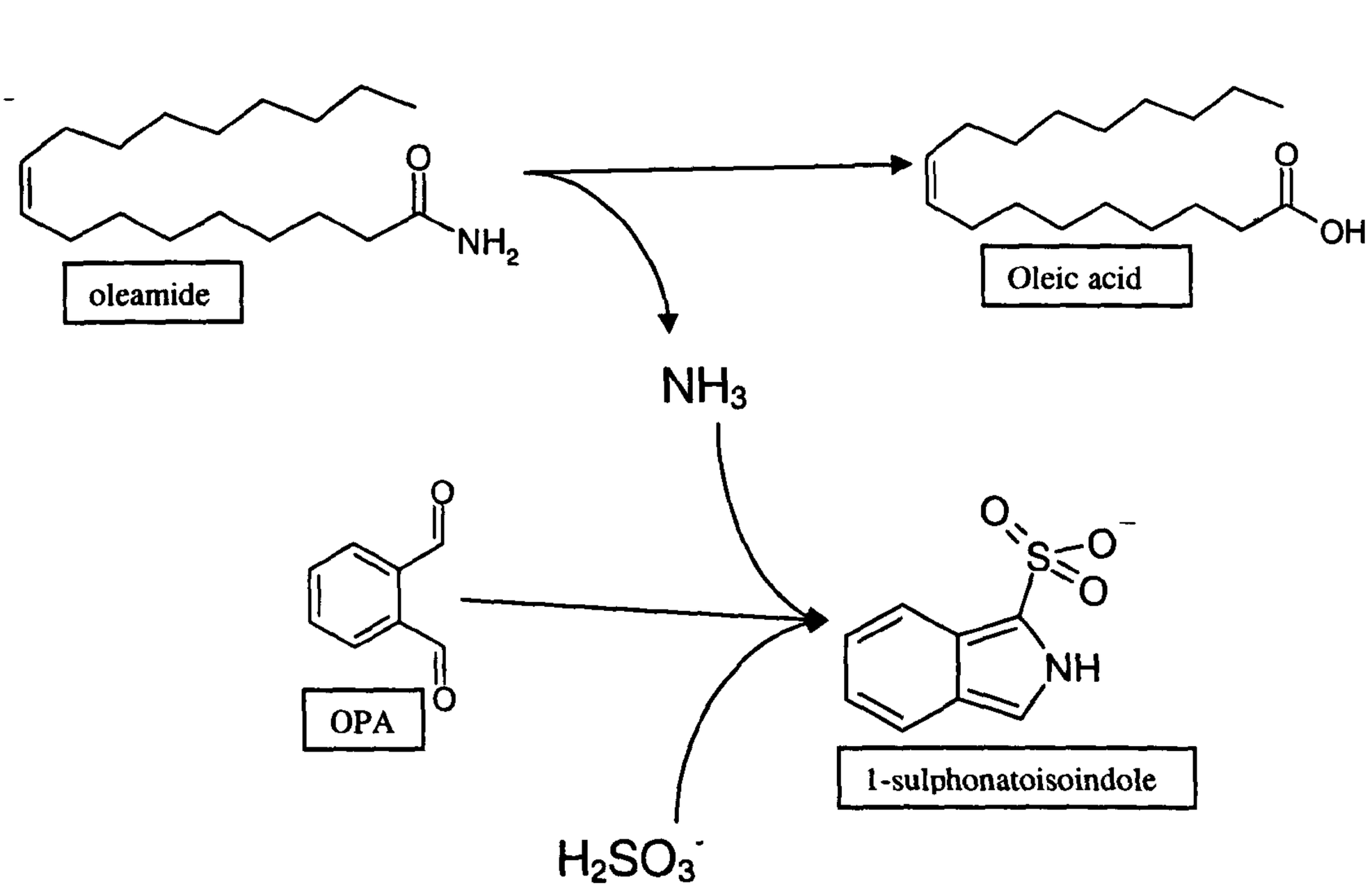

Scheme 2.1 **Reaction mechanism of FAAH-catalysed oleamide hydrolysis with reactant product ammonia's reaction with o-phthalaldehyde (5 mM) and sulphite (5 mM) to produce the highly fluorescent 1-sulphonatoisoindole derivative.**

2.3 Materials and Methods

2.2.1 FAAH assay development

There are many individual factors which can cause variation in assays. This chapter identifies a number of such factors allowing optimisation of an assay which can relate measured fluorescence to specific enzyme-substrate activity.

2.2.2 Preliminary optimisation

In preliminary experiments to identify assay parameters, assay volumes of 500 µL or greater were employed with a view to later scaling down the volumes for microtitre plate usage.

Tissue preparation

Fresh rat liver, which expresses high FAAH activity (Giang and Cravatt, 1996), was cut into pieces, hand homogenised in 1:10 weight/volume (w/v) phosphate (PO_4) buffer (0.2M, pH 7.4) on ice and centrifuged for 15 minutes at 1000 g and 4°C. The pellet was discarded and supernatant layer centrifuged for 30 minutes at 30000g and 4°C. The supernatant, cytosolic fraction was discarded and the pellet, membrane fraction was re-suspended 1:1 in PO_4 buffer and stored in 1.5 mL Eppendorf tubes at -80°C until required.

FAAH preliminary assay method

FAAH substrates were prepared as 10 mM stock solutions in 100% dimethyl sulfoxide (DMSO). A reaction mix was made up with 90% 0.2M PO_4 buffer, 10% Magnesium Sulphate ($MgSO_4$) (5 mM), 1% triton X-100 (TX-100) (0.01%), 1%

membrane fraction. 1 mL reaction mix was then incubated with 10 µL inhibitor (URB597, final concentration 5 µM) or DMSO and 10 µL endocannabinoid substrate (100 µM) in 4 mL polystyrene tubes. These components were incubated for 30 minutes at 37°C, before termination of the reaction by the addition of 0.5 mL 5% trichloroacetic acid (TCA), followed by centrifugation for 5 min at 5000 g. A developing buffer was made up using 5 mM o-phthalaldehyde (OPA) dissolved in 0.5 mL ethanol, 5 mM hydrosulphite and 20 mL 0.4 M potassium phosphate buffer, pH 11.4. 80 µL aliquots of the incubation mix were added to 160 µL OPA solution and then incubated for 30 minutes at room temperature, after which the samples were read at wavelengths of exitation (ex.) 360 emission (em.) 490 nm. Enzyme blanks were run alongside the test conditions, as well as standards using 100 µM ammonium sulphate to allow quantification of evolved ammonia.

2.4 Results

2.4.1 Substrate specificity

FAAH is a membrane bound enzyme which hydrolyses a number of primary and secondary fatty acid amides. The structurally related compounds erucamide (docosa-13,14Z-enamide), stearamide (octadecanamide), elaidamide (octadec-9,10E-enamide) and oleamide (octadec-9,10Z-enamide) were employed as substrates over a range of concentrations (**Figure 2.1**).

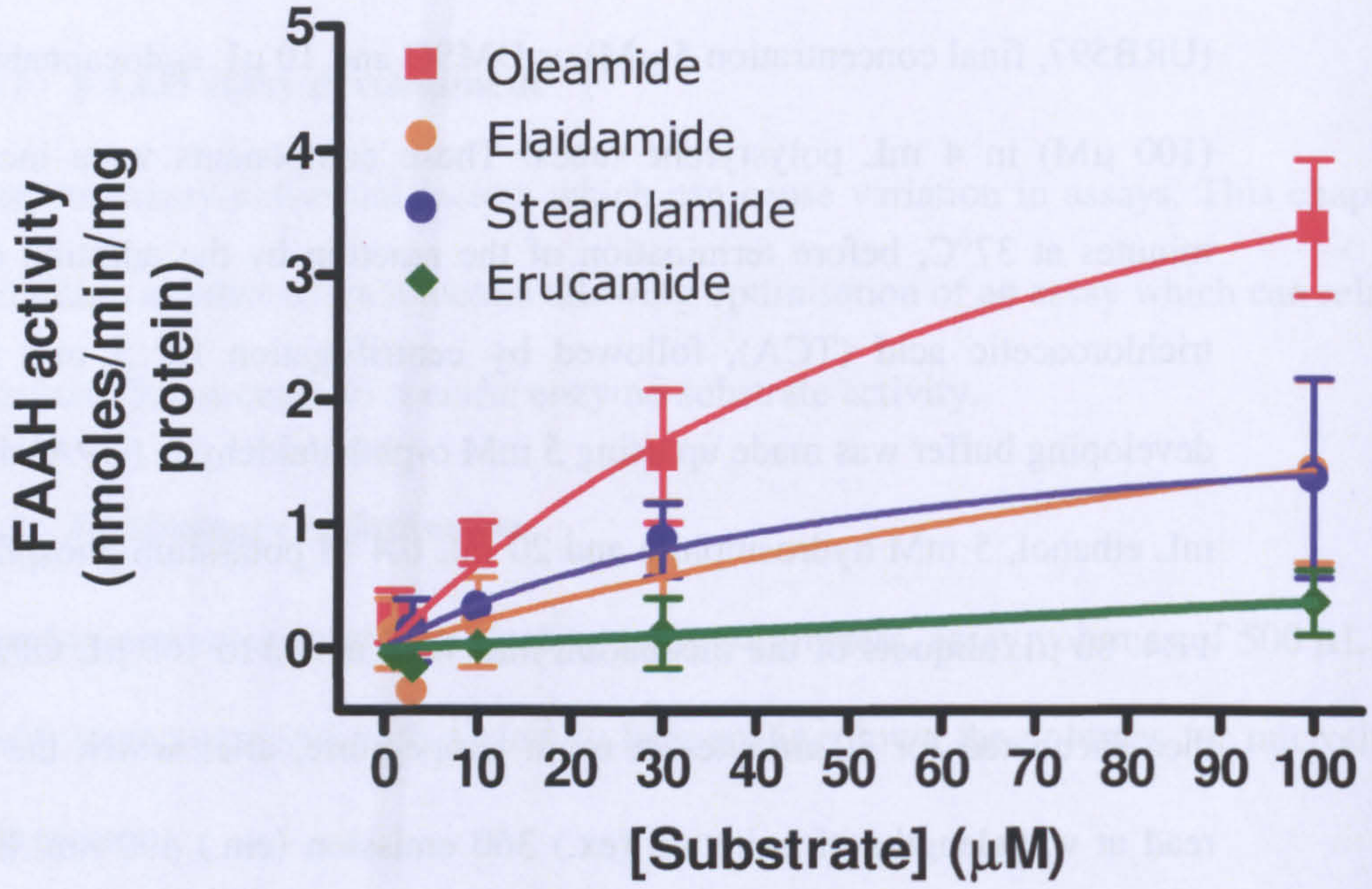

Figure 2.1 FAAH activity using ECL's as substrates

Activity of rat liver preparations against four primary amides in a fluorescence-based FAAH assay. The data are mean ± Standard error of mean (SEM) from six preparations, with four individual replicates; curves were fitted to rectangular hyperbolae using GraphPad Prism.

Of the four substrates investigated, oleamide appeared to be the 'best', with stearamide and elaidamide showing lower activity and erucamide exhibiting almost no hydrolysis (**Figure 2.1**). These results, although limited in nature, highlight the influence of fatty acid chain length and the presence & orientation of the unsaturation on FAAH activity. Although a comparing the activities of oleamide and erucamide indicates that increasing the chain length from 18 carbons to 22 carbons greatly reduces enzymatic hydrolysis. Although kinetic parameters for oleamide as a FAAH substrate were measurable, it was only possible to estimate erucamide hydrolysis at

100 μM (**Table 2.1**). Similarly, changing the orientation of the unsaturation (oleamide vs. elaidamide) reduced enzymatic hydrolysis, as did saturation of the double bond (oleamide vs. stearamide) (Table 2.1).

Substrate	**K_m** (μM)	**V_{max}** (nmoles/min/mg protein)	**Rate of hydrolysis at 100 μM** (nmoles/min/mg protein)
Oleamide	77	5.9	3.37 ± 0.54
Elaidamide	170	3.9	1.42 ± 0.73
Stearamide	48	2.0	1.36 ± 0.79
Erucamide	NC	NC	0.37 ± 0.26

Table 2.1 **V_{max} and K_m values for four FAAH substrates calculated from the FAAH assay (n=6). NC – not calculable**

2.4.2. Incubation Time

The longer an enzyme is incubated with its substrate the greater the amount of product formed, at the same time, however, enzyme denaturation and product inhibition can lead to a loss of catalytic activity. Enzyme activity was, therefore, investigated up to 60 minutes with a range of oleamide concentrations (**Figure 2.2**).

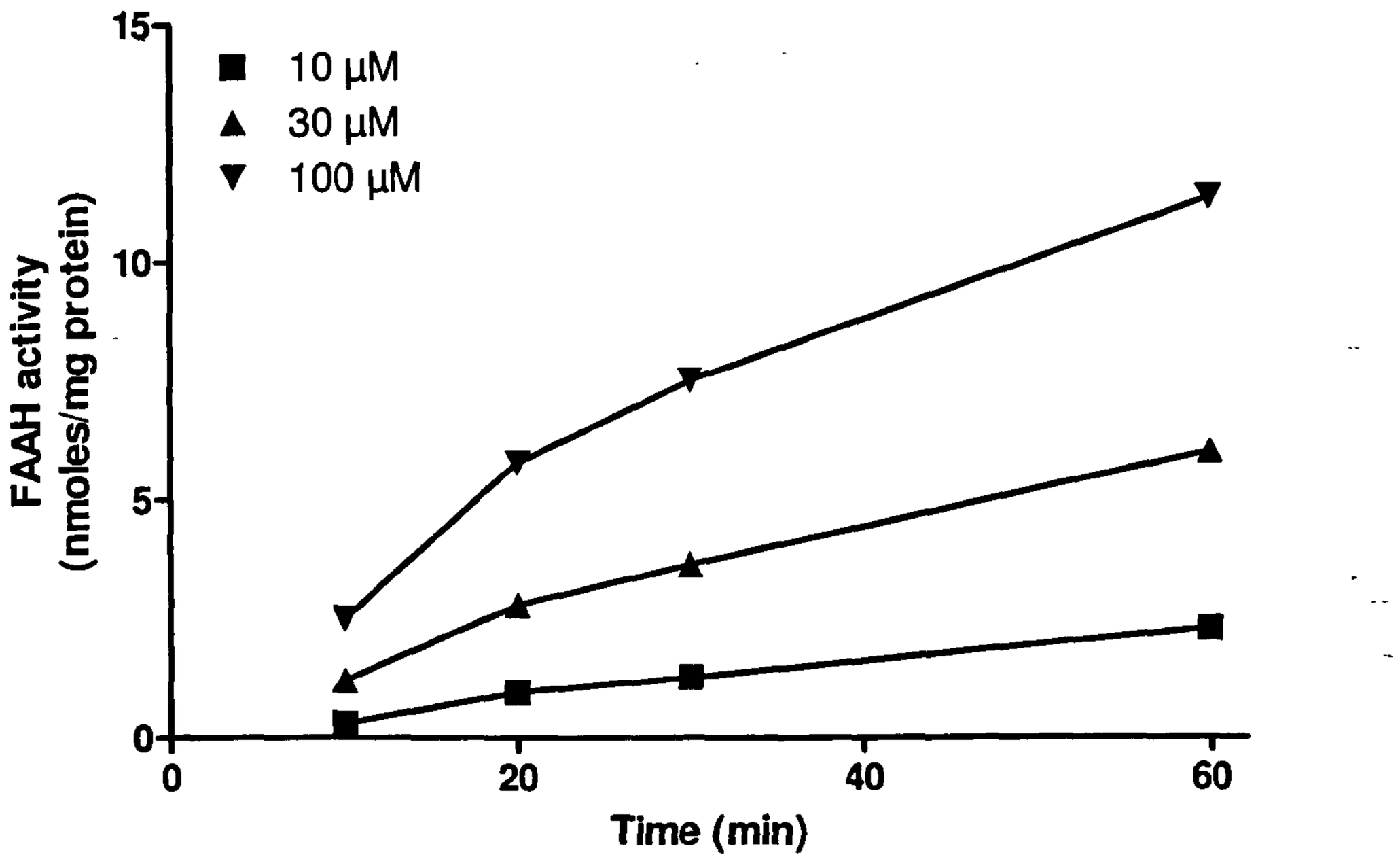

Figure 2.2 **Effect of incubation time on FAAH-oleamide hydrolysis using solubilised rat liver membrane fraction with varied concentrations of oleamide. The data represent mean ± SEM values obtained from four tissue preparation, with four individual replicates.**

Results of varied incubation times on FAAH activity can be seen in **figure 2.2**. Rates of hydrolysis are dependant of time and oleamide concentration. Higher concentrations of oleamide (100 µM) show a more linear response in hydrolysis with

an increase in time.

For later screening of potential inhibitors, a time point of 30 minutes was chosen as a compromise between rapidity of assay and accumulation of product.

2.4.3 The influence of plastics on substrate preparation

Since fatty acids and their derivatives are capable of adhering to plastics, a comparison was made of preparing 10 mM oleamide stocks in DMSO in either Eppendorf (polycarbonate polypropylene) or LP4 (polycarbonate polystyrene) tubes (**Figure 2.3**).

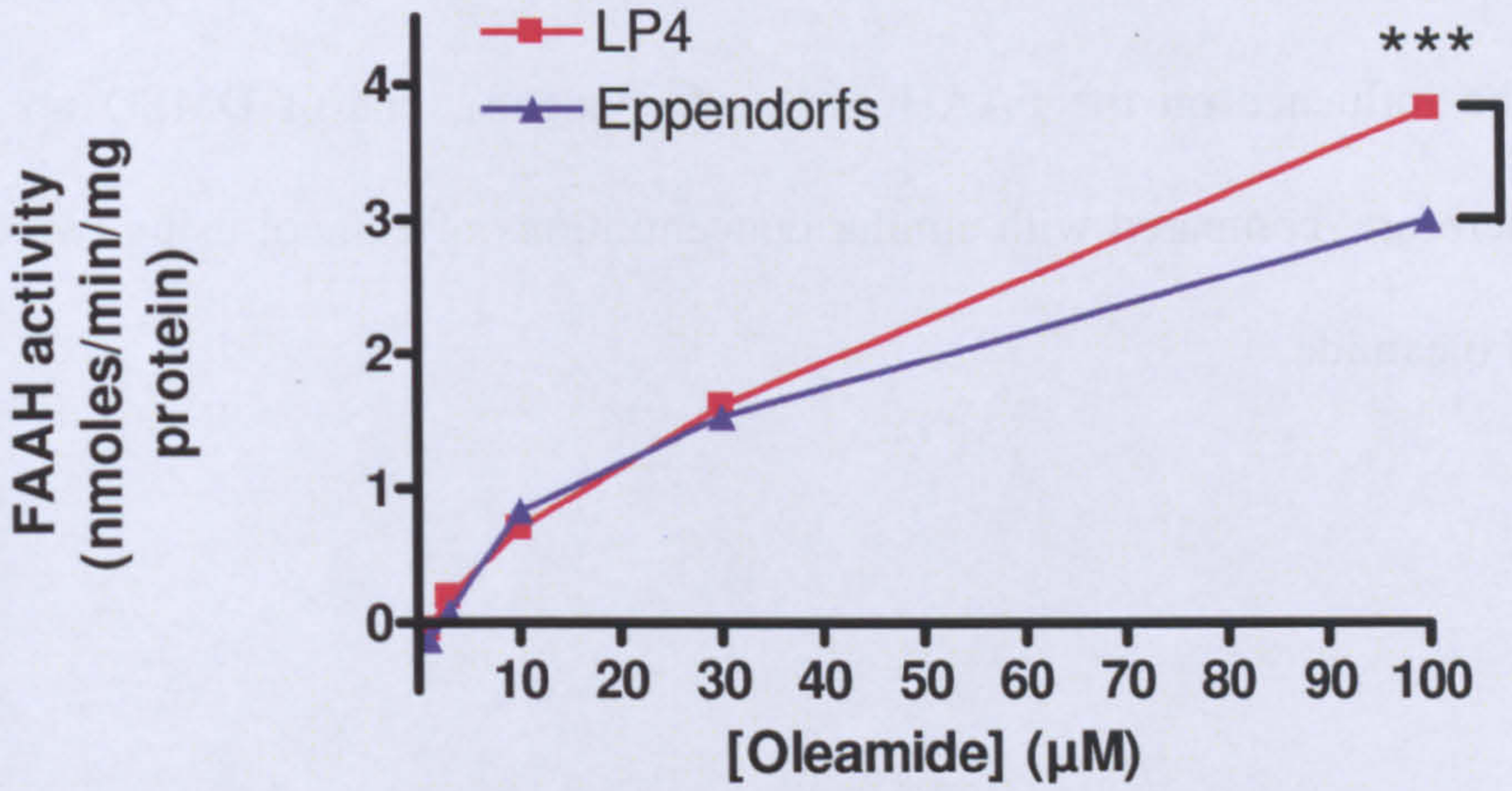

Figure 2.3 Effects of preparation materials on sample preparation in polycarbonate polypropylene Eppendorf or polycarbonate polystyrene LP4 tubes. 10 mM oleamide stocks were diluted in glass vials and assessed for FAAH-catalysed hydrolysis, using solubilised rat liver membrane fractions. Data are expressed as the mean ± SEM of triplicate values obtained from three independent experiments and were analysed by two-way ANOVA with Bonferroni *post-hoc* test (*P<0.001).**

Given the apparently higher level of FAAH activity with substrate prepared in LP4 tubes compared with Eppendorf tubes (at least at the highest concentration), it appears that the polycarbonate polypropylene plastics retain some of the oleamide (**Figure 2.3**) and so these were avoided in future substrate preparation.

2.4.5 The influence of DMSO on the FAAH assay

Dimethylsulfoxide (DMSO) is a widely used solvent able to dissolve both polar and non-polar compounds, with good miscibility in a wide range of aqueous and organic solvents, making it popular for drug dissolution in biochemistry/pharmacology. Preliminary investigations suggested that oleamide was soluble in 1 % DMSO up to 100 μM, while concentrations above 100 μM required higher DMSO concentrations. The influence on the FAAH assay of concentrations of DMSO up to 10% were, therefore, compared with similar concentrations of ethanol using two concentrations of oleamide.

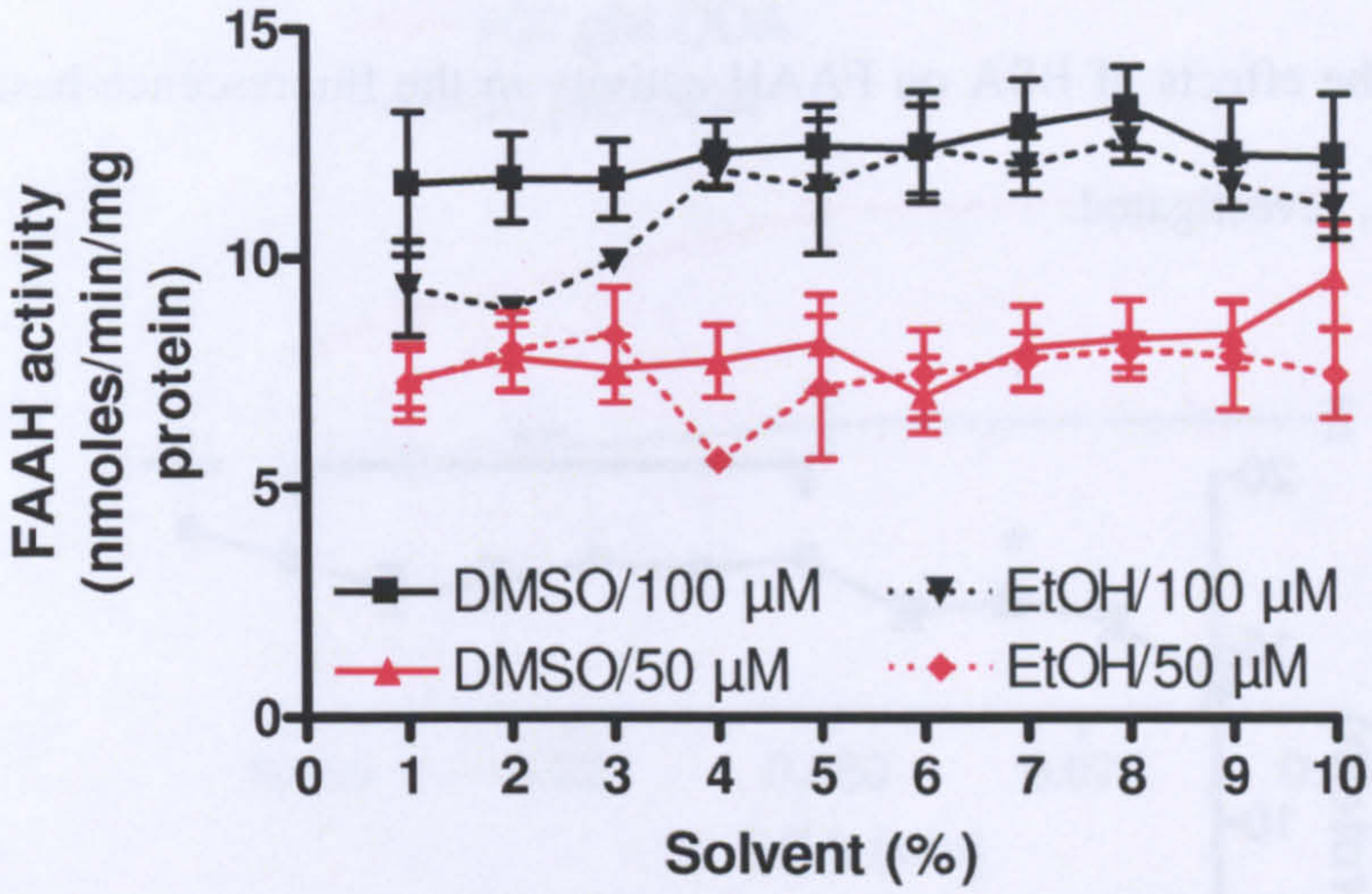

Figure 2.4 **The effect of the presence of increasing solvent concentrations of 0-10% DMSO/EtOH on the FAAH-catalysed hydrolysis of 50 µM and 100 µM oleamide in solubilised rat liver. Data, conducted in triplicates, are expressed as the mean ± SEM from three independent experiments.**

It appeared that the presence of either solvent up to 10 % was well tolerated in the FAAH assay (**Figure 2.4**). However, the increased variability of activity observed with ethanol suggested DMSO was a better solvent for later investigations.

2.4.6 The influence of Bovine serum albumin (BSA) on FAAH activity

Bovine serum albumin appears to stabilise many enzyme activities by acting as a weak anti-oxidant as well as preventing adhesion of enzymes to reaction material surfaces. Additionally, albumin has been found to bind reversibly a wide variety of ligands, and is described as the principle carrier of fatty acids that would otherwise be insoluble in circulating plasma (Spector *et al.,* 1978), including the endocannabinoids

(De Petrocellis *et al.*, 2001; Ross *et al.*, 2001; Parolaro *et al.*, 2002; Hillard *et al.*, 2003). The effects of BSA on FAAH activity in the fluorescence-based assay were, therefore, investigated.

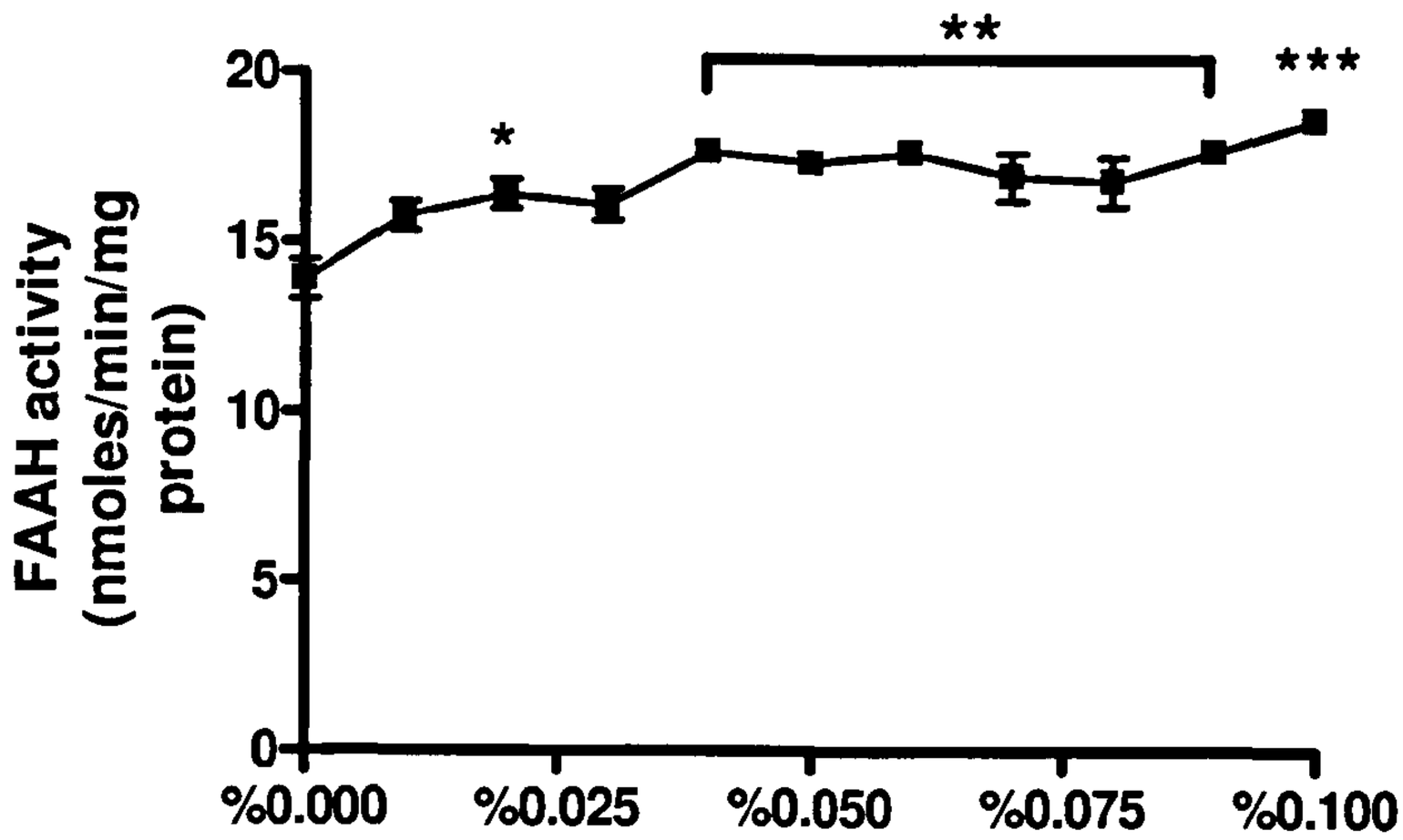

Figure 2.5 **The effects of pre-incubation with varied concentrations of BSA during FAAH-catalysed hydrolysis of 100 μM oleamide using rat liver microsomal preparations. Data, conducted in triplicates, are expressed as the mean ± SEM from four individual experiments analysed using two-way ANOVA with Bonferroni *post-hoc* test, compared with the absence of OEA (*P<0.05,**P<0.01,***P<0.001).**

BSA increased apparent FAAH activity in a concentration-dependent manner (**Figure 2.5**). It is possible that BSA enhances the 'presentation' of oleamide to the enzyme, or alternatively, binds the oleate product reducing the possibility of product inhibition. The BSA concentration-effect curve was, therefore, repeated at two different substrate concentrations (30 and 100 μM).

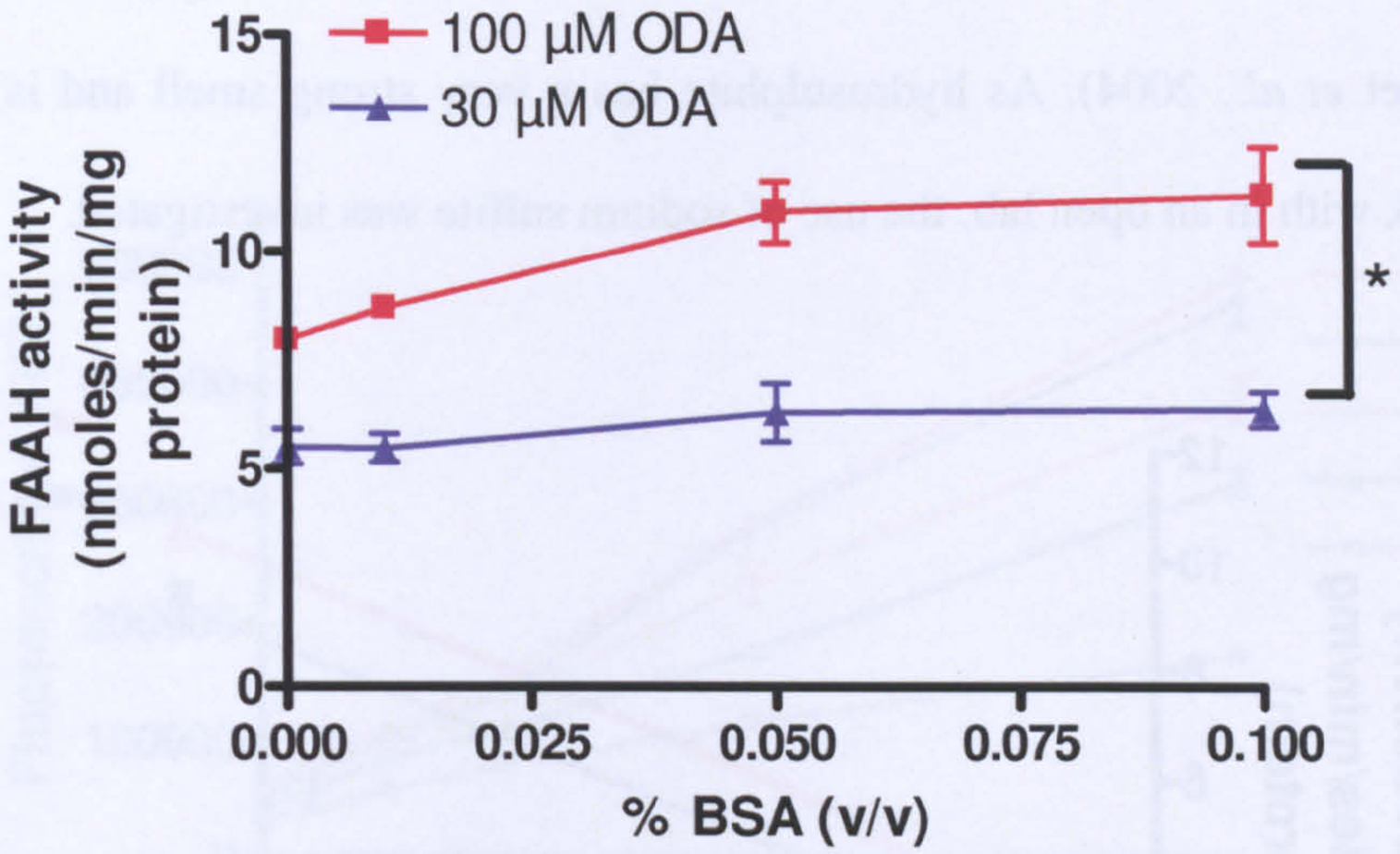

Figure 2.6 **The effects of varied BSA concentrations preincubation on FAAH-catalysed hydrolysis of oleamide at 100 µM and 30 µM using rat liver membrane fractions. Data, conducted in triplicates, are expressed as the mean ± SEM from four rat tissues analysed using one way ANOVA (*P<0.05).**

Although a complete range of substrate concentrations was not investigated, it appears that BSA had more of an effect on the oleamide concentration above the K_m (100 µM), than the concentration below the K_m (30 µM, **Figure 2.6**), implying that BSA might have increased the V_{max} without altering the K_m. This could be taken to imply that BSA doesn't alter substrate presentation, but increases enzymatic conversion, possibly by removing product inhibition.

2.4.7 Effect of developing reagents in fluorescence generation

As illustrated in **Scheme 2.1,** (hydro) sulphite ion reacts with o-phthalaldehyde in the presence of ammonia to generate the stable fluorescent isoindole derivative (Rowley

et al., 1995; Groves *et al.,* 2005; Kerouel *et al.,* 1997; Westra *et al.,* 2002; Meseguer Lloret *et al.,* 2004). As hydrosulphite has a very strong smell and is unpleasant to work with in an open lab, the use of sodium sulfite was investigated.

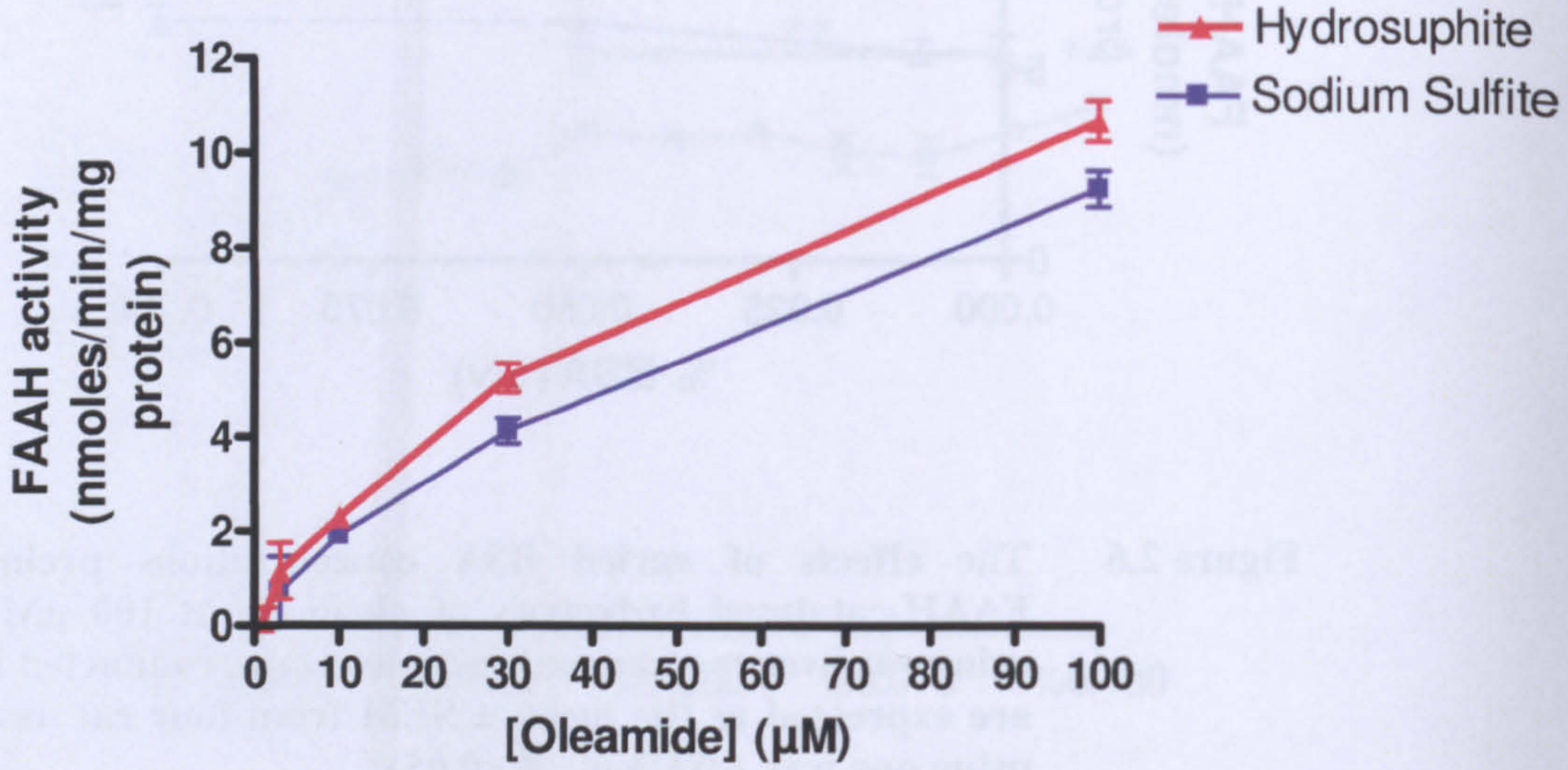

Figure 2.7 **The effects of fluorescence generation using OPA solutions with either hydrosulphite or sodium sulfite reacting with ammonia. Data, conducted in triplicates, are expressed as the mean ± SEM of three individual experiments. Analysis of data using one way ANOVA showed no significant difference between sulfite sources on fluorescence development.**

There were no obvious differences in the observed fluorescent Bovine serum albumin (**figure 2.7**) product using sodium hydrosulphite or sodium sulfite, and so subsequent investigations employed sodium sulfite in the fluorescence development solution with OPA.

The potential influence of an excess of sulfite on fluorescent product generation was

also investigated.

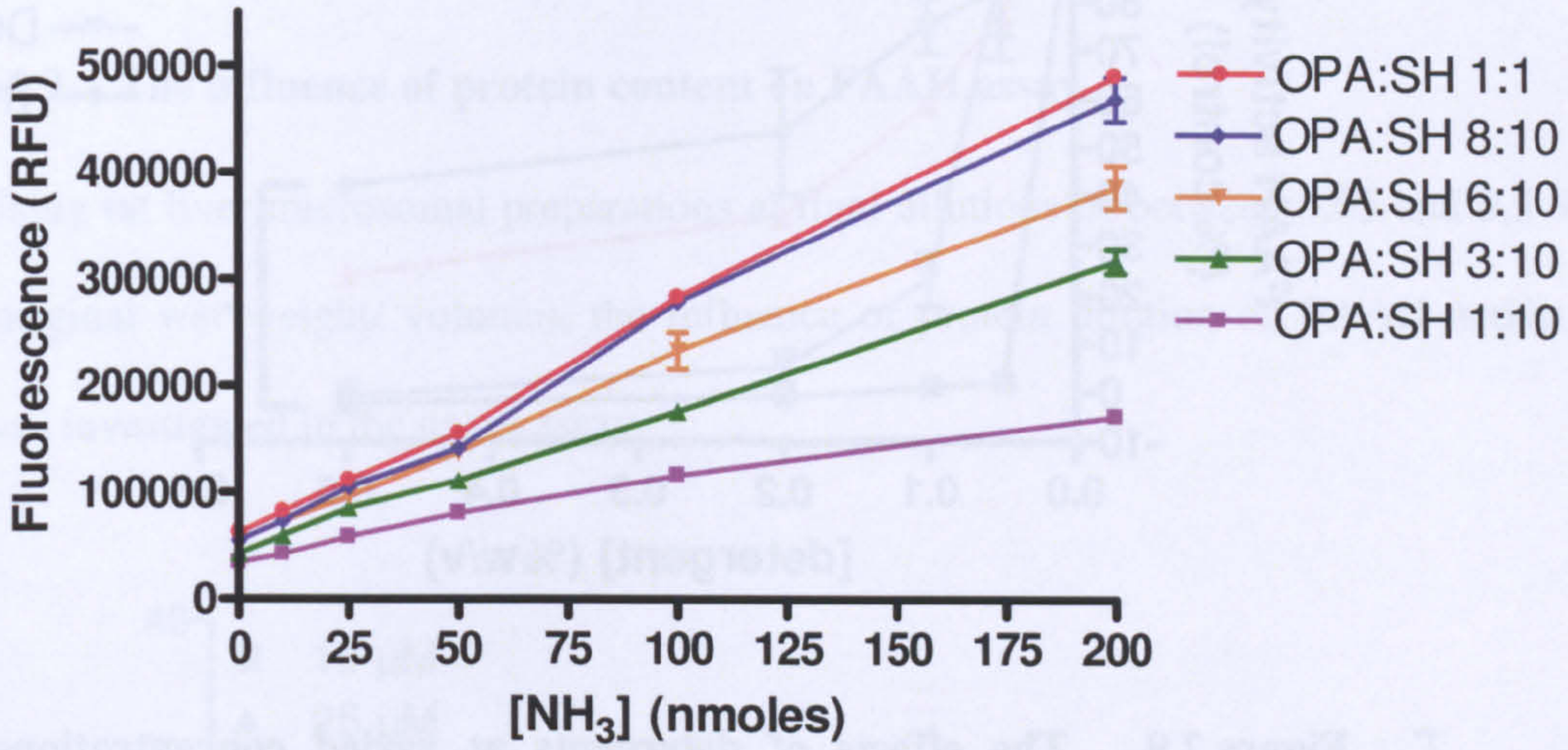

Figure 2.8 The effect of differing OPA:SO_3 ratios on fluorescence generation from an ammonia standard curve (0-200 nmoles), with fluorescence read at 60 min post-addition of OPA/sulfite mix. Data, conducted in triplicates, are expressed as mean ± SEM of three individual experiments.

Equimolar ratios of OPA and sulphite in the development buffer showed highest levels of detectable fluorescence (**Figure 2.8**) and longest fluorescent compound stability, with little variation in levels of fluorescence between 30, 60 and 90 minute measurements (data not shown).

2.4.8 The influence of detergents on FAAH activity

As FAAH is a membrane-bound enzyme, the effect of detergents, which should increase substrate availability, was investigated, investigating different classes of detergent.

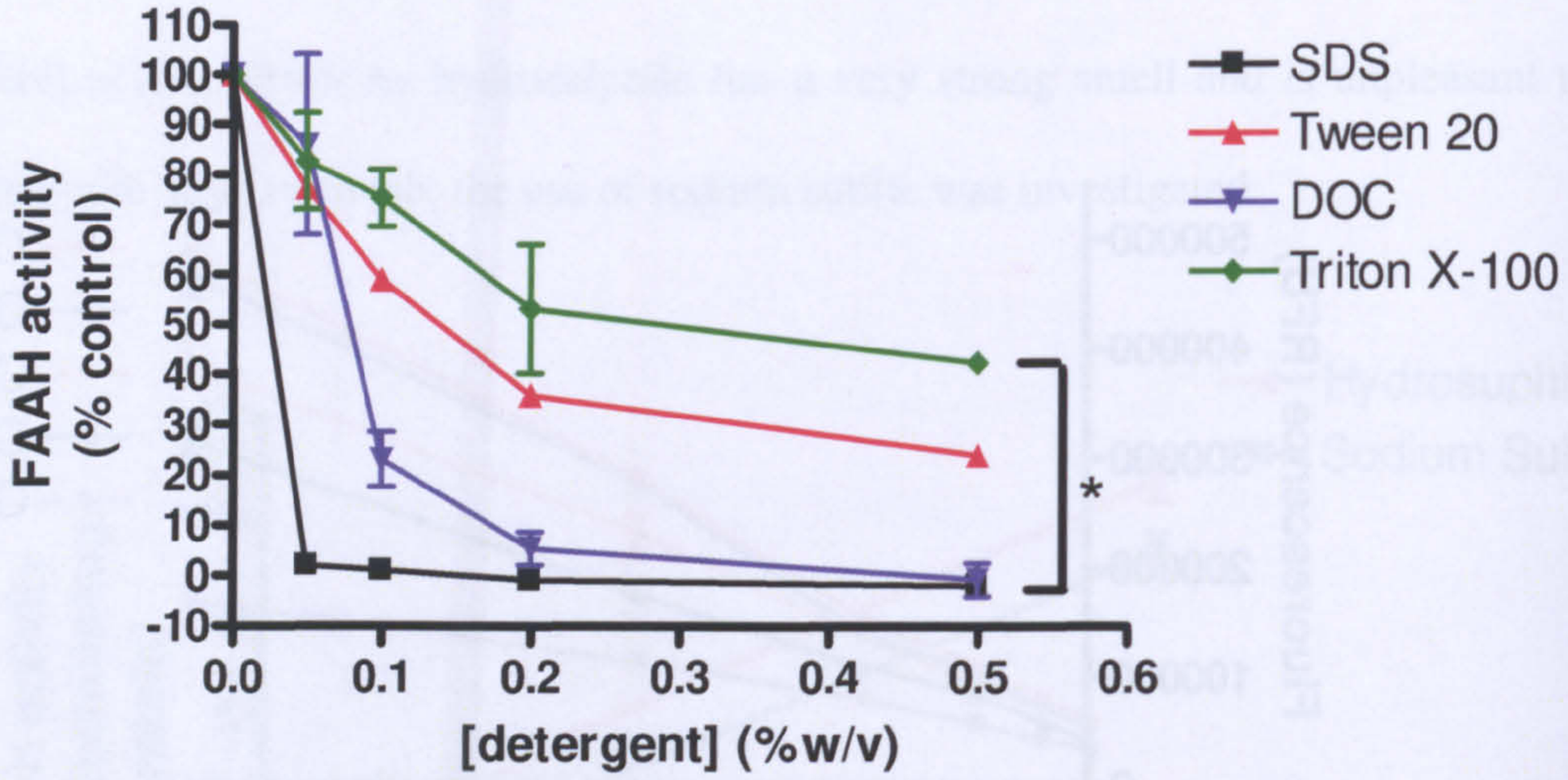

Figure 2.9 **The effects of detergents at varied concentrations on FAAH-catalysed oleamide hydrolysis at 100 μM, using solubilised rat liver membrane fractions. Data, conducted in triplicates, are expressed as mean ± SEM from five liver microsome preparations, conducted in duplicate. Data analysed using one way ANOVA (*P<0.05).**

The presence of all four detergents resulted in a concentration-dependent inhibition of enzyme activity (**Figure 2.9**). However, enzyme activity appeared most sensitive to the anionic detergent sodium dodecyl sulphate (SDS), with concentrations as low as 0.05 % (~ 2 mM) completely inhibiting FAAH activity. Sodium deoxycholate (DOC), another anionic detergent, albeit structurally distinct from SDS, was also deleterious to FAAH activity, while the non-ionic detergents Tween 20 and Triton X-100 were reasonably well tolerated. Concentrations of Triton X-100 less than 0.1 % appeared to allow retention of >75 % of enzyme activity, indicating that this

combination would be usable in FAAH assays.

2.4.9 The influence of protein content on FAAH assay

Using rat liver microsomal preparations at final dilutions of between 0.05 and 0.5 % (original wet weight/ volume), the influence of protein dilution on FAAH activity was investigated in the novel assay.

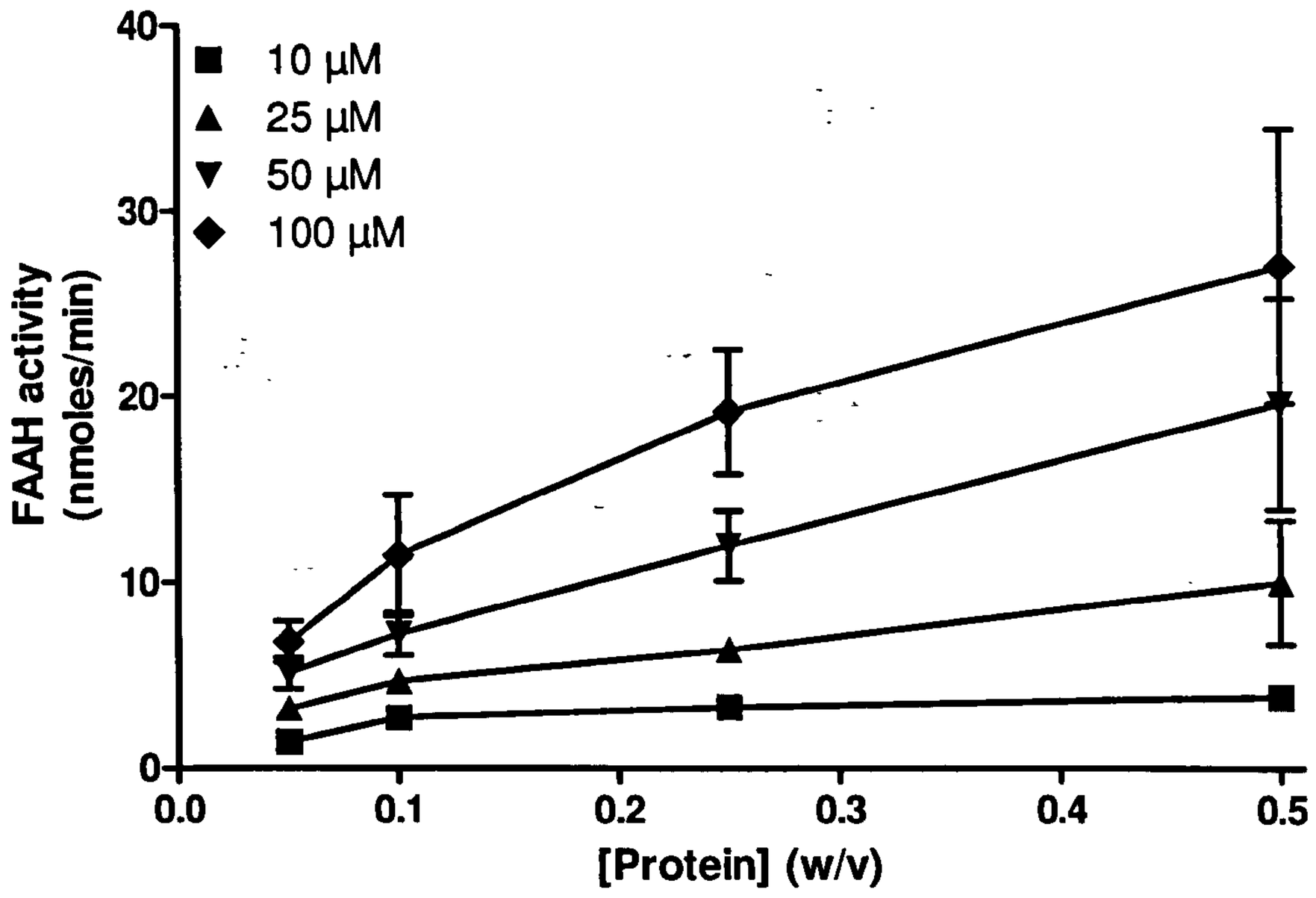

Figure 2.10 **The effects of increased protein concentration of rates of FAAH-catalysed oleamide hydrolysis at concentrations of 10 – 100 µM using rat liver membrane fractions. Data, conducted in duplicates, are expressed as the mean ± SEM of experiments using four different liver preparations. Data were analysed using two-way ANOVA with Dunnett's post-hoc test (Protein 0.05% compared with 0.25% at 100 µM $P<0.05$; protein 0.05% compared with 0.5% at 50 µM $P<0.01$, at 100 µM $P<0.001$; protein o.1% compared with 0.5% at 50 µM $P<0.05$, at 100 µM $P<0.01$).**

Increasing protein content evoked a concentration-dependent increase in enzyme activity (**Figure 2.10)** yet there was no significant interaction between protein and oleamide concentrations. Results suggest mid to high concentrations of OEA (50 μM +) are required to distinguish levels FAAH activity at differing protein concentrations, helping to determine an adequate protein concentration for use in the assay. The highest concentration of oleamide showed the most linear rates of FAAH activity, with increasing concentrations of protein, yet there was no significant increase observed in the assay enzyme blanks, showing that increased protein concentration in the assay did not cause a significant increase in the background noise.

This method used a test tube-based assay, with transfer of product, to 96-well plates to provide a fluorescence assay reading to determine levels of FAAH activity. Assay development allowed identification of a useful substrate for use in this assay, allowing determination of a measurable level of FAAH activity. Investigation identified a range of incubation times that provide high levels of FAAH activity, which will lead to further flexibility towards development of a HTS assay methodology. Other conditions including substrate preparation materials, assay solvent tolerance, sulfite source for fluorescence development buffers and effects of detergents and BSA on FAAH activity levels were established, allowing direct development of a HTS assay.

2.4.10 FAAH HTS assay development

Inhibition of FAAH leads to an increase in the endogenous tone of endocannabinoids (Jhaveri et al., 2008) and, therefore, it is a potential target for various therapeutic areas which exploit cannabinoid receptor agonism. However, screening large libraries of compounds as potential inhibitors using existing FAAH activity assays would be impractical, laborious and expensive. As previously mentioned, the FAAH assay development was a precursor to scaling down the assay volumes used, allowing inexpensive, facile and rapid HTS of compound libraries for their effects on inhibiting FAAH activity, using a 96, 384 or 1536-well microtitre plates.

2.4.11 Preliminary optimisation – measurement of FAAH activity using a microtiter plate assay

Tissue preparation

Membrane fragments were prepared from livers of male Wistar rats (150g – 250g) as described previously in section 2.2.1. and stored as 1:10 original wet weight aliquots at -80 °C.

FAAH HTS assay method

FAAH substrates were prepared as 10 mM stock solutions in 100% DMSO. Tissue was thawed from -80 °C and diluted further to 0.01g/g wet weight liver (1:100) using 0.2M PO_4 buffer, pH 7.4. 25 µL of URB597 (final concentration 5 µM, in 10% DMSO) (where 25 µL of 10% DMSO was used in the absence of an inhibitor) or other inhibitor screening compounds (final concentration 100 µM) were pre-incubated with 25 µL tissue at 37 °C for 15 minutes in a 96-well plate on a plate

warmer. 50 µL of ODA (final concentration 100 µM) was added to each well and incubated at 37 ºC for 30 minutes. The developing buffer (OPA solution) as described in *FAAH preliminary assay method* (section 2.2.1) was prepared and 100 µL was added to each well to terminate FAAH activity. The 96-well plate was then incubated at room temperature for 30 minutes, after which the samples were read at wavelengths of ex. 360 em. 490 nm. Enzyme blanks were run alongside the test conditions as well as standards using 100 µM ammonium sulphate to allow quantification of evolved ammonia.

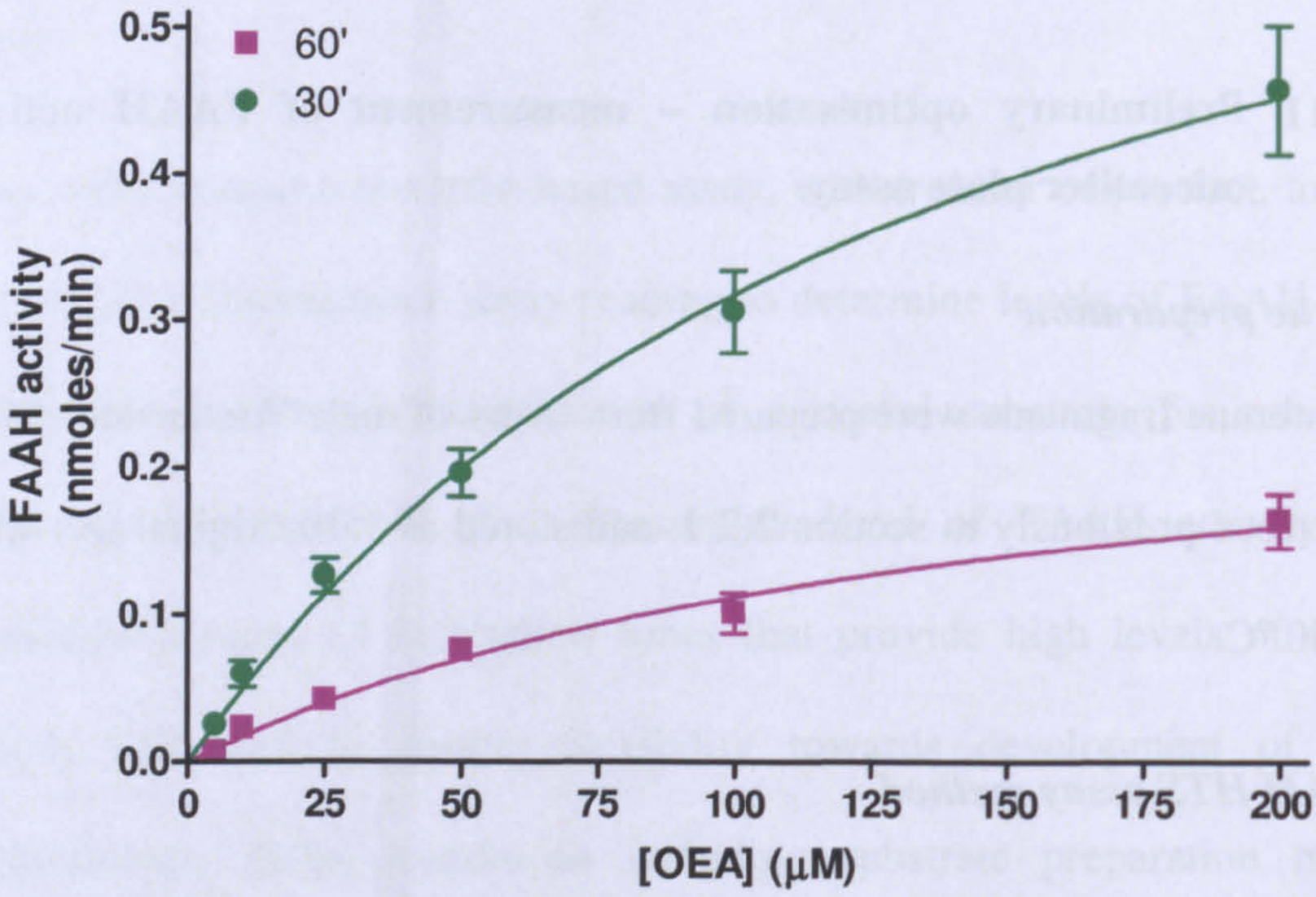

Figure 2.11 Oleamide hydrolysis by FAAH from rat liver preparations (n=4), measured following 30 minute and 60 minute incubations at 37°C. Data, conducted in triplicates, are expressed as the mean **± SEM and analysed using two-way ANOVA.**

As seen in **figure 2.11** oleamide hydrolysis measured following 30 minute incubation is similar to levels of oleamide hydrolysis seen in the previous assay. There is a loss of linearity over the time course and FAAH activity levels seem much lower, albeit

non-significant, following a 60 minute incubation, suggesting an optimum time point for measurement of maximum oleamide hydrolysis by FAAH in this assay.

2.4.12 Investigation of the effect of URB597 on FAAH activity using a HTS FAAH assay

To determine the viability of this assay for HTS of FAAH activity, the effect of varying concentrations of URB597 on the rate of FAAH hydrolysis of 100 μM oleamide was assessed.

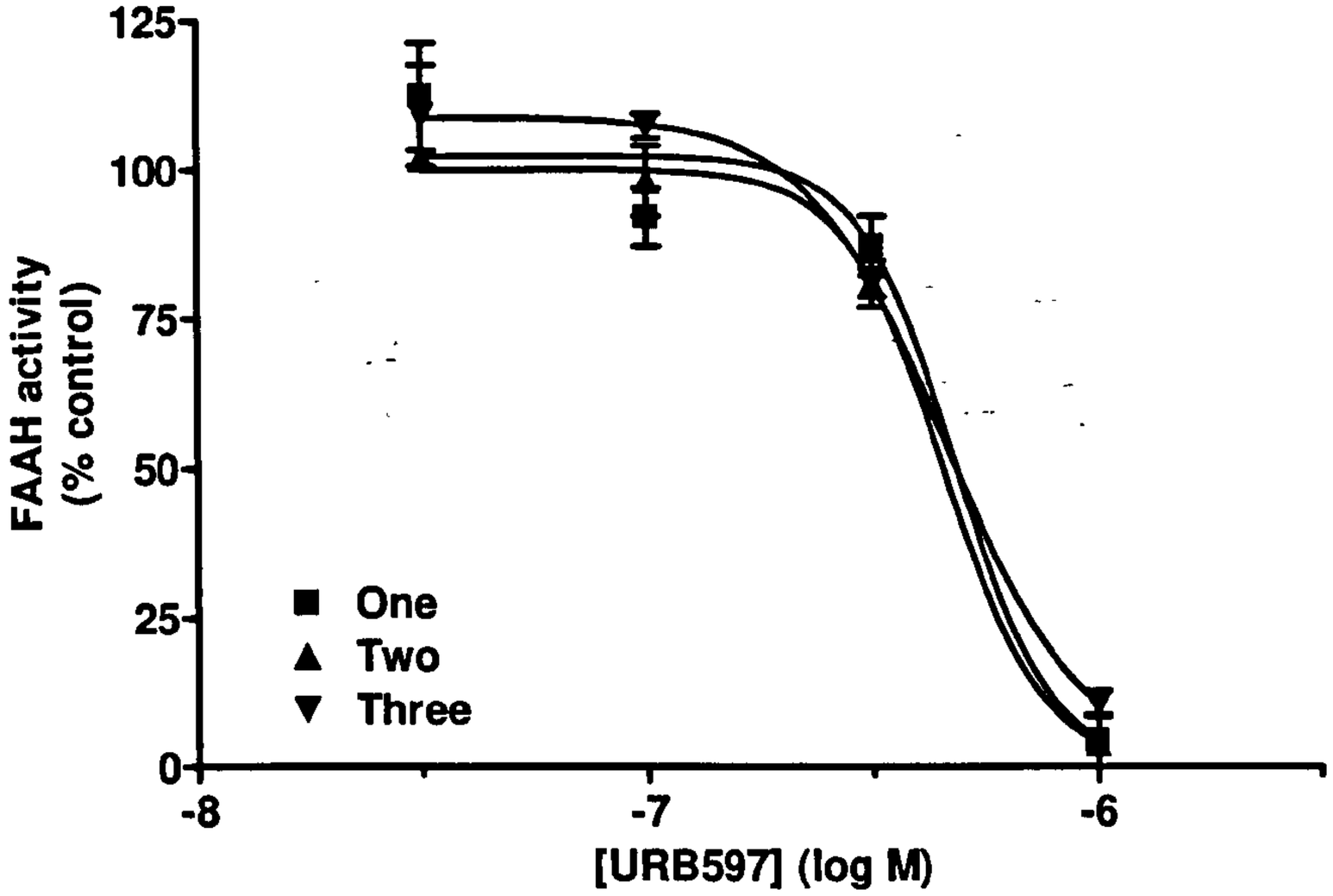

	One	Two	Three
Best-fit values			
BOTTOM	0.0	0.0	0.0
TOP	102.3	100.1	109.0
LOGEC50	-6.318	-6.343	-6.339
HILLSLOPE	-4.128	-3.994	-2.851
EC50	4.812e-007	4.543e-007	4.579e-007
Goodness of Fit			
Degrees of Freedom	9	9	8
R^2	0.9292	0.9854	0.9624

Figure 2.12 **Effects of URB597 on FAAH mediated ODA hydrolysis following 30 minutes of incubation at 37°C shown as % of control activity (n=3). Data were collected in triplicate values. The table below the graph shows quantitative parameters as determined by Prism.**

	One	Two	Three
Best-fit values			
BOTTOM	0.0	0.0	0.0
TOP	97.96	103.9	110.3
LOGEC50	-6.315	-6.416	-6.432
HILLSLOPE	-4.505	-8.589	-8.948
EC50	4.845e-007	3.841e-007	3.699e-007
Goodness of Fit			
Degrees of Freedom	9	9	9
R^2	0.9497	0.9689	0.9775

Figure 2.13 Effects of URB597 on FAAH mediated ODA hydrolysis following 60 minutes of incubation at 37°C shown as % of control activity. The table below the graph shows LogEC50 values for each independent tissue tested (n=3).

The effects of URB597 (**figure 2.12** and **figure 2.13**) indicate that ODA hydrolysis was fully inhibited at both 30 and 60 minute time points with 1 x 10^{-6} M URB597. This compares well with our previously described method which showed URB597 to

fully inhibit 100 μM ODA hydrolysis in a larger format assay. LogEC_{50} values were -6.35 for both time points, which compares well to the previously described method.

2.4.13 The effects of TX-100 on FAAH activity

The use of detergents in biochemical assays is useful to ensure cell lysis and facilitate substrate access to membrane-associated enzymes (Qui *et al.*, 2008). The effect of TX-100 in solubilisation of the enzyme was investigated to assess it's influence on FAAH activity in the assay.

We compared the effects of Triton X-100 using unsolubilised membranes, membranes exposed to detergents (using 0.01% TX-100 (v/v)) on ice for 30 minutes and *post-hoc* tissue exposure, where 0.01% TX-100 (v/v) was added with the development buffer (OPA solution).

TX-100 enzyme solubilisation method

An aliquot of membrane fraction was thawed and solubilised with 0.01% TX-100 on ice for 30 min. Following centrifugation at 20 000 g for 15 minutes, the supernatant layer was decanted and diluted a further 1:10 in 0.2 M phosphate buffer, pH 7.4, containing 1 mM ethylenediaminetetraacetic acid (EDTA).

TX-100 post-hoc enzyme solubilisation method

Development buffer (5 mM OPA, 5 mM sodium sulfite, 0.4 M potassium phosphate buffer, pH 11.4) was made up including 0.01% TX-100 (v/v), and then used to halt the enzyme substrate incubation.

FAAH HTS assay method

Assay volumes previously described were changed to 5 µL inhibitor (URB597, final concentration 5 µM), 20 µL ODA (final concentration 100 µM) and 75 µL tissue. 100 µL OPA solution was used post-incubation.

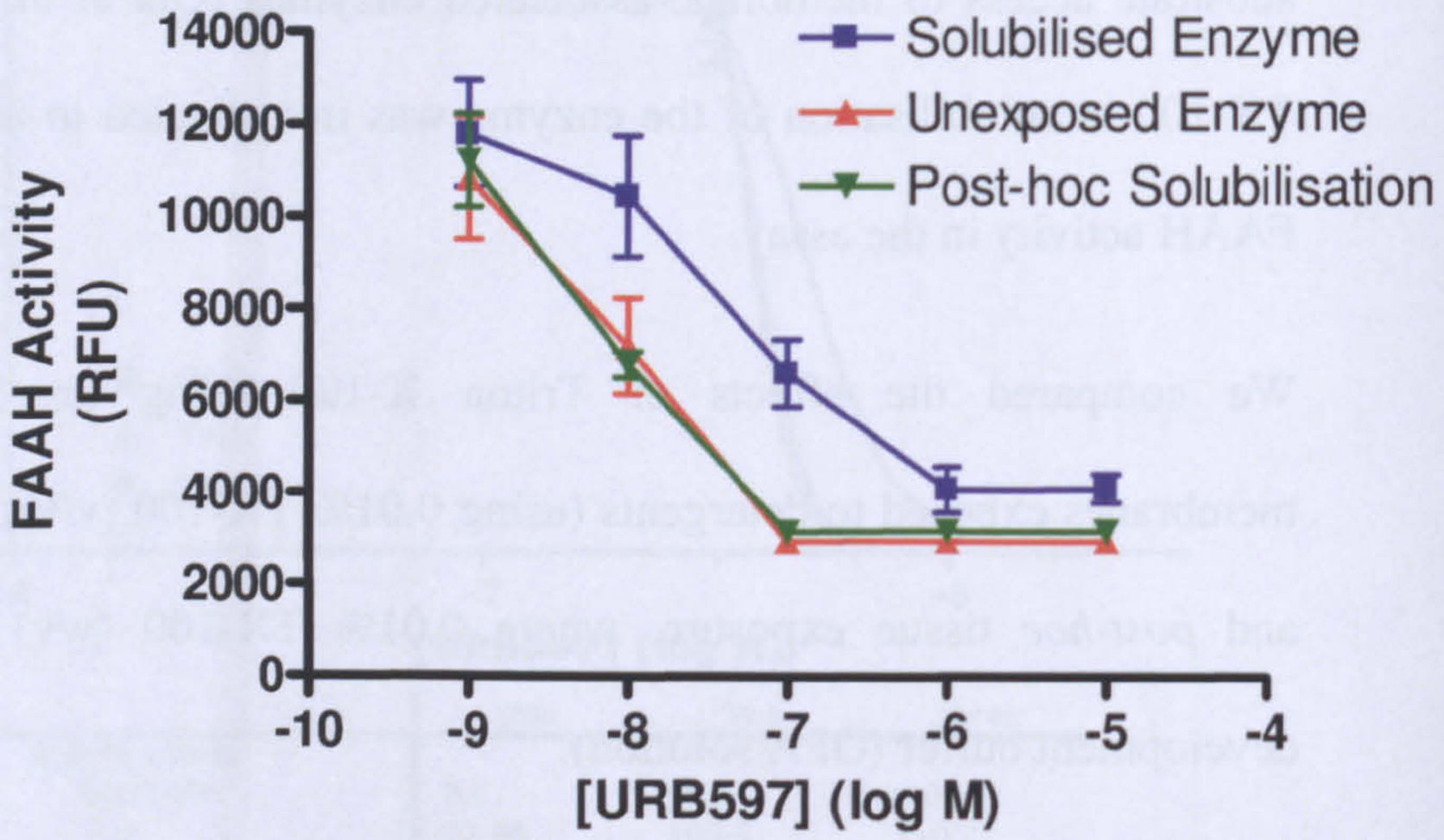

Figure 2.14 **Effects of TX-100 detergent based enzyme solubilisation on levels of FAAH activity. Comparing levels of inhibitable FAAH by URB597 in pre solubilised enzyme, post-hoc solubilised enzyme and neat enzyme preparations prepared from rat liver tissue. Data are means ± SEM for three independent preparations assessed in triplicate (n=4). LogEC_{50} values were -7.3, -7.9 and -8.0 for the solubilised, unexposed and post-hoc solubilised enzymes respectively.**

Figure 2.14 indicates that prior solubilisation of liver membranes with 0.001% TX-100 leads to recovery of similar levels of FAAH activity as using membranes without solubilisation. However, solubilisation resulted in a decrease in potency of URB597

and there was no difference in fluorescence readings between unexposed enzyme and post-hoc solubilised enzyme.

2.4.14 The influence of DMSO on the FAAH assay

Our previous studies indicated ODA to be soluble in 1% DMSO up to 100 μM, while concentrations above this required higher DMSO concentrations. Since other compounds used to test FAAH inhibition using this HTS method may also require higher solvent concentrations, we investigated the influence of DMSO (0-30%) on FAAH activity.

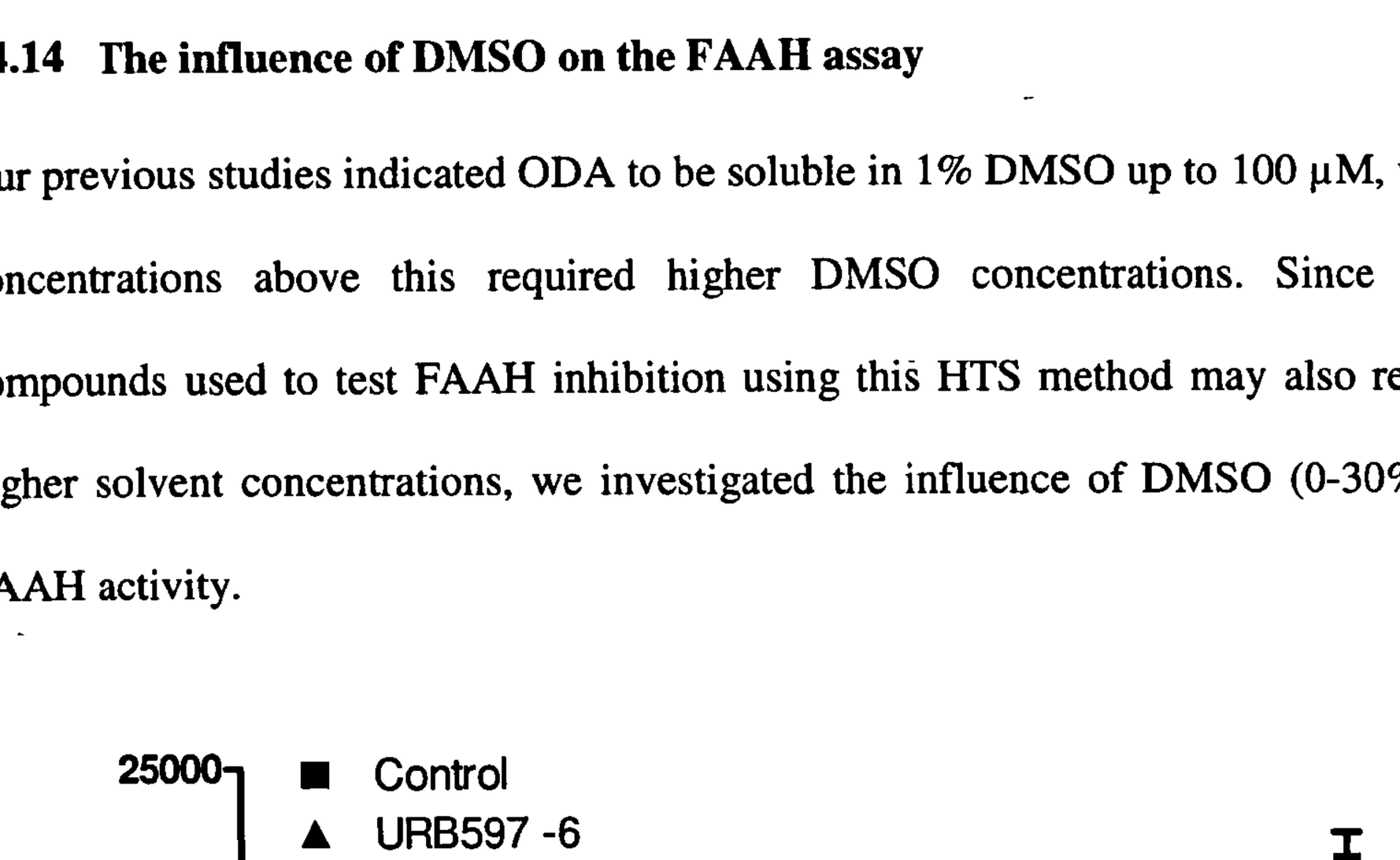

Figure 2.15 **Effects of varying concentrations of DMSO on FAAH activity (using 100 μM ODA, in the absence and prescence of two**

concentrations of FAAH inhibitor URB597. Data are expressed as means ± SEM of 3 individual experiments, conducted in triplicate (n=3).

As shown in **figure 2.15** concentrations of DMSO up to 30% were well tolerated in this HTS FAAH assay, allowing us the use of large libraries of compounds to be screened as inhibitors of FAAH, not limited by their level of solubility.

This method used a 96-well plate-based method to allow high throughput screening of FAAH activity. Results indicated high rates of FAAH mediated oleamide hydrolysis following 30 minutes of incubation which were similar to levels measured in previous assays. At 60 minutes FAAH mediated oleamide hydrolysis was still detectable but rates were much lower compared to 30 minute incubations for reasons which remain unclear. A 30 minute incubation period is more favourable in allowing greater throughput in screening. This method displayed more sensitivity to URB597, with $logEC_{50}$ values of -7.9 in untreated enzyme sources compared to previous assay experiments, using the same enzyme preparation methods, where $logEC_{50}$ values of URB597 were -6.3. Results indicate that solubilisation of enzyme sources provide no further benefit toward FAAH hyrolysis in this method, therefore unexposed (neat) enzyme shall be used in future. The assay also showed excellent tolerance of the common solvent DMSO (used widely for screening compound solubilisation). DMSO tolerance of up to 20% allows for a much bigger range of compound use.

These data clearly show that this assay can successfully be used for the HTS of compound libraries as potential FAAH activity inhibitors.

2.4.15 Application of HTS FAAH assay: Compound screening to investigate potential inhibitors of FAAH activity

The effects of groups of known compounds on the hydrolysis of 100 μM oleamide by rat liver FAAH were examined using the HTS FAAH assay methodology. On each 96-well plate, test compounds were arranged in columns of 8, assessing FAAH activity in four different liver preparations. For each preparation, one well was a test which contained compound, enzyme and substrate. In the other well of the pair, compound and enzyme were mixed but substrate was only added after OPA development solution, to provide a test compound blank. Thus, the two wells contained identical mixtures and differed only in the 30 minute incubation period allowing enzymatic hydrolysis of the ODA. The screening method assessed FAAH hydrolysis of ODA at a final concentration of 100 μM, with final solvent concentration (DMSO) at 10%. Each test compounds blank value was subtracted from its test value, the percentage inhibition of oleamide hydrolysis by each compound was calculated as a percentage of the control level of FAAH activity on each individual plate. The mean ± range percentage inhibition was then calculated. The results from this screen are shown in **figure 2.16.**

2.4.16 FAAH activity HTS assay method

Tissue preparation

Membrane fragments were prepared from livers of male Wistar rats (150g – 250g) as described previously in **chapter 2.2.1**, and stored as 1:10 original wet weight aliquots at -80 ℃.

FAAH HTS assay method

Fresh oleamide was prepared as 10 mM stock solutions in 100% DMSO. Four sets of rat liver tissue sources for FAAH activity were thawed from -80 °C and diluted further to 0.01g/g wet weight liver (1:100) using 0.2M PO_4-EDTA 5mM buffer pH 7.4. 25 µL of URB597 (final concentration 5 µM, in 5% DMSO) or 25 µL of inhibitor (final concentration of 100 µM in 5% DMSO) were pre-incubated with 25 µL of each tissue at 37 °C for 15 minutes in a 96-well plate on a plate warmer. Corresponding blanks (n=4) were set-up for each inhibitor compound, without ODA, where 50 µL of ODA (100 µM) was added to each well post-incubation. To all wells with test inhibitors, ODA was added and incubated at 37 °C for 30 minutes. The developing buffer (OPA solution as described in *FAAH preliminary assay method* chapter 2.2.1) was prepared and 100 µL was added to each well to terminate FAAH activity. The 96-well plate was then incubated at room temperature for 30 minutes, after which the samples were read at wavelengths of ex. 360 em. 490 nm. Enzyme blanks were run alongside the test conditions as well as standards using 100 µM ammonium sulphate to allow quantification of evolved ammonia.

2.4.17 Application of FAAH HTS assay: HTS of compounds as potential FAAH inhibitors

The following graphs show results of a high throughput screening of a large group of compounds. FAAH activity is indicated as % of control oleamide hydrolysis. For those samples exposed to URB597, FAAH activity was not different from tissues blanks.

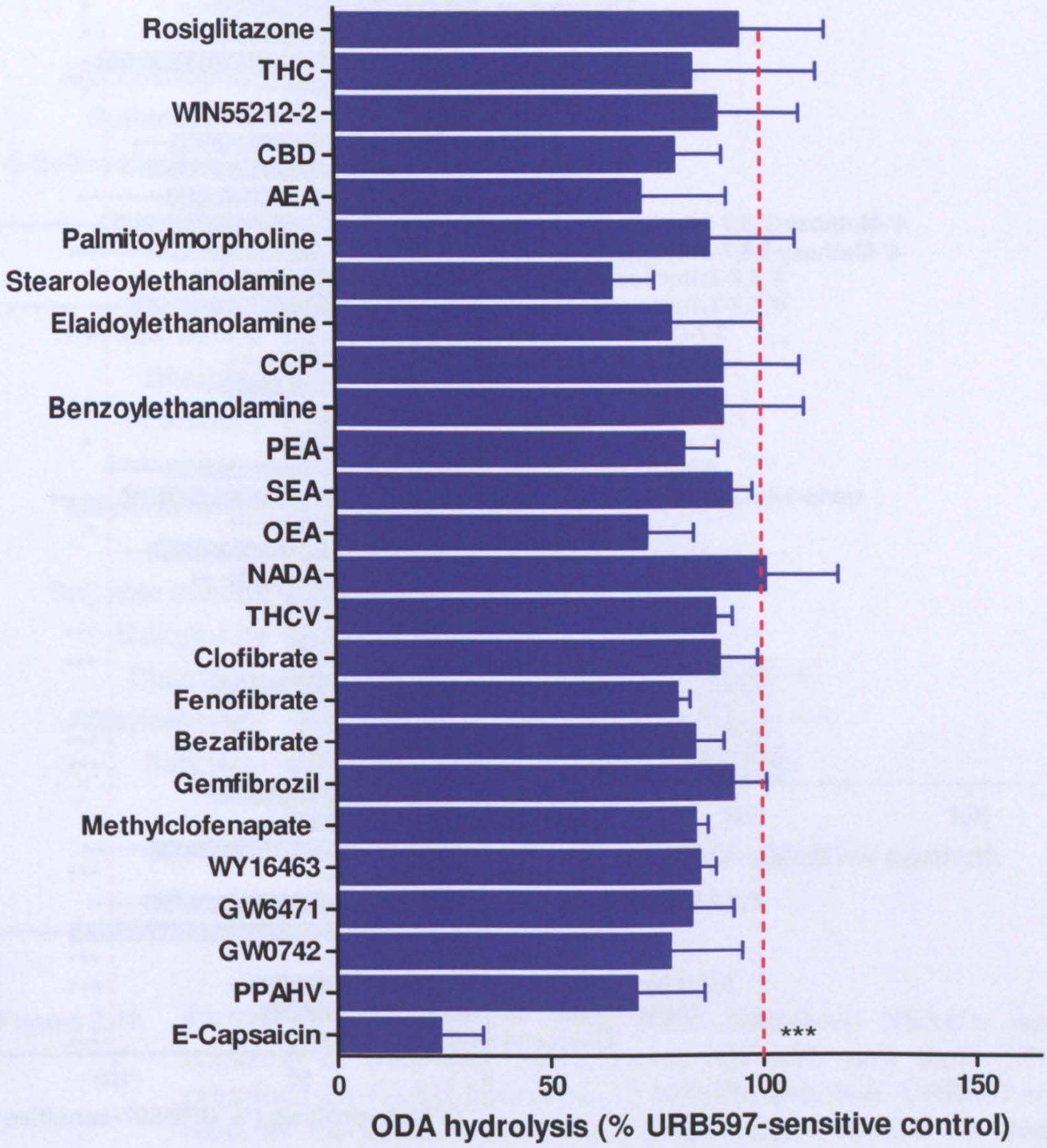

Figure 2.16 **FAAH HTS of cannabinoid ligands as potential inhibitors. Cannabinoid ligands were screened as potential inhibitors at 100 µM, and their effect examined on FAAH hydrolysis of 100 µM oleamide. URB597 was used as an inhibitor standard. Data were collected in single replicates (n=4). Data were analysed using one-way AVOVA (***P<0.001).**

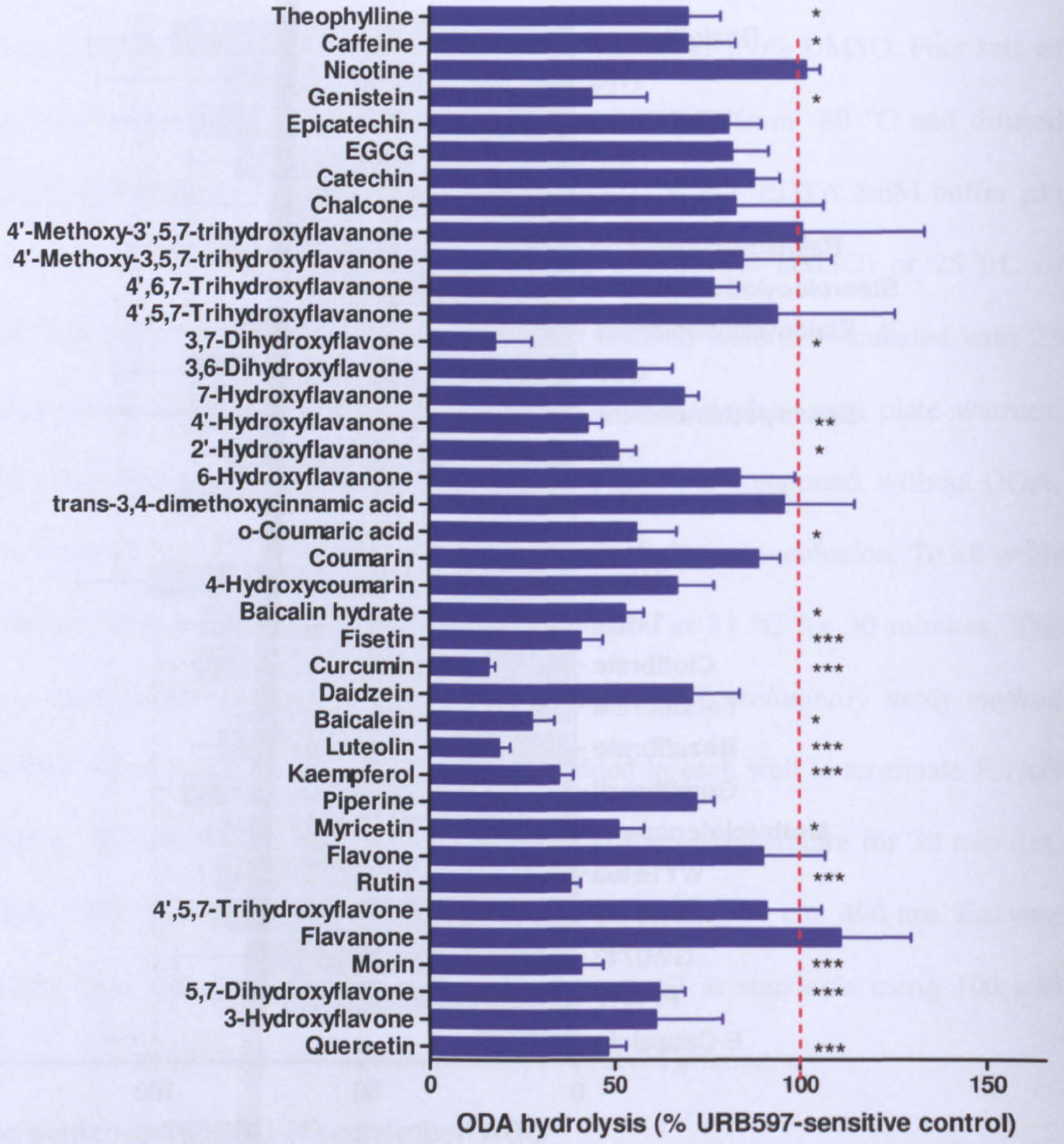

Figure 2.17 FAAH HTS of natural products as potential inhibitors. Natural products were screened as potential inhibitors at 100 μM, and their effect examined on FAAH hydrolysis of 100 μM oleamide. URB597 was used as an inhibitor standard. Data were collected in s (n=4). Data were analysed using one-way AVOVA (*P<0.001;**P<0.01;*P<0.05).**

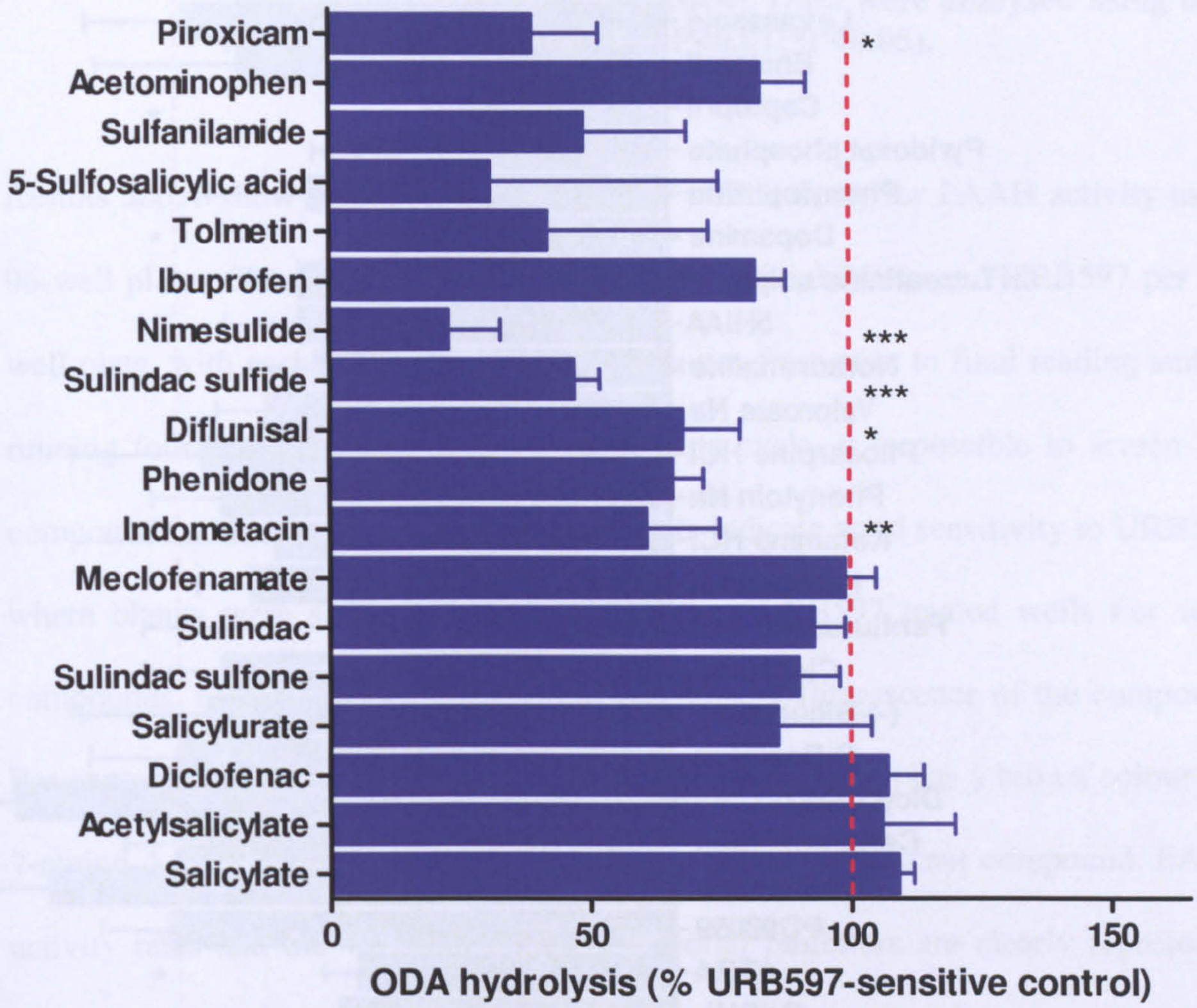

Figure 2.18 **FAAH HTS of NSAIDs as potential inhibitors. NSAIDs were screened as potential inhibitors at 100 µM, and their effect examined on FAAH hydrolysis of 100 µM oleamide. URB597 was used as an inhibitor standard. Data were collected in single replicates (n=4). Data were analysed using one-way AVOVA (***P<0.001;**P<0.01;*P<0.05).**

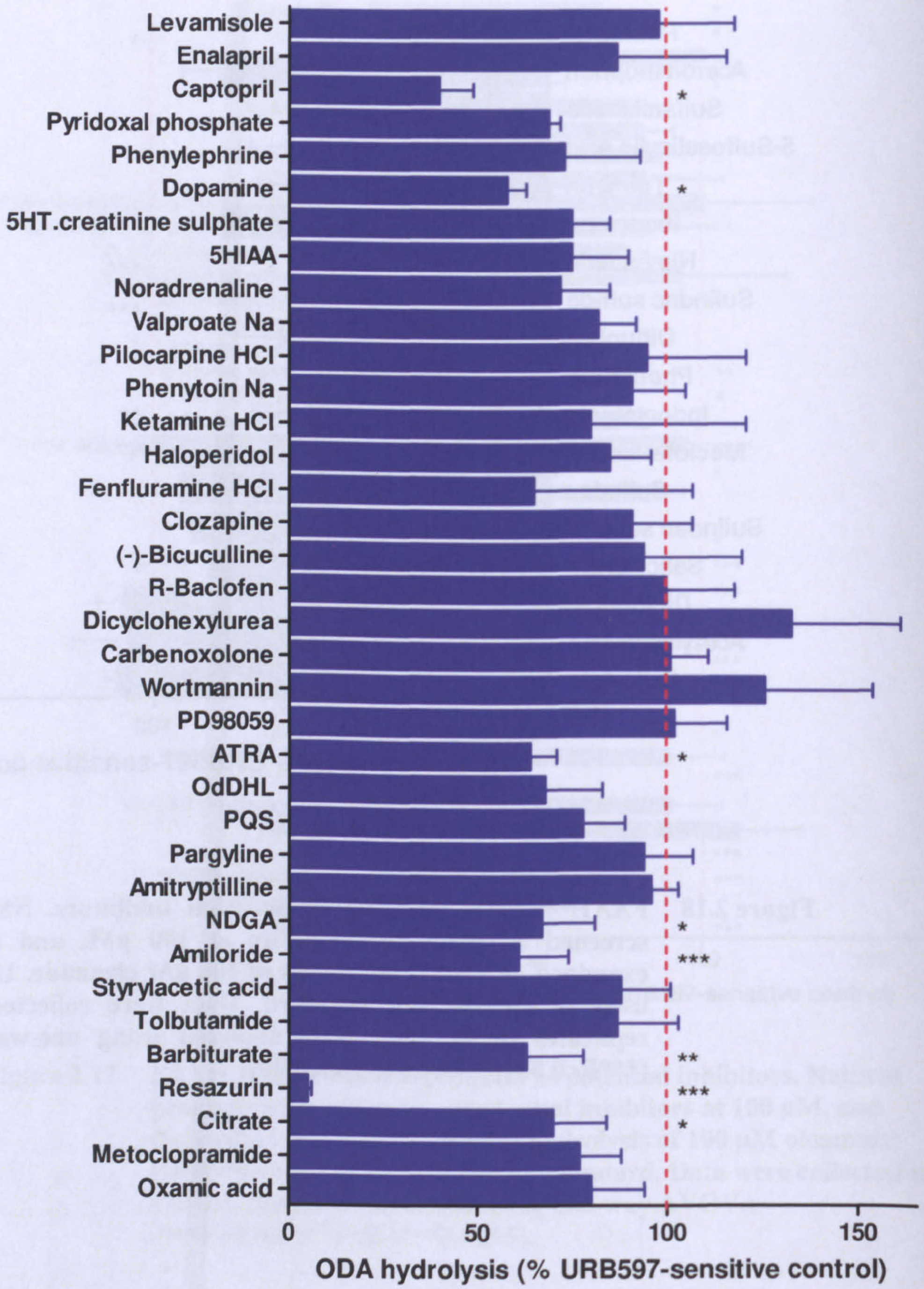

Figure 2.19 **FAAH HTS of miscellaneous compounds as potential inhibitors. Miscellaneous compounds were screened as potential inhibitors at 100 μM, and their effect examined on FAAH hydrolysis of 100 μM**

oleamide. URB597 was used as an inhibitor standard. Data were collected in single replicates (n=4). Data were analysed using one-way AVOVA (*P<0.001;**P<0.01;*P<0.05).**

Results above show successful application of a HTS assay for FAAH activity using 96-well plates. The assay allows for screening of 10 inhibitors and URB597 per 96-well plate, with each plate screened in 75 minutes from start to final reading and by running four parallel plates for each 75 minute cycle, it is possible to screen 250 compounds without the use of robotics. Results indicate good sensitivity to URB597, where blanks were seen to be no different than URB597 treated wells For some compounds, blanks were higher due to the colour or fluorescence of the compound. For example, resazurin, which is deep blue, curcumin, which has a brown colour and 7-amino-4-methylcoumarin, which is a highly planar fluorescent compound. FAAH activity rates and the variation between potential inhibitors are clearly represented visually. The cannabinoid compounds showed little effects on rates of FAAH activity, with capsacin producing the only significant reduction (**figure 2.16**). Rates of FAAH inhibition allow a structure-activity relationship to be suggested. Some have been observed in this screen, mainly within the group of NSAIDs and flavones. There were various compounds shown in **figure 2.17** which significantly inhibit FAAH activity, for example dopamine, amiloride and captopril, none of which are structurally related and therefore do not lend themselves towards development of structure activity related effects on FAAH as inhibitors.

Results clearly show that the HTS FAAH activity assay can be applied to screen compound libraries of potential inhibitors in industry to easily identify new FAAH

inhibitors compared to known FAAH inhibitor URB597 and with the use of ODA as FAAH substrate.

2.4.18 Application of FAAH HTS assay: further investigation into potential FAAH inhibitor compounds

The compounds screened as potential FAAH inhibitors showed no trend within groups of compounds, and inhibition of FAAH observed within the results in **chapter 2.4.2** was compound specific. We looked at each compound individually and further investigated compounds that inhibited activity by greater than 55% by conducting a concentration-response of each compound, at concentrations of $1 \times 10^{-6} - 1 \times 10^{-4}$, to obtain an estimate of potency as a potential FAAH inhibitor.

2.4.19 FAAH activity HTS concentration-response assay method

Tissue preparation

Membrane fragments were prepared from livers of male Wistar rats (150g – 250g) as described previously in **chapter 2.2.1** and stored as 1:10 original wet weight aliquots at -80 °C.

FAAH HTS assay method

The assay was conducted as described in **section 2.4.1**.

2.4.20 Further investigation (concentration-response curves) of compounds a potential inhibitors of FAAH activity

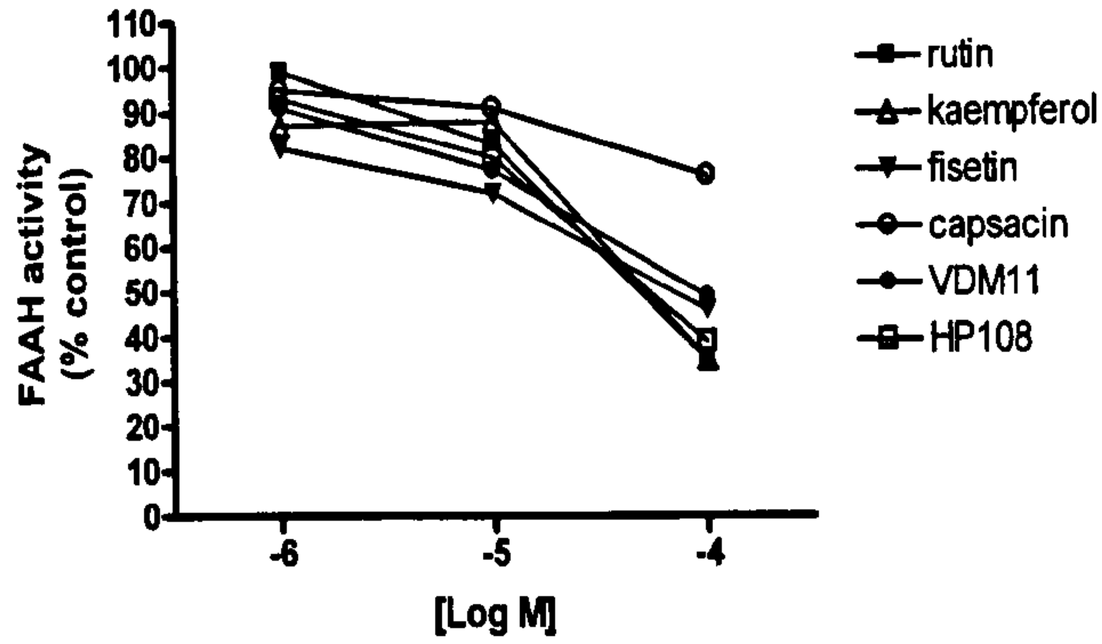

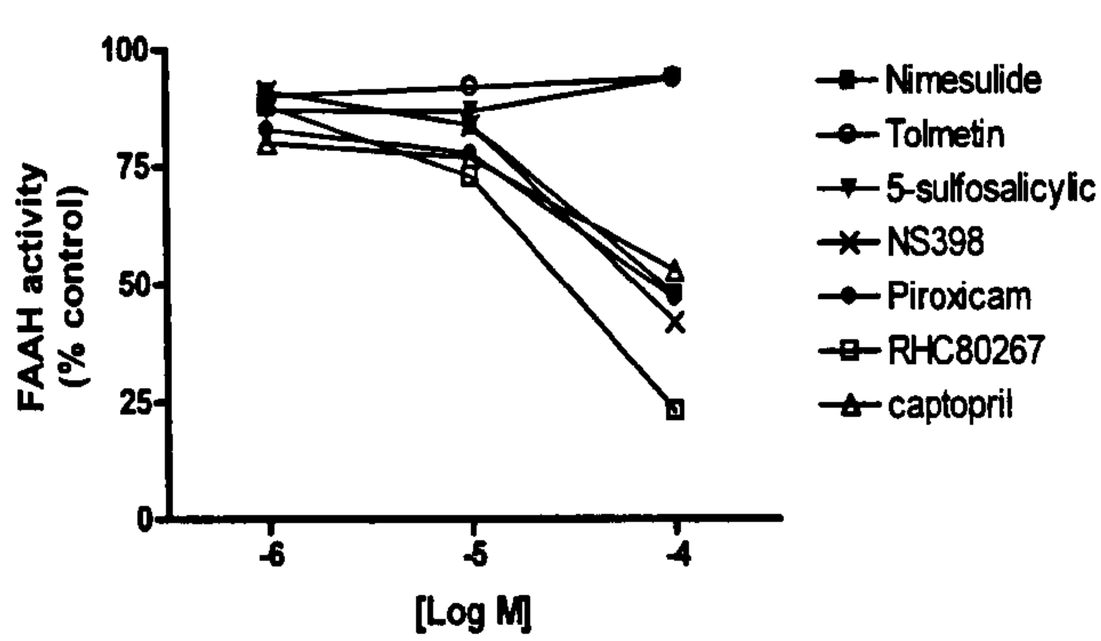

Figure 2.20 **Concentration response curves on all compounds exhibiting <40% control in HTS screen. All compounds screened at 10^{-4}-10^{-6} log M. Data collected in single replicates, n=4, data are expressed as % control.**

Compound	logEC50	SEM
rutin	-4.5	0.3
kaempferol	-4	0.3
fisetin	-4.7	0.5
capsacin	-4.6	0.2
VDM11	-4.9	0.1
HP108	-4.5	0
Nimesulide	-4.5	0
Tolmetin	-5.9	0.4
5-sulfosalicylic	-4.9	0.8
NS398	-4.5	0.1
Piroxicam	-5.1	0.3
RHC80267	-4.5	0.3
captopril	-5.5	0.5

Table 2.2 **LogEC50 values of all potential inhibitors of FAAH activity. This table displays the mean logEC_{50} value obtained for each obtained from four replicates, with the last row displaying standard error of the mean.**

In comparison with URB597 (logEC_{50} of -6.35), none of the further investigated compounds as FAAH inhibitors in section 2.5 were as potent. This experiment shows that potential inhibitors can be further investigated to obtain logEC_{50} values which allow for a point of comparison with the known logEC_{50} of the selective FAAH inhibitor URB597. This will help to rapidly determine whether any compounds would potentially provide a stronger level of inhibition compared to that provided by URB597.

2.4.21 Z-Factor

The Z-factor is a statistical analysis and measure of the size of effect within a given assay. It has been used in high throughput assays, used for multiple compound screening, to determine whether the response in an assay is large enough to warrant further attention, and provides an indication of the quality of the assay itself [Zhang 1999]. The final Z-factor value reflects both the assay signal dynamic range as well as the data variation associated with the signal measurements and therefore provides a through assay quality assessment. It is a value which clearly aids the process of assay optimization.

Calculation

Calculation of the Z-factor requires input of four parameters, the means and standard deviations of both positive (p) and negative (n) controls (χ_p. σ_p and χ_n. σ_n).

Given these values the Z-factor is defined by:

$$\textbf{Z-Factor} = 1 - 3 \times (\sigma_p + \sigma_n) / (\chi_p - \chi_n)$$

Interpretation

Z-Factor	Interpretaion
1.0	Ideal. Z-Factor can never exceed 1.
0.5 - 1.0	Excellent assay.
0 - 0.5	Marginal assay.
less than 0	Too much overlap of positive and negative control for assay to be useful.

HTS FAAH assay calculation

positive control (ODA)	negative control (URB)
13208	-66
15554	-241
20999	403
19913	181
19578	456
18534	-212
17964	28
mean	**17964**	**78**
st dev	**2518**	**259**
Z-Factor	**0.53**	

Table 2.3 **Z-factor value calculated using data from HTS FAAH inhibitor screening, with the use of 100 μM ODA and 5 μM URB597.**

2.5 Discussion

This chapter describes the characterisation of a novel fluorescence-based 96-well plate high throughput FAAH activity assay to provide a cheap and rapid assay tool for use in industry towards the development and identification of potential FAAH inhibitors. Application of this assay was successful in identification of potential FAAH inhibitors, and provided an easy route for further investigation to determine the potency of the potential inhibitors picked out from an initial screen. It has few additions and can therefore be easily applied to industrial lab robotics, with raw data easily manipulated by computer macro applications allowing for fast identification of potential inhibitors within a large library of screened compounds. Tolerance of the assay to high concentrations of solvents, used to solubilise compounds, provide further flexibility in the range of compounds that can be used and screened in the assay, with URB597 as a useful tool for comparison of new and potential inhibitors. Using this methodology the K_M and V_{MAX} values for FAAH-catalysed oleamide hydrolysis were determined and found to be similar to that obtained in using the previous non-HTS methodology. In addition, inhibition of FAAH by URB597 was observed in a concentration-dependant manner with similar IC_{50} values obtained using the previous methodology. We have seen that pre-incubation is necessary in application of this assay towards potential new inhibitors, as there was an increased sensitivity when URB597 was pre-incubated for 15 minutes prior to addition of substrate. It was shown that there was no difference in the use of pre or post-hoc solubilised enzyme preparations, therefore provides a simpler and quicker option and preparation of an enzyme source. The Z-factor calculation (Z-Factor = 0.53) (**table**

2.3) also provides an indication of a very useful assay in the use of HTS screening towards the identification of potential inhibitors of FAAH.

2.5.1 The HTS Assay

Figure 2.16 shows the majority of the cannabinoid compounds failed to significantly affect FAAH activity. Capsaicin is a vanniloid receptor $TRPV_1$ agonist, which may stimulate eCB generation through calcium mobilization. **Figure 2.16** shows its use at 100 μM is high enough to activate $TRPV_1$ receptors and also cause FAAH inhibition. These two independent effects may lead to an even further increase in endogenous levels of eCBs potentially contributing to capsaicin-evoked analgesia. This possibility requires testing in intact cells, such as dorsal root ganglion cells.

AEA and cannabidiol (CBD) have been reported to divert or inhibit FAAH activity, where the IC_{50} of CBD has been reported to be 27.5 μM (Bisogno et al., 2001). Our assay provided adequate concentrations of CBD to cause such an inhibition on FAAH, yet inhibition of its activity was not observed in **figure 2.16**.

Figure 2.17 allows assessment of structure:activity relationships amongst the flavonoids as FAAH inhibitors to be identified. For example, glycosylation, compound saturation and hydroxylation are potential influences on FAAH inhibitory activity. Flavone has a C2 – C3 double bond, whereas flavanone is unsaturated in its structure. Neither compound exhibited significant inhibition of FAAH activity (FAAH activity (% control) = 90 ± 17 and 111 ± 19, respectively). Rutin, a glycosylated derivative of quercetin, seemed as effective as quercetin itself. The soya-derived isoflavone genistein was more effective than it's flavones isomer

apigenin (4',5,7-trihydroxyflavone) (44 % vs. 92 %). In summary, though, there was no clear-cut pattern allowing the identification of the importance of hydroxylation number or position on inhibition of FAAH activity. Chris Fowler's group have previously established SAR to the favonoids on their inhibition of FAAH. Kaempferol was reported to be the least potent , displaying FAAH inhibition, using a radiolabelled AEA hydrolysis assay, with a Ki value of 5 μM. 7-hydroxyflavone and 3,7-dihydroxyflavone were amongst the most active, displaying IC_{50} values of 1 μM and 2.2 μM respectively (Thors et al., 2008). Our results correlate with this study, as seen in **figure 2.17**, we observed the most potent effect on FAAH activity to be by 3,7-dihydroxyflavone, which was more potent compared with 7-hydroxyflavone. Kaempferol inhibited FAAH activity with a value in between that of the above hydroxyflavones. Fowler's group conducted their study using radiolabelled AEA hydrolysis, which is widely regarded as the current gold standard for measuring FAAH activity, although it doesn't allow the high-throughput of our HTS FAAH assay. It will clearly be vital to determine whether methodological differences in the assays are responsible for these discrepancies in inhibitor potency..

Flavonoids are present in the diet and are ingested daily in our diets. They are present at μM concentrations in plasma and from our data in **table 2.3** we see that 10+ μM concentrations are required to produce an inhibitory effect on FAAH activity. It appears unlikely, therefore, that individual dietary flavonoids will influence FAAH activity levels significantly, although, but it may be possible for several flavonoids to have additive effects on FAAH inhibition, especially if their mechanisms of FAAH

inhibition differ from each other – producing a more potent effect overall.

Although the compounds itemised in **table 2.2** are less potent inhibitors when compared with URB597, they may well still provide therapeutic benefit. Lower potency as a FAAH inhibitor may provide lower levels of eCBs available for CB receptor activation. Low level cannabinoid receptor activation has been reported to be beneficial in disease (for example in the treatment of MS (Baker et al., 2001).

There are no existing studies in the literature to match the screening conducted here, although some individual compounds have been reported to inhibit FAAH activity, in particular the NSAIDs. Fowler's group have previously shown the COX inhibitor ibuprofen to inhibit FAAH activity, while the COX2 inhibitor nimesulide was inactive (Fowler et al., 2003). Our findings **(figure 2.18)** show no significant levels of FAAH inhibition, compared with control. Differences in the methodologies may have caused these different findings, as suggested above.

In summary, it appears likely that this assay will provide a highly useful tool to extend cannabinoid research as there is growing interest in the therapeutic use of FAAH inhibitors.

Chapter 3: Development of MAGL HTS assay

3.1 Introduction

Monoacylglycerol lipase (MAGL) is a key enzyme in the hydrolysis of the endocannabinoid 2-arachidonoylglycerol (Dinh et al., 2002; Makara et al., 2005). It converts monoacylglycerols to the free fatty acid and glycerol. 2-AG is a naturally occurring monoglyceride that acts as a full agonist at both cannabinoid receptors and is present in the brain (Mechoulam et al., 1995) (Sugiura et al., 2006). Levels of 2-AG in the brain have been found to be 170-fold higher than those of anandamide. It is produced by neurons in an activity- and calcium-dependent manner, and is rapidly eliminated (Stella 1997). The contribution of MAGL to total brain 2-AG hydrolysis activity has been estimated to be ~85% (Blankman et al., 2007). This *in vitro* estimation of MAGL activity has recently been confirmed *in vivo* with the use of a selective MAGL inhibitor JZL184 The subcellular localisation of MAGL was first studied in rat adipocytes, where the enzyme activities were mainly found in the plasma membrane and in the cytosol fractions, with activity levels being similar between the two fractions (Sakurada and Noma, 1981). It was originally found to function with hormone-sensitive lipase (HSL) in the hydrolysis of adipocyte triglyceride stores (Fredrikson et al., 1986), which led to the investigation of its ability to hydrolyse other monoglycerol compounds, such as 2-AG and its analogues.

Previously used methods to determine MAGL activity involve measurement of free fatty acid release from a monoacylglycerol substrate using a gas or liquid chromatography mass spectrometry (GC/LC-MS) system or measurement of radiolabelled substrate 2-

oleoyl-[^{3}H]-glycerol.

The radiolabelled substrate assay is the most commonly used. It allows the labelled 2-OG to react with either use of cytosolic of membrane bound enzyme preparations for a set period of time. The reaction is then stopped using either charcoal (Boldrup et al., 2004) or the Folch extraction procedure based on the use of 1:1 aqueous/organic mixtures, in this case, methanol:chloroform, which allows separation of the hydrophilic and lipophilic fractions (Folch et al., 1957). Pure chloroform is then used to bring the aqueous phase to the top, which contains the radiolabelled hydrophilic glycerol moiety release following hydrolysis by MAGL. The free fatty acid moiety remains in the organic phase along with any unhydrolysed 2-OG, providing complete separation of the hydrolysed product. The amount of hydrolysed 2-OG is then measured using liquid scintillation spectroscopy (Dinh et al., 2002) (Omeir et al., 1995). Methods using LC-MS commonly estimate 2-AG as a MAGL substrate and amounts of arachidonic acid (AA) cleaved off from 2-AG hydrolysis by MAGL. The released AA is then measured by GC/LC-MS. (Muccioli and Stella, 2008). Both methods are laborious and time consuming. Even though the radiolabelled assay is more sensitive and accurate in the measurement of monoglycerol hydrolysis by MAGL compared with the GC/LC-MS methodology and can be used in a 96-well format (Brengdahl and Fowler, 2006), the use of radiolabelled substrates has the drawback of being expensive.

The most recently developed assay used to measure MAGL activity is a colorimetric assay (Muccioli and Stella, 2008) using recombinant human MAGL (Labar et al., 2007). It is a simple and inexpensive method that can be applied to high throughput screening of

potential inhibitors of MAGL with the use of a chromogenic substrate 4-nitrophenolacetate (4-NPA). Hydrolysis of substrate following incubation with recombinant enzyme results in development of a yellow colour which allows kinetic measurement over time to measure 4-NPA hydrolysis. A drawback to this assay is that NPA is not a specific substrate for MAGL and thus 4-NPA hydrolysis activity will be influenced by other non-specific esterases. Hence, the radiolabelled assay may be used alongside the colorimetric assay to determine, confirm and quantify the level of MAGL activity (using the MAGL inhibitor MAFP) and determine the contributed activity from non-specific esterases.

We have applied Muccioli's method towards native tissues, to investigate it's potential as a more accessible and cheaper HTS assay for potential inhibitors of MAGL.

3.2 Method

3.1.1 Tissue preparation

Membrane and cytosolic fragments were prepared from various tissues of male Wistar rats (150g – 250g) as described previously in chapter 2.2.1. and stored as 1:10 original wet weight aliquots at -80 °C. Homogenate preparations of tissues were also stored at -80 °C.

3.1.2 Preliminary MAGL HTS assay method

4-NPA was prepared as 100 mM stock solutions in 100% EtOH and stored at -20 °C. Tissue was thawed from -80 °C and diluted further to 0.01 g/g wet weight tissue (1:100) using 50 mM Tris-EDTA buffer, pH 7.4. Concentration response curves were generated using 10^{-1} to 10^{-4} NaF as an esterase inhibitor, with and without the presence of 1 µM MAFP (in 10% DMSO) or other inhibitor screening compounds (100 µM) were pre-incubated with n=4 of enzyme source at 37 °C for 15 minutes in a 96-well plate on a plate warmer. 250 µM NPA was added to each well, making an assay volume of 200 µL. Colour development as a result of 4-NPA hydrolysis was measured kinetically at a wavelength of 405 nm on a spectrophotometer for 60 minutes. Data generated after 15 minutes were isolated and analysed.

3.1.3 Data Analysis

Following kinetic measurement of 4-NPA hydrolysis, data were extracted at a time point of 15 minutes. 4-NPA hydrolysis with MAFP alongside a NaF concentration curve was deducted from 4-NPA hydrolysis with NaF levels providing baseline data, which was

then normalised to control 4-NPA hydrolysis without presence of inhibitors and graphs were generated as % of control activity, with log IC_{50} values calculated.

3.3 Results

3.2.1 Comparison of skeletal muscle and adipose tissue as a source of MAGL activity

As discussed in section **2.1** both skeletal muscle and adipose tissue have previously shown levels of MAGL activity. Here we investigated levels of MAFP inhibitable activity in the presence of the non-specific esterase inhibitor NaF, from soluble, particulate and homogenate tissue preparations. We collected Wistar rat (150-250 g) adipose tissue and skeletal muscle from the thigh and prepared it as in section **2.2**. We used dilutions of tissue preparations determined in preliminary investigations to give maximal substrate hydrolysis levels from each tissue fraction. Cytosolic preparations were diluted 1:10, particulate preparations were diluted 1:40 and homogenate, showing highest levels of activity was diluted to 1:50.

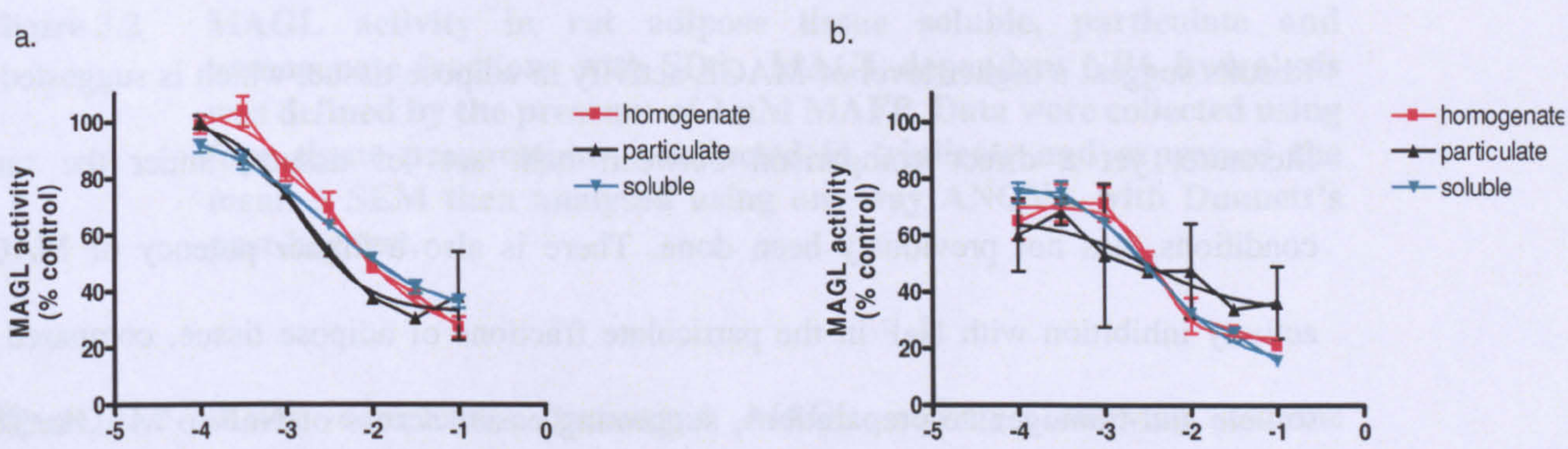

Figure 3.1 **MAGL activity as determined by NPA hydrolysis in rat adipose (a) and rat skeletal muscle tissue (b), in soluble, particulate and homogenate fractions against a concentration response curve of NaF. Data were collected using four tissue preparations, conducted in triplicate and expressed the mean ± SEM then analysed using one-way**

ANOVA with Dunnett's post-hoc test.

	log IC50 (logM)			Mean (logM)
Adipocyte	-2.41	-2.86	-2.52	**-2.6**
Skeletal	-2.38	-2.49	-2.41	**-2.43**

Table 3.1. **Log IC_{50} values of 4-NPA hydrolysis by NaF in both adipocyte and skeletal muscle tissues, using homogenate, particulate and cytosol (from left to right, respectively).**

Analysis of data show activity from all fractions of adipocyte tissue, as a source of MAGL activity, to be higher than observed in skeletal muscle. Log IC_{50} values calculated for NaF (table 3.1) were reasonably consistent in adipose and skeletal muscle tissue. MAGL activity was highest in the adipose particulate fraction, providing the lowest log IC_{50} value (-2.86) where log IC_{50} values for both soluble and homogenate fractions were similar (-252 and -2.41 respectively).

Results suggest a higher level of MAGL activity in adipose tissue, which is suggested in literature, yet a direct comparison between both sets of tissues, under the same conditions, has not previously been done. There is also a higher potency of MAGL activity inhibition with NaF in the particulate fractions of adipose tissue, compared to soluble and homogenate preparations, suggesting easier access of NaF to MAGL. This was unexpected as it is well documented that MAGL is primarily a cytosolic enzyme and therefore access of inhibitors should be greater in the soluble fractions ((Somma-Delpero et al., 1995) 25mM NaF=10% control MAGL activity).

3.2.2 The effects of SDS on adipose tissue NPA hydrolysis

To try to isolate the MAGL component of NPA hydrolysis, the effects of the detergent SDS were examined in adipose tissue preparations.

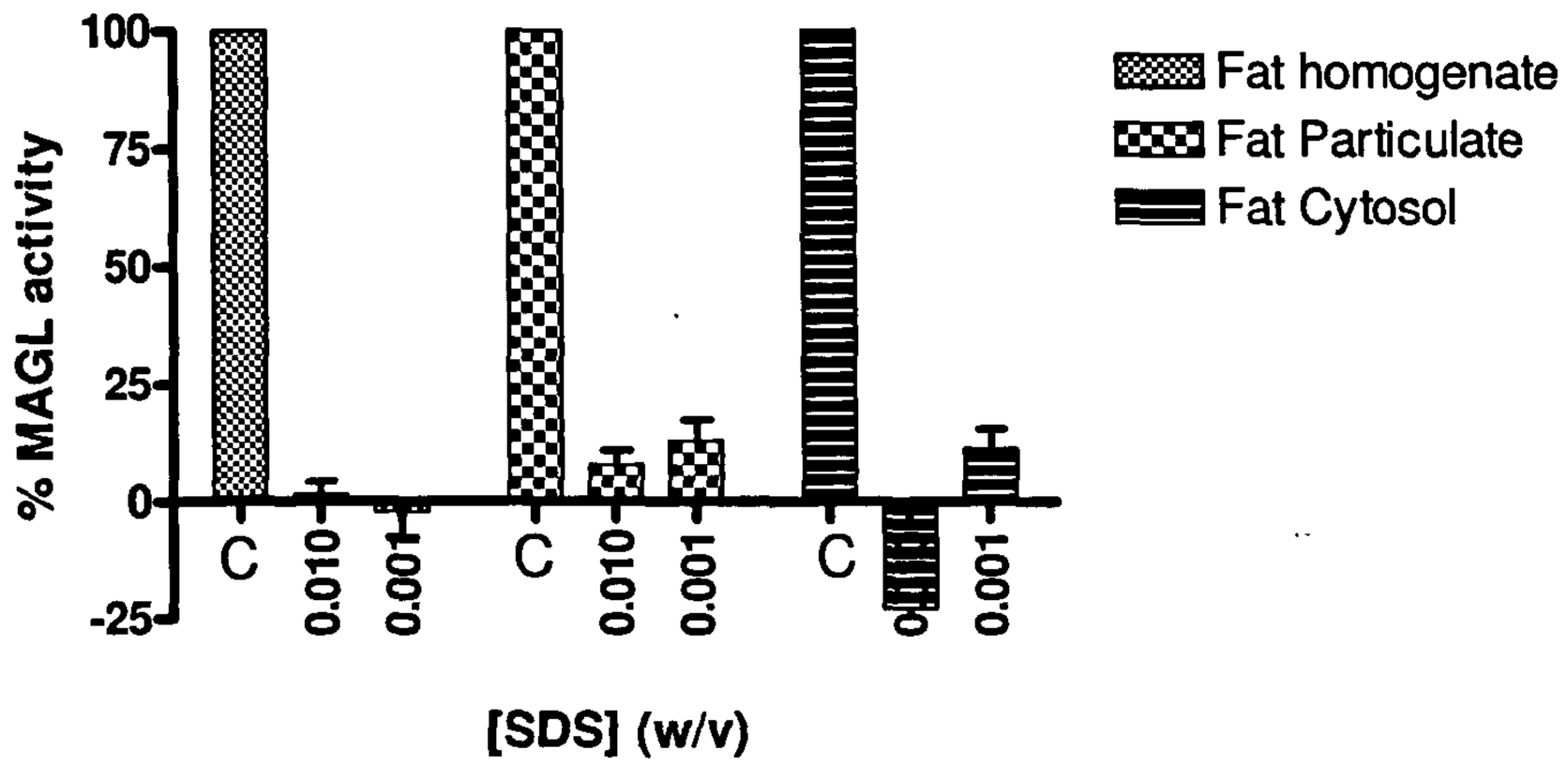

Figure 3.2 **MAGL activity in rat adipose tissue soluble, particulate and homogenate fractions with SDS. MAGL-dependent NPA hydrolysis was defined by the presence of 1 μM MAFP. Data were collected using four tissue preparations, conducted in triplicate and expressed the mean ± SEM then analysed using one-way ANOVA with Dunnett's post-hoc test.**

Figure 3.2 shows completely diminished MAGL activity following enzyme solubilisation with 0.01% and 0.001% SDS in all adipose tissue fractions.

MAGL solubilisation should make the suggested plasma membrane location of MAGL (Sakurada and Noma, 1981) more accessible for substrate hydrolysis. Following enzyme solubilisation, we would expect similar or increased levels of MAFP inhibitable activity.

Figure 3.2 suggests 4-NPA is not hydrolysed by solubilised enzymes. Previous studies assessing lipase activity (hormone-sensitive lipase) from adipocyte preparations have not been successful due to interactions of enzymes with lipid, producing large lipid-protein aggregates, which would cause major light scattering when used in our assay. This group also encountered difficulties when trying to extract lipids with solvents of detergents (Fredrikson et al., 1986). This problem then led into detergent-based solubilisation of adipocyte tissue preparations which then allowed for HSL solubilisation and partial purification to use as an enzyme source. Solubilisation of MAGL was achieved by Tornqvist and Belfrage (1976) using apolyoxyethylene alcohol detergent which did not cause changes in biological activity. They found attempts at solubilisation of homogenate with sonication at various combination of ionic strength and pH without detergent was not successful. The non-ionic detergent nonipol was therefore used for solubilisation. This group also identified that protection of the functional sulfhydryl groups of MAGL increased stability of enzyme activity.

We observed complete loss of biological activity in the presence of the anionic detergent SDS, which suggests disruption of the structure of the enzyme, for example, by interfering with sulfhydryl groups. Use of non-ionic detergents may prove to be a more successful approach.

3.2.3 Adipose tissue as a source of MAGL activity

We investigated levels of NPA hydrolytic activity in adipose tissue using different dilutions of the particulate fraction. We extracted rat adipose tissue from three male

Wistar rats (150-200 g), and tissue was prepared as in section **3.2.**

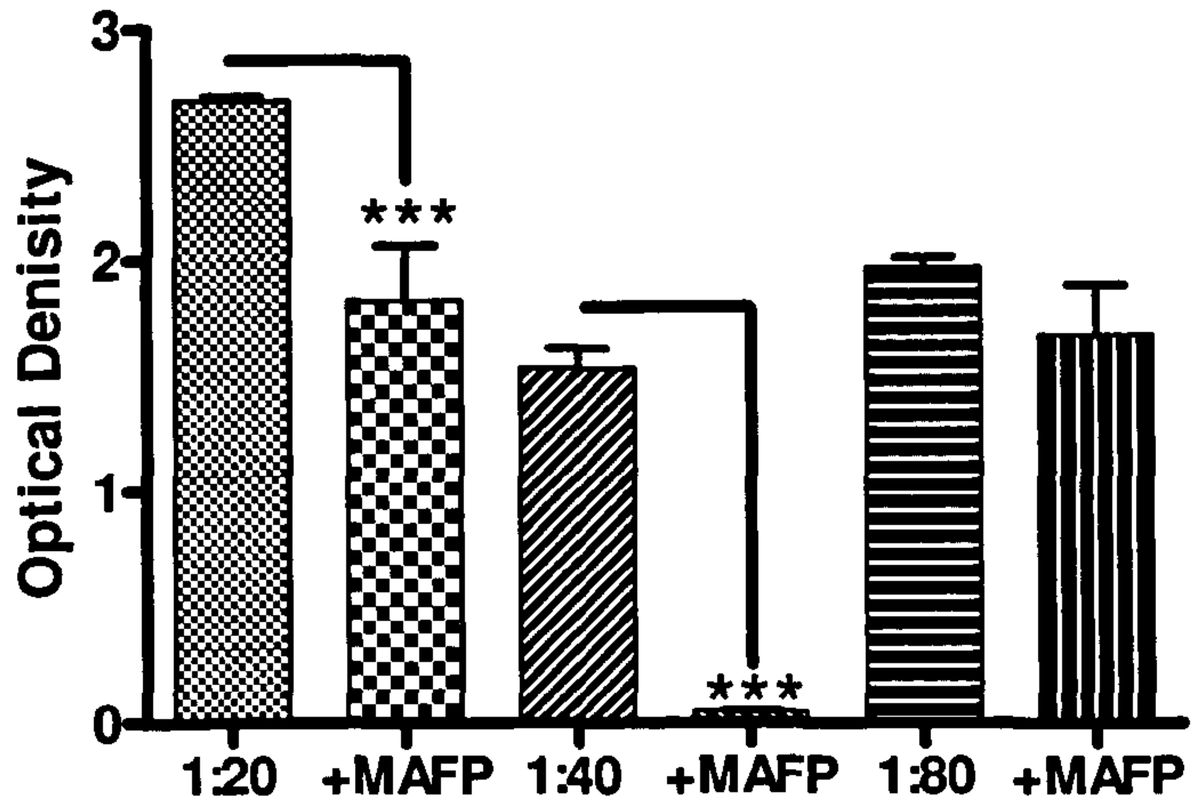

Figure 3.3 **MAGL activity in rat adipose particulate fractions at a range of tissue dilutions, with and without 1 μM MAFP. Data were collected using four tissue preparations, conducted in triplicates and expressed the mean ± SEM then analysed using one-way ANOVA with Bonferroni's post-hoc test (***p<0.001).**

Figure **3.3** shows 4-NPA hydrolysis is present in all three adipose particulate dilutions, with activity being the highest in the least diluted preparation (1:20) which displays highly significant levels of MAFP inhibitable activity (MAGL-specific), with clearly a high level of activity still present from other esterases. 1:80 dilution of the particulate also displays a high level of 4-NPA hydrolysis, albeit lower than 1:20 diluted tissue, yet it shows a very low level of MAFP inhibitable activity which is not significant. The 1:40 dilution of adipocyte particulate provides the lowest amount of 4-NPA hydrolysis of the three tissue dilutions, yet it appears to have the greatest contribution of MAFP inhibitable activity, with the least influence of other esterases.

Figure **3.3** shows a 1:40 dilution of adipocyte particulate tissue to be the most favourable

to apply to the HTS MAGL assay, as there is a high level of MAFP inhibitable activity, which displays MAGL specific 4-NPA hydrolysis. This tissue preparation provides the lowest levels found of 4-NPA hydrolysis resulting from other esterases. The description of the recent MAGL colorimetric assay by Muccioli (2008) suggests that non-specific esterases this MAGL specific activity difficult to determine in native tissues. Hence, the lower the levels of NSE activity we have, the easier it is to determine a MAGL specific effect. Results shown in figure **3.3** were generated from the same experiment, where the same tissues were used and diluted to be run directly in the experiment. However, the unusual pattern of MAFP-inhibitable activity observed, where activity at the greatest dilution appeared to derive entirely from NSEs, while only a 2-fold more concentrated protein preparation appeared to be entirely due to MAGL activity, suggests some complex interactions. Experiments previous to this, which were run to determine optimal protein dilutions in adipose particulate preparation showed a variety of sensititivity to MAFP, indicating adipose tissue may not be suitable without additional manipulation as a MAGL source for application in a high throughput spectrophotometry assay.

3.2.4 Brain tissue as a source of MAGL activity

We therefore investigated the use of a more traditional source for ECB turnover, rat brain cytosol (Dinh et al., 2002); (Blankman et al., 2007). Rat brain cytosol is used in radioligand assays for ^{3}H-2-OG hydrolysis by MAGL (Ghafouri et al., 2004). In the right conditions, it was anticipated that there should be an abundance of MAGL activity in this tissue preparation for high throughput application.

Tissue fractions were kept in 1:10 w/v stock at -80°C and then further diluted according

to the tissue fraction. Homogenate was further diluted 1:50, particulate 1:10 and cytosol 1:40, to assess all fractions from the rat brain for preliminary levels of MAGL present.

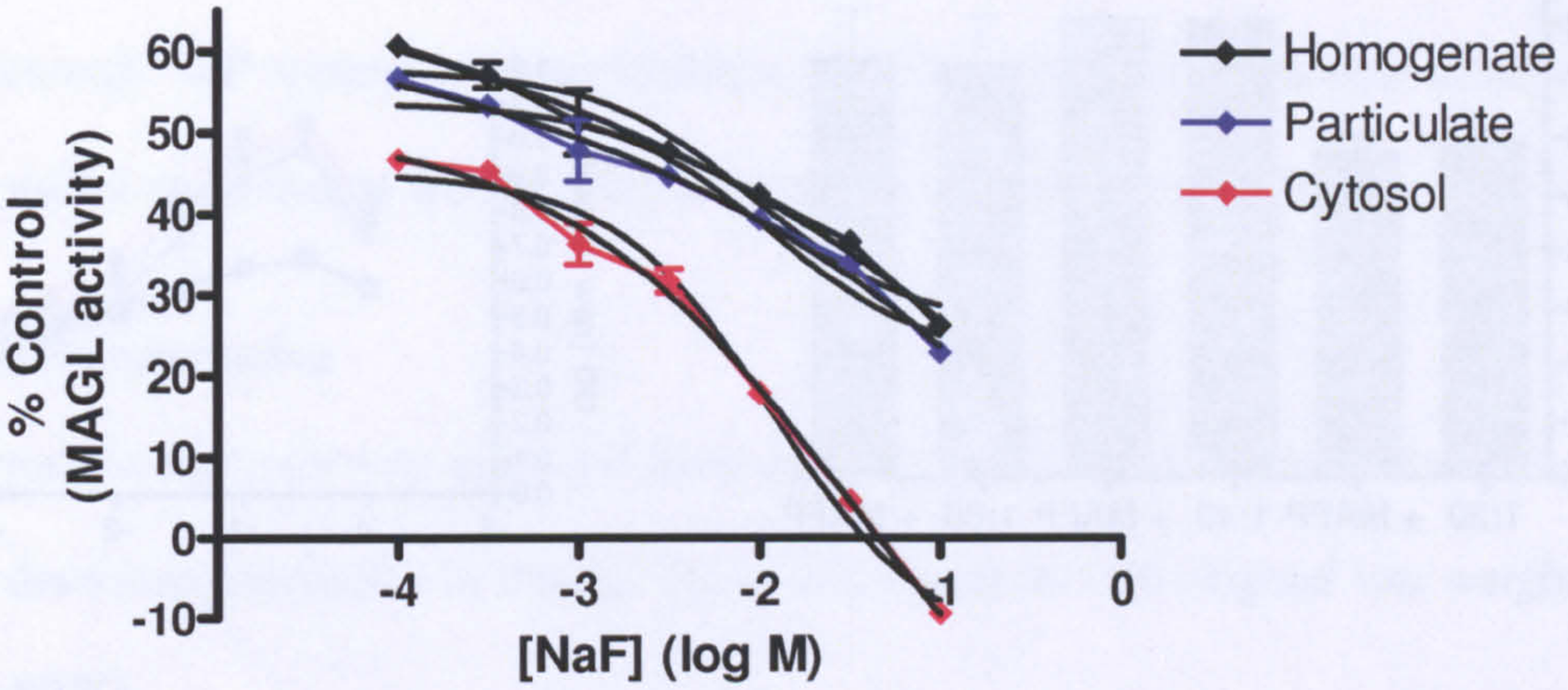

Figure 3.4 **Levels of 4-NPA hydrolysis by MAGL in rat brain homogenate, particulate and cytosolic preparations, and the influence of varying concentrations of NaF. Data were collected using four tissue preparations, conducted in triplicates and expressed the mean ± SEM. Data were normalized and expressed as percentage of control MAGL activity.**

	Homogenate	Particulate	Cytosol
Log EC50	**-2.02**	**-1.93**	**-1.93**

Table 3.2. **Log EC50 values calculated using sigmoidal dose response (variable slope) of MAGL 4-NPA hydrolysis in rat brain homogenate, particulate and cytosolic fractions.**

Results show high levels of MAGL activity in the rat brain, which is inhibitable by NaF at log EC_{50} values of between -2.02 and -1.93. Intriguingly, the cytosolic fraction appeared to be inhibited by NaF more than homogenate and particulate fractions.

The effects of MAFP were investigated on rat brain cytosolic NPA hydrolysis, to attempt

to define the contribution of MAGL.

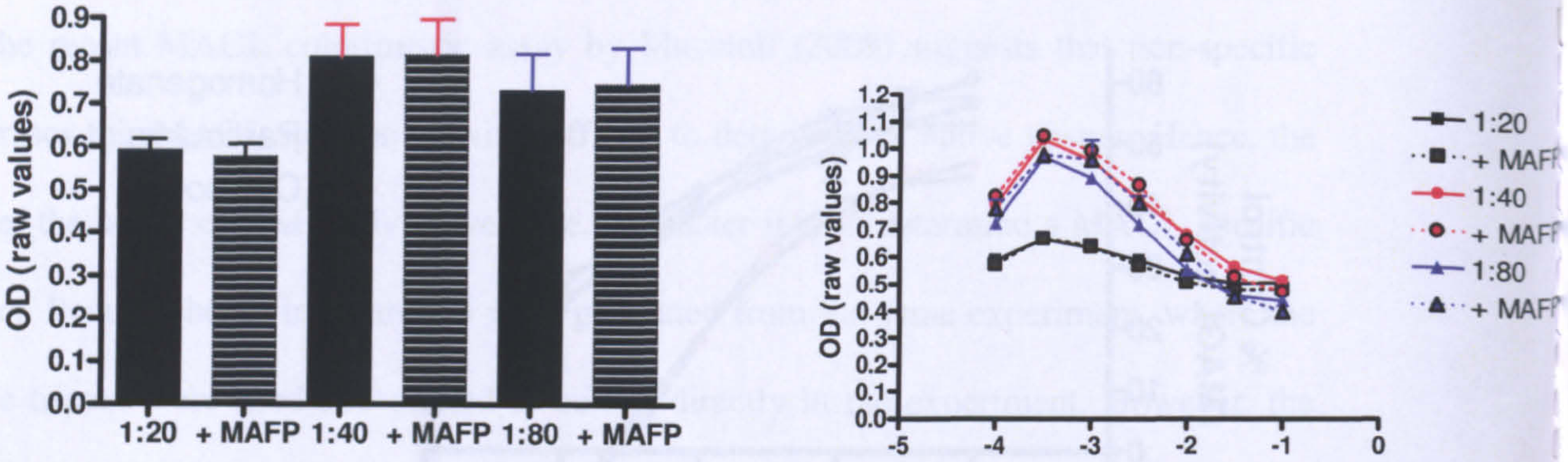

Figure 3.5 **Levels of 4-NPA hydrolysis in rat brain cytosol preparations, and MAFP inhibitable levels (a) Concentration-response curve of NaF on 4-NPA hydrolysis in rat brain cytosol preparations with and without MAFP (b). Data were collected in triplicates and expressed the mean ± SEM of three individual experiments then analysed using one-way ANOVA with dunnett's post-hoc test.**

	1:20	1:40	1:80
control	**-2.52**	**-2.38**	**-2.48**
+ MAFP	**-2.55**	**-2.24**	**-2.20**

Table 3.3 **Log EC_{50} values obtained for 4-NPA hydrolysis (control) in the presence of MAFP (+ MAFP) alongside a NaF concentration gradient (10^{-1}-10^{-4}) using rat brain cytosolic fractions at differing dilutions.**

Figure 3.5 indicates that NPA hydrolysis by rat brain cytosol was not greatly affected by dilution of the tissue over the range 1:20 to 1:80. At all three dilutions, MAFP was without significant effect. Neither did MAFP alter the effects of different concentrations of NaF, which were complex.

Since these results were not consistent with evidence from the literature and the labs at

Nottingham for high levels of MAGL activity in the rat brain cytosol, the use of the more traditional radiometric assay for MAGL activity was investigated.

3.2.5 MAGL inhibition by NaF – radiometric assay

Although NaF appears to be an inhibitor of NPA hydrolysis in multiple tissues, it would be useful to determine whether NaF has any direct inhibition of MAGL.

Tissue preparation

Cytosolic fractions were prepared from various tissues of male Wistar rats (150g – 250g) as described previously in chapter 2.2.1. and stored as 1:10 original wet weight aliquots at -80 ℃.

MAGL radioligand binding assay (^{3}H-2-OG)

Tissue was thawed from -80 ℃ and diluted further to 0.01 g/g wet weight tissue (1:100) using 50 mM Tris-EDTA buffer, pH 7.4. Enzyme source was pre-incubated with NaF and MAFP, as required, at 37 ℃ for 15 minutes in 0.5 mL Eppendorf tubes. 100 µM ^{3}H-2-OG was added to each tube, making an assay volume of 100 µL. These were incubated in a water bath for 30 minutes at 37 ℃ and then stopped using 200 µL of a 1:1 mixture of methanol:chloroform, followed by the addition of 200 µL chloroform to allow separation of the upper aqueous layer containing radiolabelled glycerol. 100 µL of this layer was removed and added to 3 mL scintillation fluid and counted overnight.

Data Analysis

Following scintillation counts of radiolabelled sample content. ^{3}H-2-OG hydrolysis with MAFP alongside a NaF concentration curve was deducted from ^{3}H-2-OG hydrolysis with

NaF levels providing baseline data, which was then normalised to control ^{3}H-2-OG hydrolysis without presence of inhibitors and graphs were generated as % of control activity.

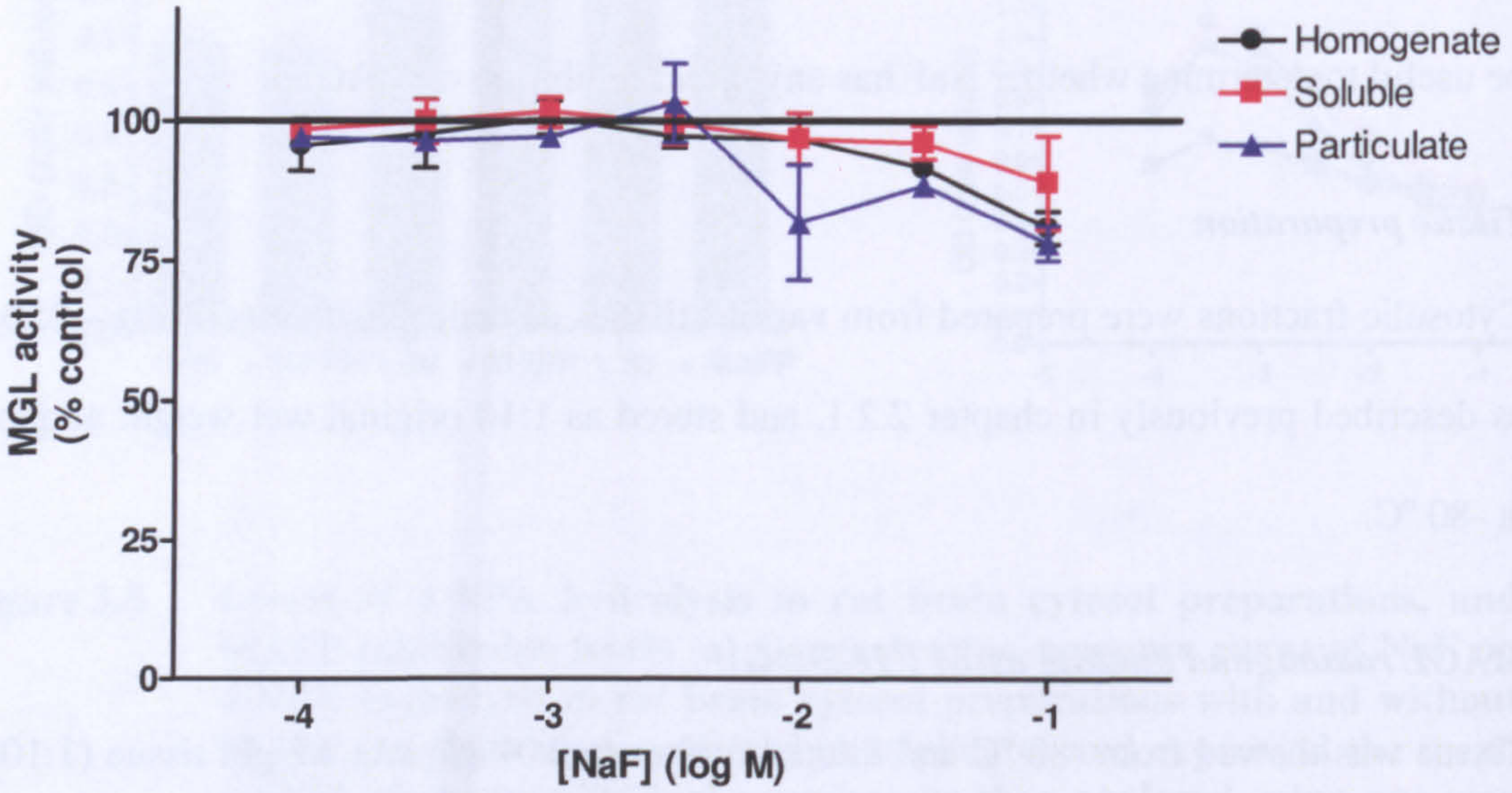

Figure 3.6 Effect of NaF concentration response on MAGL activity assessed using radiolabelled 2-OG as substrate in radioligand binding MAGL assay in homogenate, particulate and soluble fractions of rat brain tissue. Data were collected in triplicates and expressed the mean ± SEM of three individual experiments and expressed as % control of ^{3}H 2-OG hydrolysis.

Data suggest there to be no significant MAGL inhibition by NaF at concetrations of 100 µM to 3 mM, with modest, non-significant inhibitory effects at higher concentrations (**figure 3.6**). Interestingly, the highest concentration of NaF applied (100 mM) evoked an inhibition to 74% control MAGL activity response, whereas it has been reported in literature that the use of 25 mM NaF produces 10% control MAGL activity response (Somma-Delpero et al., 1995).Differences in the assays, such as their use of purified

MAGL on radiometricassay methods may well account for the difference in responses observed, nevertheless there is a large difference between these two results.

3.2.6 HTS MAGL inhibitors in rat liver and brain

As section **3.3.4** suggests rat brain is a good source of MAGL activity and the well known knowledge of the high levels of enzyme activity in the liver, we compared MAGL activity rates using the HTS methodology to see how inhibitor actions varied between the tissues and which one provided the highest levels of MAGL activity and hence able to display the best sensitivity to MAGL inhibitors. We extracted rat brain and liver tissue from three male Wistar rats (150-200 g), and tissue was prepared as in section **3.2.**

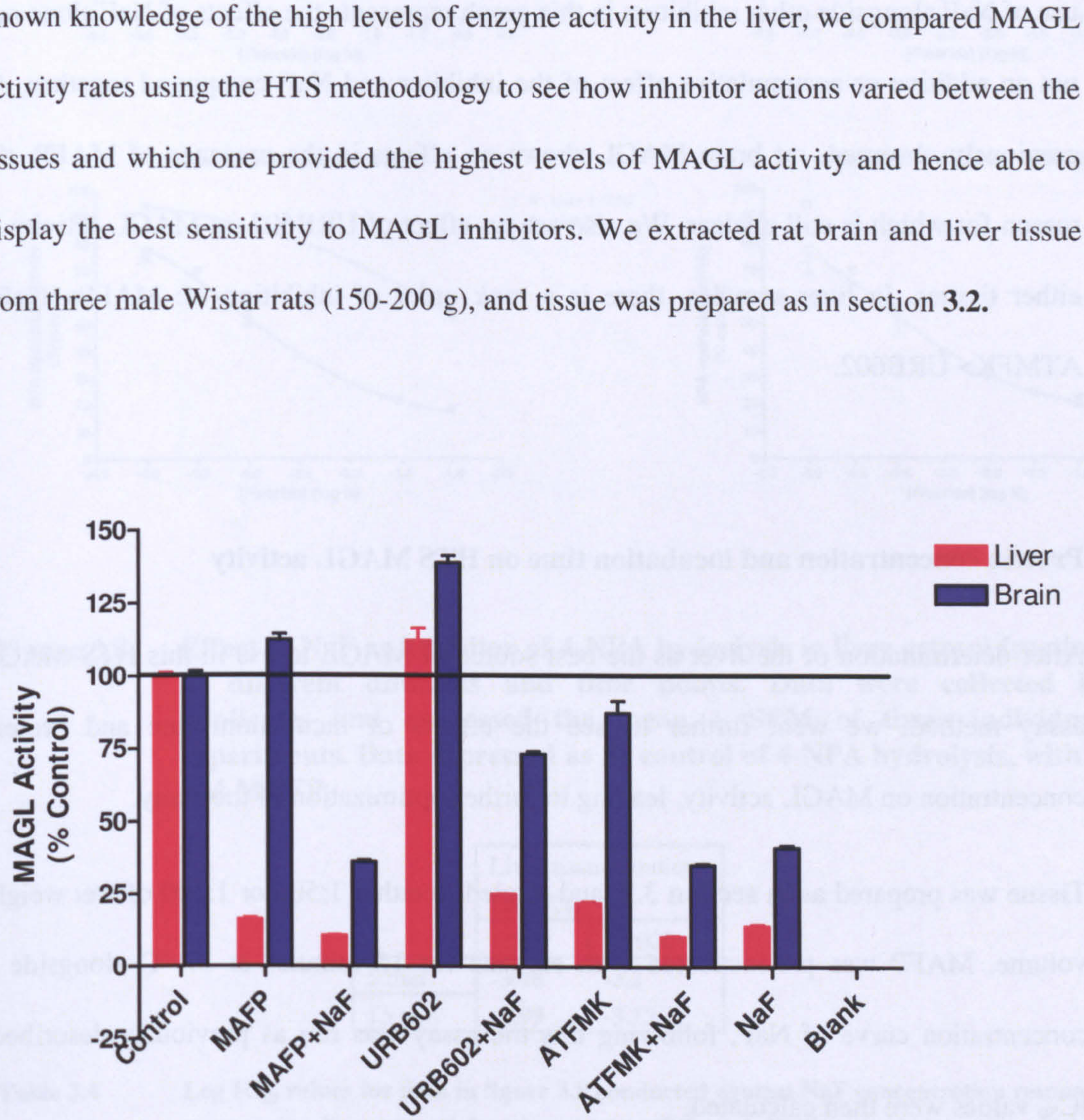

Figure 3.7 **Effects of potential MAGL inhibitors in liver and brain cytosolic fractions, with the use of 100 mM NaF, 1 μM MAFP, 10 μM ATFMK and 100 μM URB602. Data were collected in triplicates and expressed**

as the mean ± SEM from three individual experiments and expressed as % control of 4-NPA hydrolysis.

Figure 3.7 clearly shows the liver to be more sensitive to MAGL inhibitors, compared with brain. There is a clear indication of non-specific esterase activity as treatment with inhibitor in the HTS assay is further reduced in the presence of NaF – in all cases. The use of NaF alongside other inhibitors in this graph represents the effects of NaF alone and not an additive or accumulative effect of the inhibitor and NaF compound together. As previously observed, rat brain MAGL shows no effects in the presence of MAFP, the reason for which is still unclear. We also see no effect of URB602 on MAGL activity in either tissues. In liver samples, there is a rank order of inhibition of: MAFP> NaF> ATMFK> URB602.

Protein concentration and incubation time on HTS MAGL activity

After determination of the liver as the best source of MAGL to use in this HTS MAGL assay method, we went further to see the effects of incubation time and protein concentration on MAGL activity, leading to further optimization of the assay.

Tissue was prepared as in **section 3.2.** and diluted to either 1:500 or 1:100 of wet weight volume. MAFP was pre-incubated with enzyme for 15 minutes at 37 °C alongside a concentration curve of NaF, following this the assay was run as previously described. IC_{50} values were then calculated.

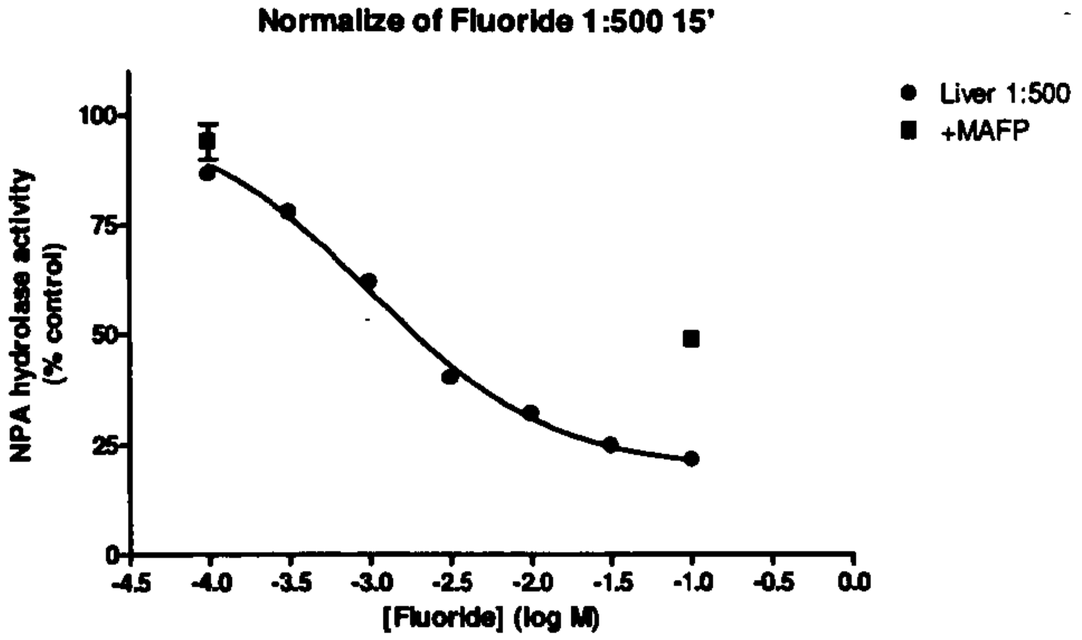

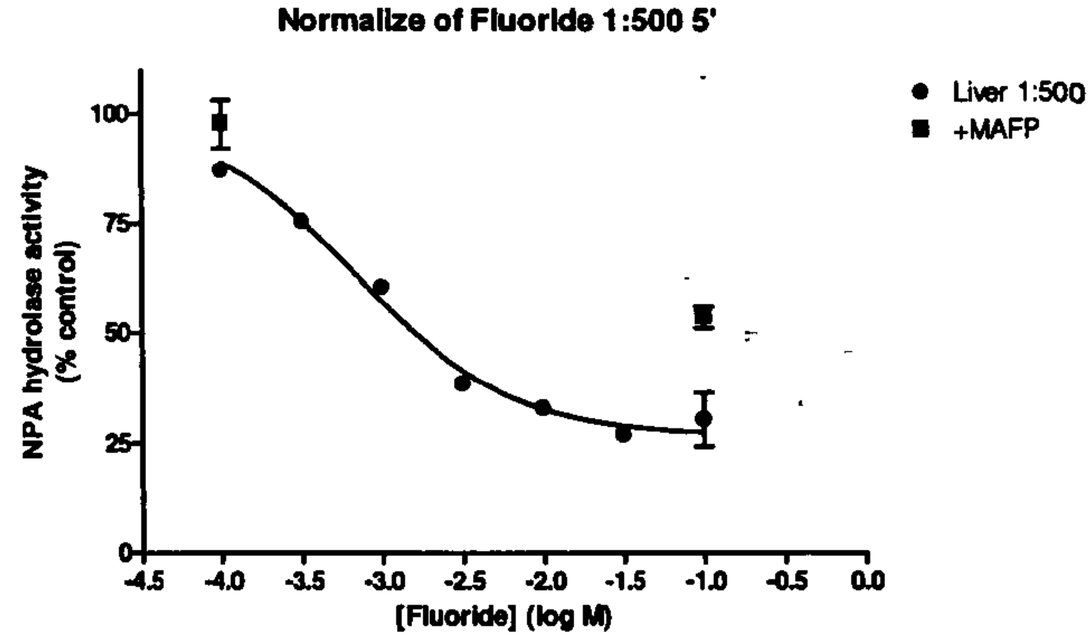

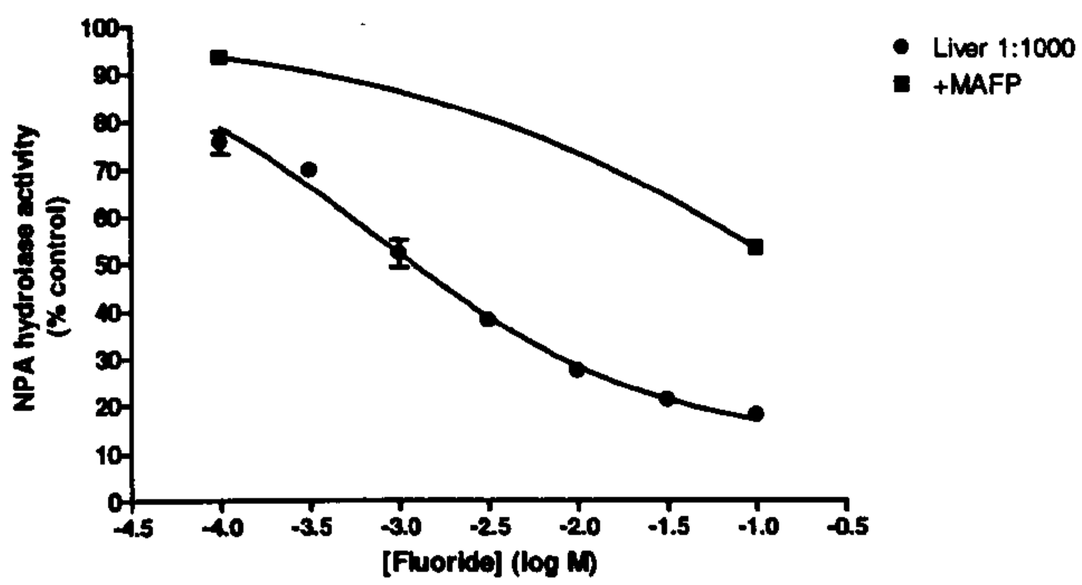

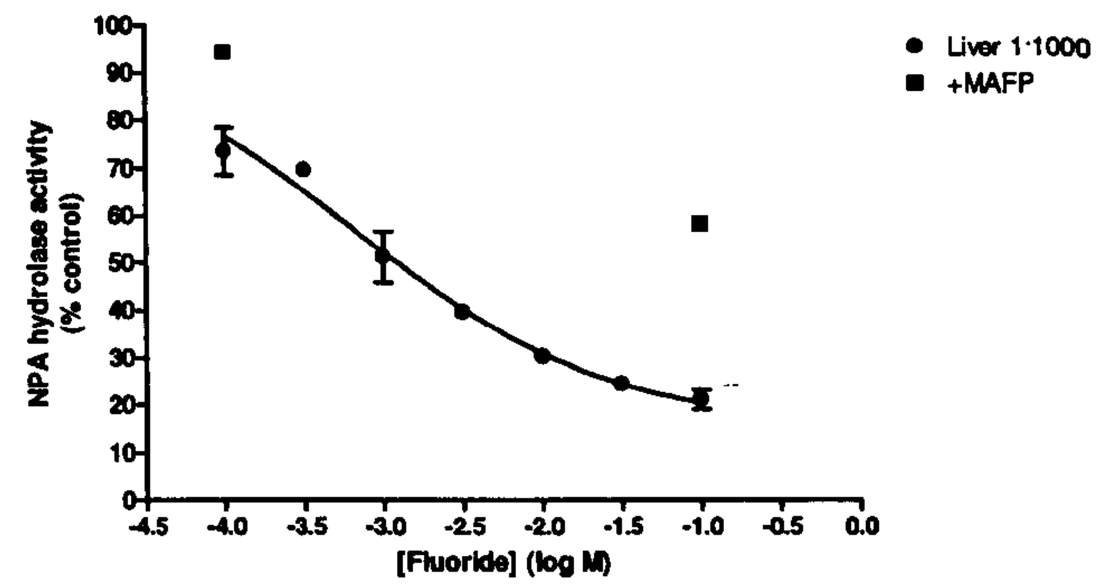

Figure 3.8 **Effect of NaF as inhibitor of 4-NPA hydrolysis in liver cytosol fraction at different dilutions and time points. Data were collected in triplicates and expressed the mean ± SEM of three individual experiments. Data expressed as % control of 4-NPA hydrolysis, with 1 μM MAFP.**

	Liver tissue dilution Log IC_{50}	
	1:500	1:1000
5 min	**-3.16**	**-3.2**
15 min	**-2.99**	**-3.12**

Table 3.4 **Log IC_{50} values for data in figure 3.8 conducted against NaF concentration response curve using liver cytosol fractions at two different dilutions and data extracted at two different time points.**

Results indicate IC_{50} values to be unaffected with increased protein concentration. Such

marginal changes between time and protein concentration allows for choice towards low cost and efficiency. The use of low protein concentration enzyme source will provide more use out of each tissue sample preparation and a 15 minute incubation time will ensure all inhibitory effects of screened compounds to be observed, yet with large compound library screening, it provides the choice of an alternative 5 minute incubation time, to allow screening of more compounds, within the same time frame. Therefore a 15 minute incubation time and 1:1000 enzyme dilutions were chosen for further experiments, unless stated otherwise.

3.2.7 Validation of MAGL HTS assay

To validate the assay, we assessed the effects of two MAGL inhibitors and a MAGL substrate, conducted as concentration response curves.

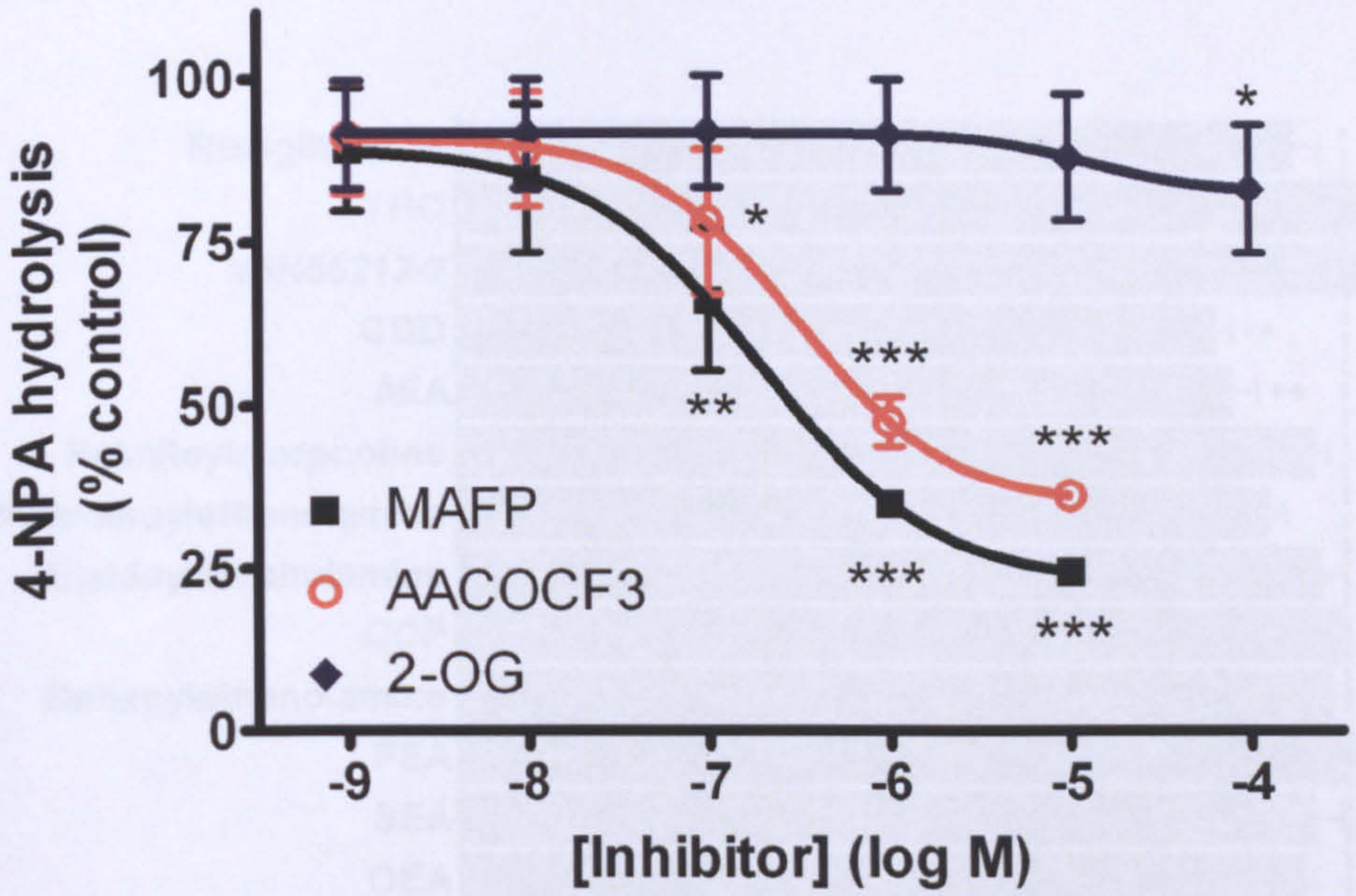

Figure 3.9 **Concentration response curves of MAGL inhibitors on liver soluble fractions. Data collected in triplicates from three individual experiments and expressed as the expressed as % control ± SEM of 4-NPA hydrolysis.**

	MAFP	AACOCF3	2-OG
LOGEC50	**-6.7**	**-6.5**	**>-4**

Table 3.5 **Log EC_{50} values for MAGL inhibitors on 4-NPA hydrolysis.**

The assay displays good sensitivity to inhibitors MAFP and $AACOCF_3$ (**figure 3.9**), with comparable IC_{50} values to literature (Ahn et al., 2008), while 2OG only evoked a

significant inhibition of NPA hydrolysis at 100 μM. In comparison, Ghafouri et al. (2004) observed an log IC_{50} value for 2OG-mediated inhibition of rat brain MAGL activity of 4.9.

3.2.8 Application of MAGL HTS assay: HTS of compounds as potential MAGL inhibitors

The following graphs show results of a high throughput screening of a large group of compounds. MAGL activity is indicated as % of control 4-NPA hydrolysis. For those samples exposed to MAFP, NPA hydrolysis was not different from tissues blanks.

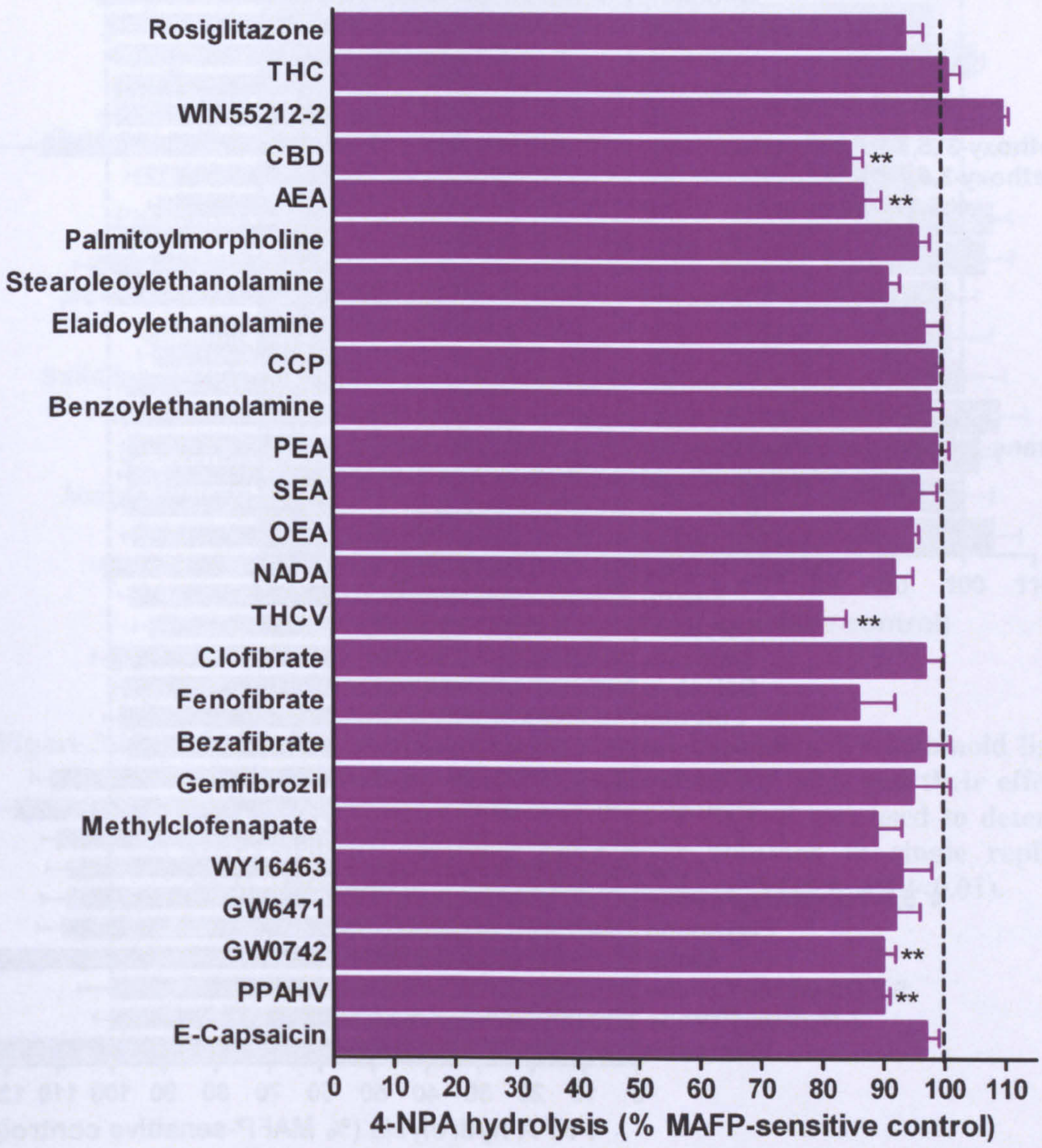

Figure 3.10 MAGL HTS of cannabinoid ligands as potential inhibitors.

Cannabinoid ligands were screened as potential inhibitors at 100 µM, and their effect on MAGL hydrolysis of 250 µM 4-NPA. MAFP was used to determine MAFP-sensitive activity. Data were collected in single replicates (n=4). Data were analysed using one-way AVOVA (P<0.01).**

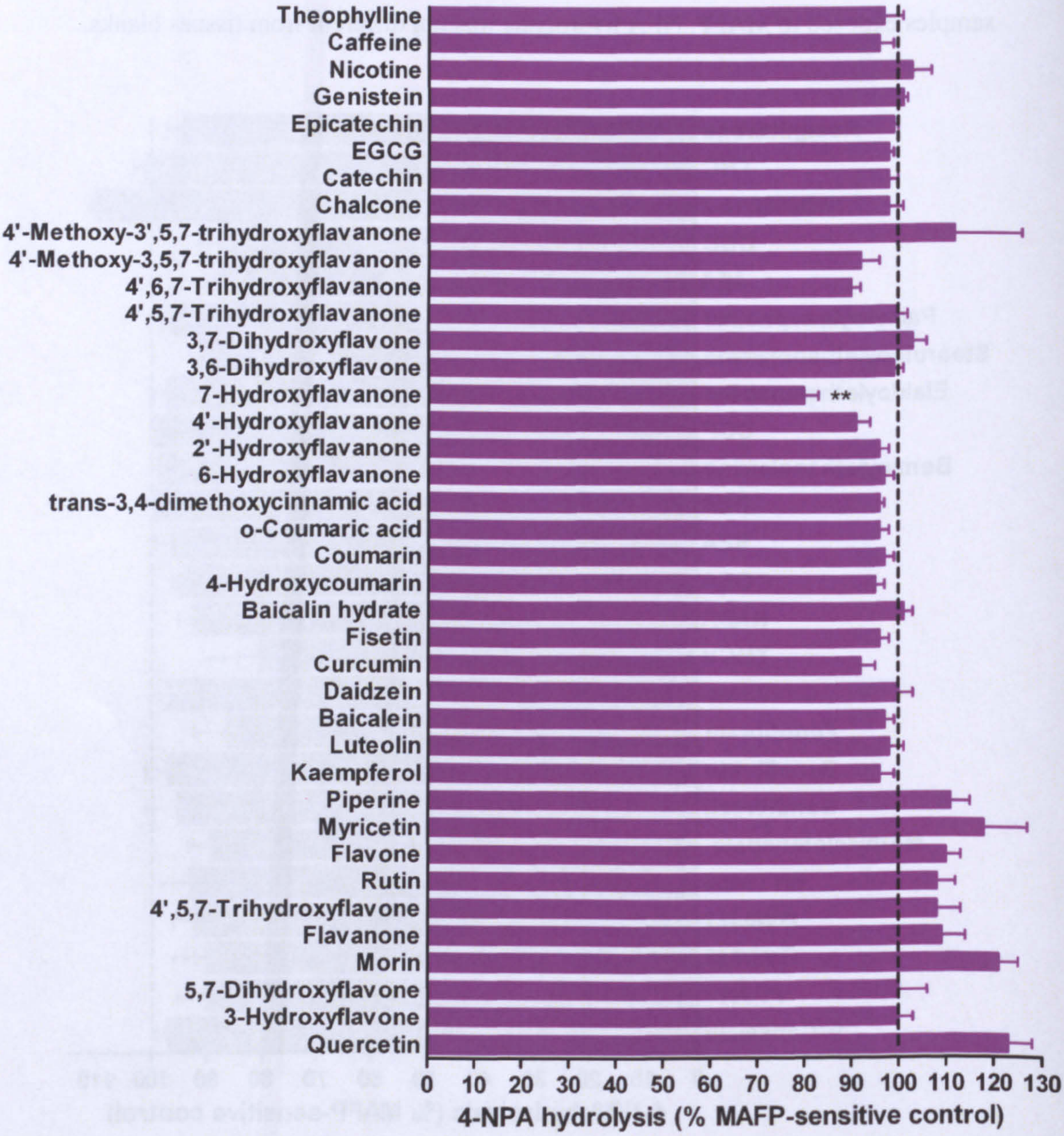

Figure 3.11 MAGL HTS of natural ligands as potential inhibitors. Cannabinoid

ligands were screened as potential inhibitors at 100 µM, and their effect on MAGL hydrolysis of 250 µM 4-NPA. MAFP was used to determine MAFP-sensitive activity. Data were collected in single replicates (n=4). Data were analysed using one-way AVOVA (**P<0.01).

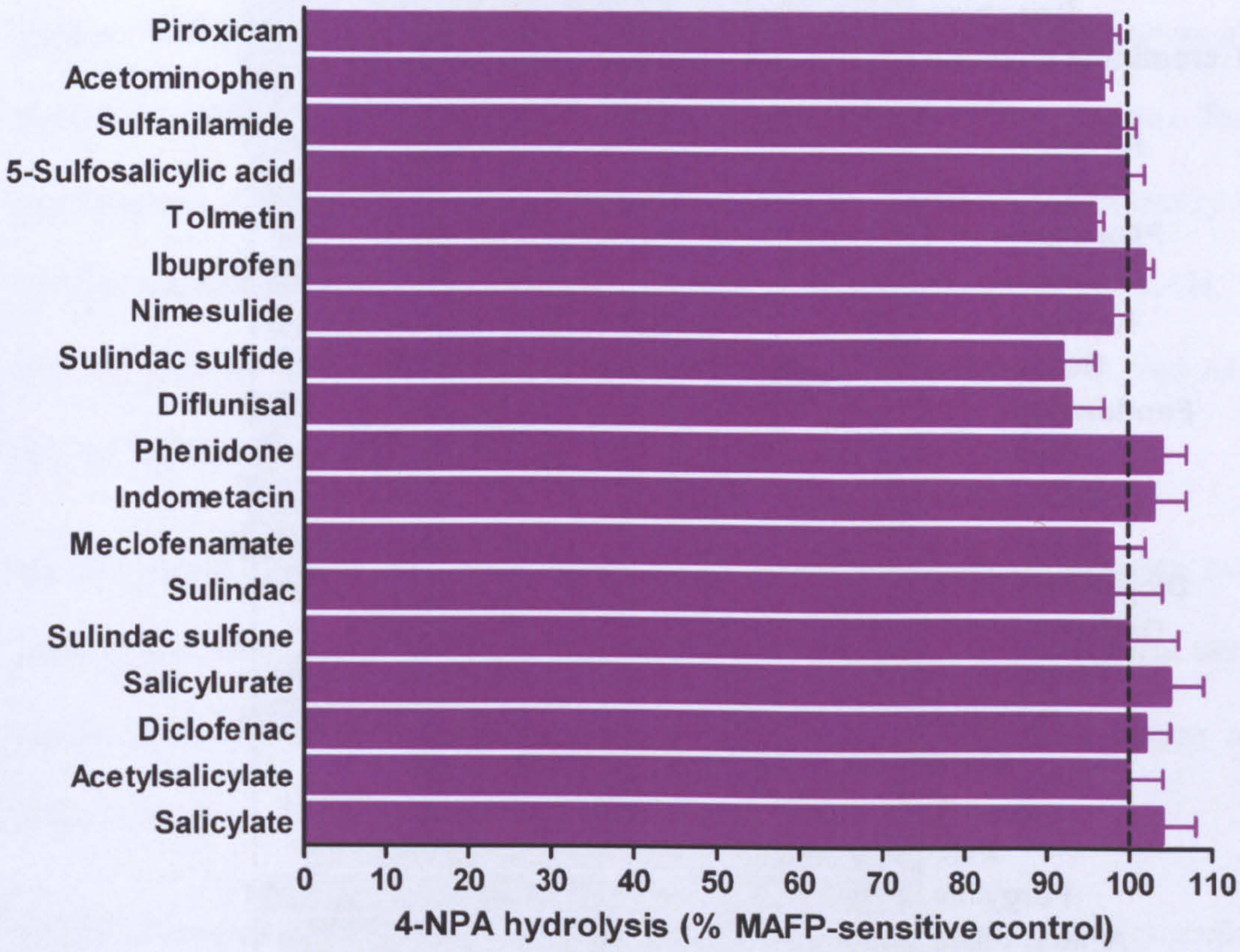

Figure 3.12 **MAGL HTS of NSAIDs as potential inhibitors. Cannabinoid ligands were screened as potential inhibitors at 100 µM, and their effect on MAGL hydrolysis of 250 µM 4-NPA. MAFP was used to determine MAFP-sensitive activity. Data were collected in single replicates (n=4). Data were analysed using one-way AVOVA (**P<0.01).**

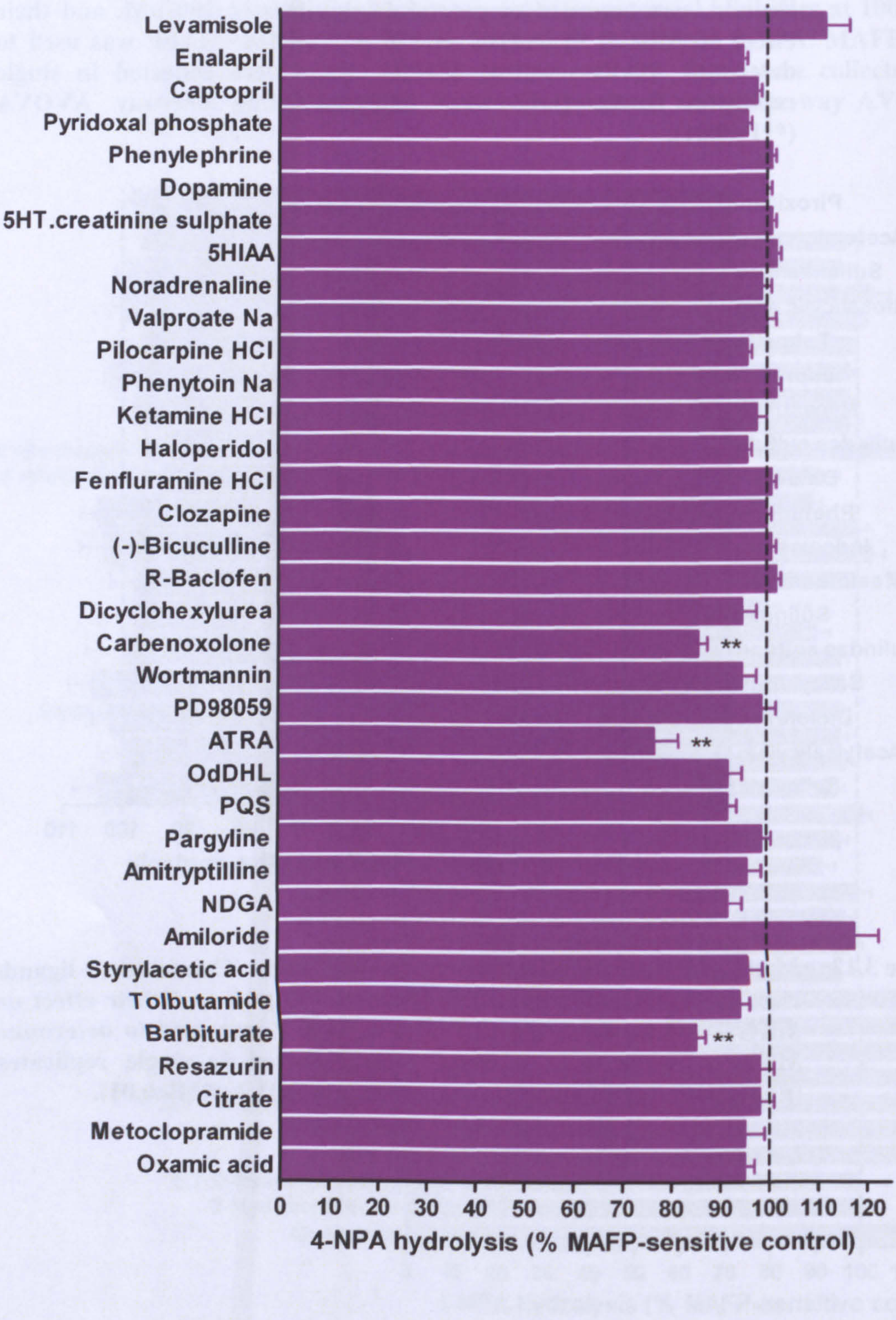

Figure 3.13 **MAGL HTS of miscellaneous compounds as potential inhibitors. Cannabinoid ligands were screened as potential inhibitors at 100 μM, and their effect on MAGL hydrolysis of 250 μM 4-NPA. MAFP was**

used to determine MAFP-sensitive activity. Data were collected in single replicates (n=4). Data were analysed using one-way AVOVA (P<0.01).**

Figures 3.10-3.13 show the majority of compounds to be ineffective as inhibitors of NPA hydrolysis, either in the absence (pictured) or presence of MAFP (not shown). The non-psychoactive cannabinoid compound CBD, THCV and eCB AEA significantly inhibit MAGL activity, but to a much lesser degree compared to their effects on FAAH. THCV was the most effectiveMAGL inhibitor, closely followed by CBD (85 %), and AEA (83 %), PPAHV and GW0742 also caused small, butsignificant inhibition.

Of the natural ligands (**figure 3.11**) only the flavonoid 7-hydroxyflavanone caused a small (70 % control) yet significant MAGL inhibition. There was insufficient inhibition observed by the other natural compounds to allow generation of structure activity relationships.

NSAIDs showed no inhibitory action on MAGL (**figure 3.12**), but a few miscellaneous compounds (**figure 3.13**) inhibited MAGL activity, namely carbenoxolone (86 %), ATRA and barbiturate (85 %).

Overall, this HTS MAGL assay provides a good tool for the identification of potential MAGL inhibitors, in a rapid, inexpensive and facile manner. More conventional and MAGL specific assays would be required to investigate further potential 'hits' identified from this method.

3.2.9 Z-Factor calculation

The Z-factor, as previously mentioned in chapter 2, is a statistical analysis and measure of the size of effect within a given assay. It has been used in high throughput assays, to determine whether the response in an assay is large enough to warrant further attention, and provides an indication of the quality of the assay itself (Zhang et al., 1999). The final Z-factor value reflects both the assay signal dynamic range as well as the data variation associated with the signal measurements and therefore provides a through assay quality assessment. It is a value which clearly aids the process of assay optimization.

Calculation

Calculation of the Z-factor requires input of four parameters, the means and standard deviations of both positive (p) and negative (n) controls (χ_p. σ_p and χ_n. σ_n).

For the positive control values, the rate of reaction of OEA hydrolysis by FAAH in rat liver microsome fractions were used. For the negative control values of rates of reaction of OEA hydrolysis following FAAH incubation with its inhibitor URB597 were used.

These values were obtained using the high throughput screening method as described in this chapter.

Given these values the Z-factor is defined by:

$$\textbf{Z-Factor} = 1 - 3 \times (\sigma_p + \sigma_n) / (\chi_p - \chi_n)$$

Interpretation

Z-Factor	Interpretaion
1.0	Ideal. Z-Factor can never exceed 1.
0.5 - 1.0	Excellent assay.
0 - 0.5	Marginal assay.
less than 0	Too much overlap of positive and negative control for assay to be useful.

HTS MAGL assay calculation

	positive control (ODA)	negative control (URB)
	1.46	0.024
	1.33	0.024
	1.46	0.020
	1.30	0.023
	1.46	0.023
	1.36	0.024
mean	**1.393**	**0.023**
st dev	**0.073**	**0.002**
Z-Factor	**0.84**	

Table 3.2 Z-factor value calculated using data from HTS FAAH inhibitor screening, with the use of 100 µM ODA and 5 µM URB597.

The Z-factor score shows the HTS MAGL assay to be (at least from this parameter) an excellent tool in the screening identification of new potential MAGL inhibitors. Through

interpretation of the Z-factor values from both the FAAH (0.53) and MAGL (0.84) HTS assays, we can determine that the MAGL seems to be stronger, yet we know the FAAH to be more enzyme specific and that 'hits' from the MAGL assay would require follow-up investigations of the compounds using more conventional assays.

3.4 Discussion

4-nitrophenylacetate (NPA) has been identified as a useful substrate for MAG lipase using recombinant enzyme preparations, although hydrolysis by esterases other than MAG lipase in rat tissues limits its usefulness (Muccioli and Stella, 2008). In this chapter, we have identified that NPA can be utilised in a high-throughput screen for MAG lipase from native rat liver enzyme preparations, although there are significant limitations associated with it's use. It is likely that a better methodology would be to make use of human recombinant MAGL as the enzyme source for future inhibitor screening, thereby allowing some assurance of the validity of the assay.

With the development of a selective MAGL inhibitor JZL184 (Long et al., 2009), a growing understanding of the physiological role of MAGL is beginning to emerge and will continue to provide information of its involvement in various pathological states. In turn, there will be an increasing need to identify potential inhibitors of MAGL which may alter its role in the presence of inhibitory ligands, especially endogenously active ones. Therefore such a simple, cheap and facile HTS assay will provide rapid screening of compounds of libraries as well as known compounds, to indicate possible inhibitors for further investigation.

Chapter 4: THE ROLE OF OEA IN FOOD INTAKE AND SATIETY IN THE MOUSE

4.1 Introduction

Phytocannabinoids and synthetic cannabinoids are appetite stimulants through activation of CB1 receptors located in the CNS. Endocannabinoids (eCB) and endocannabinoid-like molecules (eCBL) can also activate CB1 receptors to work in the same way (Guzman et al., 2004). Hence, drugs that can diminish eCB activity at CB1 receptors (for example, rimonabant) provide good appetite suppression and show efficacy in the treatment of obesity and type-2 diabetes (Fu et al., 2005). OEA has been shown to lack binding affinity to CB_1 receptors, which has led to further investigation into the role of endogenous OEA and its involvement in other receptor mechanism pathways. As with other eCB compounds and eCBL molecules, OEA is a naturally occurring lipid thought to be produced on demand. Its synthesis in the GI tract appears to be stimulated upon feeding (Fu et al., 2005), suggesting OEA may participate in regulating satiety. Investigation into OEA's locus of action found that feeding stimulated OEA mobilisation in proximal areas of the small intestine. It was found not to be mobilised in other areas of the gastrointestinal tract, CNS or other peripheral tissues. This mobilisation local of OEA was accompanied by enhanced accumulation of OEA-generating NAPE, increased activity and expression of OEA-synthesising NAPE-PLD, decreased activity and expression of OEA-degrading FAAH (Fu et al., 2007).

As described in **section 1.7** exogenous administration of OEA (20 mg.kg, i.p.) in rats has

been shown to cause a dose-dependant delay in feeding onset of free-feeding animals, without altering meal size or post-meal intervals. OEA also delayed feeding onset in food deprived rats, and reduced meal size (Gaetani et al., 2003). The anorexic effects of OEA do not occur when directly injected into the brain but only when injected i.p (OEA #1), with actions being independent of appetite regulating hormone mechanisms (Proulx et al., 2005), and requiring intact sensory fibres (Gaetani et al., 2003), further indicating a peripheral receptor target. One likely target would be through activation of receptors expressed in the walls of the small intestine sending signals through vagal sensory neurons directly to the hypothalamus to induce satiety (Fu et al., 2005).

PPARα is a nuclear receptor reported to be highly expressed in the small intestine in close proximity to the vagal sensory neurone and is known to be involved in the handling of fats in the blood and liver (Fu et al., 2005). PPARα agonists, such as fenofibrate, lower triglyceride levels in blood and also have beneficial effects on cholesterol, yet they have not been reported to affect appetite. OEA exhibits a nanomolar-range binding affinity for PPARα, this may therefore account for the effects of OEA on appetite (Fu et al., 2003). OEA, in vivo and in vitro, behaves as a PPARα agonist by decreasing natural lipid content in hepatocytes by enhancing fatty acid oxidation, reducing serum cholesterol and reducing triglyceride levels (Guzman et al., 2004) as well as reducing food intake, effects that are not observed in PPARα$^{-/-}$ rats (Fu et al., 2003).

An alternative explanation for the role of OEA in the regulation of food intake may be through the entourage effect. This hypothesis suggests that OEA, as well as other eCBL molecules have indirect effects on CB1 receptors by diverting the hydrolytic activity of FAAH, thereby leading to an accumulation of canonical eCB molecules (Mechoulam et

al., 1997), potentially activating CB1 receptors.

Given these alternatives, we have attempted to investigate the nature of OEA influences on feeding behaviour, making use of pharmacological and genetic models, as well as analytical methods, to determine the locus of action of OEA.

4.2 OEA dose response and locomotor activity effects in mice

4.2.1 Introduction

Cannabinoid compounds are known to produce unwanted physiological responses, such as the psychotropic effects of cannabis, alterations in cognition and memory, sedation and immobility. These are thought to be largely mediated by the CB_1, and to a lesser extent CB2 receptors (Sun et al., 2007) (Howlett, 1995). The eCBL compounds, such as OEA, are structurally related to cannabinoids, yet have been described not to activate CB receptors (Fu et al., 2003) (Fu et al., 2005). There is still much to be learnt of the receptor targets and subsequent physiological effects exerted by the eCBL compounds.

In the literature, previous doses of OEA administered intraperitoneally to mice and rats have ranged from 10-15 mg/kg (Thabuis et al., 2008). Here we investigate the effect of a range of doses of OEA on sedation, locomotor activity and other behavioural effects prior to investigating the effects of OEA on food intake.

4.2.2 Method

Eight C57bl6 male adult mice were given i.p injections of 1, 10 and 20 mg/kg OEA and vehicle (5% Tween 80, 5% PEG 300, 90% sterile saline), on a 7 day cycle. Mice were on a 12 hour dark:light cycle and were dosed at 4 hours into the dark phase. They were then placed in individual LMA Perspex boxes and the distance moved by each mouse was electronically measured electronically for 60 minutes.

LMA equipment

Each mouse was placed into a 30 cm x 60 cm clear Perspex box with a solid coloured digitising base. Above each box was a video camera linked (live) to a computer to track the movement of each mouse. Tracking of the animal was achieved by the computer calculating the difference between two sequential pictures, taken 10 - 15 frames per second. The differences add up to provide the total distance moved by the mouse.

4.2.3 Results

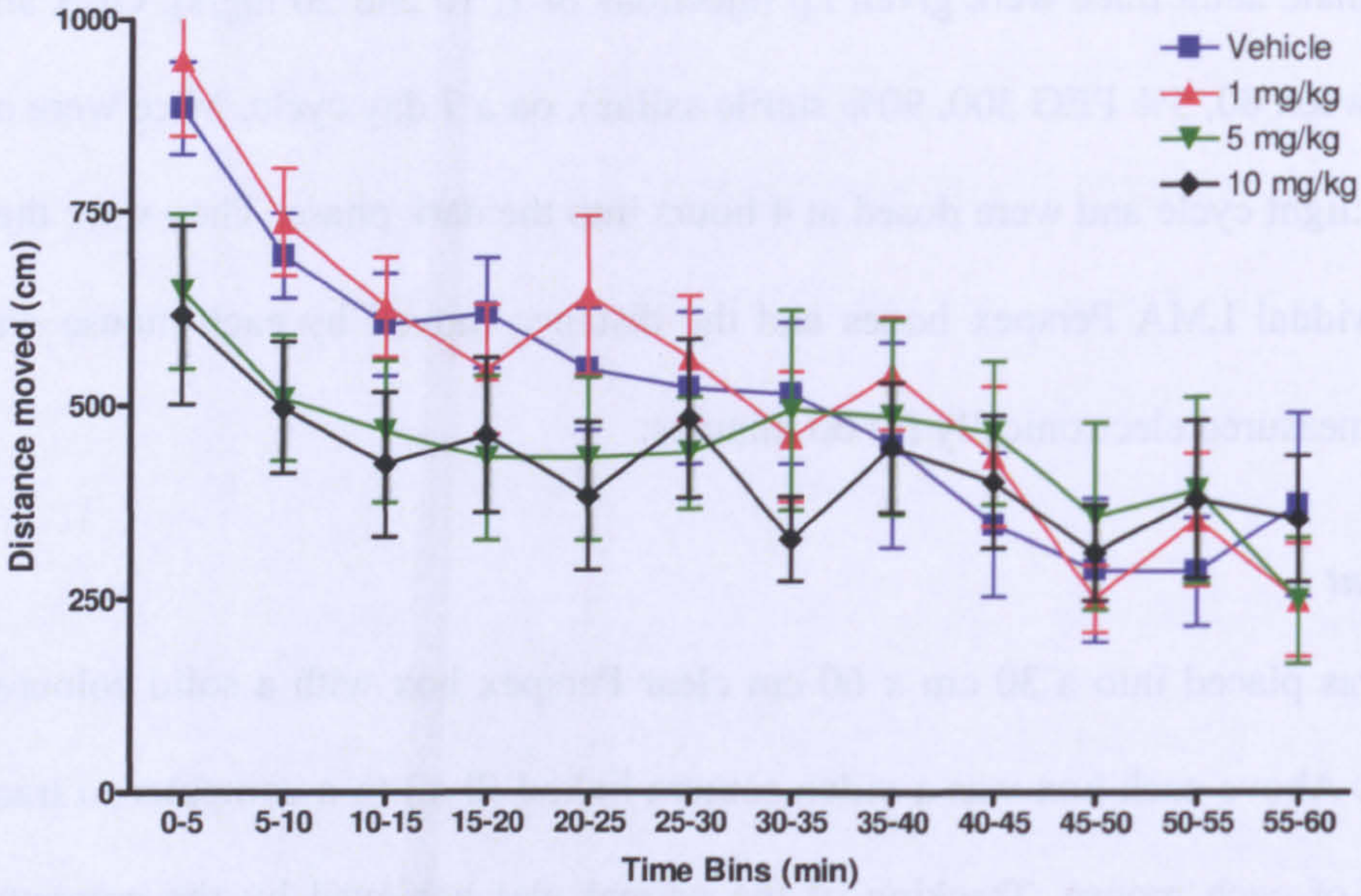

Figure 4.1 Dose dependant effects of OEA on locomotor activity. Eight C57bl6 adult male mice, counted from point of injection in 5 minute time bins up to 60 minutes post-injection. Data were analysed using two-way ANOVA with Bonferroni's post-hoc test.

There was a small, non-significant reduction in activity evoked by OEA compared with vehicle treatment at early time points following injection. For all treatments, including vehicle, there was a decline in locomotor activity following injection.

The mice achieved a steady state level of activity 45 minutes post-injection. .

4.2.4 Discussion

The locomotor activity observed post-injection with vehicle and 1 mg/kg OEA is probably associated with the disturbance and discomfort associated with the injection. The lower levels of locomotor activity observed at doses of 5 and 10 mg/kg OEA suggest

that these doses are not painful {Wang, 2005 13076 /id}, and in fact may actually evoke analgesia or sedation. All sedative effects of cannabinoids previously described have involved CB receptor-mediated mechanisms (Howlett *et al* 1995). There is no evidence in the literature highlighting any sedative effects caused by eCB or eCBL compounds through non-CB receptor-mediated mechanism pathways.

There was no significant difference between the doses of OEA in observed behaviour and locomotor activity. These doses were, therefore, investigated for effects on the reduction of food intake .

4.3 Dose dependant effects of OEA on food intake

4.3.1 Introduction

OEA (10 mg/kg, i.p.) was observed to significantly reduce food intake over 0-12 hours in PPARα$^{+/+}$ mice and not in PPARα$^{-/-}$ mice (Lo Verme et al., 2005). It has been suggested that OEA's effects on feeding are short lived suggesting OEA is rapidly eliminated after systemic administration (Piomelli, 2003). Measured OEA plasma levels in free-feeding rats, following a single acute i.p. injection of 5 mg/kg OEA showed OEA concentrations to sharply increase and return back to baseline levels within 60 minutes post-injection, where there were significant differences between test and control values for up to 30 minutes but not 60 minutes (Piomelli, 2003). This reflects the rapid distribution and catabolism of OEA by eCBL hydrolysing enzymes. OEA has also been described to show a dose dependant relationship (5, 10, 20 mg/kg) with latency of feeding, with no change

in meal sizes or post meal intervals, as well as a reduction in meal frequency with the higher doses of OEA (10 and 20 mg/kg) (Lo Verme et al., 2005).

In this next section, I have examined the effects of a range of OEA doses on parameters of food intake, latency of feeding, post meal intervals, activity, oxygen consumption and respiratory quotient.

4.3.2 Methods

Animals

Experimental animals were obtained from a colony of C57bl6 strain mice, maintained at the University of Nottingham BMSU, Medical School. They were housed in individual cages under controlled temperature (21˚C) and light (12 hr light, 12 hr dark cycle; lights off at 16:00). All animals had ad libitum access to food intake and water. All animal procedures were approved by the University of Nottingham Local Ethical Review Committee and were carried out in accordance with the Animals Scientific Procedures Act (UK) 1986.

CLAMS: OxyMax comprehensive lab animal monitoring system

This is a metabolic closed-circuit metabolic system consisting of eight calorimetric chambers capable of simultaneously monitoring eight mice individually. It is able to measure, non-invasively, several physiological and behavioural parameters. This study focussed on total feeding, feeding bouts, total activity counts, oxygen consumption, carbon dioxide consumption and hence respiratory quotients. These parameter measurements are linked to automated computerised recordings using *OxyMax* software

collecting recordings every 6-8 minutes. All measurements were taken at an ambient temperature of 21–22°C.

Picture 1: This picture displays the CLAMS setup as used in the following experiments described in this chapter. There are eight Perspex boxes all in a closed metabolic measurement system. Each animal setup is completely sealed so all metabolic gases, waste and food intake are accurately measured through computerised calibration systems. Data on those parameters as well as all movement and activity are electronically transferred and available for analysis.

Oxygen consumption (VO_2):

VO_2 for each chamber is calibrated to the relative change in pressure following the removal of carbon dioxide and water from the system using soda lime. VO_2 was measured as ml O_2 per minute per kilogram metabolic body weight (ml/min/$kg^{0.75}$). The system was operated with an air intake of 0.6 litres/min per chamber, and an extracted outflow of 0.4 litres/min.

Respiratory Quotient (RQ)

RQ was calculated from the ratios of measured oxygen consumption and the amount of

carbon dioxide removed from the closed-circuit system using soda lime.

Total activity

Infra-red lasers crossing the Y, X and Z axis allow monitoring of a complete range of movement by the mouse within the chamber, including running, rearing and sleeping. Activity was recorded when two or more consecutive infrared beams positioned approximately 2 cm apart were broken. Total activity counts were assessed over the 0-24 hour period post injection.

Feeding

Each chamber holds a food hopper positioned in the middle of the chamber containing ground chow and linked to a digital scale with information automated fed into *OxyMax* computer software, where all removal of food was recorded. Parameters measured included total food intake, meal frequency and duration of feeding bouts and food consumption per bout. A bout of food intake (meal) was defined as an intake of greater than 0.02 g. Water was provided by dropper bottles, but water intake was not recorded.

Picture 2: The above picture shows the food hopper which is independently filled and put in place on the base containing a digital scale, measuring the food hopper contents, with the

Perspex metabolic box sealed and fitted over the food hopper with it entering inside the box providing a small space allowing for the mice to scurry food out of the hopper. Food which the mice do not eat can only fall back on the food hopper and nowhere inside the Perspex box, giving a constantly accurate measure of the direct food intake of the mouse in that box.

Experimental procedure

Eight adult male mice were separated into four treatment groups, where all mice received all treatments over a period of four weeks (allowing for a drug washout period) in a pseudo random order, allowing each mouse to act as its own control. The mice were placed into individual CLAMS chambers for a 24 hour habituation period pre-dosing. They were then injected (10 μL/g, i.p) with their respective doses at the onset of the dark phase and then placed back into their respective CLAMS chambers and all parameters were measured for a further 24 hour period. Vehicle was 5% Tween 80, 5% PEG 300, 90% sterile saline.

	Group 1		Group 2		Group 3		Group 4	
→ mouse	**1**	**2**	**3**	**4**	**5**	**6**	**7**	**8**
Week 1	Vehicle		OEA (1 mg/kg)		OEA (5 mg/kg)		OEA (10 mg/kg)	
Week 2	OEA (10 mg/kg)		Vehicle		OEA (1 mg/kg)		OEA (5 mg/kg)	
Week 3	OEA 5 mg/kg)		OEA (10 mg/kg)		Vehicle		OEA (1 mg/kg)	
Week 4	OEA (1 mg/kg)		OEA (5 mg/kg)		OEA (10 mg/kg)		Vehicle	

Table 4.1 **The experimental dosing plan of all eight mice in a pseudo-random order with varying doses of OEA over four weeks.**

Statistical analysis

Measurement of food intake, activity, VO_2 and RQ

The doses of OEA were compared with vehicle treatments using repeated measures ANOVA by a Dunnett's procedure for post-hoc comparisons between groups of treatments.

All data shown in this section were collected from eight individual animals, unless stated otherwise.

4.3.3 Results

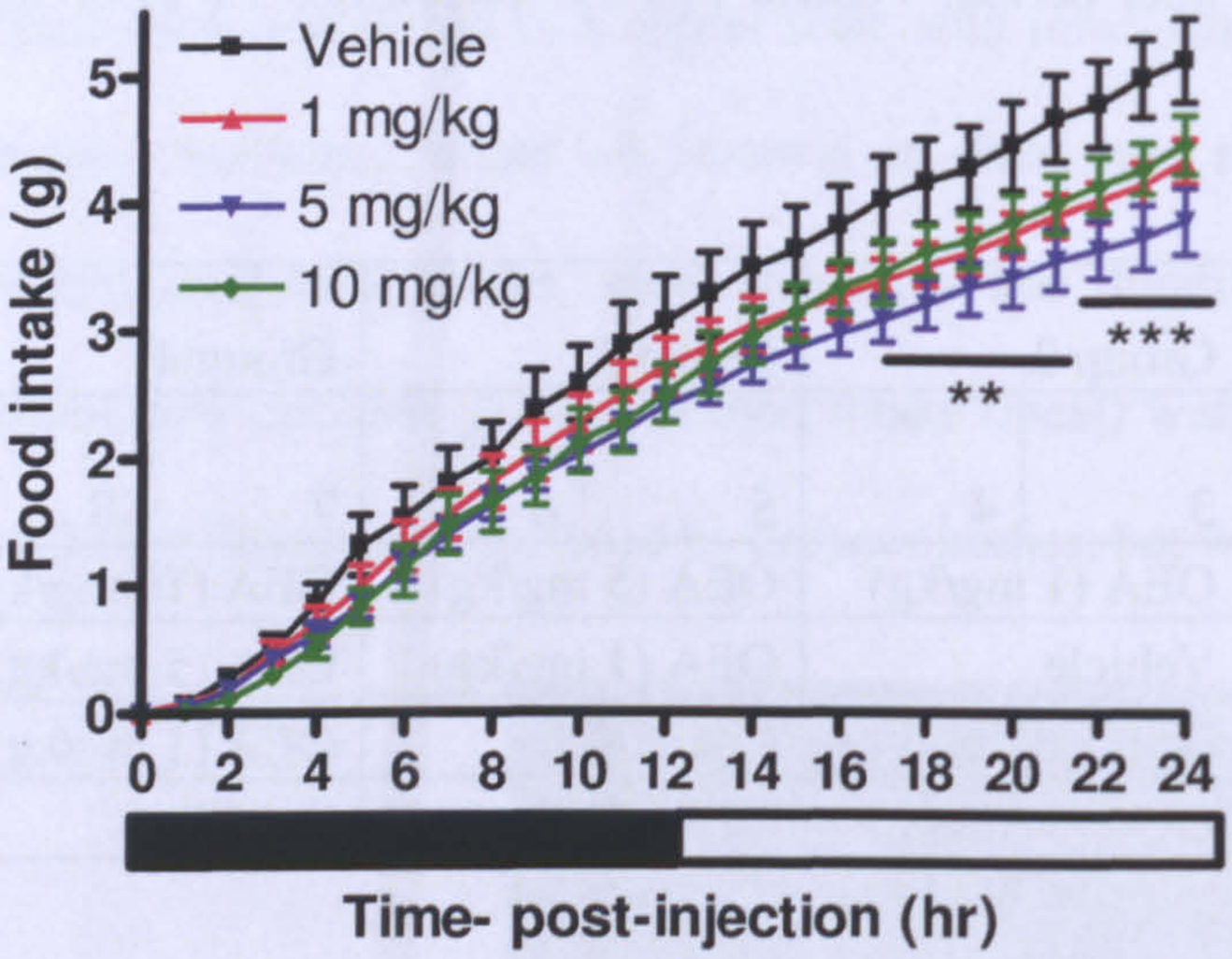

Figure 4.2 **Cumulative food intake for 0-24 hours post-injection. Mice treated with 1, 5, 10 mg/kg OEA and vehicle (n=8). The bars below the graph indicate 12 hour dark and light phase. 0-24 hour data were analysed comparing OEA treated against vehicle, using two-way ANOVA with Bonferroni's post-hoc test.**

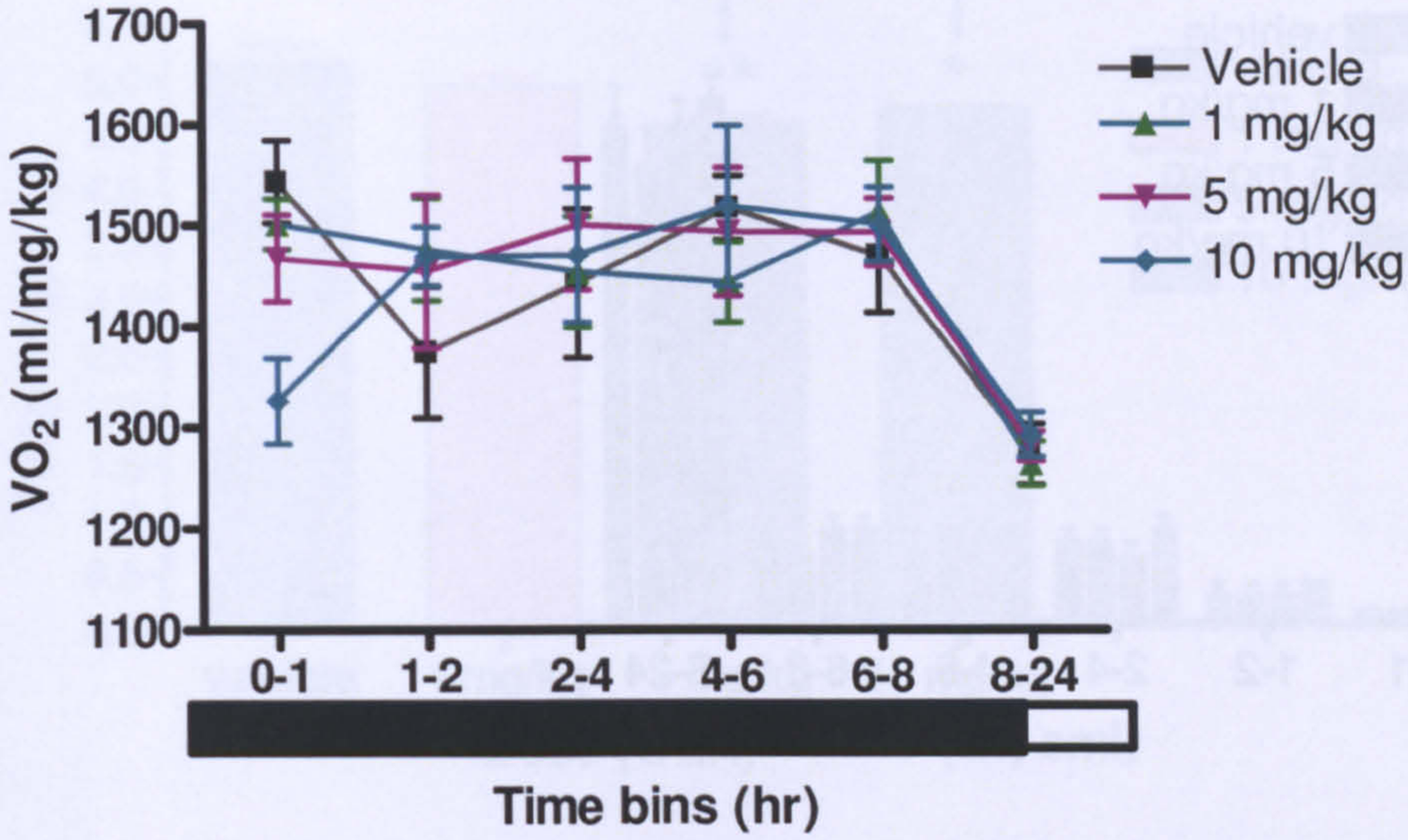

Figure4.3 **Oxygen consumption of mice 0-24 hours post-injection. Mice treated with 1, 5, 10 mg/kg OEA and vehicle (n=8). Data were grouped into 6 time bins and were analysed using two-way ANOVA with Dunnett's Post-hoc test.**

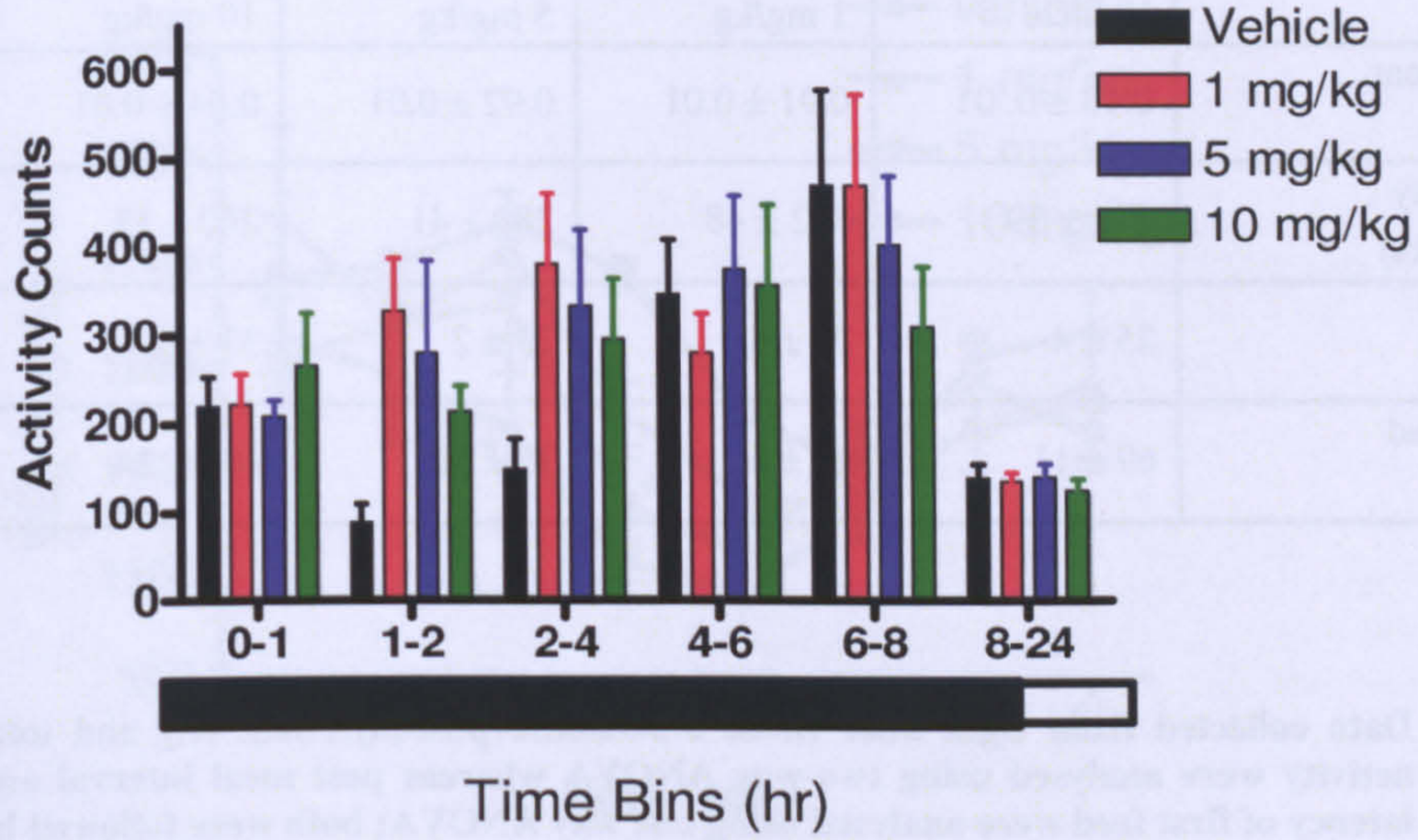

Figure 4.4 **Locomotor activity 0-24 hours post-injection. Activity measured in eight mice (n=8) in 6 time bins over 0-24 hour period. Data were analysed using two-way ANOVA with Dunnett's post-hoc test.**

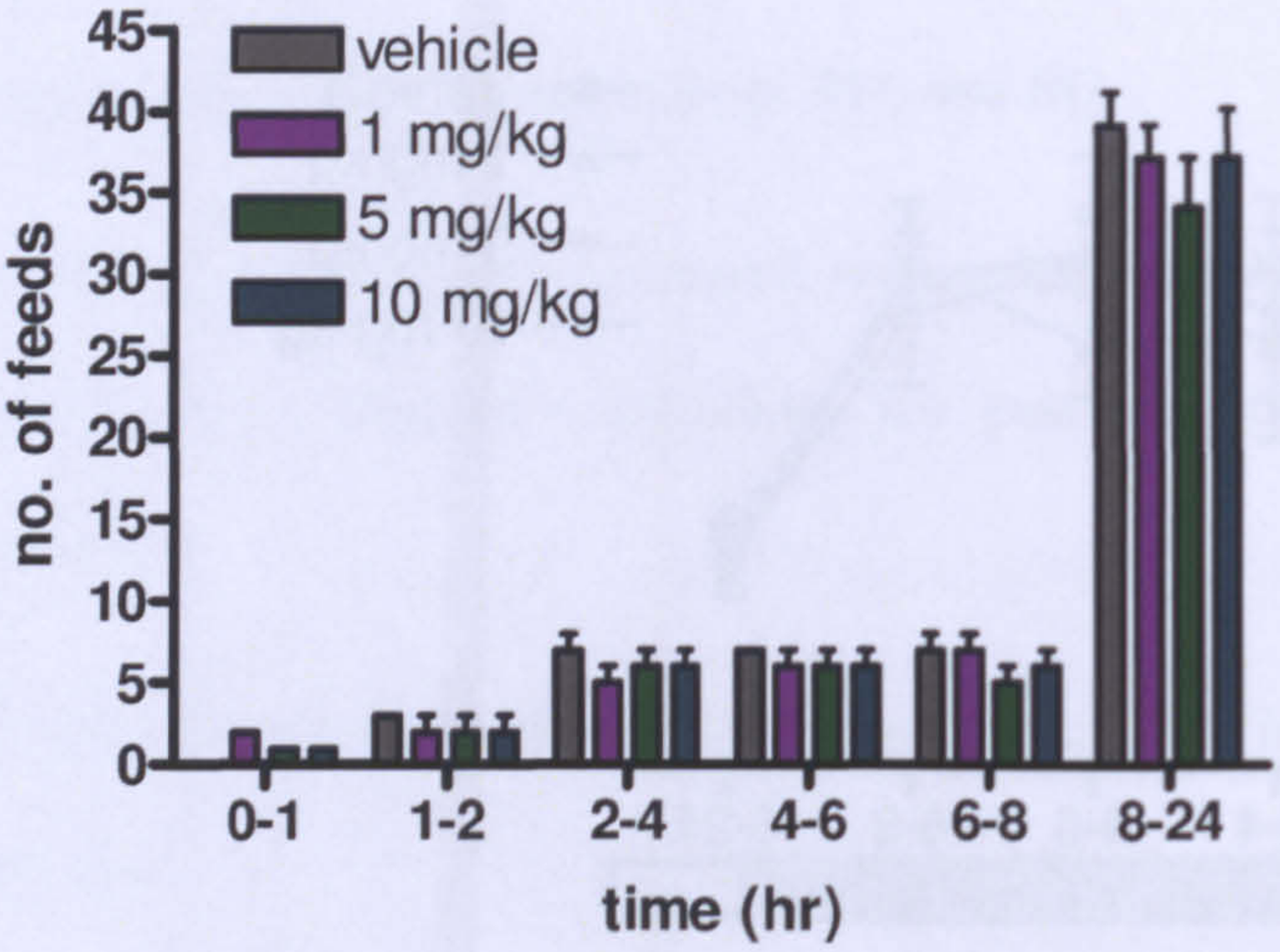

Figure 4.5 **Feeding bouts in eight mice (n=8) over the 24 hours following injection. Data were analysed using one-way ANOVA with Dunnett's post-hoc test.**

	OEA			
	Vehicle	1 mg/kg	5 mg/kg	10 mg/kg
Respiratory Quotient (mg/kg/hr)	0.93 ± 0..01	0.91 ± 0.01	0.92 ± 0.01	0.94 ± 0.01
Locomotor Activity (no. of beam breaks)	235 ± 59	302 ± 48	289 ± 41	260 ± 33
Post meal interval (min)	25 ± 4	27 ± 4	29 ± 2	33 ± 9
Latency of first feed (min)	69 ± 11	33 ± 6	71 ± 17	104 ± 24

Table 4.2 **Data collected from eight mice (n=8) 0-24 hours post-injection. RQ and total activity were analysed using two-way ANOVA whereas post meal interval and latency of first feed were analysed using one way ANOVA; both were followed by Dunnett's post hoc test.**

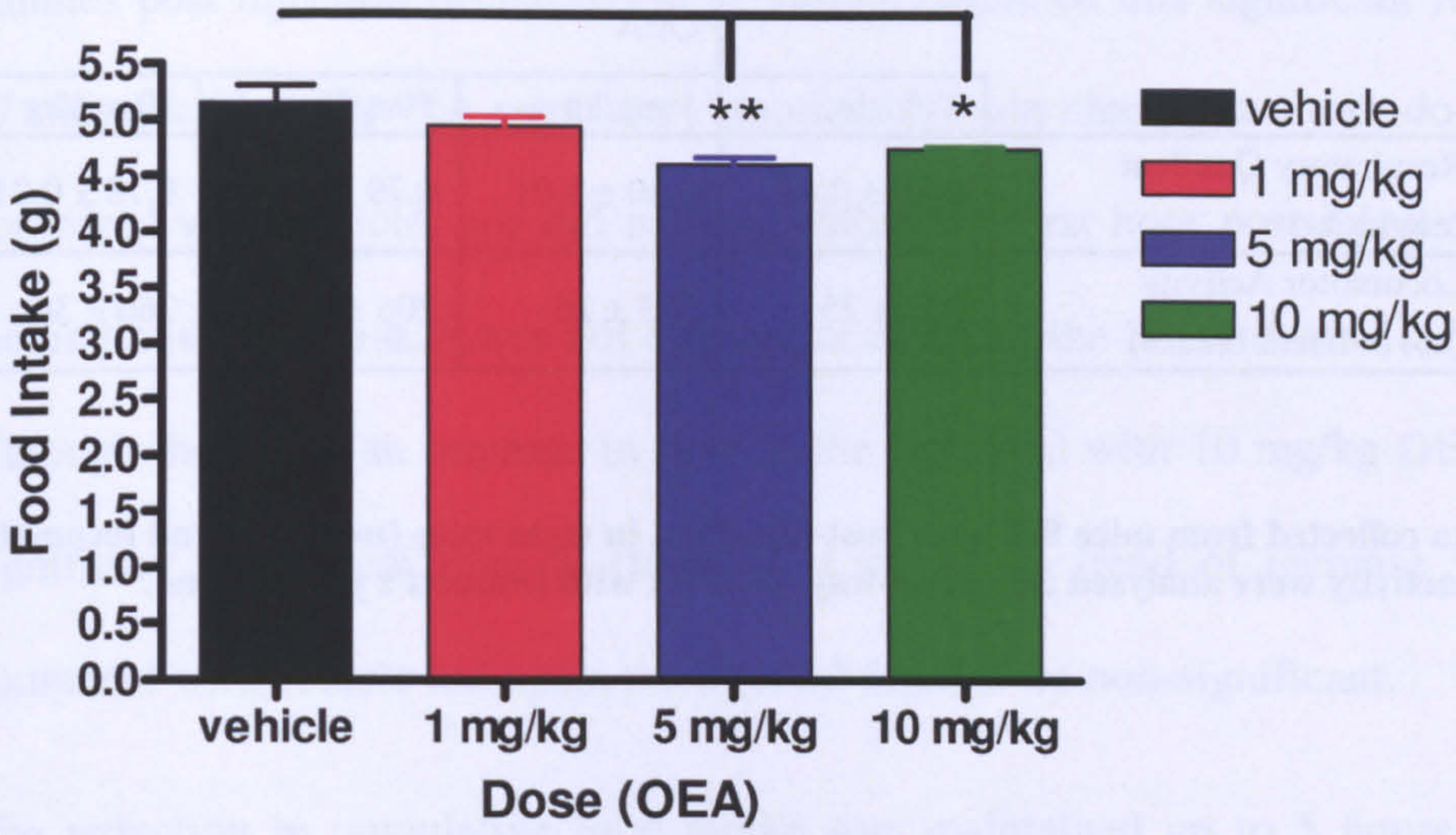

Figure 4.6 **Food intake for the first hour following injection, in eight mice (n=8). Data were analysed using one-way repeated measures ANOVA.**

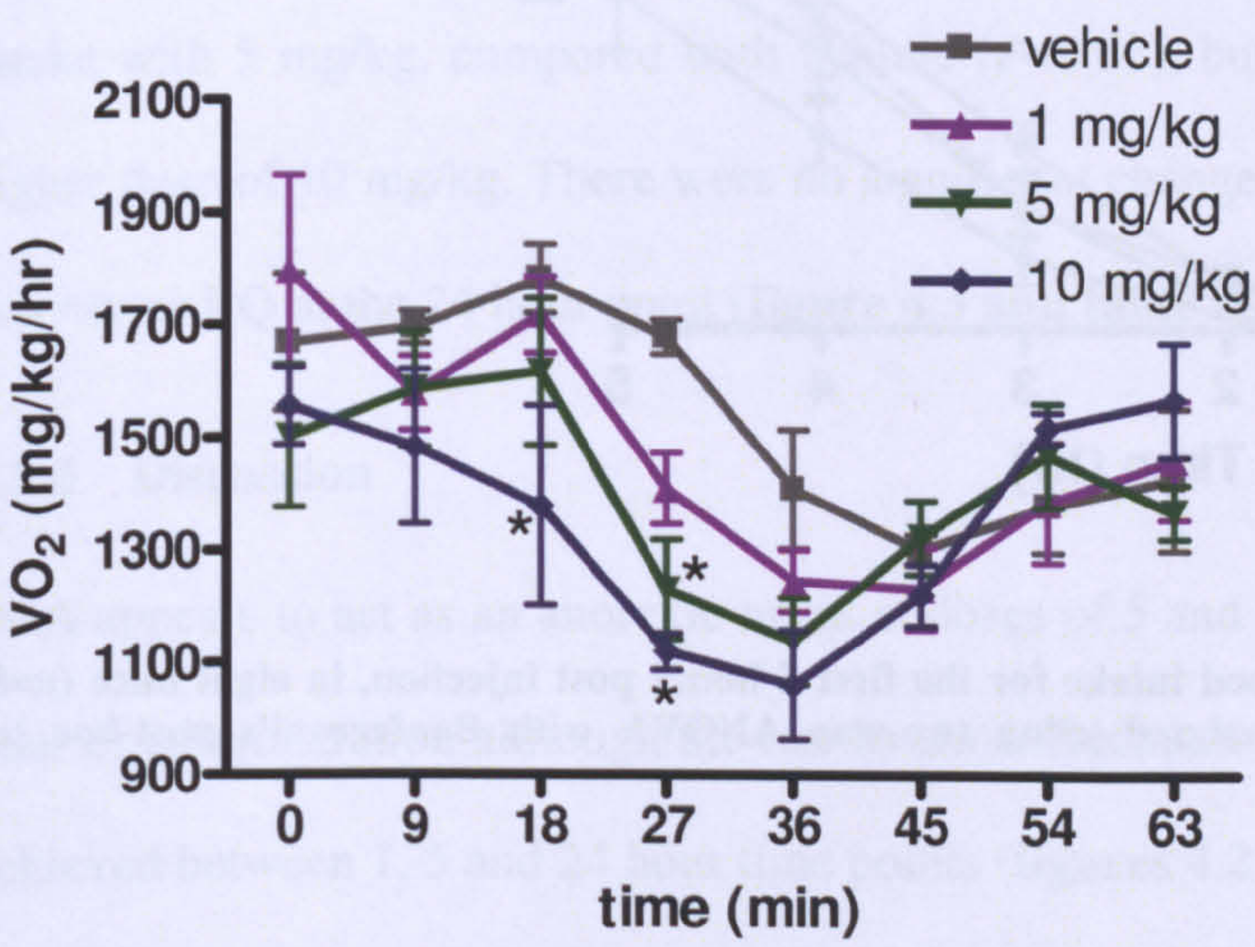

Figure 4.7 **Oxygen consumption for the first hour post-injection, in eight mice (n=8). Data were analysed using two-way ANOVA with Bonferroni post-hoc test.**

		OEA		
	Vehicle	1 mg/kg	5 mg/kg	10 mg/kg
Respiratory Quotient (mg/kg/hr)	0.80 ± 0.01	0.80 ± 0.01	0.79 ± 0.01	0.78 ± 0.01
Locomotor Activity (no. of beam breaks)	237 ± 25	223 ± 26	206 ± 19	266 ± 36

Table 4.3 Data collected from mice 0-1 hour post-injection, in eight mice (n=8). RQ and locomotor activity were analysed using two-way ANOVA with Dunnett's post hoc test.

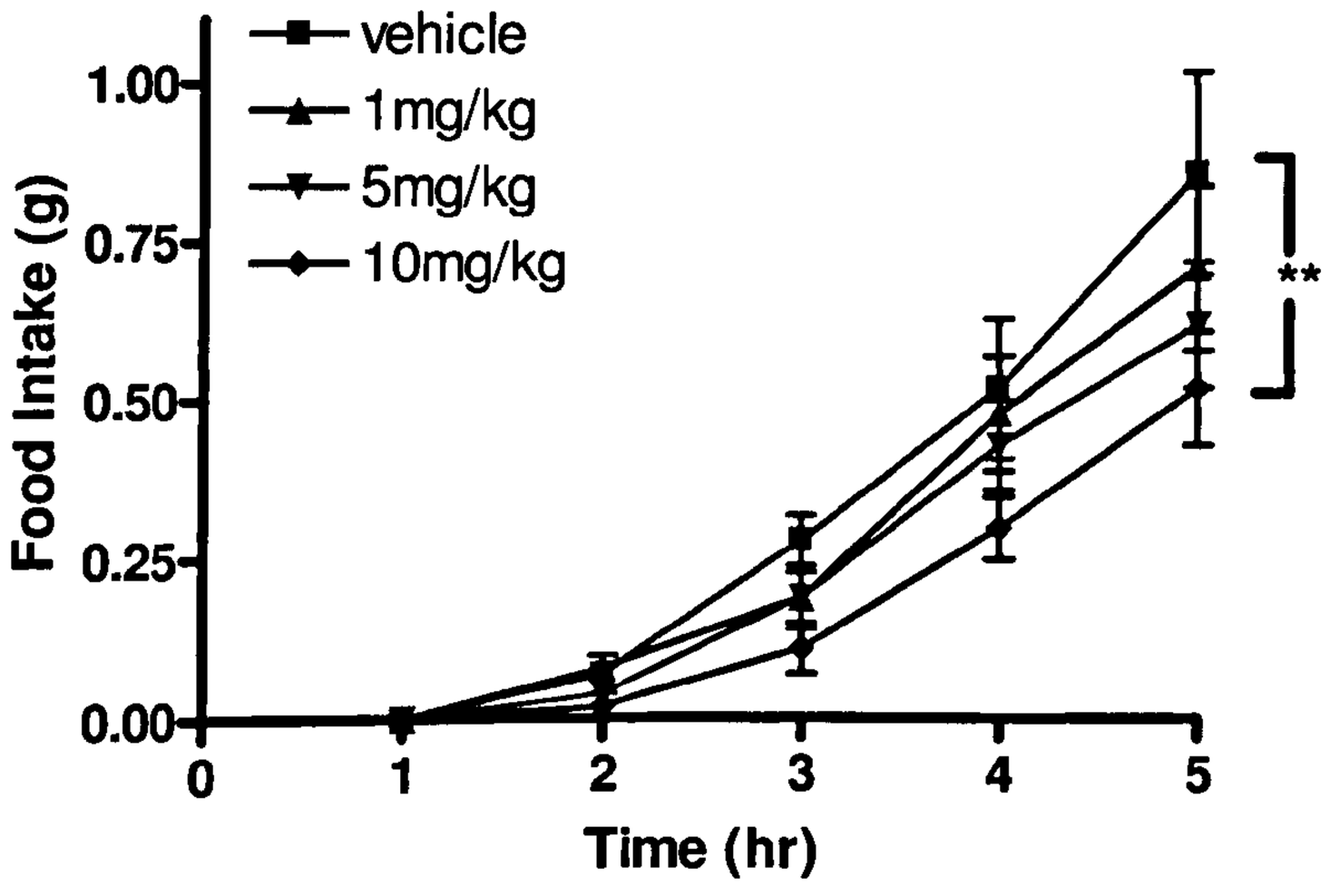

Figure 4.8 **Cumulative food intake for the first 5 hours post injection, in eight mice (n=8). Data were analysed using two-way ANOVA with Bonferroni's post-hoc test (**P<0.01).**

OEA significantly reduced food intake at doses of 5 mg/kg and 10 mg/kg, in the first hour (**figure 4.6**) following administration compared with vehicle treated animals ($P<0.01$ and $P<0.05$ respectively). This coincided with an acute reduction in VO2 at both doses (**figure 4.7**), where the dose of 5 mg/kg evoked a significant reduction at 18

minutes post injection ($P<0.05$) and 10 mg/kg sustained this significant reduction up to 27 minutes ($P<0.05$) The respiratory quotient did not change at either dose (**table 4.3**), compared with vehicle, nor did activity within the first hour post-injection. Latency of feeding onset (**table 4.2**) was not affected at either of the lower doses (1, 5 mg/kg OEA) although there was an increase in time to the first feed with 10 mg/kg OEA, albeit non-significant. Post meal interval (**table 4.2**) showed a trend of increase with all doses compared with vehicle but again the interval times were non-significant.

The reduction in cumulative food intake was maintained up to 5 hours post-injection (**figure 4.8**) with the highest dose of OEA (10 mg/kg; $P<0.01$) yet 5 mg/kg OEA did not maintain its significant reduction, indicating a transient effect of OEA on food intake. Results up to 24 hours post-injection (**figure 4.2**) show a significant reduction in food intake with 5 mg/kg, compared with vehicle ($P<0.05$), but this was not shown with the higher dose of 10 mg/kg. There were no significant changes observed in VO2, locomotor activity or RQ at the 24 hour point (**figure 4.3 and table 4.2**).

4.3.4 Discussion

OEA appears to act as an anorexic agent at doses of 5 and 10 mg/kg (i.p.) within the first hour of administration although the results show fluctuations in the levels of significance achieved between 1, 5 and 24 hour time points (**figures 4.2** and **4.8**).

OEA at 5 mg/kg reduced food intake more significantly than 10 mg/kg with effects observed only up to one hour post-injection. 10 mg/kg OEA's effects lasted up to 5 hours. At 24 hours post-injection, OEA at 5 mg/kg and not 10 mg/kg was able to significantly reduce food intake, compared with vehicle.

Despite the higher level of significant reduction in food intake observed with 5 mg/kg OEA compared with 10 mg/kg, in the first hour post-injection (**figure 4.2**), there was not much difference in levels of food intake between both doses. Results suggest a dose of 10 mg/kg OEA to be more effective in the reduction of food intake as it maintained its significant reduction up to 5 hours post-injection (**figure 4.8**).

These results support literature that suggests OEA's actions to be transient due to its rapid catabolism by eCBL hydrolysing enzymes (Rodriguez de Fonseca et al., 2001).

Mice were injected at the onset of the dark phase to ensure regular feeding patterns, where food intake is higher in the dark phase than the light.

The level of significant reduction in food intake achieved by 5 mg/kg OEA and not 10 mg/kg at 24 hours post-injection (**figure 4.2**), may be due to compensatory effects in the reduction of food intake up to the 5 hours point with the dose of 5 mg/kg (**figure 4.8**), which may have caused an overall increase (above significance) at the 24 hour point.

No significant change was observed in parameters of VO2, locomotor activity and RQ at 24 hours post injection (**figure 4.3** and **table 4.2**), suggesting the effects of OEA are diminished by this time point, presumably due to its catabolism. The only significant effect we observed as a result of OEA administration is in the acute reduction of VO2 at 18 and 27 minutes following injection (**figure 4.3**). As all other measured parameters showed no change at this time point compared with vehicle values, it is difficult to determine the mechanism of action that has caused this acute reduction in VO2. OEA showed no change in RQ or locomotor activity throughout the 24 hours following injection (**table 4.2**) alongside no significant change in latency of feeding onset and number of feeds (**table 4.2**), strongly suggesting that the OEA-evoked response on food

intake is not a result of a change in the animals basal metabolic rate, but supports a mechanism involving direct signalling to the satiety centre resulting in the reductions of food intake.

Previous studies have shown OEA levels to decrease in rats during food deprivation, and increase during re-feeding (Rodriguez de Fonseca et al., 2001). Yet the presence of OEA also causes changes in levels of the expression of its pre-cursor and the activity of its synthesising and metabolising enzymes, orchestrating a rapid response. We may therefore expect, when administered exogenously, the body to utilise OEA and metabolise it rapidly.

The same group (Rodriguez de Fonseca et al., 2001) found endogenous levels of OEA to localise largely in proximal areas of the small intestine, suggesting a gastrointestinal locus of action. This led us further to investigate the possibility of a peripheral mechanism mediating OEA's effect.

4.4 The role of OEA and PPARα receptor on energy balance and metabolism

4.4.1 Introduction

The actions of OEA on food intake have not been fully characterised. It is thought to act through various peripheral receptors located in the small intestine, one of which is the nuclear receptor PPARα, another is the recently de-orphanised GPCR named GPR119 (Overton et al., 2006) as well as the vanilloid receptor TRPV1 (Ahern, 2003). OEA's peripheral activity has been shown to decrease food intake and have an action on satiety. Given the multiple potential mediators of OEA-evoked changes in feeding behaviours,

the local availability of PPARα knockout mice and interest in these receptors led us to investigate the role of a key mediator PPARα using pharmacological and, later, genetic means.

The overall aim of this investigation was to understand the role of OEA in regulating feeding behaviour and to determine the involvement of this peripheral receptor to the effects observed on satiety.

4.4.2 Method

Given the results on food intake shown with doses of OEA in the previous study, we have administered OEA at a dose of 10 mg/kg, alone or alongside fenofibrate at a dose of 20 mg/kg (equal to the maximum recommended human dose).

Experimental procedure

The same experimental procedure was applied as described in section **3.3.2.**

	Group 1		Group 2		Group 3		Group 4	
Mouse →	**1**	**2**	**3**	**4**	**5**	**6**	**7**	**8**
Week 1	Vehicle		OEA (10 mg/kg)		Fenofibrate (20 mg/kg)		OEA(10mg/kg) + Fenofibrate (20 mg/kg)	
Week 2	OEA (10 mg/kg) + Fenofibrate (20 mg/kg)		Vehicle		OEA (10 mg/kg)		Fenofibrate (20 mg/kg)	
Week 3	Fenofibrate (20 mg/kg)		OEA (10 mg/kg) + Fenofibrate (20 mg/kg)		Vehicle		OEA (10 mg/kg)	
Week 4	OEA (10 mg/kg)		Fenofibrate (20 mg/kg)		OEA (10 mg/kg) + Fenofibrate (20 mg/kg)		Vehicle	

Table 4.4 **Experimental dosing plan. Eight mice were treated in a pseudo-random order with treatment of Vehicle, OEA (10 mg/kg), fenofibrate (20 mg/kg) and dual administration of both OEA and fenofibrate, over a four week period.**

4.4.3 Results

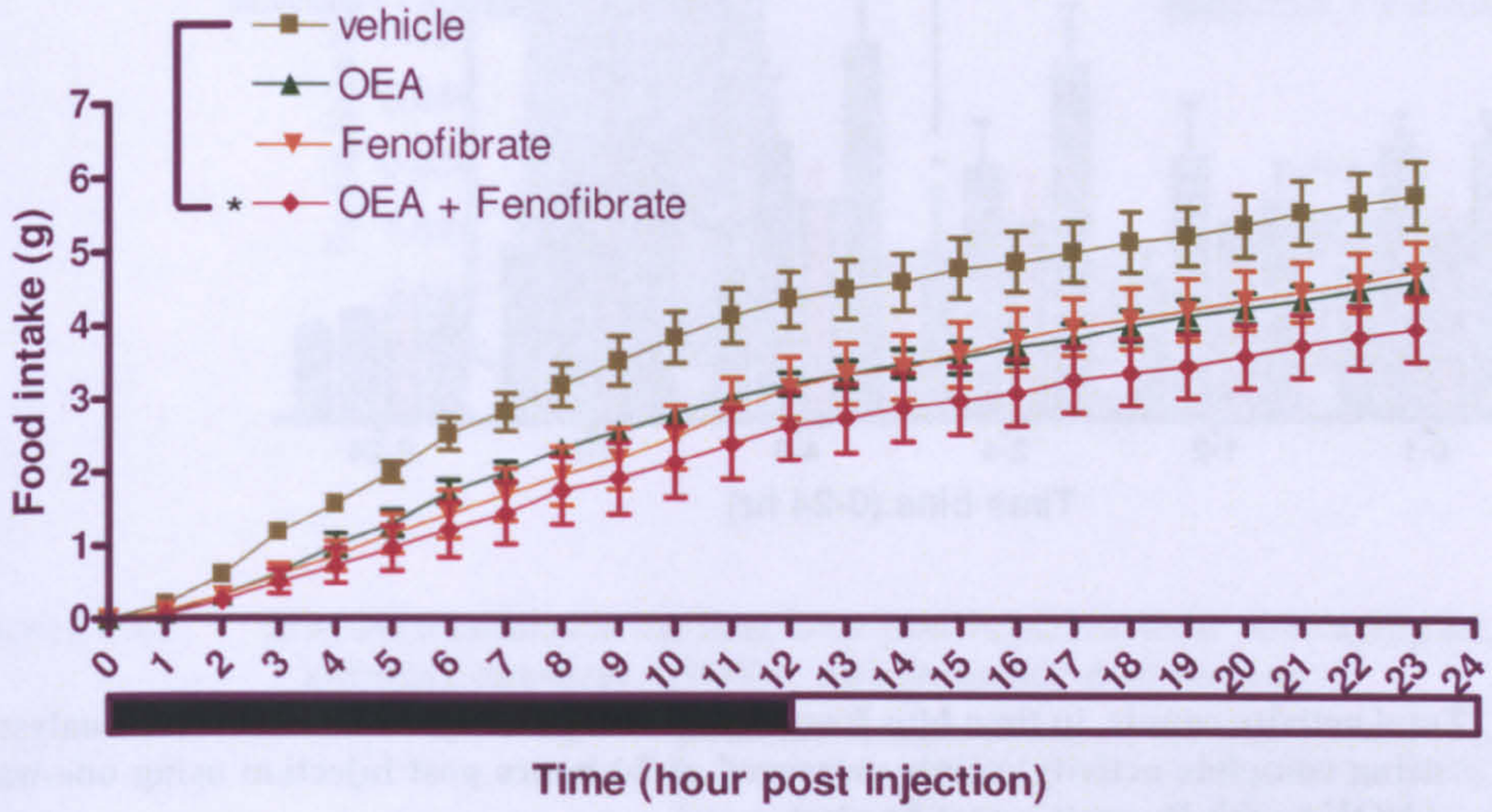

Figure 4.9 **Cumulative food intake for mice for 24 hours post-injection. All experiments shown in this section have n=8 of data. The bars below the graph indicate 12 hour dark and light phase. 0-24 hour data were analysed comparing all treatments against vehicle, using one-way ANOVA with Dunnett's post-hoc test.**

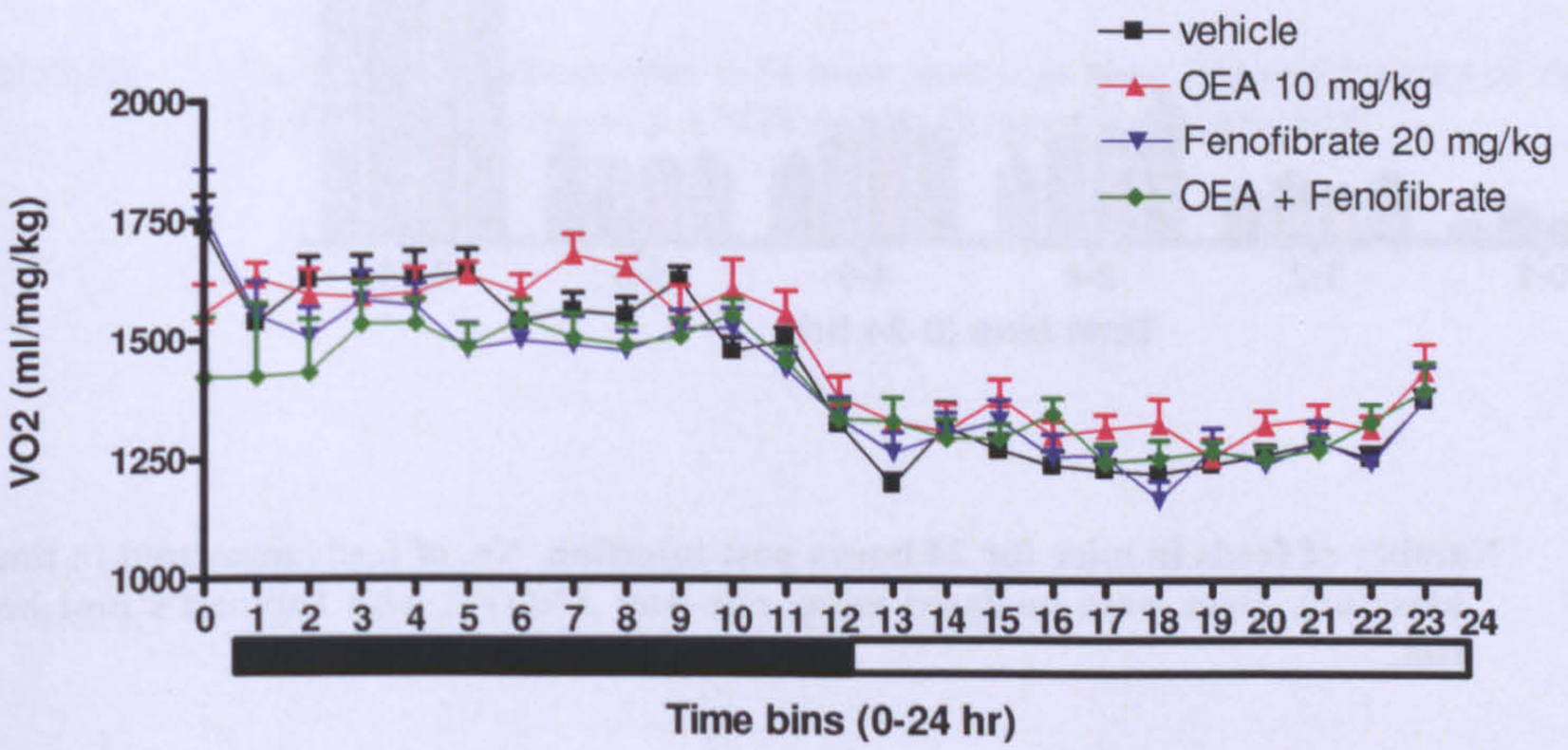

Figure 4.10 **Oxygen consumption of mice for 24 hours post-injection. Data were analysed using one-way ANOVA with Dunnett's post-hoc test.**

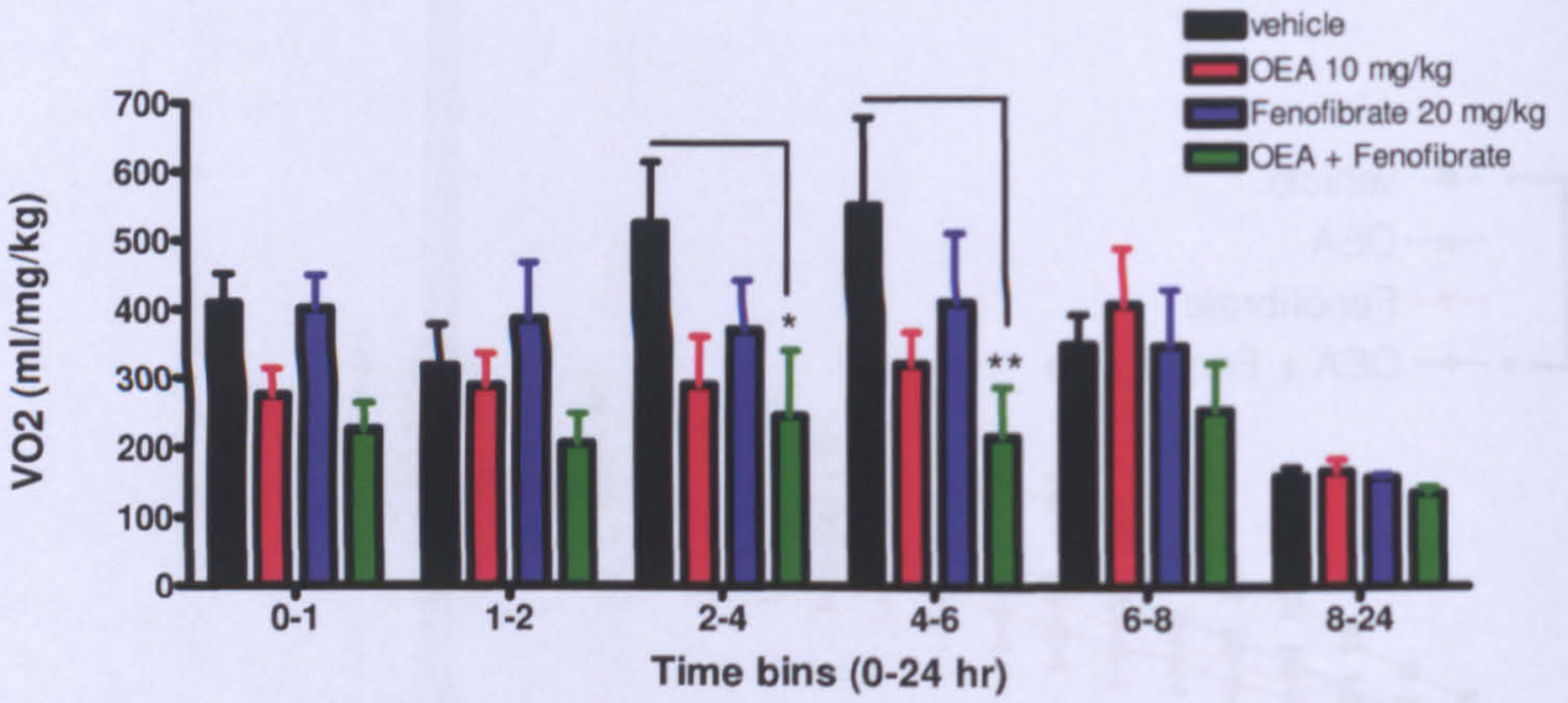

Figure 4.11 **Total activity counts, in time bins from 0-24 hours post-injection. Data were analysed using complete activity counts measured at 24 hours post injection using one-way ANOVA with Dunnett's post-hoc test.**

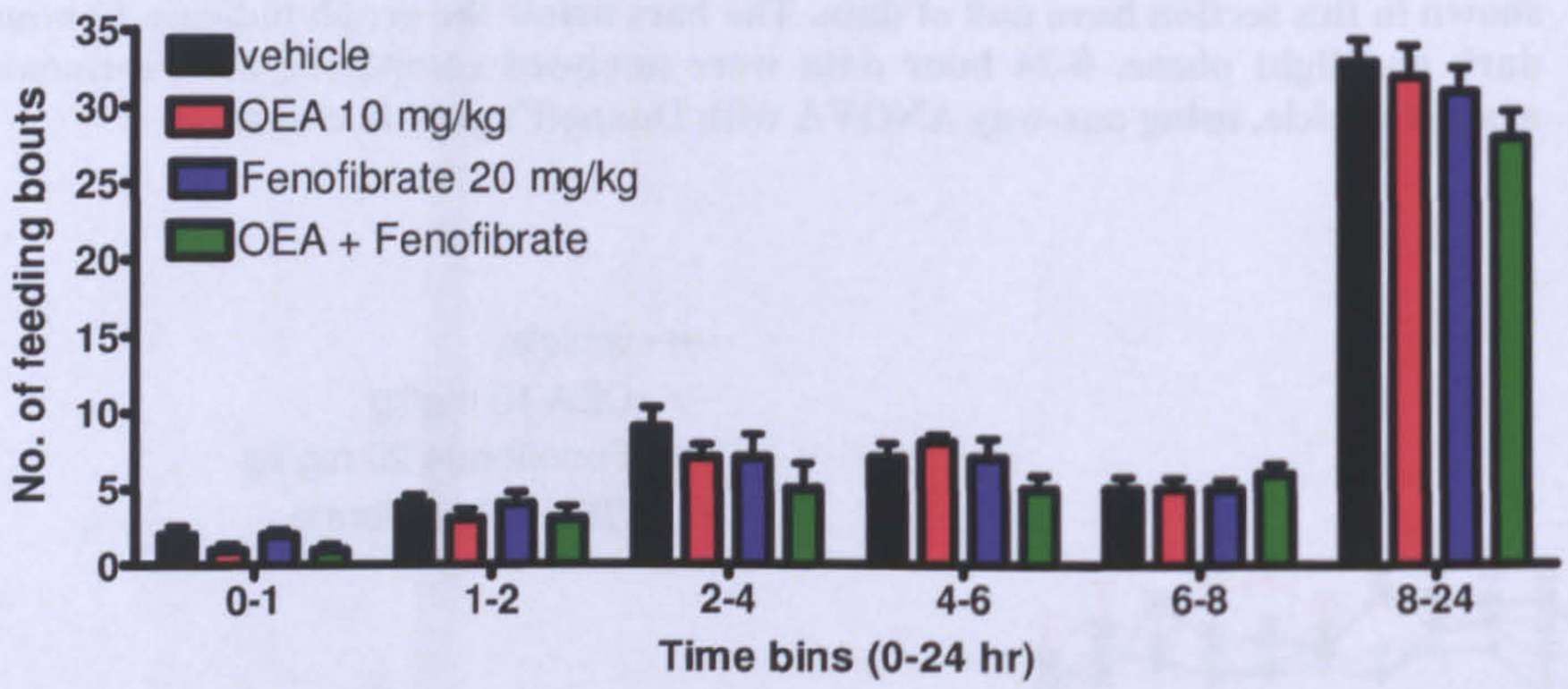

Figure 4.12 **Number of feeds in mice for 24 hours post-injection. No. of feeds measured in time bins (hr). Data were analysed using one-way ANOVA with Dunnett's post-hoc test.**

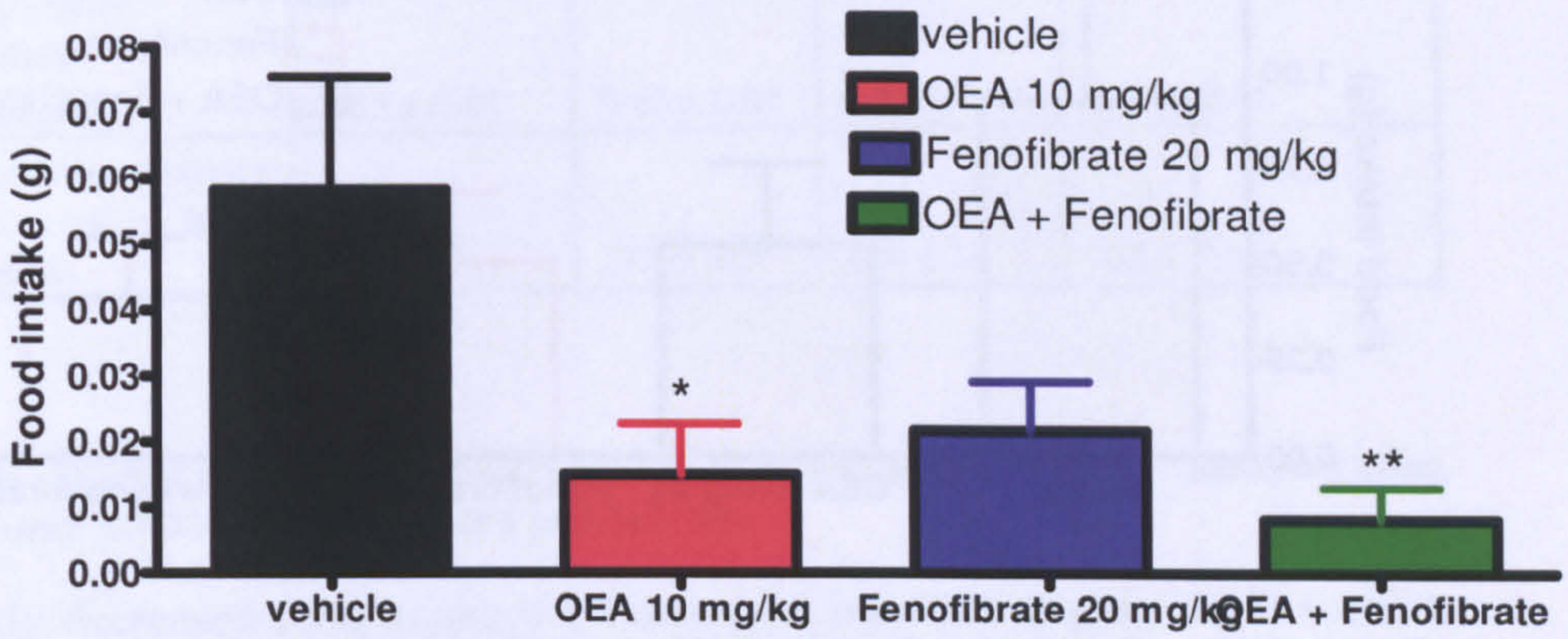

Figure 4.13 **Total food intake for the first hour post-injection. Data were analysed using one-way repeated measures ANOVA, with Dunnetts' post-hoc test.**

	Vehicle	OEA 10 mg/kg	Fenofibrate 20 mg/kg	OEA + Fenofibrate
Respiratory Quotient (mg/kg/hr)	0.95 ± 0..01	0.92 ± 0.01	0.92 ± 0.01	0.90 ± 0.01**
Latency of first feed (min)	24 ± 4	68 ± 20	78 ± 5	68 ± 37

Table 4.5 **Data collected from mice 0-24 hour post-injection. RQ and latency of first feed were analysed using one-way ANOVA with Dunnett's post hoc test.**

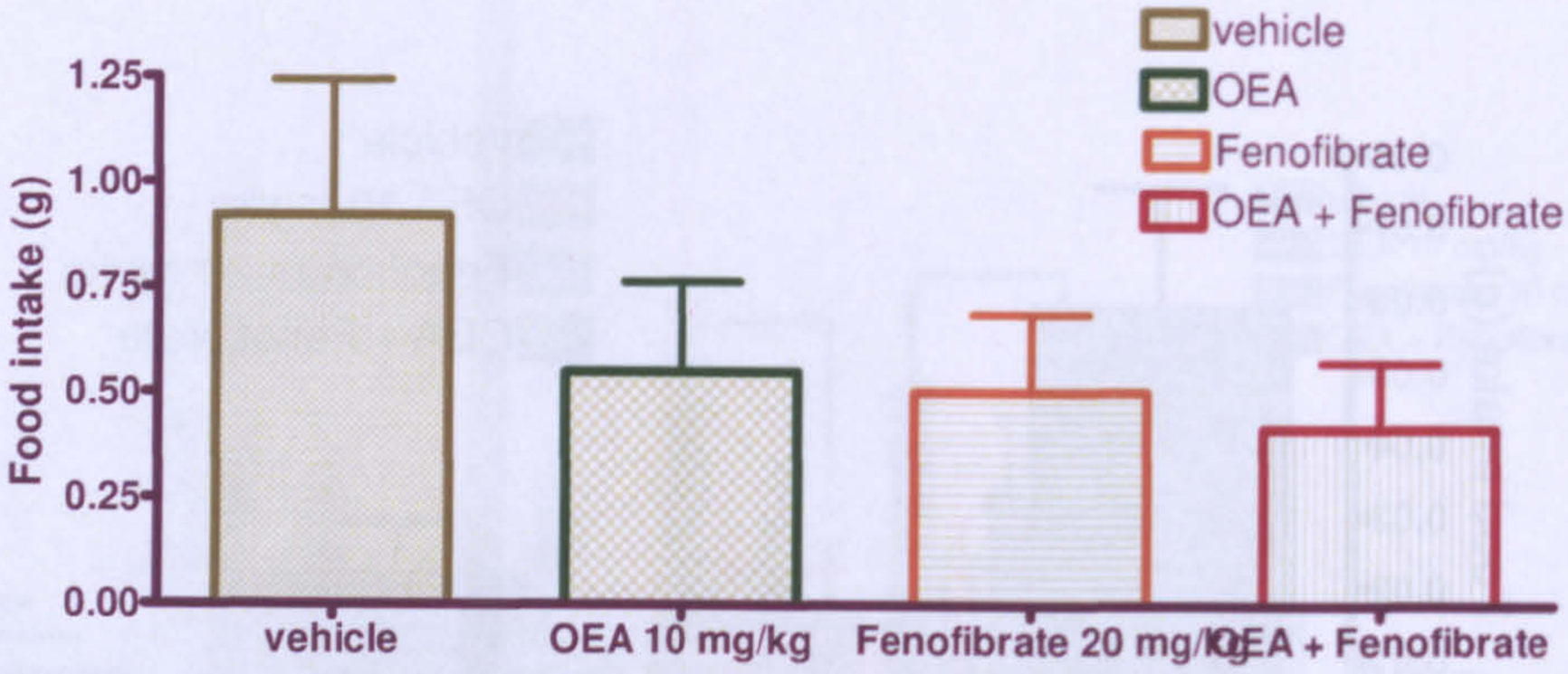

Figure 4.14 **Cumulative food intake in mice for the first 5 hours post-injection. Data were analysed using one-way ANOVA with Dunnett's post-hoc test.**

	Vehicle	OEA 10 mg/kg	Fenofibrate 20 mg/kg	OEA + Fenofibrate
No. of feeds (>0.06g)	21 ± 2	15 ± 2	21 ± 1	10 ± 3

Table 4.6 **Data collected from mice 0-5 hour post-injection. No. of feeds were analysed using one-way ANOVA with Dunnett's post hoc test.**

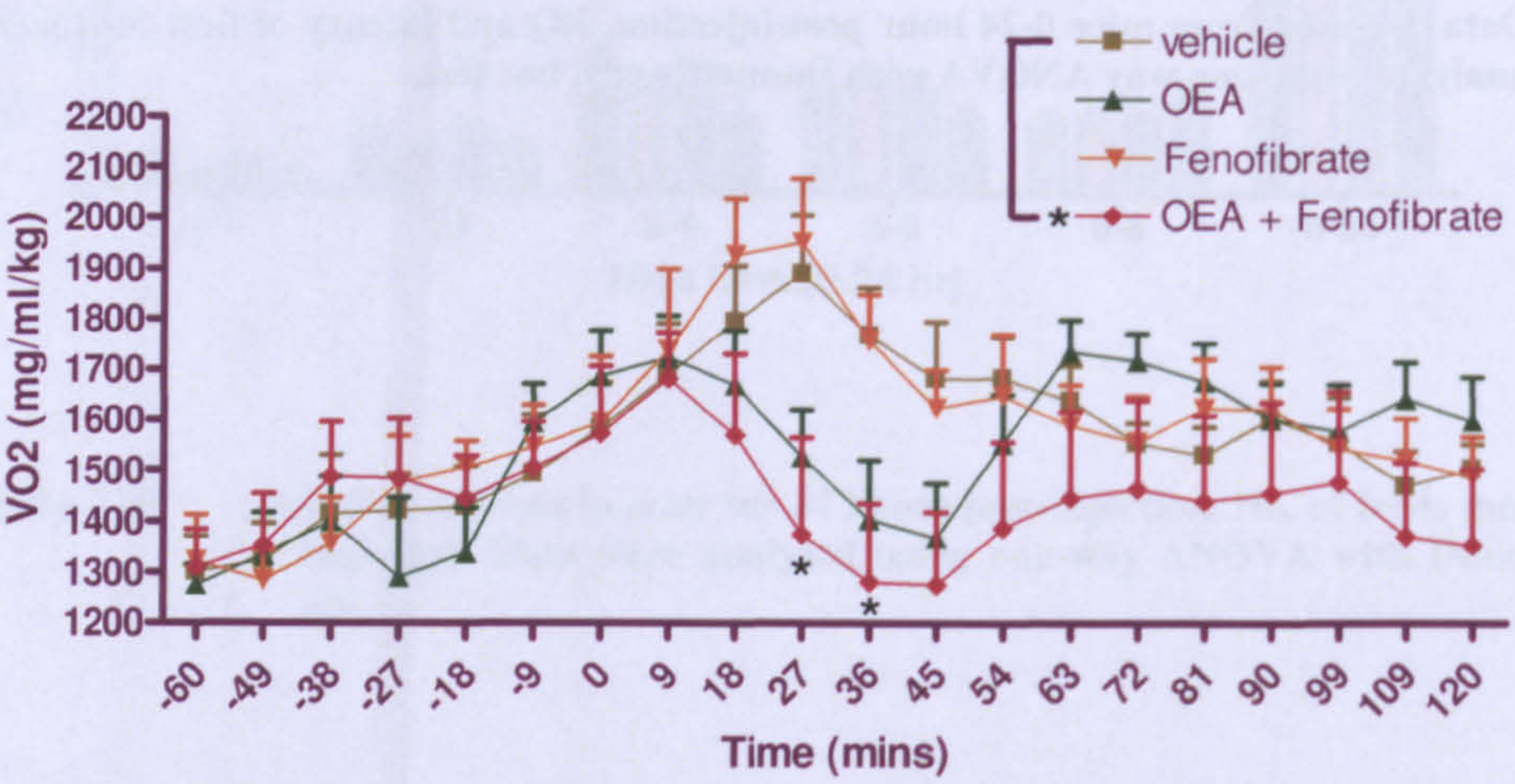

Figure 4.15 **Oxygen consumption from an hour pre-injection to 60 min post- injection. Data were analysed using Two-way ANOVA with Bonferroni's post-hoc test (*P<0.05).**

	Vehicle	OEA 10 mg/kg	Fenofibrate 20 mg/kg	OEA + Fenofibrate
Respiratory Quotient (mg/kg/hr)	0.83 ± 0.01	0.83 ± 0.01	0.83 ± 0.01	0.80 ± 0.01
Locomotor Activity (no. of beam breaks)	411 ± 35	271 ± 32*	388 ± 34	234 ± 29**

Table 4.7 Data collected from mice 0-1 hour post-injection. No. of feeds were analysed using one-way ANOVA with Dunnett's post hoc test.

OEA significantly decreased food intake 0-1 hours post injection (**figure 4.13**) (vehicle 0.19 ± 0.02, OEA 0.075 ± 0.02; $P<0.05$). Fenofibrate, in comparison, had a marginal reduction (0.10 ± 0.04 g), although administration of the two compounds together evoked a significant reduction in food intake (0.06 ± 0.03 g; $P<0.01$). The effects of OEA and fenofibrate were lost after 2 hours, indicating a short acting response or rapid metabolism. In contrast, however administration of both agents simultaneously significantly maintained this reduction in food intake for up to 5 hours post-injection (**figure 4.15**), compared with vehicle ($P<0.01$). Combined administration of OEA and fenofibrate suppressed food intake over 0-24 hours post injection (**figure 4.9**) (vehicle 6.94 ± 1.07; dual 4.02 ± 0.46 g; $P<0.05$), when neither OEA nor fenofibrate had any significant effect in the response at 0-24 hours when administered alone. Alongside this we observed a trend of increased latency of feeding onset with all treatments (**table 4.5**), in the order of fenofibrate, OEA and combined administration, compared with vehicle, albeit non-significant.

The decrease of food intake with both OEA and the combined administration of OEA and fenofibrate was associated with an acute reduction in oxygen consumption 0-1 hour post

injection (**figure 4.15**), where OEA elicited an acute significant reduction in VO_2 (1369 ± 108 mg kg^{-1} hr^{-1}; $P<0.05$) 36 minutes post-injection, where combined administration showed a significant reduction (1277 ± 143; $P<0.05$), compared with vehicle, at both 27 and 36 minutes post-injection, which was rapidly reversed, whereas fenofibrate alone had no effect on this parameter. There was no significant change over the 24 hour period following administration in VO_2 (**figure 4.10**).

Alongside this the respiratory quotient remained unaffected by any treatment within the first hour post injection (**table 4.7**), yet significant reduction of RQ was seen with dual administration, at 24 hours post-injection (**table 4.5**). No hyperactivity or sedation was evident, but decreased activity was observed in the first hour (**table 4.7**), in the order of fenofibrate, OEA and dual administration, where OEA and combined OEA and fenofibrate administration caused a significant reduction ($P<0.05$ and $P<0.01$ respectively), compared to vehicle. Mice treated with OEA lost this effect on activity but over the 0-24 hour period activity (**table 4.5**) remained significantly reduced, when compared with vehicle, for mice treated with both OEA and fenofibrate together.

4.4.4 Discussion

One potential interpretation of these results is that OEA is acting at PPARα nuclear receptors, located in the walls of the small intestine. Pharmacodynamically, the maintenance in the reduction of food intake suggests potentiation of the effect of OEA when administered with fenofibrate, although the time profile of OEA indicates the possibility that this response is an additive effect, with OEA being involved in a different peripheral mechanism adding to the effects of fenofibrate at PPARα on food intake.

Various receptors have been investigated for their affinity for eCBLs. OEA has been reported to be an endogenous agonist at GPR119, whose physiological response is yet undetermined, as well as the vanilloid receptor $TRPV_1$. Anorexic effects mediated by these receptors have not been reported in literature and their possible involvement with OEA in the reduction of food intake would need to be further investigated (Wang et al., 2005) (Overton et al., 2006). Pharmacokinetically, it can be hypothesised that fenofibrate may be able to inhibit OEA metabolism or displace it from a non-functional binding site, therefore increasing its bioavailability.

The acute reduction in VO_2 observed with OEA, but not by fenofibrate, supports acute effects on VO_2 observed in the previous chapter with OEA alone, yet the mechanism by which this occurs is still undetermined.

The reduced RQ may be evidence for an additive effect of OEA and fenofibrate mediated response in direct activation of PPARα (for example), as neither compound alone induced a reduction of RQ. This may be a result of high potency binding and activation of the PPARα receptor by both OEA and fenofibrate, both of which are able to cause changes in transcriptional activity (Sun et al., 2006) and drive the mice more towards protein metabolism than carbohydrate as seen with the other treatments, this may also be possible in the time of 24 hours post-injection. Dual administration also showed a significant reduction in activity compared to vehicle between 2-6 hours post-injection, again indicating a response to mechanisms involving both compounds as this was not observed though administration of either compound alone.

Results so far suggest a different time course in the effects of both compounds when

administered individually, yet the additive effect observed through dual administration of both compounds indicate an additive effect towards the overall effects on satiety. The different effects of OEA and fenofibrate administration suggest distinct mechanisms of action or differences in their pharmacokinetic profiles *in vivo*, while the extended duration of action of OEA with fenofibrate co-administration suggests a potentially novel indirect effect of PPARα receptors on food intake.

4.5 The role of OEA on energy balance and metabolism independent of PPARα

4.5.1 Introduction

GW6471 has only been used once previously *in vivo*, in a recent local study in which it was administered through an intraplantar injection at a dose of 0.12 mg/kg for the investigation of local effects. Informal discussions with GSK personnel suggested that the compound had a poor bioavailability profile *in vivo*. The dose of GW6471 chosen (20 mg/kg) was based on previous *in vitro* assays, drawing parallels with effects of PPARα agonists.

4.5.2 Method

GW6471 has only been used once previously *in vivo*, administered through an interplantar injection at a dose of (0.12 mg/kg) for the investigation of local effects and has been reported to have a poor absorption profile in vivo. The dose of GW6471 was therefore based on previously used *in vitro* assays which led to a dose selection of 20 mg/kg for the investigation of the effects of GW6471 as a PPARα antagonist *in vivo*.

Experimental procedure

The same experimental procedure was applied as described in **section 3.3.2.**

→	Group 1		Group 2		Group 3		Group 4	
mouse	**1**	**2**	**3**	**4**	**5**	**6**	**7**	**8**
Week 1	Vehicle		OEA (10 mg/kg)		GW6471 (20 mg/kg)		OEA + GW6471	
Week 2	OEA + GW6471		Vehicle		OEA (10 mg/kg)		GW6471 (20 mg/kg)	
Week 3	GW6471 (20 mg/kg)		OEA + GW6471		Vehicle		OEA (10 mg/kg)	
Week 4	OEA (10 mg/kg)		GW6471 (20 mg/kg)		OEA + GW6471		Vehicle	

Table 4.8 **Experimental dosing plan. Eight mice treated in a pseudo-random order with treatment of Vehicle, OEA (10 mg/kg), GW6471 (20 mg/kg) and dual administration of both OEA and GW6471, over a four week period.**

4.5.3 Results

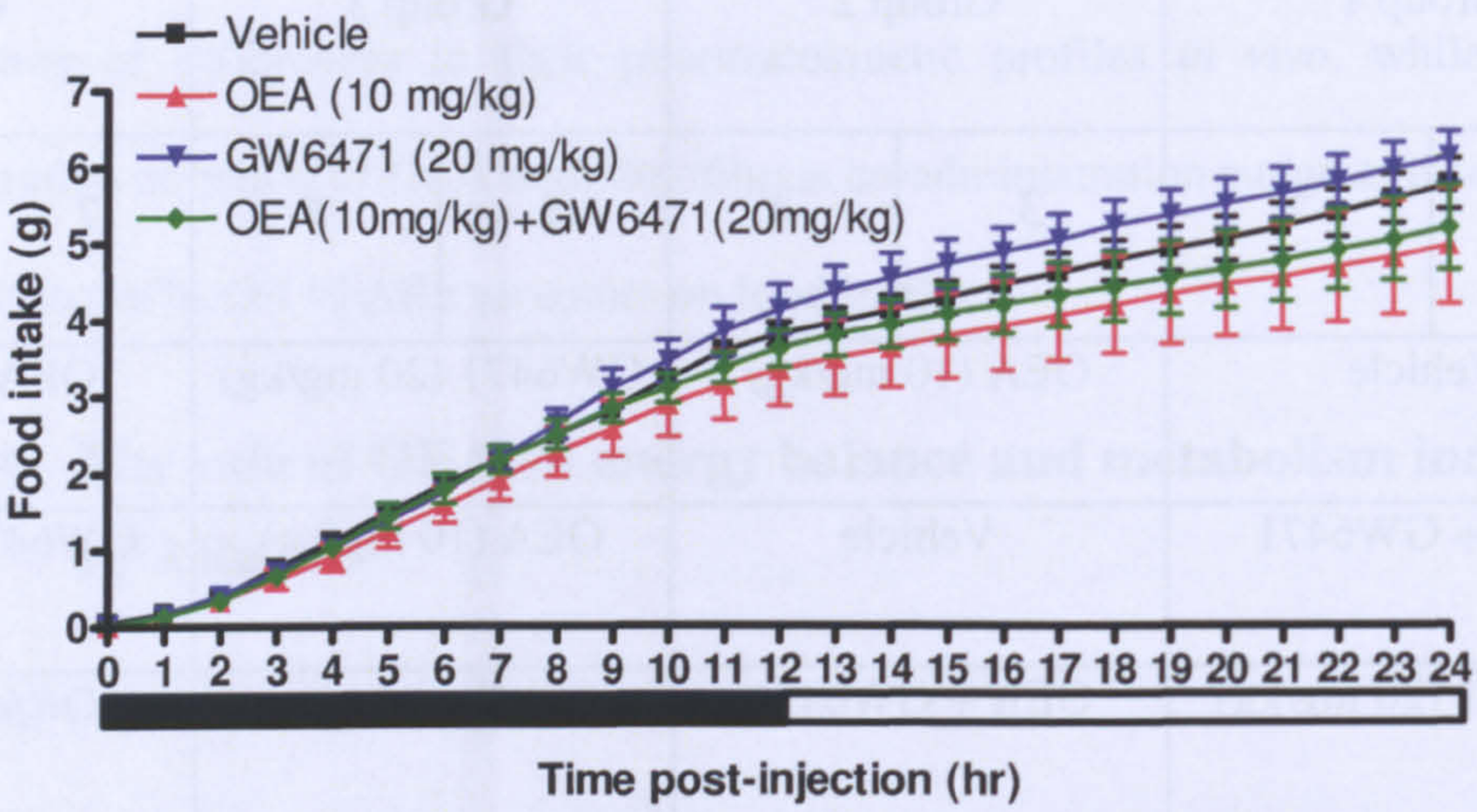

Figure 4.16 **Cumulative food intake for mice for 24 hours post-injection. All data are n=8 for this and all other results shown in this section. The bars below the graph indicate 12 hour dark and light phase. Data were analysed comparing all treatments against vehicle, using two-way ANOVA with Dunnett's post-hoc test.**

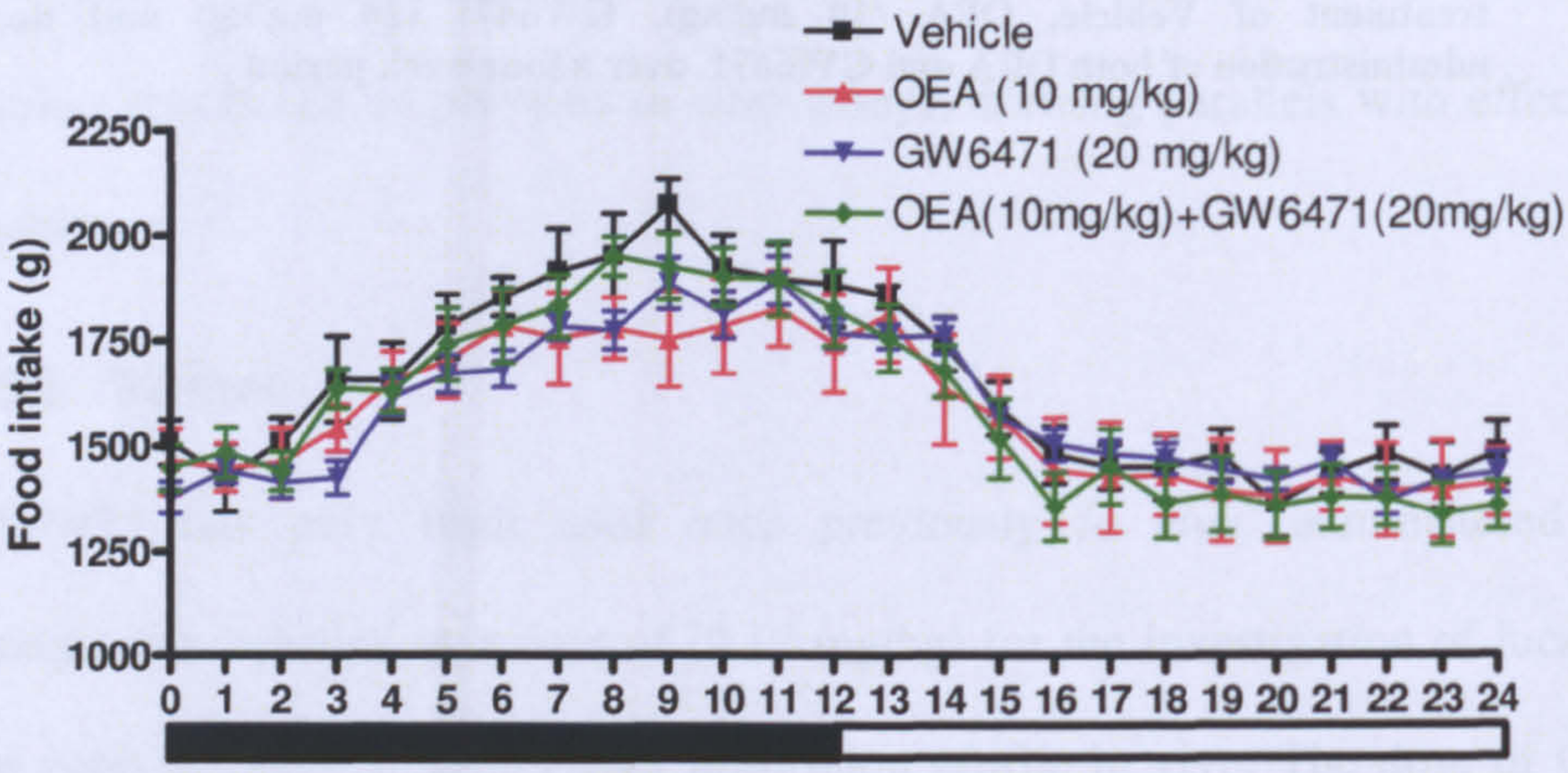

Figure 4.17 **Oxygen consumption of mice for 24 hours post-injection. Data were analysed using one-way ANOVA with Dunnett's post-hoc test.**

	Vehicle	OEA 10 mg/kg	GW6471 20 mg/kg	OEA + GW6471
Respiratory Quotient (mg/kg/hr)	0.96 ± 0..01	0.94 ± 0.01	0.97 ± 0.01	0.93 ± 0.01*
Locomotor Activity (no. of beam breaks)	291 ± 43	234 ± 25	225 ± 26	261 ± 34
Latency of first feed (min)	30 ± 8	47 ± 14	47 ± 7	44 ± 11

Table 4.9 **Data collected from mice 0-24 hours post-injection. RQ and total activity were analysed using two-way ANOVA whereas latency of first feed were analysed using one way ANOVA; both were followed by Dunnett's post hoc test.**

	Vehicle	OEA 10 mg/kg	GW6471 20 mg/kg	OEA + GW6471
No. of feeds (>0.06g)	20 ± 3	8 ± 2	12 ± 2	10 ± 3
Food Intake (g)	0.66 ± 0.23	0.61 ± 0.22	0.62 ± 0.21	0.60 ± 0.23

Table 4.10 **Data collected from mice 0-5 hours post-injection. No. of feeds and food intake were analysed using two-way ANOVA with Dunnett's post hoc test.**

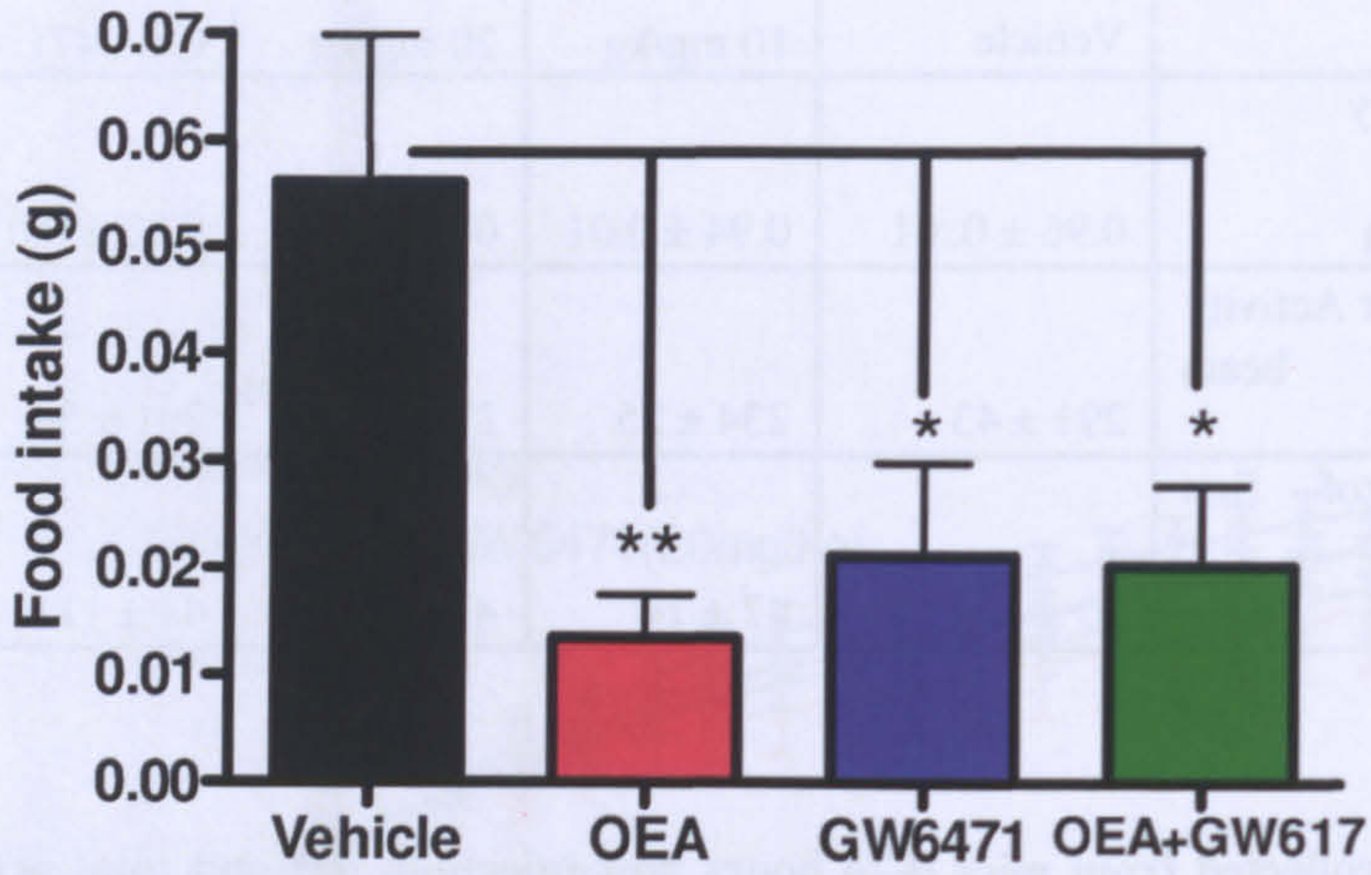

Figure 4.19 **Total food intake in mice for the first hour post-injection. Data were analysed using two-way repeated measures ANOVA, with Dunnetts' post-hoc test.**

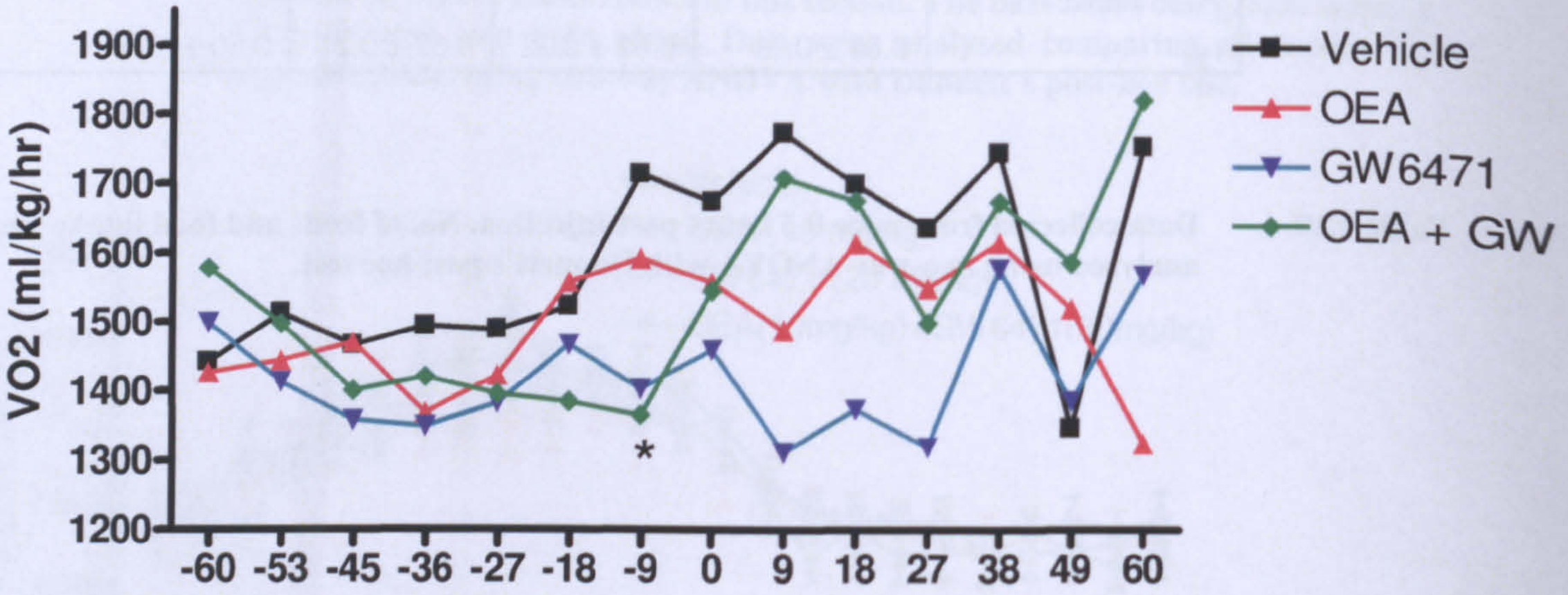

Figure 4.20 **Oxygen consumption from an hour pre-injection to 60 min post- Injection. Data were analysed using Two-way ANOVA with Bonferroni's post-hoc test (*p<0.05).**

	Vehicle	OEA 10 mg/kg	GW6471 20 mg/kg	OEA + GW6471
Respiratory Quotient (mg/kg/hr)	0.98 ± 0..01	0.96 ± 0.01	0.95 ± 0.01	0.95 ± 0.01
Locomotor Activity (no. of beam breaks)	286 ± 37	250 ± 34	209 ± 39	294 ± 36

Table 4.11 **Data collected from mice 0-1 hours post-injection. No. of feeds and food intake were analysed using two-way ANOVA with Dunnett's post hoc test.**

Administration of OEA, GW6471 or combined administration of both compounds elicited a reduction in food intake in the first hour post-injection (OEA=$P<0.01$, GW6471 and dual administration =$P<0.05$). This significant reduction was lost with all treatments by 5 hours post-injection. At 24 hours post-injection cumulative food intake appeared reduced (not significantly), compared to vehicle, in the order of OEA>dual administration yet the PPARα antagonist enhanced food intake compared to vehicle, albeit not significantly. There was a trend of increased latency of feeding onset in the order of OEA, GW6471 and dual administration of both compounds.

GW6471 administration produced the highest reduction in activity in the first hour following administration although it was not significant. At 24 hours, combined administration caused a significant reduction in RQ ($p<0.05$) suggesting a switch towards protein metabolism in the mice, as observed in the previous chapter with combined OEA and fenofibrate administration (RQ=0.821).

OEA showed the only trend of decrease in VO_2 following injection (at 30 minutes, albeit

non-significantly), and treatment with GW6471 alone significantly reduced VO_2 at 9 minutes post-injection ($p<0.05$), but displayed a quick recovery as seen with OEA in previous *in vivo* experiments. All other compounds followed the profile displayed by vehicle treatment. There was no significant effect of any compound 24 hours post-injection on oxygen consumption.

4.5.4 Discussion

The PPARα antagonist GW6471 was employed to allow us to determine the involvement of PPARα receptor in the OEA-mediated effects on food intake. Due to the lack of *in vivo* use and knowledge of the pharmacokinetic profile of GW6471, GW6471 was administered alone to determine its behavioral effects *in vivo*. In our hands, GW6471 (20 mg/kg) evoked a significant reduction in food intake in either the absence or presence of OEA. The precise mechanism for this is unclear, as is the involvement of PPARα receptors. It should be noted, however, that a reduction in food intake could be induced by a non-specific feeling of malaise. If that were the case for GW6471 we would expect to see a reduction in locomotor activity, which was not present. Analysis of food intake 5 hours post-injection showed no sustained significant reduction in food intake with GW6471, indicating the effects of this compound, as well as OEA, to be transient. **Figure 4.16** shows food intake up to 24 hours post-injection and shows levels of food intake to be reduced the most by OEA treatment, and this effect is reduced with treatment of OEA with GW6471, indicating at least a partial contribution of PPARα. Further experiments would need to be conducted to determine whether a higher dose of GW6471 would inhibit the effects of OEA completely. Treatment with GW6471 alone showed a

reduction in food intake, compared to vehicle, suggesting tonic PPARα receptor activation with an endogenous ligand. This experiment is conducted with free-feeding animals and it is known that OEA is synthesized in response to feeding (Piomelli 2006). It is a distinct possibility that endogenous levels of OEA synthesized *de novo* may be acting at PPARα receptors to produce this tonic activation.

All treatments showed trends of decreased RQ within the first hour post-injection, yet at 24 hours combined administration alone showed a significant reduction in RQ, indicating a possible change to the metabolic rate of the animal. As seen in **section 4.5.3,** RQ was observed to decrease with combined administration of OEA and PPARα receptor agonist fenofibrate, indicating an involvement of OEA the change in basal metabolic rate. It was previously hypothesised that, as PPARα is a nuclear receptor, the change in RQ could be due to changes in transcriptional activity, yet this is unlikely now that the same effects have now been observed by OEA alongside a receptor antagonist. The contribution of GW6471 alone in this effect is therefore undetermined.

OEA treatment displayed a trend similar to that seen in **figures 4.14** and **figure 4.7** on VO_2, but to a lesser (not significant) degree, yet GW6471 alone produced a sudden, transient reduction in VO_2 at 9 minutes post injection ($p<0.05$). The mechanism by which this effect occurs is still unknown.

We show conflicting behavioural effects of GW6471 *in vivo* linked to feeding behaviours and the animals' metabolic profiles. The lack of knowledge and information on the bioavailability and pharmacokinetics of GW6471 makes it difficult to determine whether the doses given provide adequate concentrations of unchanged drug reaching systemic

circulation, leading to an optimal observational effect on feeding behavior by GW6471 acting as an antagonist at PPARα receptors. Further investigation is required to determine the absolute bioavaiability of GW6471 *in vivo* by obtaining plasma drug concentrations over time. A further understanding of the bioavailability and pharmacokinetics of this compound would allow us to hypothesise the pharmacological mechanisms which may cause the transient increase in food intake when GW6471 is administered alone. Due to the known non-beneficial clinical effects of PPARα receptor blockade leading to myopathy and rhabdomyeolysis and yet the beneficial effects of PPARα agonism little research has been conducted using PPARα antagonists such as GW6471 as a pharmacological tool. Therefore we have little to no available *in vivo* data to provide indications to dose related behavioral or metabolic effects *in vivo*.

Analysis of data suggest OEA to have effects on food intake at the PPARα receptor as reduction of levels of food intake induced by OEA are reduced with the PPARα antagonist, yet the mechanism involved in the enhanced levels of food intake 24 hours post-injection with GW6471 are unclear and will need further investigation. Data support OEA's role to be a direct effect on satiety and not a change in metabolic state of the mice.

4.6 OEA tissue levels following i.p. administration

4.6.1 Introduction

Investigations on the effects of endocannabinoid OEA (10 mg/kg) in mice have shown a significant reduction in food intake from the time of administration up to 5 hours, with a time of onset at 30 minutes post-dosing. Since the distribution of administered OEA post injection was unknown, we hypothesised that knowledge of tissue levels would allow

some insight into potential mechanisms of action.

4.6.2 Method

Experimental approach

As 10 mg/kg OEA evoked a significant response in previous experiments, we used this dose, with a timepoint at the peak of the behavioural effect (30 minutes). A 60 minutes timepoint was also included to indicate turnover of eCBs in those tissues. Analysis of eCBs other than OEA will also give some insight as to whether its effects are indirect, for example by diverting FAAH activity and allowing the accumulation of AEA.

Experimental design

Mice were maintained on 12L:12D, lights off 16:00, on 04:00. To comply with the previous experiments we administered OEA at the onset of the dark phase. Once the tissue had been dissected, it was weighed and frozen in liquid nitrogen before being placed in a collection tube and stored at -80°C until it was required to use as a LC-MS/MS sample to measure levels of OEA, PEA, AEA and 2-AG.

18 adult males will be split into four groups.

Endocannabinoid extraction method

Dry glass homogenizing tubes, centrifuge tubes and glass pipettes were silanised by filling with 5% dichloromethyl silane in toluene and left for 30 minutes in a fume cupboard. They were then washed out once using toluene and twice with methanol and allowed to dry.

Weighed tissue samples were placed in the homogenizing tubes, and kept on ice. 100 µL

d8 2-AG and/or 15 µL of d8 AEA was added to each homogenizing tube containing sample and vortexed. HPLC grade ethyl acetate/hexane were mixed to a 9:1 ratio and 5 mL was added to each homogenizing tube and left on ice for 15 minutes and then homogenized using a hand held pestle. 5 mL of de-ionised water was then added to each sample and each tissue re-homogenised. All of the sample was transferred from homogenizing tubes to plastic centrifuge tubes and vortexed. A further 5 mL of 9:1 ethyl acetate/hexane was added to the homogenizing tubes as a washout for any remaining samples and left on ice. Centrifuge tubes were then centrifuged at 7000 rpm for 15 minutes at 4°C. The supernatant layer was collected into silanised glass centrifuge tubes and plastic centrifuge tubes were re-filled with the remaining 5 mL ethyl acetate/hexane from each homogenizing tube. This was then centrifuged at 7000rpm for 15 minutes at 4°C. This was repeated one further time. The combined supernatant layers in glass centrifuge tubes were placed in a rotary evaporator and centrifuged until the solvent was fully evaporated.

Solid phase extraction (SPE) method

Samples were reconstituted using 1 mL anhydrous chloroform in capped glass tubes, and placed on a vibrating shaker for 4 minutes. SPE cartridges were placed on a SPE rack with silanised glass collection tubes for the elute. Each cartridge was loaded with reconstituted sample using glass silanised pipettes.

Each cartridge was then washed through in the following order:

- 4x1ml wash- anhydrous chloroform

- 2x1ml elute A – anhydrous chloroform + 2% methanol
- 4x1ml elute B – anhydrous chloroform + 2% methanol + 0.2% TEA
- 4x1ml elute C – anhydrous chloroform + 2% methanol + 0.05% TFA

The pooled elution stages were then evaporated under nitrogen at 35 °C using a sample concentrator. Samples were then stored at -80 °C until analysis.

Endocannabinoids were then quantified in samples using liquid chromatography–tandem electrospray ionization mass spectrometry methods, run by Sarir Sarmad.

4.6.3 Endocannabinoids in the Liver

a.

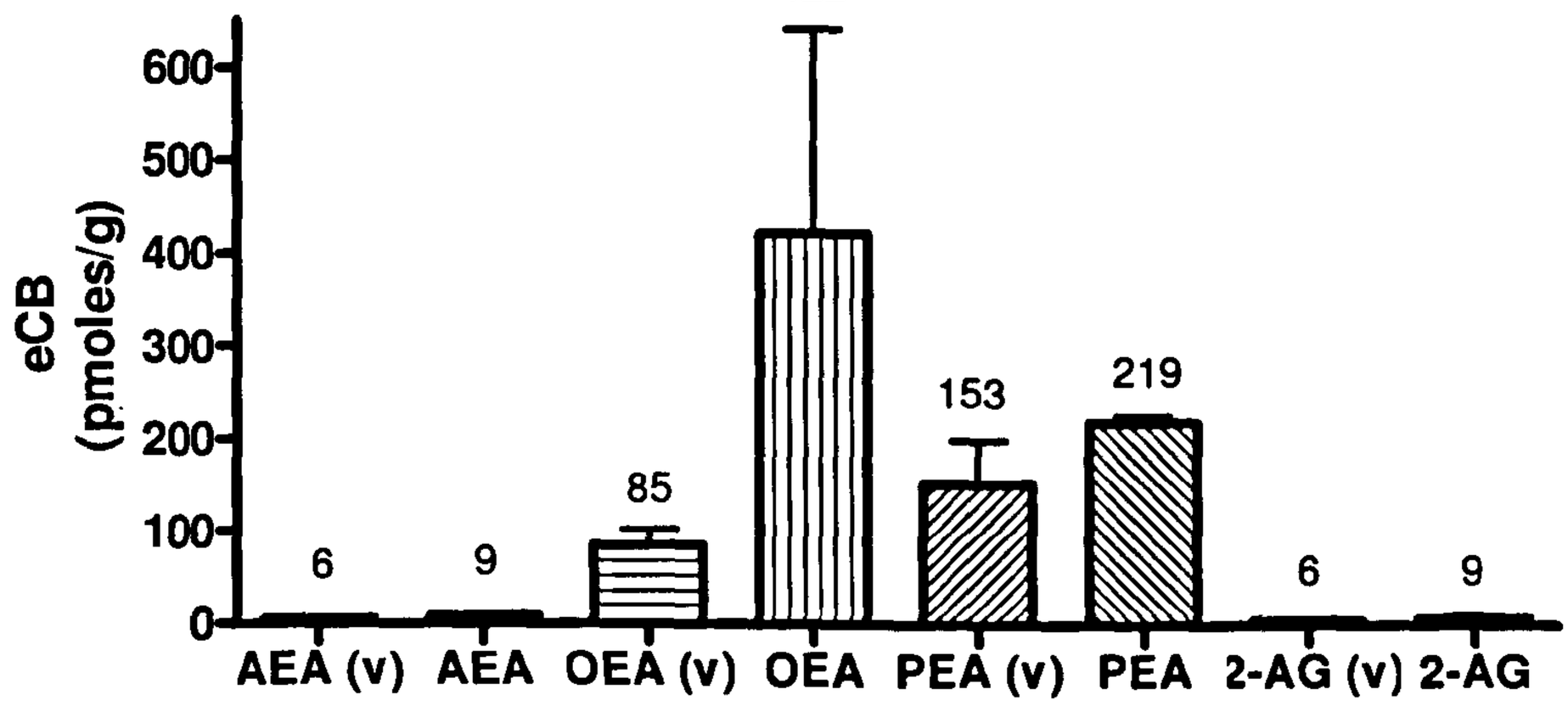

b.

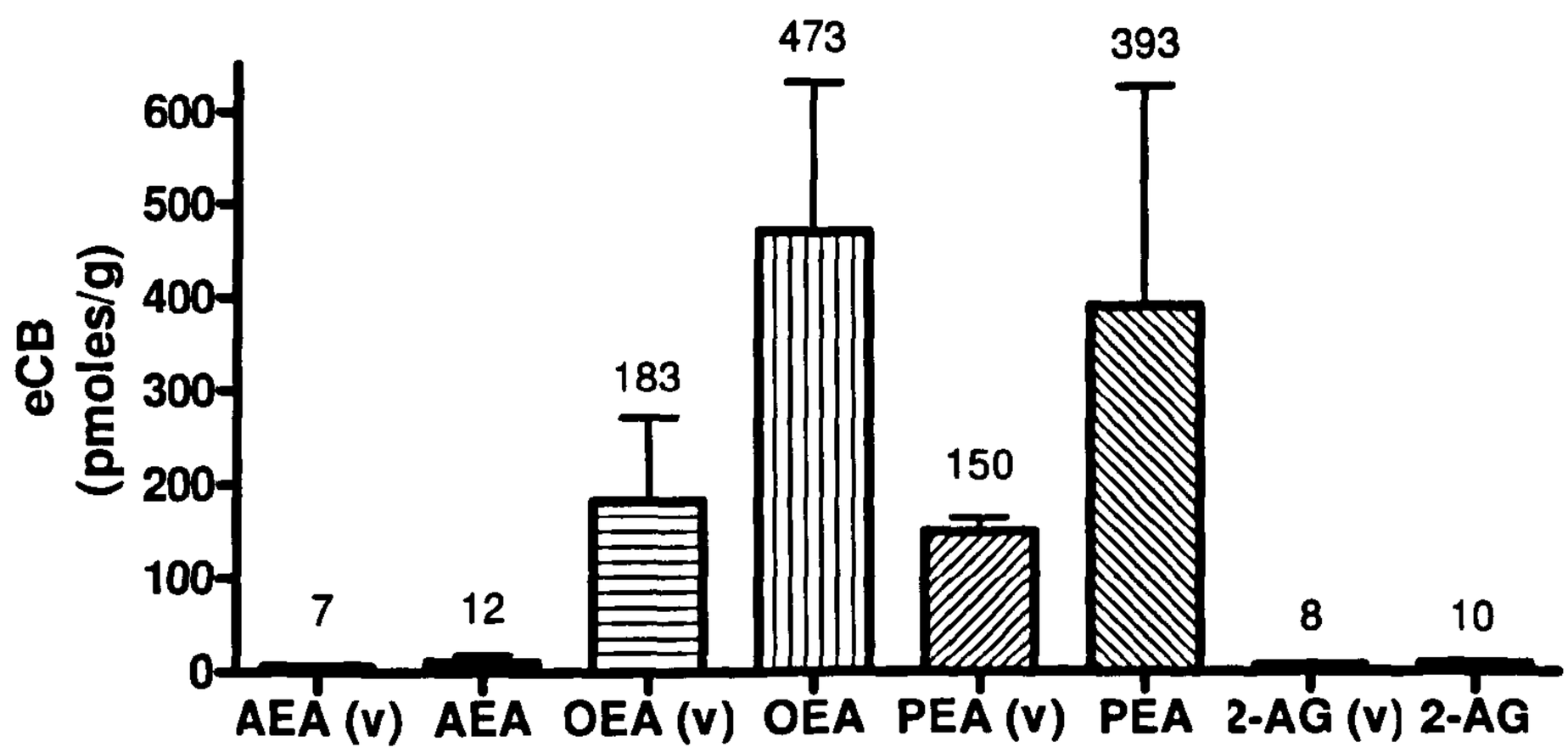

Figure 4.20 **Endocannabinoid levels quantified in mouse liver tissues, following vehicle and OEA (10 mg/kg) treatment (i.p.) and tissues collected 30 (a) and 60 (b) minutes post-injection (n=4).**

Levels of AEA and 2-AG in the mouse liver were similar and much lower than levels of OEA or PEA. 30 minutes following OEA administration, liver levels of OEA are significantly elevated; with no significant changes in PEA, AEA or 2-AG. OEA levels remain elevated at 60 minutes, with no significant changes in PEA, AEA or 2-AG.

4.6.4 Endocannabinoids in the ileum

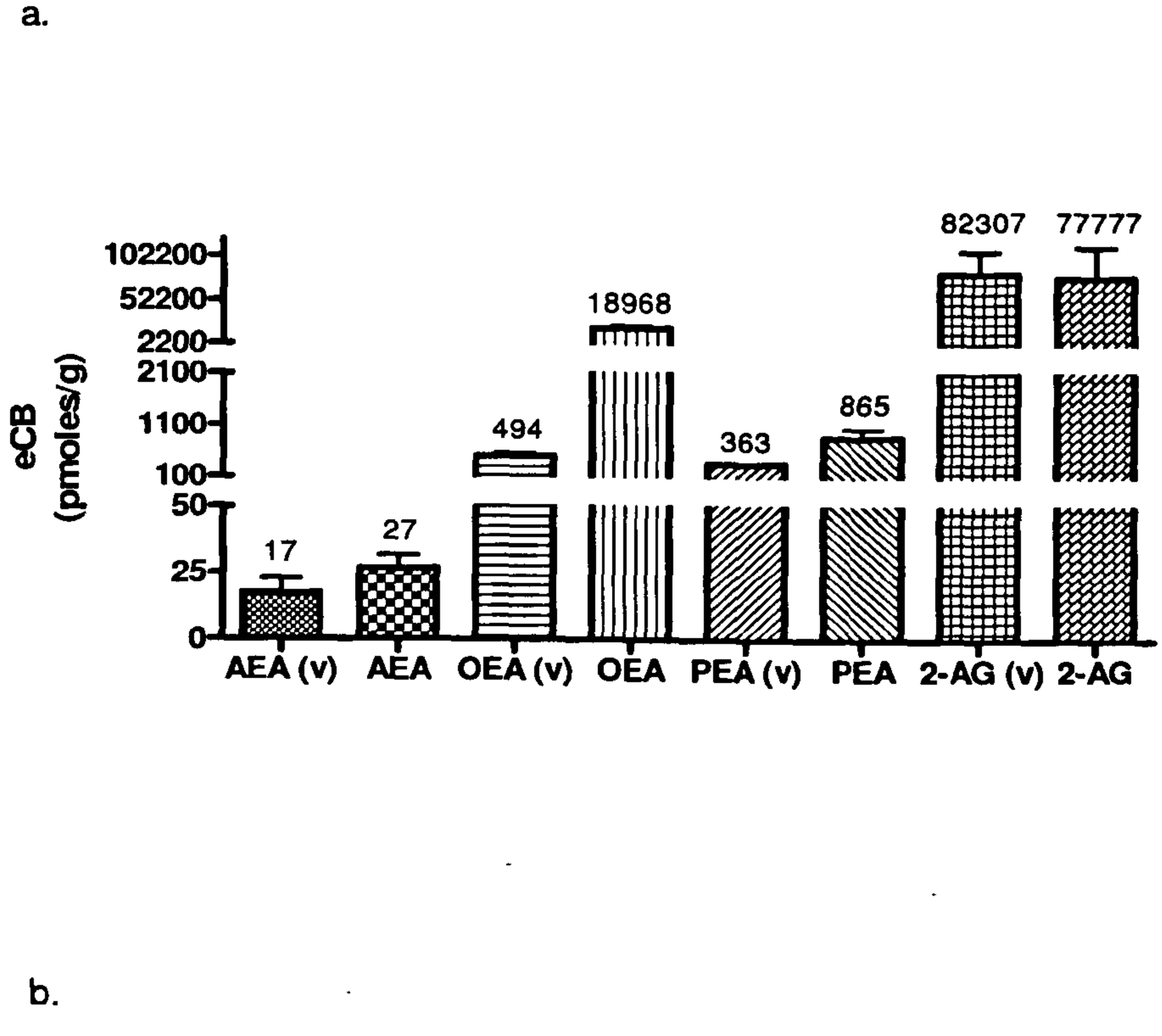

Figure 4.21 **Endocannabinoid levels quantified in mouse ileum tissues, following vehicle and**

OEA (10 mg/kg) treatment (i.p.) and tissues collected 30 minutes (a) and 60 minutes (b) post-injection (n=4).

In the ileum, basal levels of AEA were similar to those in the liver. In contrast, levels of OEA and PEA were higher, while 2-AG levels were strikingly elevated compared to the liver. As in the liver, i.p.administartion of OEA resulted in a significant elevation of OEA levels in the ileum, without significant alterations in PEA, AEA or 2-AG.

4.6.5 Endocannabinoids in the duodenum

a.

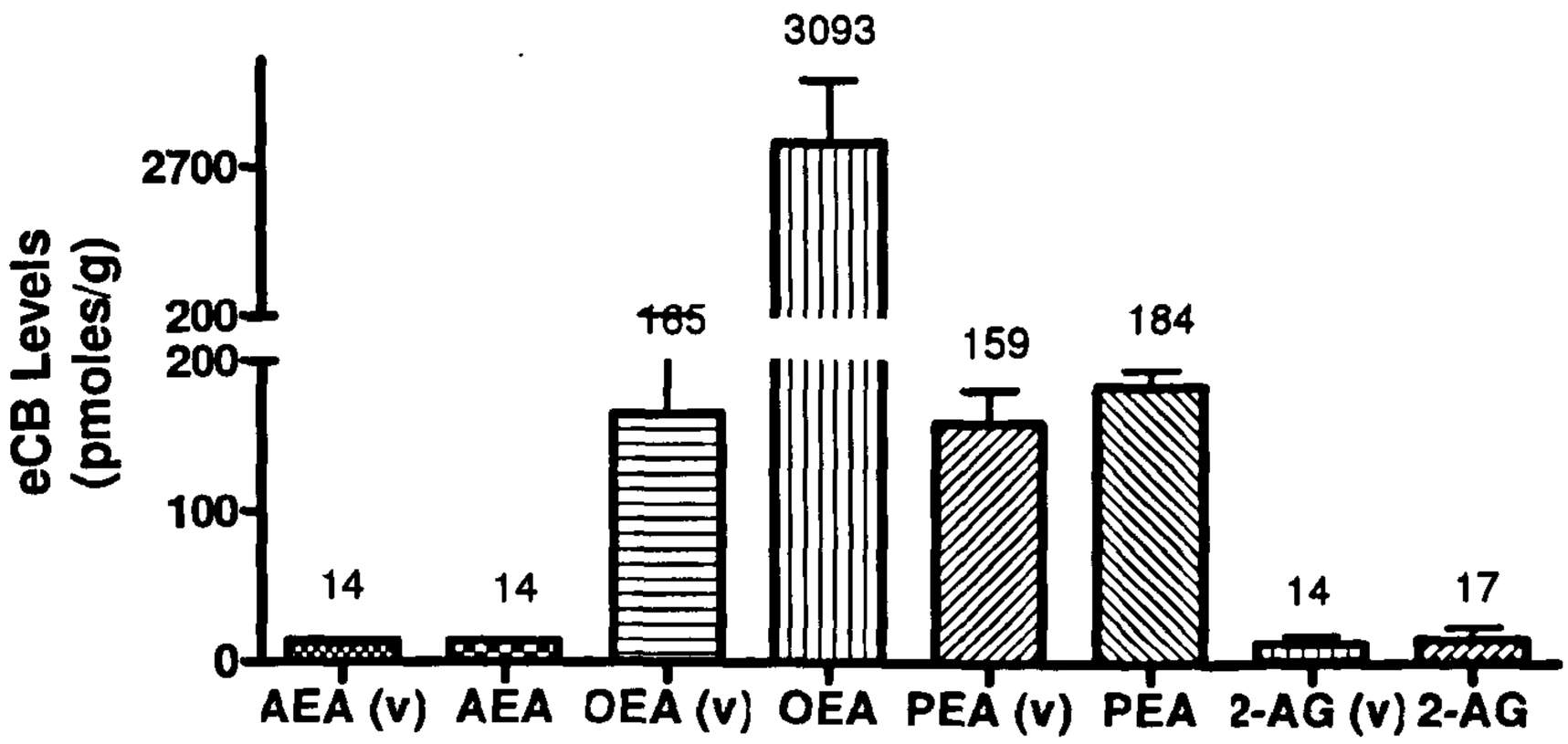

b.

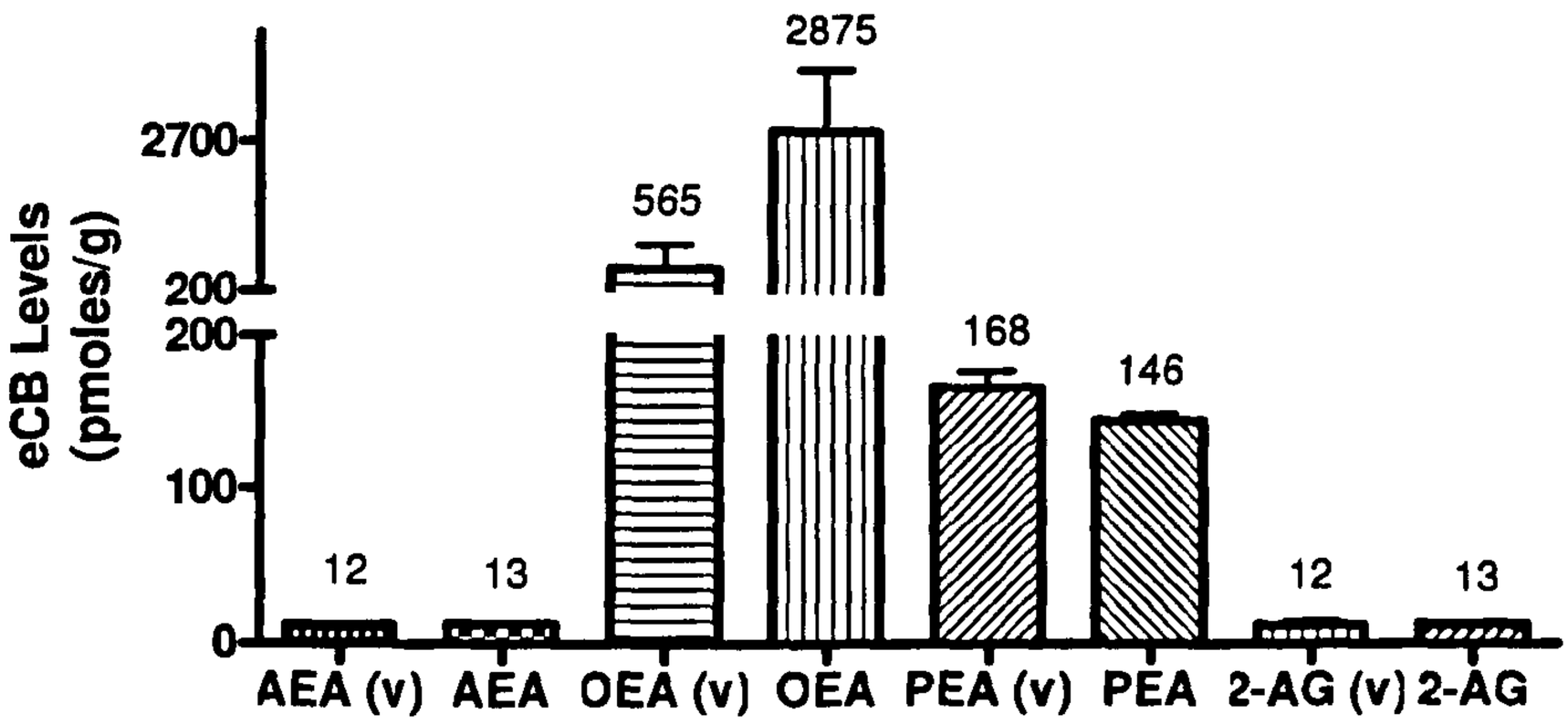

Figure 4.22 **Endocannabinoid levels quantified in mouse duodenum tissues, following vehicle and OEA (10 mg/kg) treatment (i.p.) and tissues collected 30 (a) and 60 (b) minutes post-injection (n=4).**

Basal levels of OEA in the duodenum were nearly twice that found in the liver and nearly three times lower than in the ileum. Basal levels show the amount of eCBL compounds measured to be 10-12-fold higher than levels of AEA and 2-AG. At 30 minutes OEA shows a 30-fold significant increase ($P<0.01$) compared to basal levels, with little change in PEA, AEA or 2-AG. eCB levels at 60 minutes post-injection show OEA to maintain this significant increase ($P<0.01$), again with no change in levels of PEA, AEA or 2-AG.

4.6.6 Endocannabinoids in the hypothalamus

a.

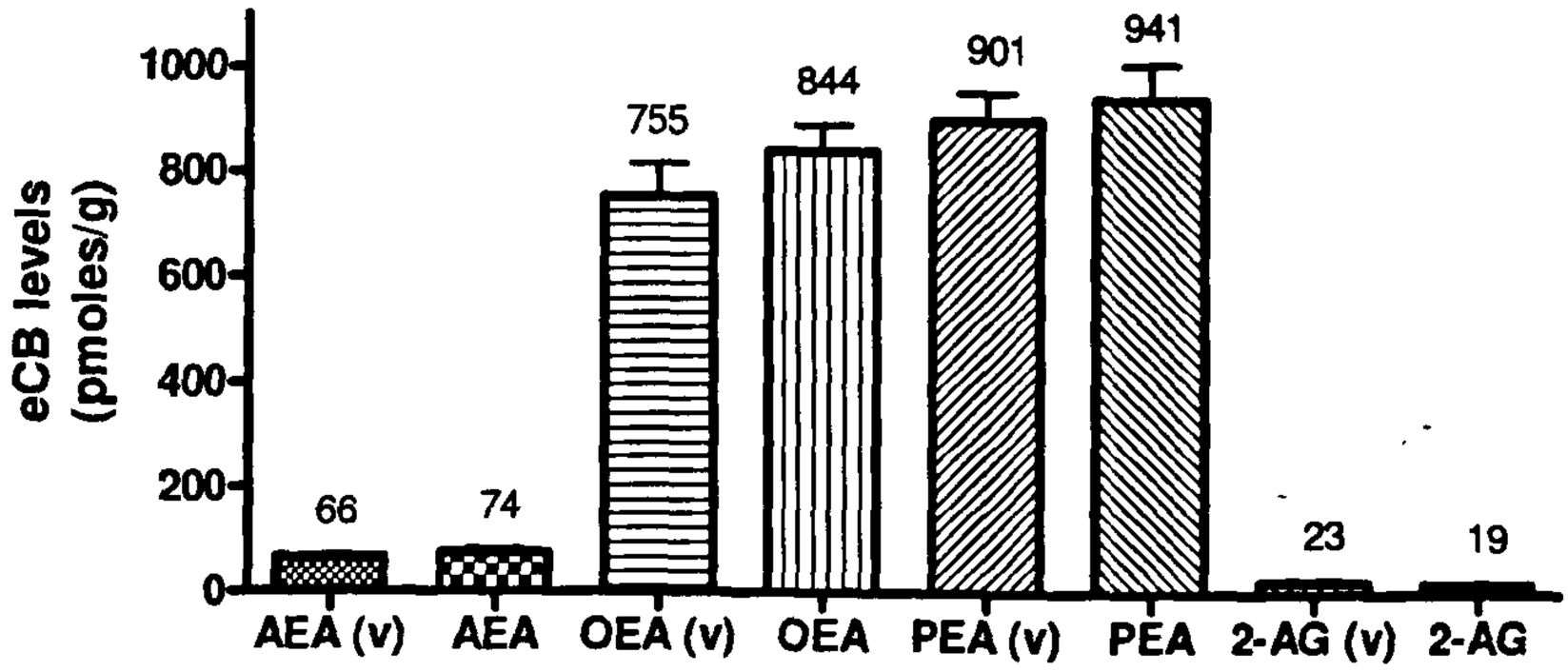

b.

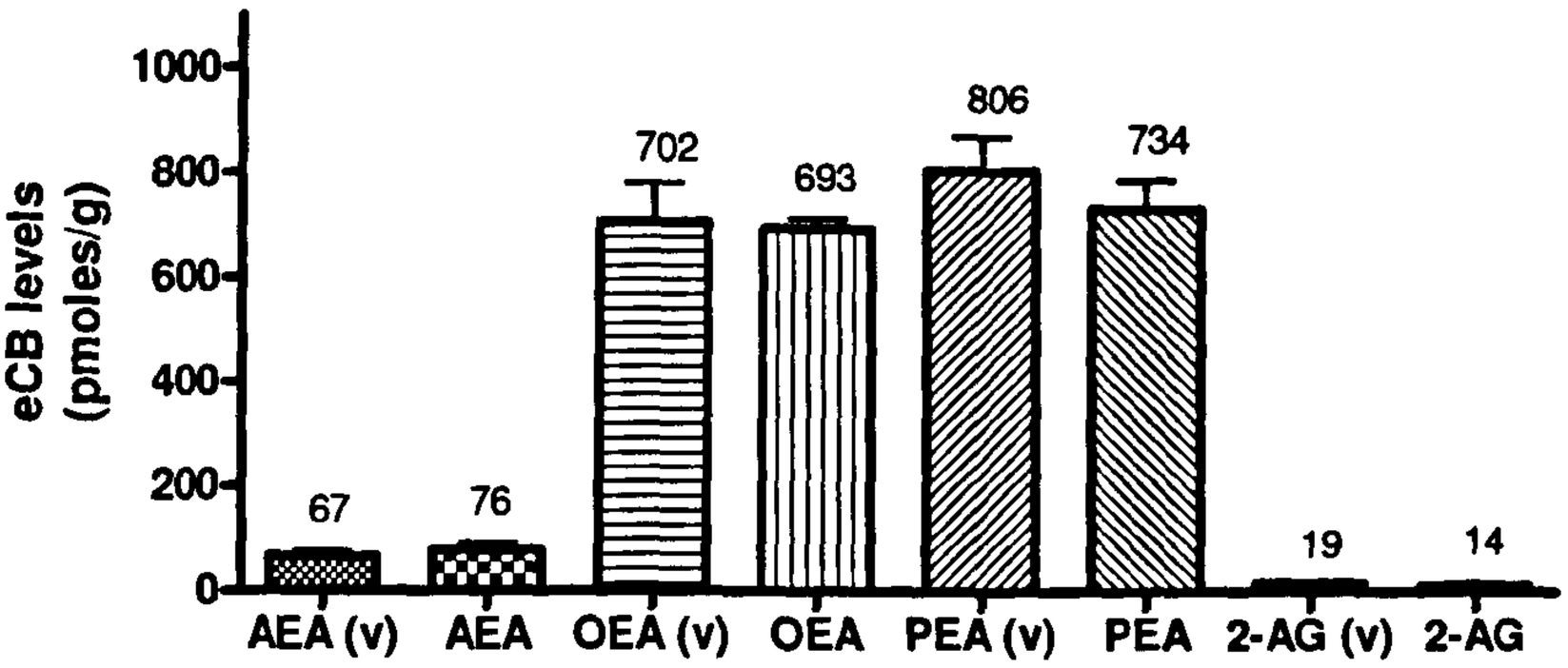

Figure 4.23 **Endocannabinoid levels quantified in mouse hypothalamus tissues, following vehicle and OEA (10 mg/kg) treatment (i.p.) and tissues collected 30 (a) and 60 (b) minutes post-injection (n=4).**

Basal levels show OEA and PEA to be 10-12 fold higher than that of AEA and 2-AG, with levels of PEA being slightly higher than that of OEA. There was no change in levels of all compounds at 30 and 60 minutes post-injection.

4.6.7 Endocannabinoids in the hippocampus

a.

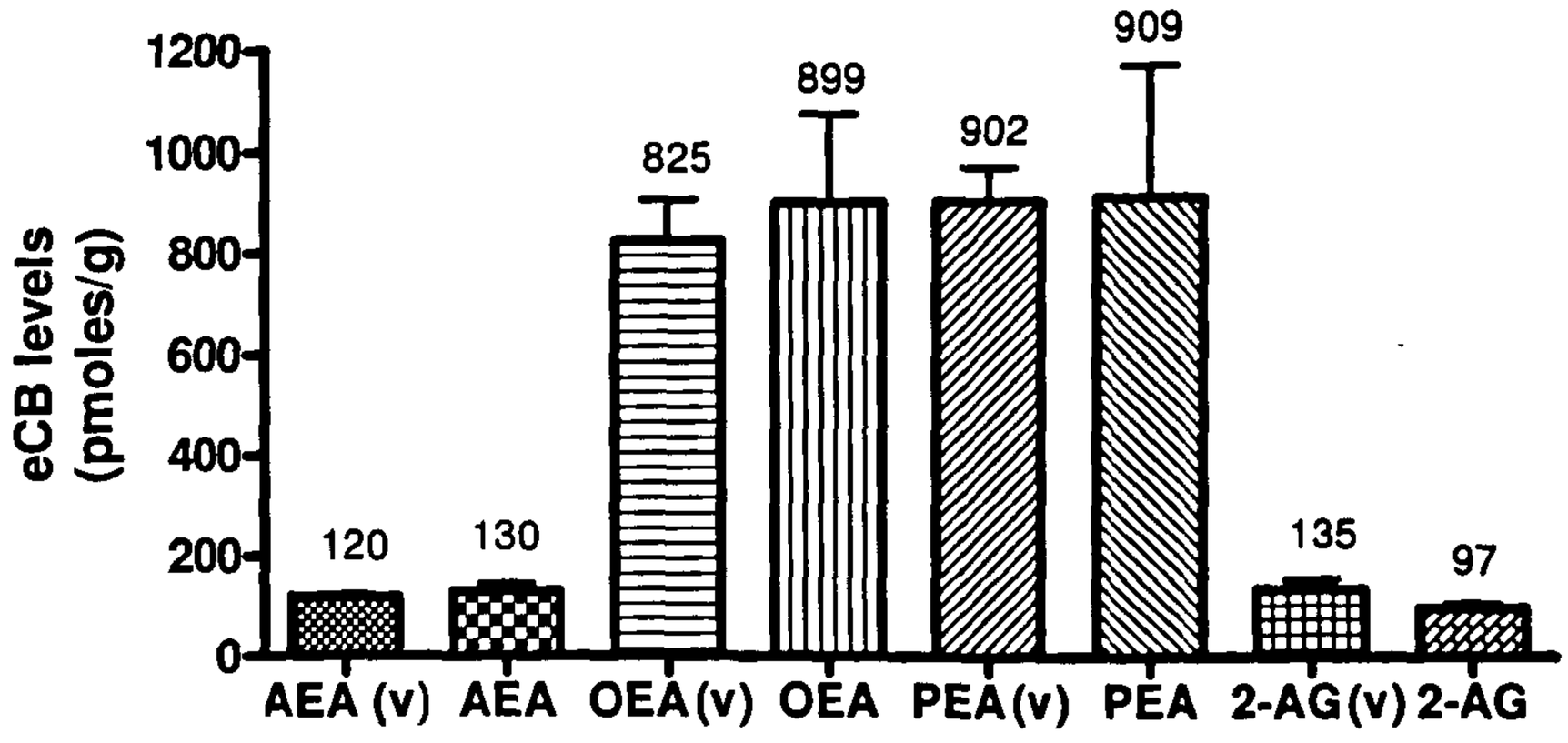

b.

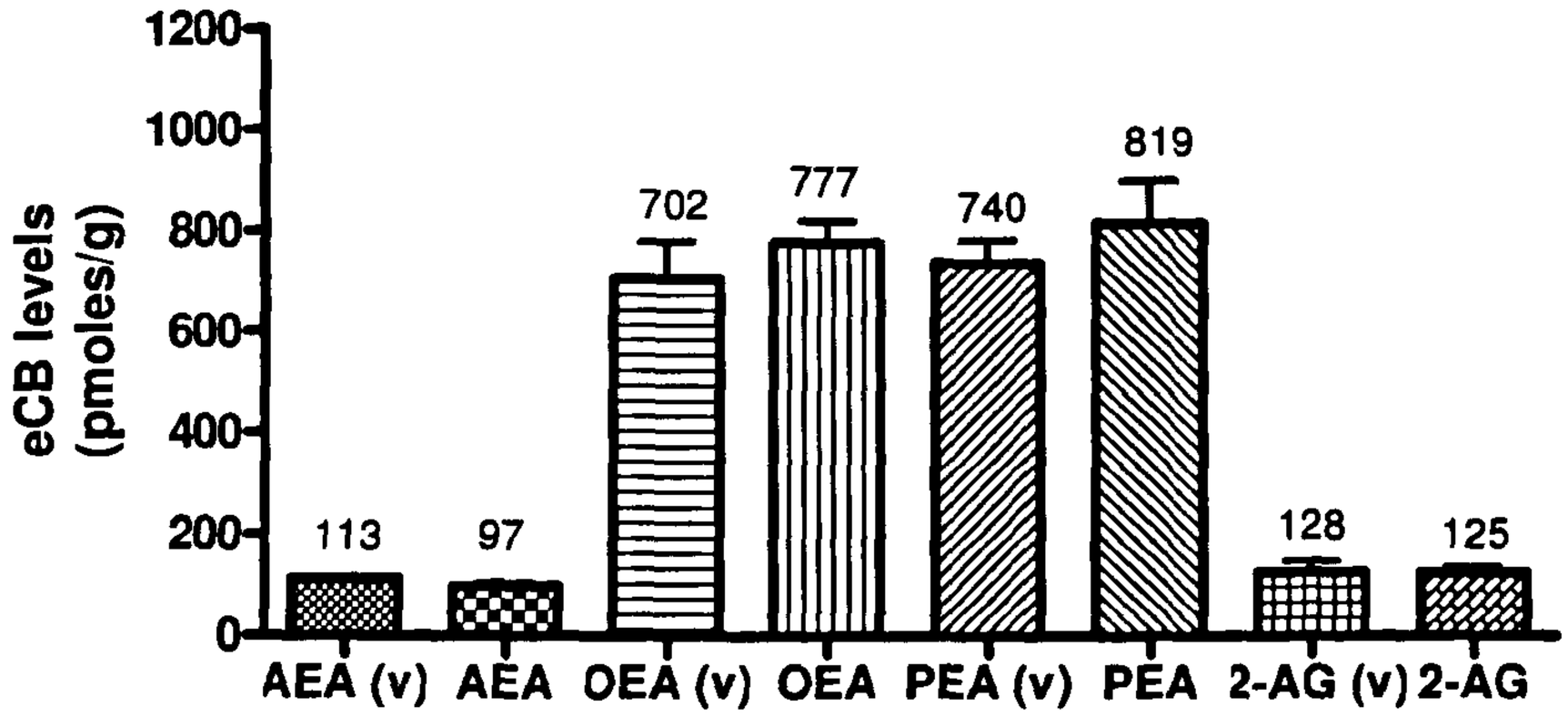

Figure 4.24 **Endocannabinoid levels quantified in mouse hippocampus tissues, following vehicle and OEA (10 mg/kg) treatment (i.p.) and tissues**

collected 30 (a) and 60 (b) minutes post-injection (n=4).

Basal levels of OEA were 7-8 fold higher than those of AEA and 2-AG, while basal levels of PEA were 8-9 fold higher also compared to the eCBs. Again, in this brain tissue, there was no change in levels measured at 30 and 60 minutes following injection with any of the compounds (**figure 4.24**).

4.6.8 OEA quantified levels

a.

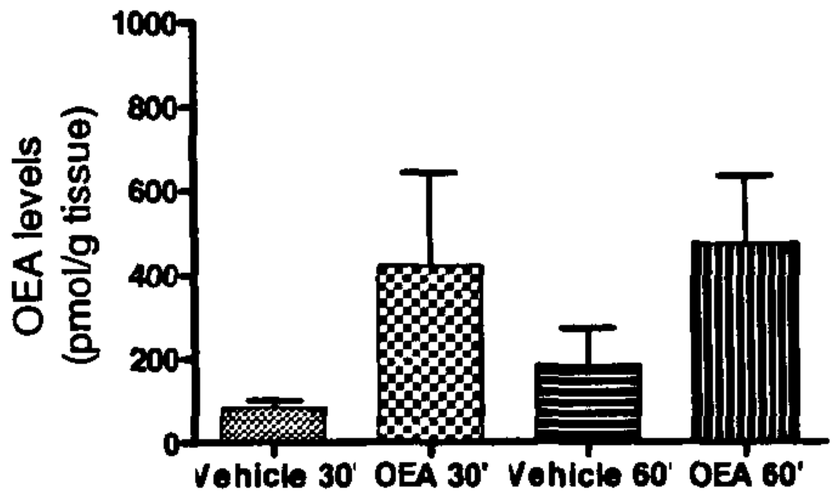

b.

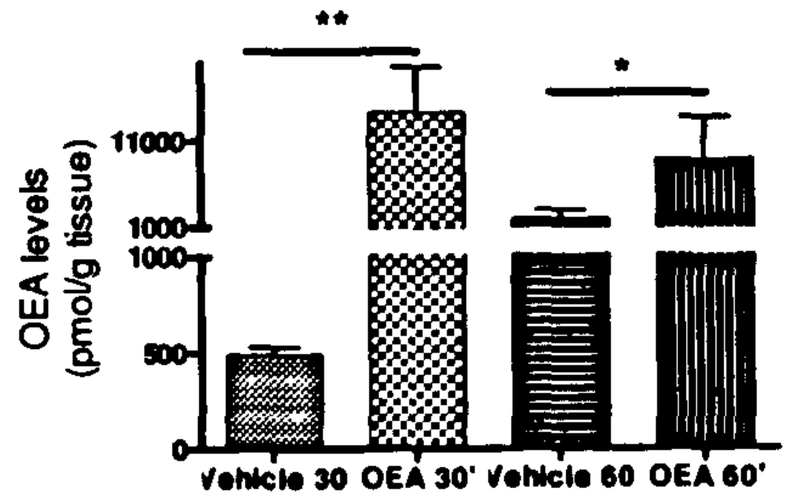

c.

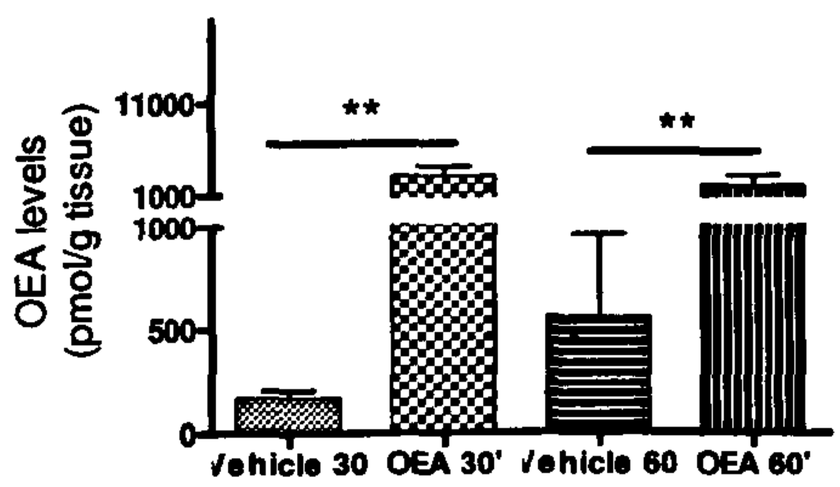

d.

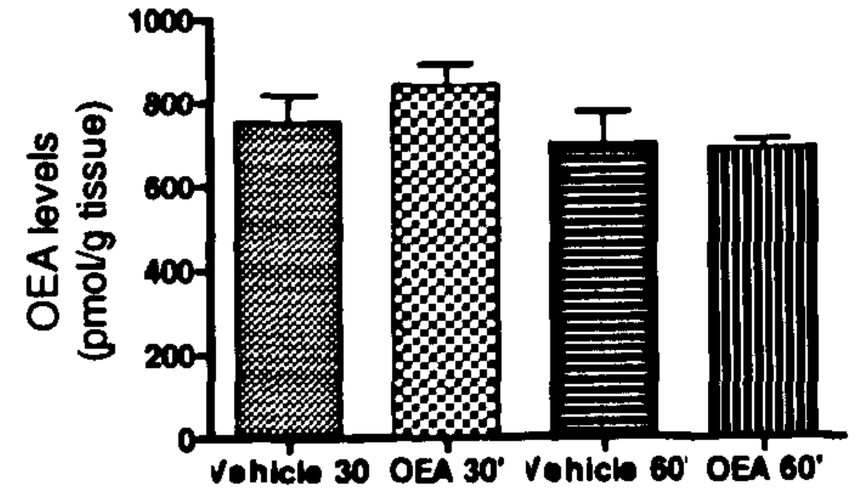

e.

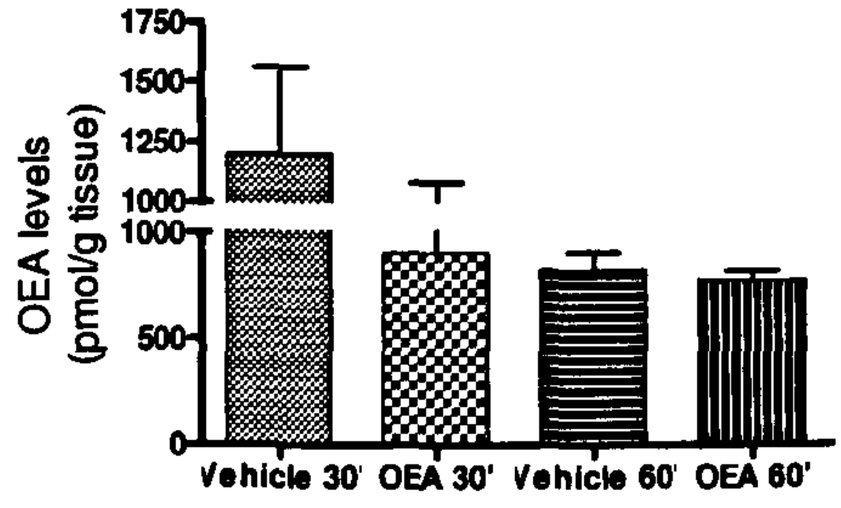

Figure 4.25 **OEA levels quantified in mouse liver (a), ileum (b), duodenum (c), hypothalamus (d) and hippocampus (e) tissues, following vehicle and OEA treatment (10 mg/kg; i.p.) and tissues collected at 30 and 60 minutes post-injection. Data were analysed using two-way ANOVA with Dunnett's post-hoc test (*p<0.05; **p<0.01).**

Figures 4.25 shows the changes in levels of OEA measured at both time points in each individual tissue. It is clear in the liver that OEA displays a trend of increase in OEA at both 30 and 60 minutes, albeit not significant. In the ileum however, OEA administration caused a significant increase at 30 minutes ($P<0.01$) which is slightly decreased, yet still significant, at 60 minutes ($P<0.05$). In the duodenum, there was a significant increase in OEA levels at 30 minutes ($P<0.01$) which was sustained up to the 60 minute point ($P<0.01$). Both brain tissues showed no significant change in levels of OEA at either 30 or 60 minutes.

4.6.9 Discussion

OEA's actions on satiety are peripheral in their site of action and do not involve PEA, AEA or 2-AG. Tissues levels are regulated by FAAH, which makes a contribution to the reduction in eCB levels measured at 60 minutes compared to 30 minutes. It is clear that exogenously administered OEA reaches the liver, ileum and duodenum, but does not seem to reach central tissues (hippocampus and hypothalamus). Levels of OEA in the liver increase as a result of mobilization of exogenously administered OEA. We know (**section 2.4.1**) FAAH activity is at its highest in the liver and this may in turn explain high, rapid rates of OEA metabolism by its primary hydrolyzing enzyme FAAH reducing levels of OEA achieved in this tissue between the 30 and 60 minute time points, and overall, causing OEA to not reach a level of significant increase in the liver.

The ileum has levels of FAAH activity lower than the liver, yet higher than measured in

the duodenum (Duncan *et al.,* 2008). OEA administration shows significant increase of OEA in this tissue within the transient time frame OEA has previously displayed its actions on satiety. These data indicate the ileum as a site of OEA mobilization, indicating a locus of action, which is further supported by literature (Fu et al., 2003; Rodriguez de Fonseca et al.). The lower levels of FAAH activity, compared to the liver may explain how OEA reached a significant levels ($P<0.01$) at 30 minutes, but the reduction in OEA from 30 to 60 minutes may still be explained by the level of FAAH activity present in this tissue. We would expect OEA hydrolysis to occur between 30 and 60 minutes causing the observed reduction in the significance ($P<0.05$) reached by OEA levels at 60 minutes compared to 30 minutes.

The duodenum shows high levels of OEA accumulation at 30 minutes following administration. Due to the lower levels of FAAH activity in the duodenum, the significant increase in levels of OEA is maintained up to 60 minutes post-administration. Overall, results indicate a gastrointestinal locus of action, which supports literature, where it has been found that endogenous levels of OEA, measured in fasted and feeding animals show mobilization in proximal areas of the small intestine (Fu et al., 2007; Piomelli et al., 2006). Piomelli's group have also reported lower levels of FAAH activity in proximal areas of the small intestine, in response to the increase of OEA levels initiated with onset of feeding. Further investigation of the effects of OEA on the expression and activity of OEA's synthesizing and hydrolyzing enzymes in various tissues may provide a better understanding of its role in the regulation of feeding.

There are high levels of PPARα expression in the walls of the small intestine, where

activation could potentially lead to signals being directly sent through the vagal sensory neurone (as describes in **section 1.7**), in response to PPARα activation, to the satiety centre, to induce satiety.

Results do not support a central locus of action as exogenous OEA is not seen to alter OEA levels at either 30 or 60 minutes, directly in the hypothalamus itself or the larger brain section of the hippocampus. If OEA-mediated effects on food intake were centrally controlled and involved direct activation within the satiety centre, we would have expected levels in the hypothalamus to have been altered following OEA administration, yet this was not seen. We do not know if OEA can directly access the brain through the blood brain barrier, but OEA has been previously found not to induce its effects on food intake when injected directly into the brain, but only when administered i.p. in the periphery (Cravatt et al., 2007; Fu et al., 2007), again supporting the hypothesis that OEA exerts its effects through a peripheral, intestinal site of action.

4.7 Investigation of the contribution of PPARα in OEA-evoked satiety responses using genetic animal models

4.7.1 Introduction

We have previously compared the effects of a known PPARα agonist, fenofibrate, PPARα antagonist GW6471, and OEA in their effects mediated through PPARα receptor. Results indicated an additive effect of OEA, suggesting reduction in food intake is in part mediated by PPARα, yet another receptor mechanism may well account for part of the response measured. OEA has been found to reduce food intake in wild-type mice, but not in mice deficient in PPAR-α (PPAR-$\alpha^{-/-}$) (Fu et al., 2005). Here we have used PPARα$^{-/-}$

mice to quantify the OEA-evoked response mediated by PPARα receptor. The overall aim was to understand the role of PPAR-α in regulating feeding behaviour; this study will determine whether a functional PPAR-α is responsible for the individual effects of OEA, fenofibrate and GW6471 on food intake and satiety.

4.7.2 Method

Our previous experiments employing administration of OEA, fenofibrate and GW6471 has allowed us to determine significant effects in food intake with doses of 10 mg/kg, 20 mg/kg and 15 mg/kg respectively. We will therefore be administering these doses to PPAR-α-null mice to determine the involvement of PPAR-α receptor-dependent mechanisms on regulation of food intake.

Experimental procedure

Eight PPARα$^{-/-}$ mice and eight wild type mice (C57bl6) were used as controls. The mice were split up into 4 knockout mice and 4 controls. Each treatment was given to one PPARα$^{-/-}$ mouse and one control (according to **table 4.13**), following the same experimental procedure was applied as described in **section 4.3.2.** After mice were measured in the CLAMS for 48 hours, the experimental procedure was repeated with another set of 4 knockout and 4 control mice, to provide n=8 of knockouts versus control data.

	Group 1		Group 2		Group 3		Group 4	
mouse	**1(P)**	**1(C)**	**2(P)**	**2(C)**	**3(P)**	**3(C)**	**4(P)**	**4(C)**
Week 1	Vehicle		OEA (10 mg/kg)		Fenofibrate (20 mg/kg)		GW6471 (15 mg/kg)	
Week 2	GW6471 (15 mg/kg)		Vehicle		OEA (10 mg/kg)		Fenofibrate (20 mg/kg)	
Week 3	Fenofibrate (20 mg/kg)		GW6471 (15 mg/kg)		Vehicle		OEA (10 mg/kg)	
Week 4	OEA (10 mg/kg)		Fenofibrate (20 mg/kg)		GW6471 (15 mg/kg)		Vehicle	

Table 4.13 **Experimental dosing plan of eight mice (4 x PPAR$^{-/-}$ ((P)) and 4 x control ((C)) (C57bl6)) in a pseudo-random order with treatment of Vehicle, OEA (10 mg/kg), GW6471 (20 mg/kg) and fenofibrate (20 mg/kg). following a CLAMS measurments session, the above table was repeated using mice 5-8 of both PPAR$^{-/-}$ and controls. The experiment was run over a 4 week period.**

4.7.3 Results

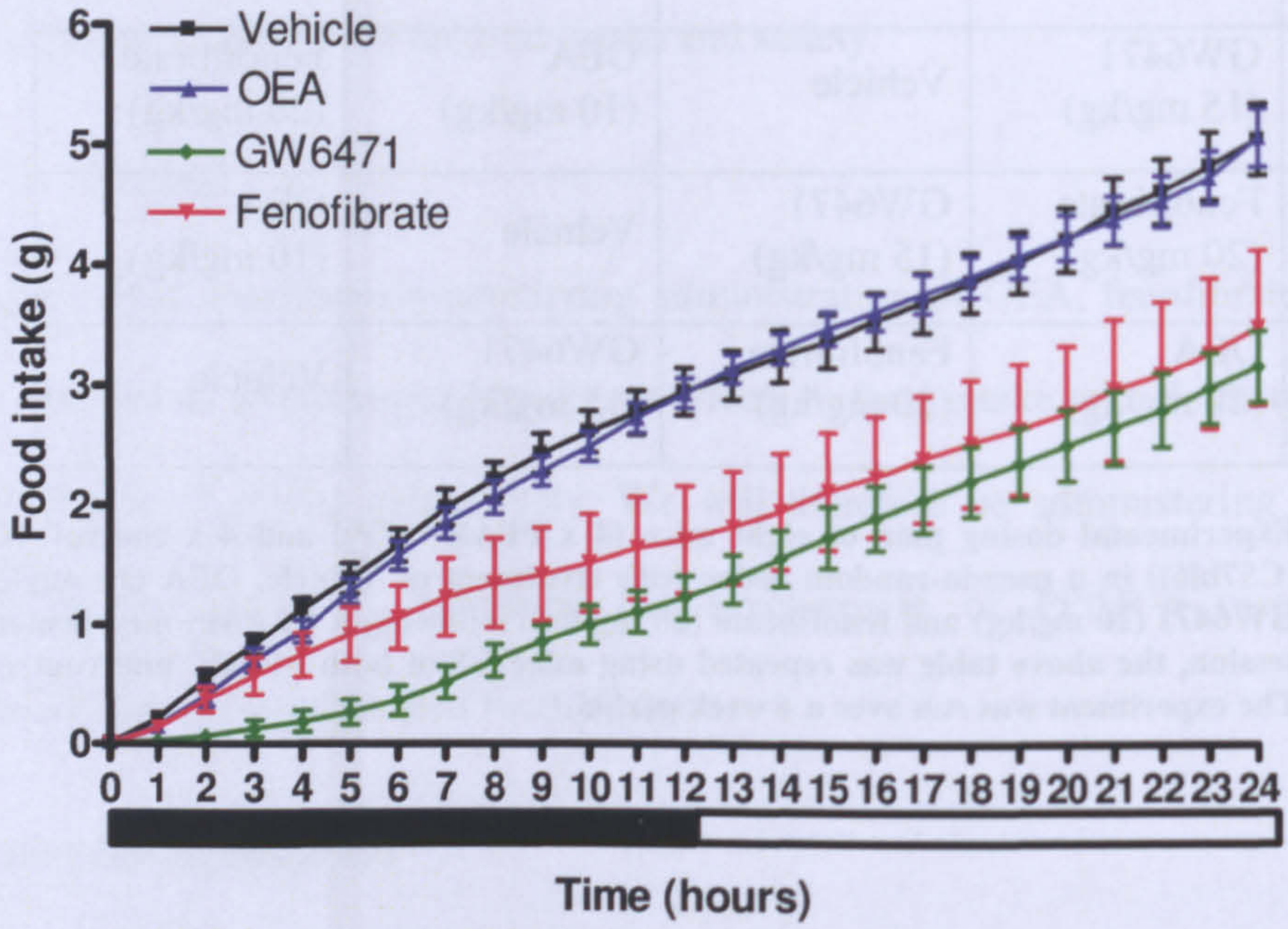

Figure 4.26 **Cumulative food intake for control wild-type mice (C57bl6) for 24 hours post-injection (all experiments shown in this section have n=8 of data). The bars below the graph indicate 12 hour dark and light phase. 0-24 hour data were analysed comparing all treatments against vehicle, using one-way ANOVA with Dunnett's post-hoc test.**

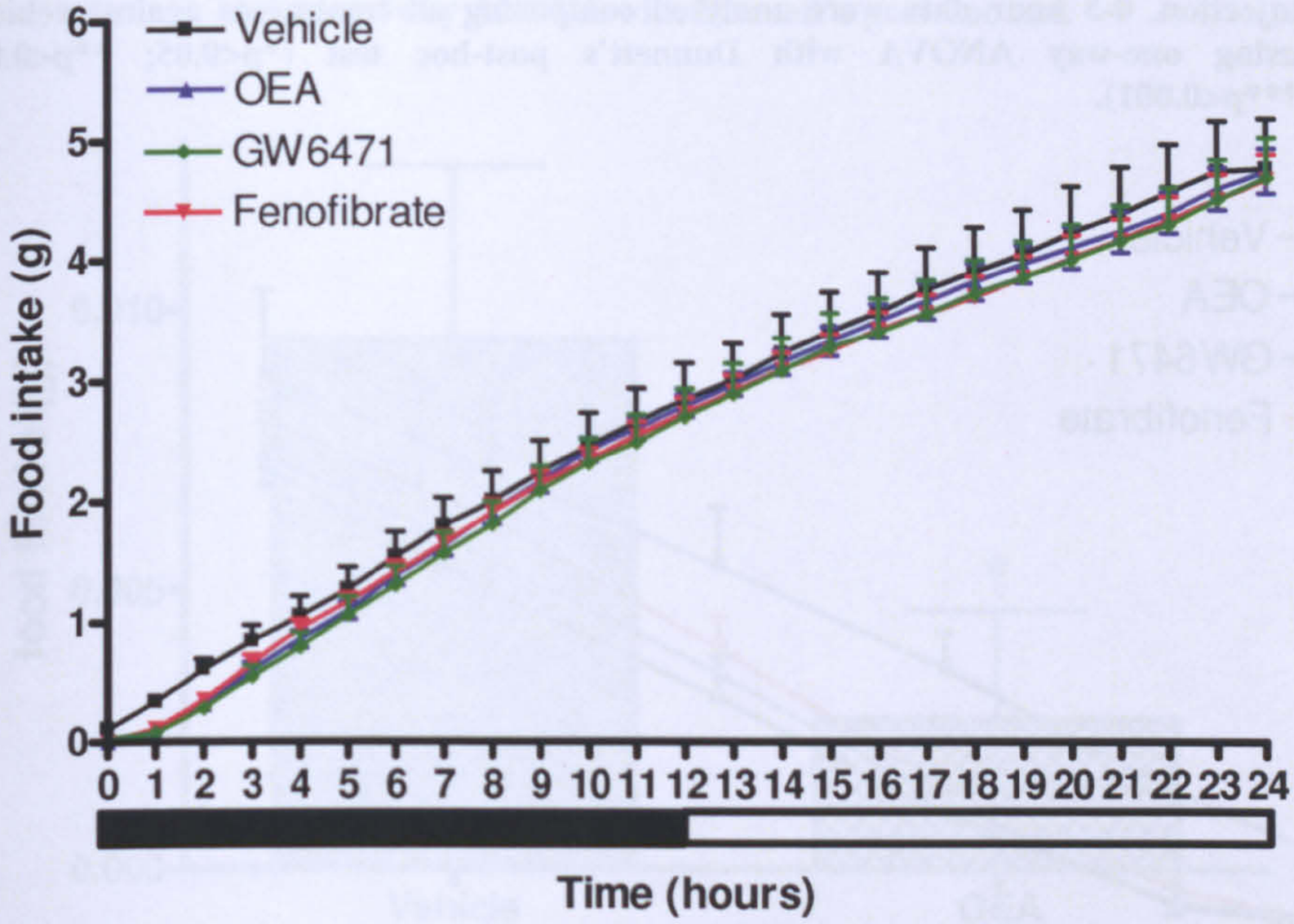

Figure 4.27 **Cumulative food intake for PPARα$^{-/-}$ in eight mice for 24 hours post-injection. The bars below the graph indicate 12 hour dark and light phase. 0-24 hour data were analysed comparing all treatments against vehicle, using one-way ANOVA with Dunnett's post-hoc test.**

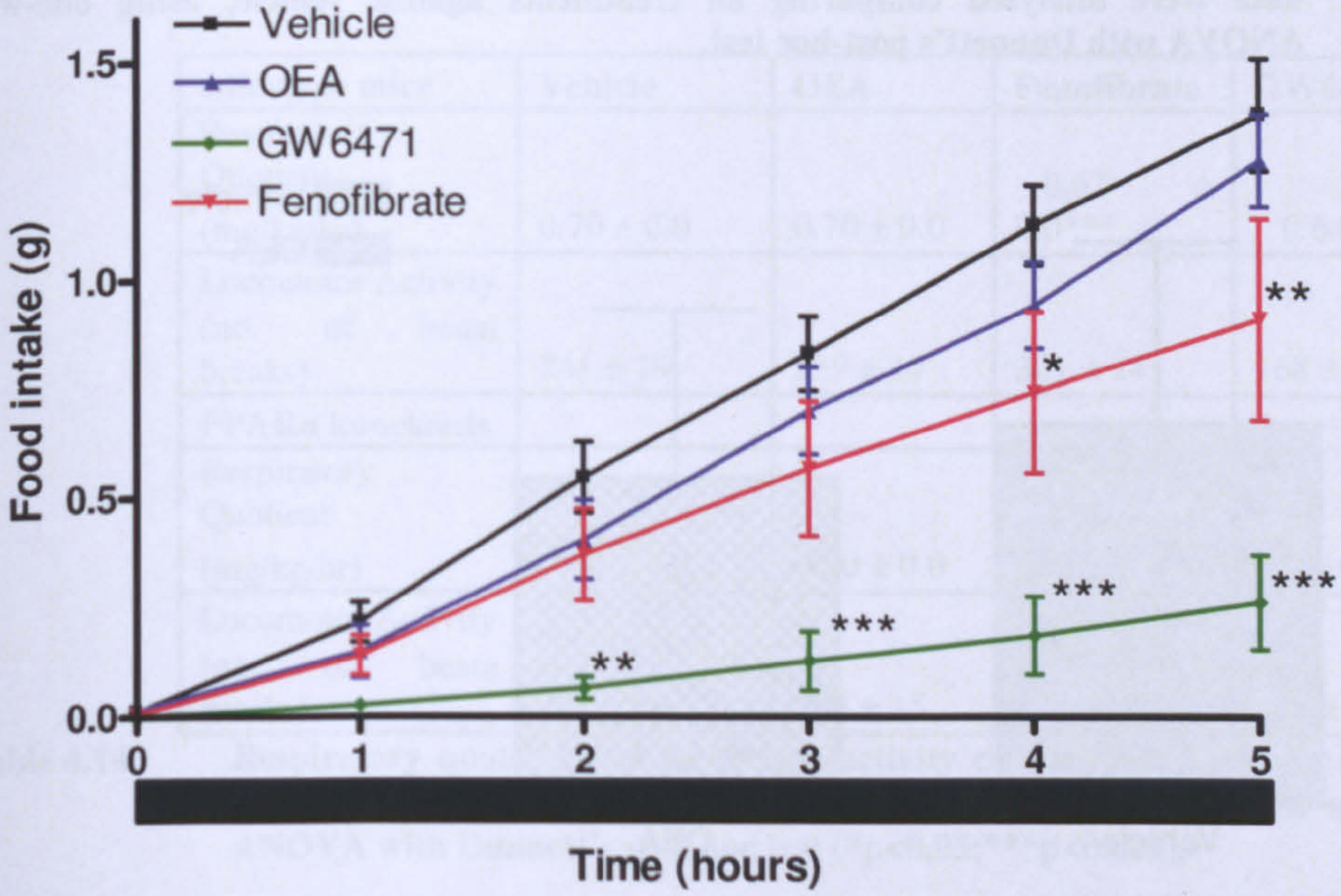

Figure 4.28 **Cumulative food intake for eight control wild-type mice (C57bl6) for 5 hours post-injection. 0-5 hour data were analysed comparing all treatments against vehicle, using one-way ANOVA with Dunnett's post-hoc test (*p<0.05; **p<0.01; ***p<0.001).**

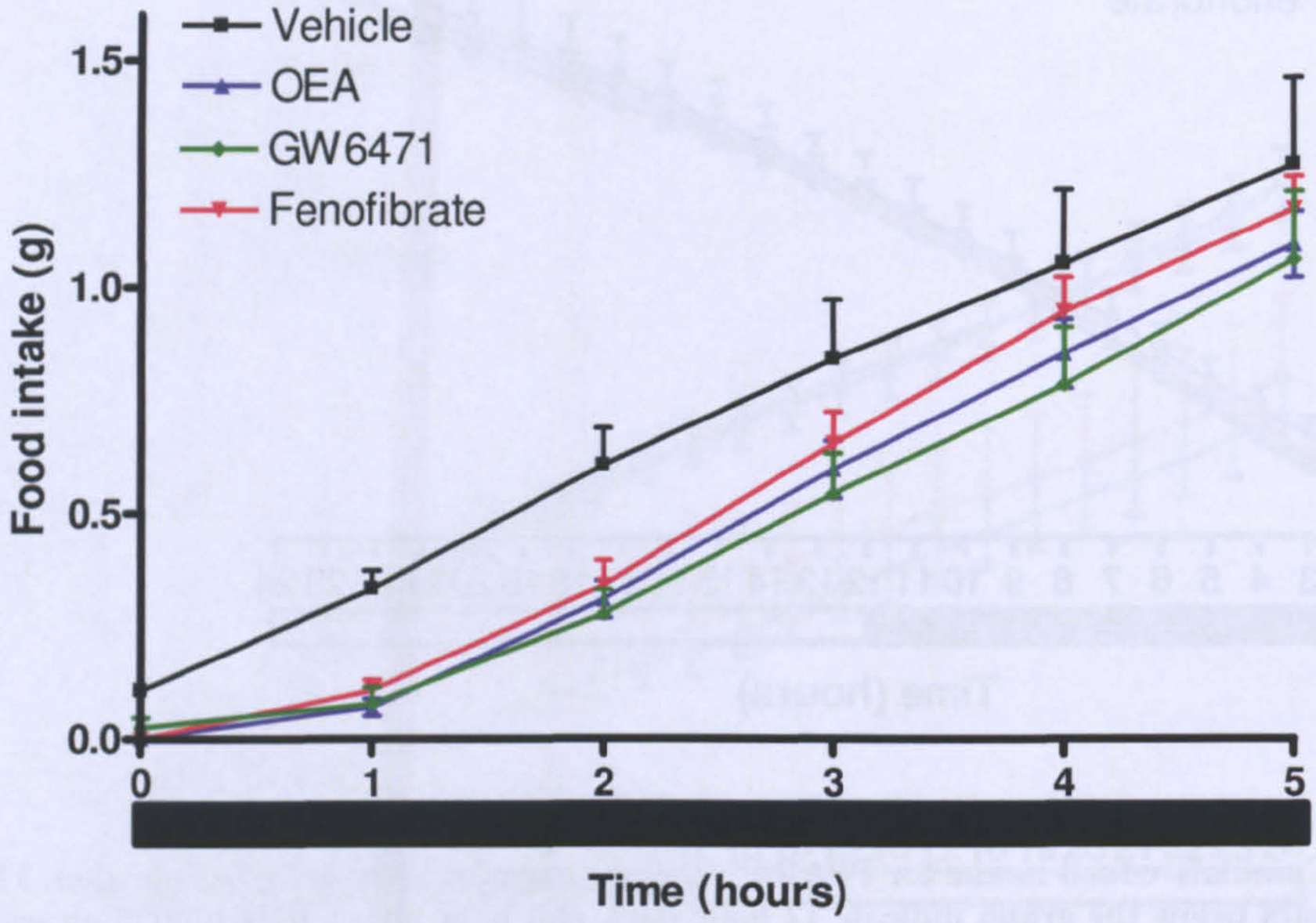

Figure 4.29 **Cumulative food intake in eight PPARα$^{-/-}$ mice for 5 hours post-injection. 0-5 hour data were analysed comparing all treatments against vehicle, using one-way ANOVA with Dunnett's post-hoc test.**

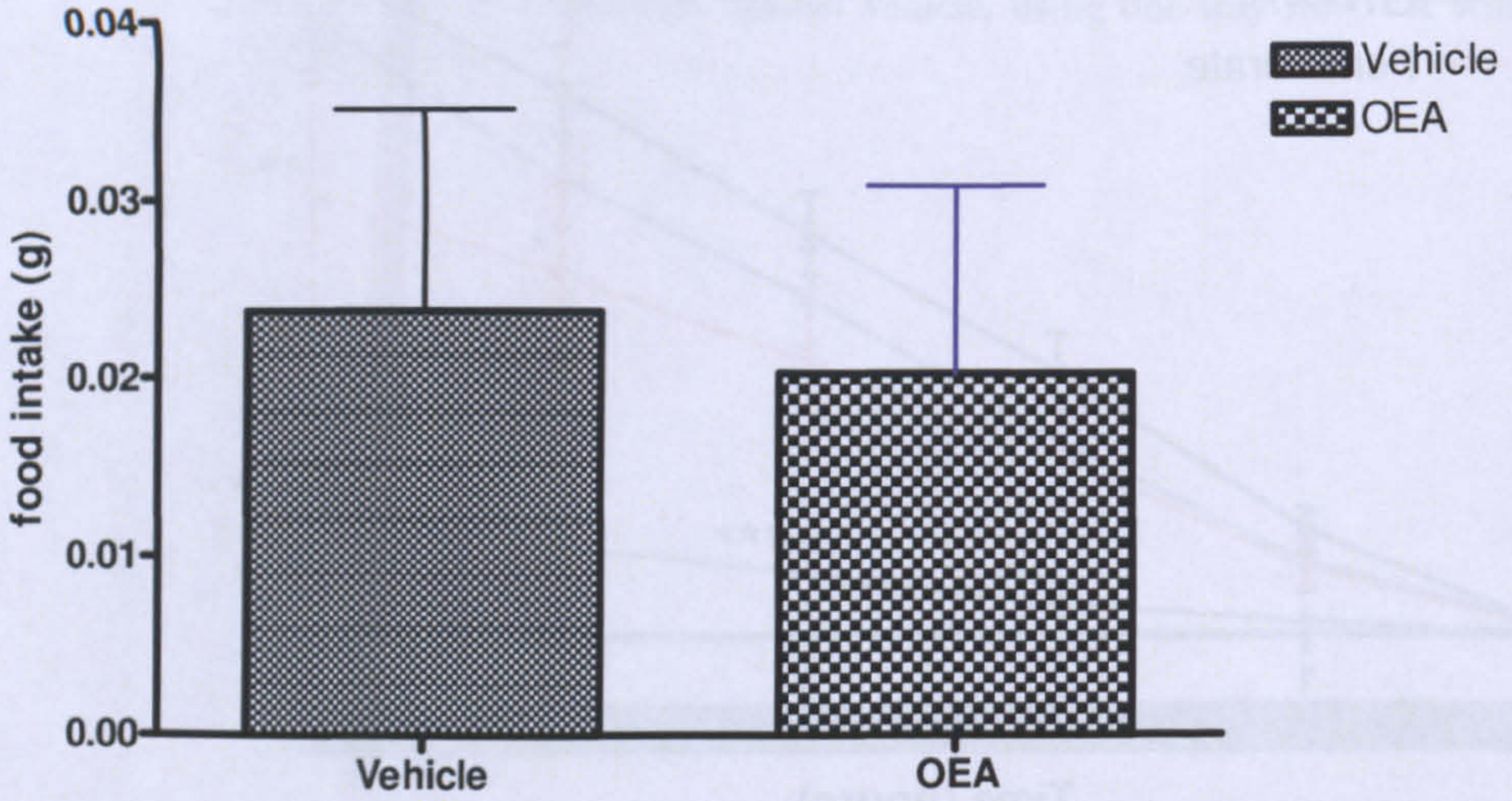

Figure 4.30 **Cumulative food intake in eight control wild-type mice (C57bl6) for 1 hour post-**

injection. 0-1 hour data were analysed comparing all treatments against vehicle, using one-way ANOVA with Dunnett's post-hoc test.

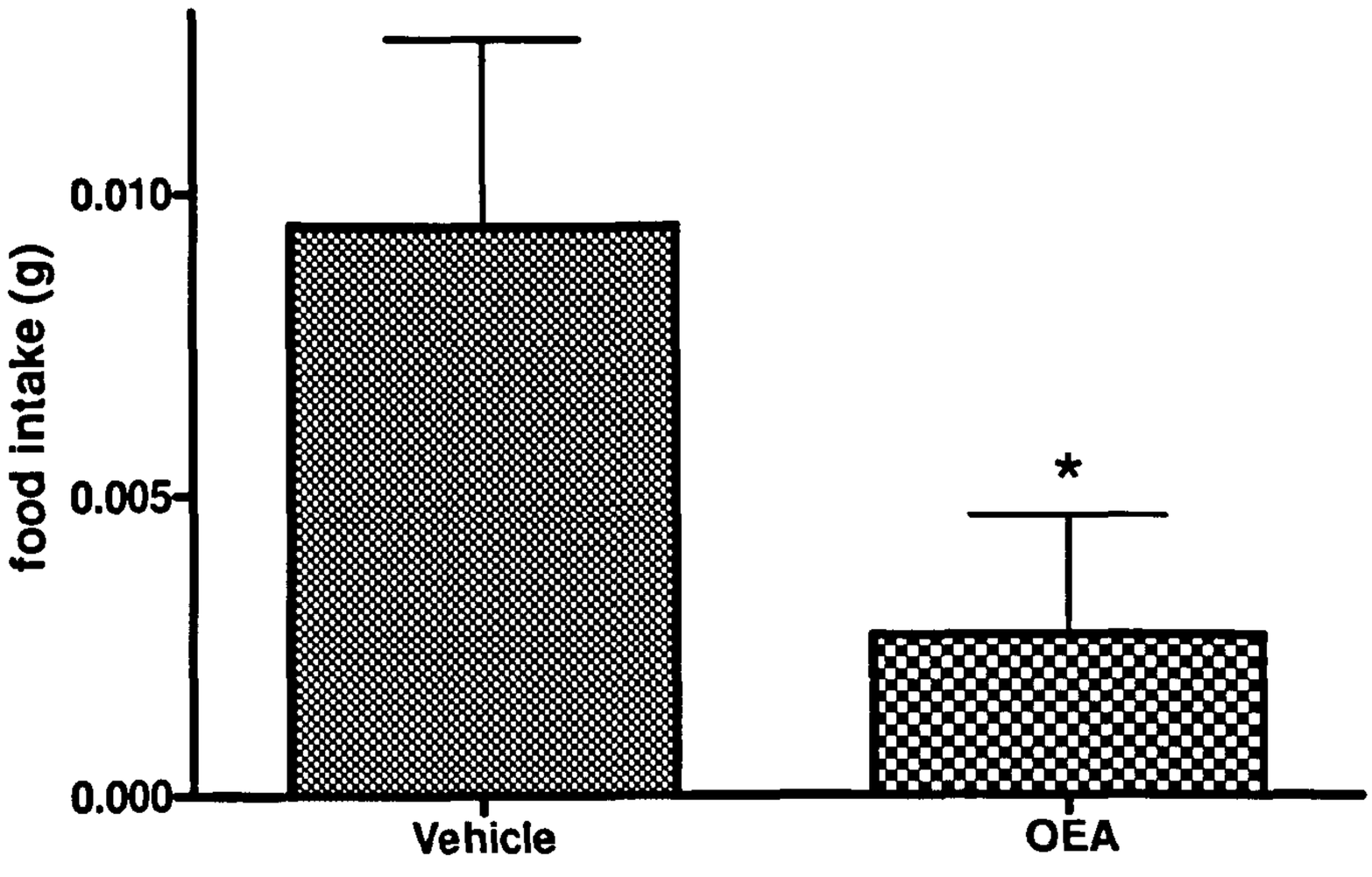

Figure 4.31 Cumulative food intake in eight PPARα$^{-/-}$ mice for 1 hours post-injection. 0-1 hour data were analysed comparing all treatments against vehicle, using one-way ANOVA with Dunnett's post-hoc test (*p<0.05).

wild-type mice	Vehicle	OEA	Fenofibrate	GW6471
Respiratory Quotient (mg/kg/hr)	0.70 ± 0.0	0.70 ± 0.0	0.67 ± 0.0***	0.64 ± 0.0***
Locomotor Activity (no. of beam breaks)	241 ± 19	239 ± 17	301 ± 24	168 ± 13*
PPARα knockouts				
Respiratory Quotient (mg/kg/hr)	0.69 ± 0.0	0.70 ± 0.0	0.69 ± 0.0	0.69 ± 0.0
Locomotor Activity (no. of beam breaks)	201 ± 13	204 ± 15	234 ± 19	249 ± 16

Table 4.14 Respiratory quotient and locomotor activity counts for 24 hours post-injection of wild-type mice (C57bl6) and PPARα$^{-/-}$ mice. Data were analysed using one-1way ANOVA with Dunnett's post hoc test (*p<0.05;***p<0.001).

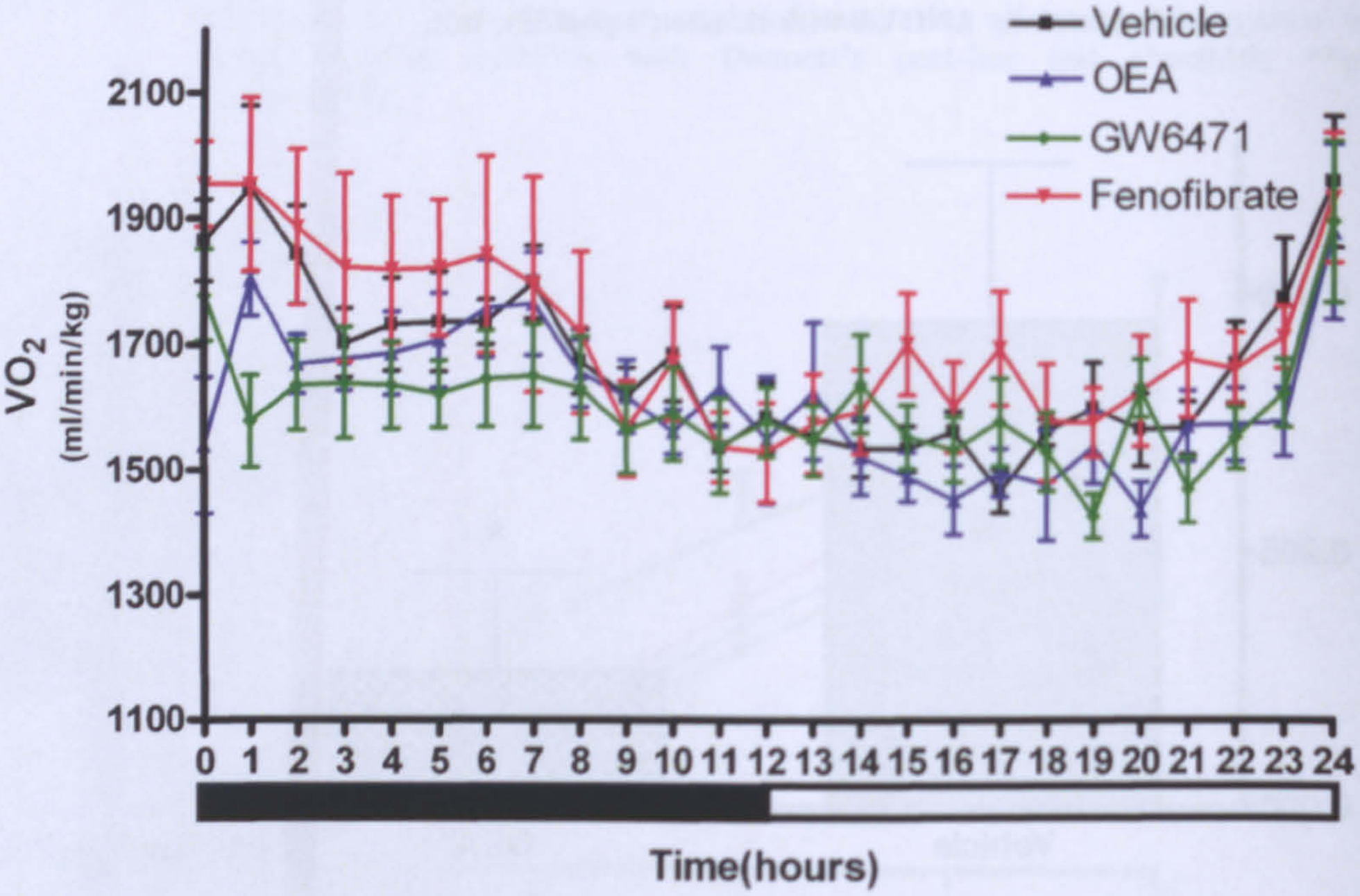

Figure 4.32 **Oxygen consumption in eight wild-type mice (C57bl6) for 24 hours post-injection. 0-24 hour data were analysed comparing all treatments against vehicle, using one-way ANOVA with Dunnett's post-hoc test.**

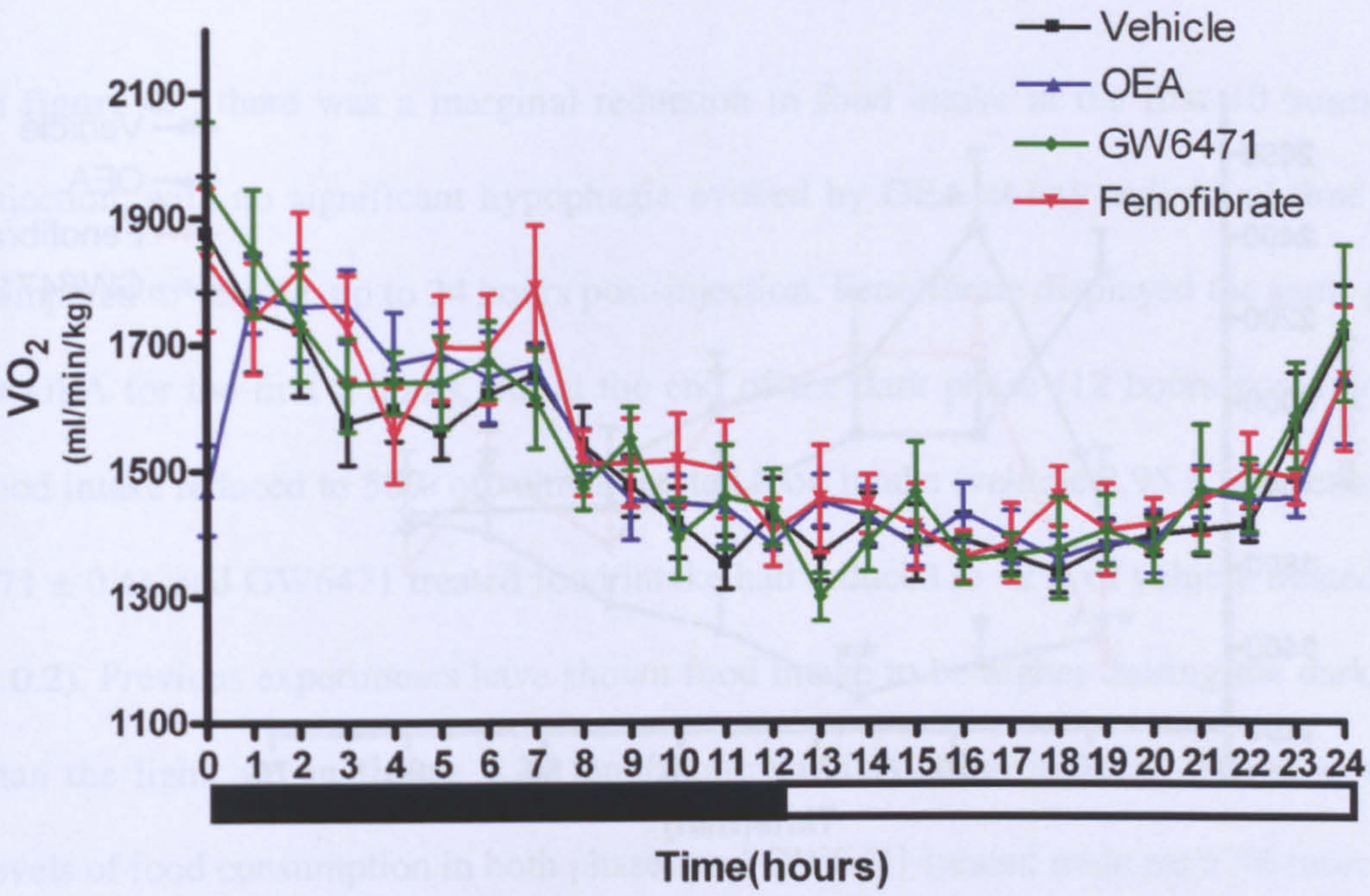

Figure 4.33 **Oxygen consumption in eight PPARα$^{-/-}$ mice for 24 hours post-injection. 0-24 hour data were analysed comparing all treatments against vehicle, using one-way ANOVA with Dunnett's post-hoc test.**

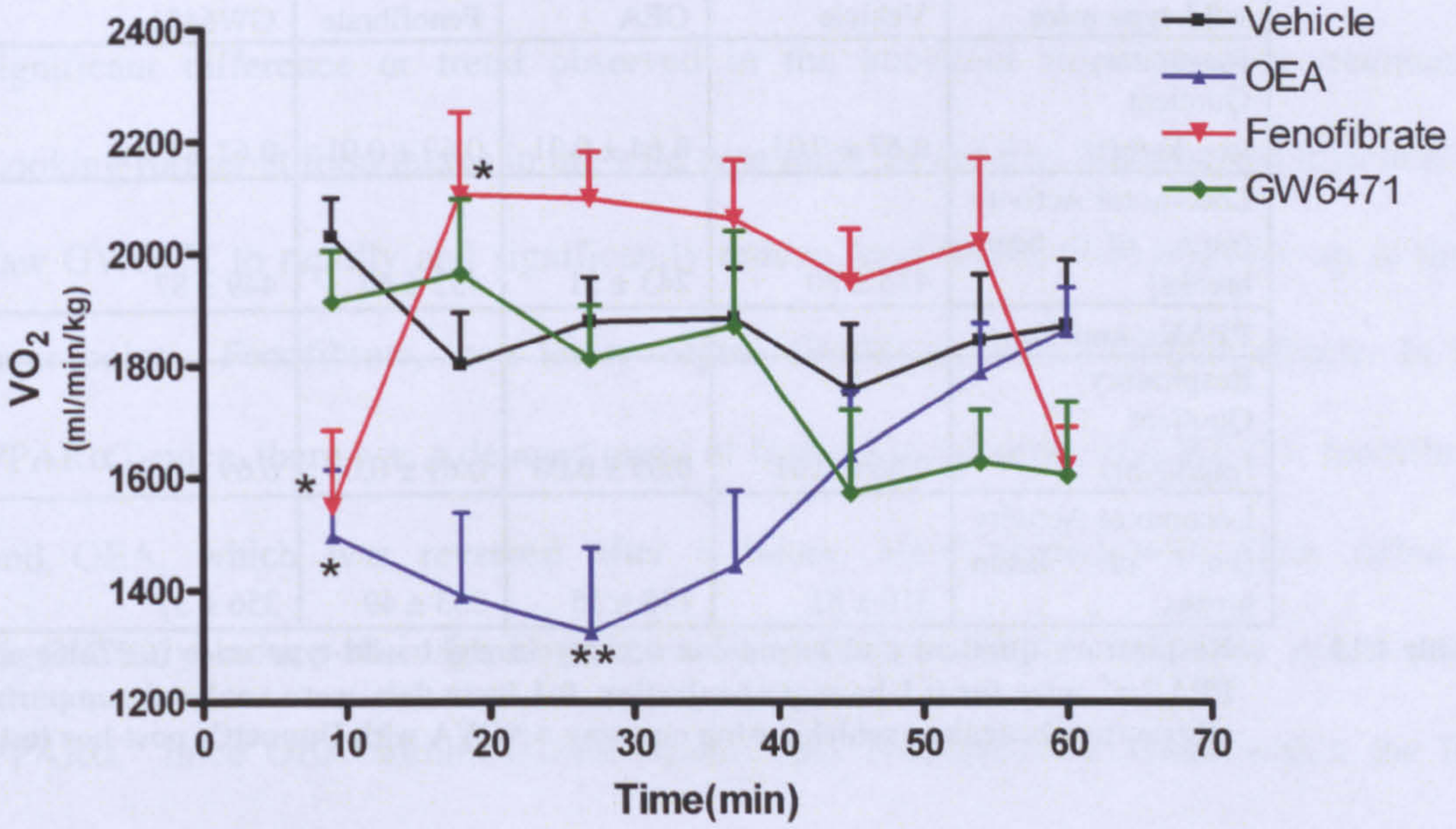

Figure 4.34 **Oxygen consumption in eight wild-type mice (C57bl6) for 1 hour post-injection. 0-1 hour data were analysed comparing all treatments against vehicle, using one-way**

ANOVA with Dunnett's post-hoc test (*p<0.05; **p<0.01).

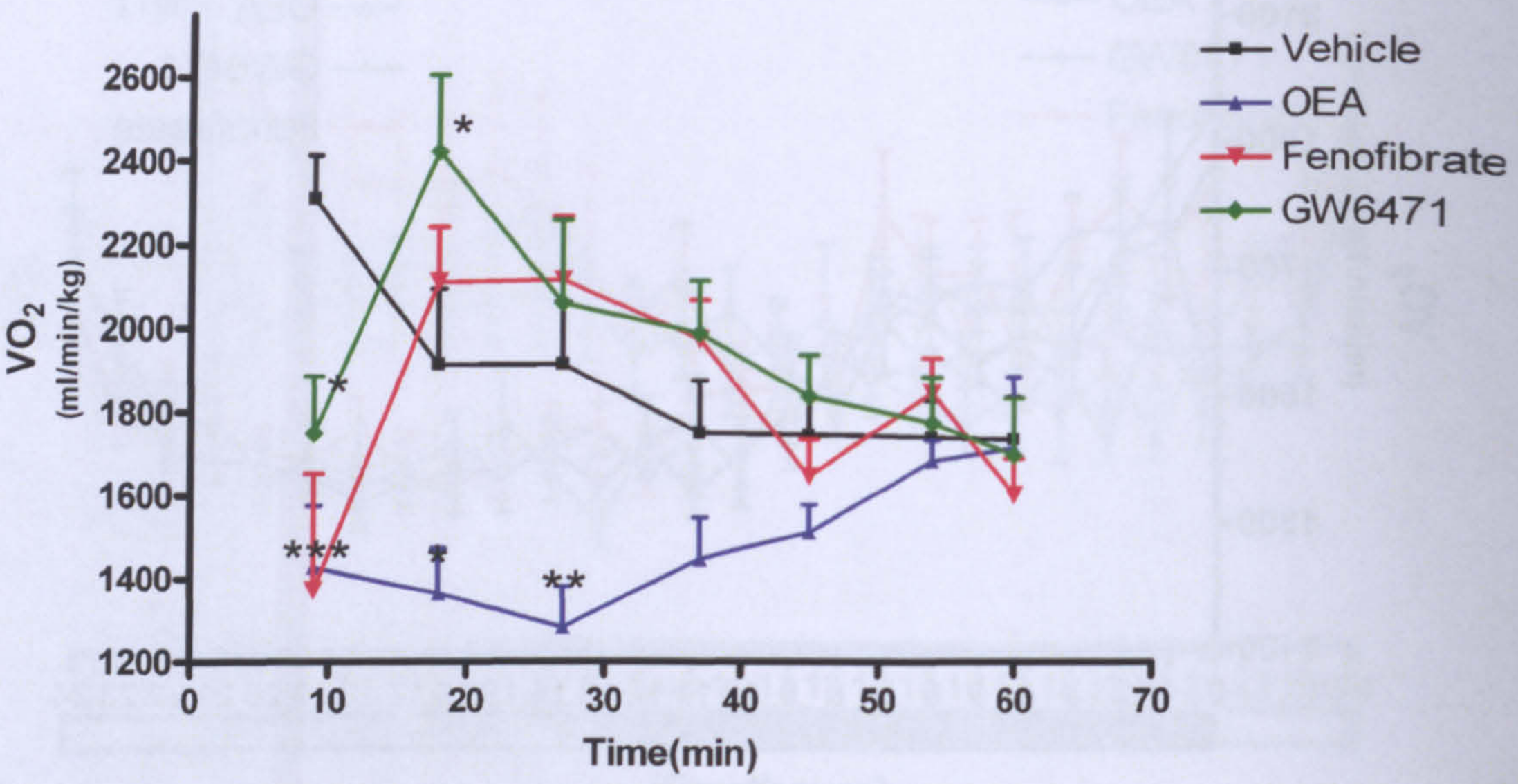

Figure 4.35 **Oxygen consumption in eight PPARα$^{-/-}$ mice for 1 hour post-injection. 0-1 hour data were analysed comparing all treatments against vehicle, using one-way ANOVA with Dunnett's post-hoc test (*p<0.05; **p<0.01; ***p<0.001).**

wild-type mice	Vehicle	OEA	Fenofibrate	GW6471
Respiratory Quotient (mg/kg/hr)	0.67 ± 0.01	0.64 ± 0.01	0.69 ± 0.01	0.67 ± 0.01
Locomotor Activity (no. of beam breaks)	415 ± 80	243 ± 51	432 ± 60	449 ± 87
PPARα knockouts				
Respiratory Quotient (mg/kg/hr)	0.66 ± 0.01	0.65 ± 0.00	0.69 ± 0.00	0.69 ± 0.01
Locomotor Activity (no. of beam breaks)	310 ± 81	149 ± 15	353 ± 49	356 ± 37

Table 4.15 **Respiratory quotient and locomotor activity in eight wild-type mice (C57bl6) and PPARα$^{-/-}$ mice for 0-1 hour post-injection. 0-1 hour data were analysed comparing all treatments against vehicle, using one-way ANOVA with Dunnett's post-hoc test.**

In **figure 4.** , there was a marginal reduction in food intake in the first 10 hours post-injection, with no significant hypophagia evoked by OEA at any individual time point, compared to vehicle, up to 24 hours post-injection. Fenofibrate displayed the same profile as OEA for the first 2 hours, but at the end of the dark phase (12 hours post-injection) food intake reduced to 58% of vehicle treated food intake (vehicle 2.95 ± 0.2; fenofibrate 171 ± 0.4), and GW6471 treated food intake had reduced to 42% of vehicle treated (1.23 ± 0.2). Previous experiments have shown food intake to be higher duiring the dark phase than the light, yet in **figure 4.26** fenofibrate administration appears to lead to similar levels of food consumption in both phases and GW6471 treated mice eat 57% more in the light phase than in the dark. In **figure 4.27** with the PPAR$\alpha^{-/-}$ animals OEA, fenofibrate and GW6471 treated mice display a slight delayed onset of feeding. Analysis of these data suggests effects observed in **figure 4.26** to be PPAR$\alpha^{-/-}$ mediated. There was significant difference or trend observed in the knockout mice between treatments. Looking further at food intake in the wild type mice for the first 5 hours post injection we saw GW6471 to rapidly and significantly reduce food intake ($P<0.001$) for up to the 5 hour point. Fenofibrate, to a lesser degree ($P<0.01$), evoked similar effects. In the PPAR$\alpha^{-/-}$ mice, there was a delayed onset of feeding in the order of GW6471, fenofibrate and OEA, which was reversed after 4 hours. Mice treated with OEA failed to significantly reduce their food intake in the first hour in the wild type mice, yet in PPAR$\alpha^{-/-}$ mice OEA administration significantly reduced food intake within the first hour.

Table 4.14 shows GW6471 treatment in wild type mice to significantly reduce activity in the first 24 hours and shows this effects to be reversed when administered to PPARα$^{-/-}$ mice, and in fact displays a trend towards stimulating locomotor activity as does fenofibrate in both wild type and PPARα$^{-/-}$ mice, albeit not significantly. We observe a depression of activity within the first hour with OEA, in wild-type mice and the same pattern in PPARα$^{-/-}$ mice. Activity in all PPARα$^{-/-}$ mice is lower than the wild-types. There was no significant effect of any treatment in oxygen consumption at 24 hours post-injection. GW6471 treated wild-type mice showed consistently lower oxygen consumption throughout the 24 hours compared to other treatments, albeit not significant, whereas this is not seen in PPARα$^{-/-}$ mice. We see a familiar observation with OEA treated wild-type mice in the first hour post-injection, an acute transient reduction in VO_2. The same is seen in the PPARα$^{-/-}$ mice. All changes in VO_2 caused by the different treatments become normalised and all treatments then follow the same profile. GW6471 produces a significant reduction in respiratory quotient in wild-type mice 24 hours following injection ($P<0.001$), which is reversed compared to PPARα$^{-/-}$ mice at 24 hours. There is no significant change with any treatment in either wild-type or PPARα$^{-/-}$ mice within the first hour post-injection.

4.7.4 Discussion

OEA produces no significant reduction in food intake at any individual time point over the first 24 hours. There is less of an effect with OEA administration (using the wild-type C57bl6 mice) seen in this investigation than in previous experiments in this chapter. This variation has provided difficulty in determining how much of the OEA-evoked response,

previously recorded on food intake, is mediated by the PPARα receptor. It is unfortunate to have not obtained data similar to that observed before using OEA to compare to effects now seen using PPARα$^{-/-}$ mice, it may be argued that we may be administering a less than optimum dose of OEA (or even that of GW6471). It is well known that cannabinoids and their endogenous ligands produce dose-response effects in a bell shaped curve, and that, unlike synthetic modulators, a maximal tolerated dose will not reflect the maximal effect of that endocannabinoid. In hindsight, maybe further investigation into the dose-response effects of OEA using a wider range of doses would have been useful to bring out its maximal regulatory effects on feeding behavior *in vivo*. In PPARα$^{-/-}$ mice, OEA showed a significant ($P<0.01$) reduction in food intake in the first hour post-injection, suggesting that OEA is able to evoke transient satiety in mice without the presence of PPARα receptor. This suggests potentiation of OEA-evoked satiety mediated through an as yet unknown mechanism – previously suggested as an additive pathway. It has previously been reported that OEA's hypophagic effects are abolished in PPARα$^{-/-}$ mice (Fu et al., 2003; Piomelli et al., 2006; Schwartz et al., 2008, Astarita et al., 2006) and there is no indication in the literature of an additive pathway, eventhough alternative receptors for OEA have been hypothesized to be involved in OEA's action on food intake **(section 1.7)**.

Throughout all feeding behaviour data, OEA alongside GW6471 and fenofibrate display delayed onset of feeding, lasting up to 4 hours in PPARα$^{-/-}$ mice. As this is only observed with PPARα ligands this could be suggested to be ligand activity at a distinct target. These effects have not previously been seen in either wild-type mice, previous

experiments or the literature and are therefore possibly due to compensatory effects of the knockout animals following administration of its endogenous and synthetic ligands.

Sedation resulting from OEA administration has not been documented in the literature and as a depression in activity with OEA was observed in both wild-type and PPARα$^{-/-}$ mice, it may be a mechanistic effect mediated through an unknown mechanism.

OEA again evoked a transient reduction in oxygen consumption, significantly sooner in PPARα$^{-/-}$ mice and for up to 30 minutes in both PPARα$^{-/-}$ and wild-type. This was reported previously in this chapter and was not seen with either of the other two ligands, implying this not to be a PPARα$^{-/-}$ mediated effect.

The rapid and long-lasting effects of GW6471 on food intake in wild-type mice has not previously been established, and its lack of effect in PPARα$^{-/-}$ mice suggest GW6471 to be acting as a PPARα agonist with higher efficacy compared with fenofibrate. With knowledge of PPARα's ability to regulate food intake and as we also know what there is endogenous tone of endocannabinoids in our system to allow for low levels of chronic activation of receptors, it may be expected that the use of GW6471 may increase food intake in the animals, as this endogenous tone of OEA may lead to the naturally reduced levels of food intake via PPARα and this is a mechanism potentially disrupted following GW6471 administration, albeit we have determined some involvement of OEA via PPARα in the regulation of food intake, but we do not see any classical antagonism of this effect with GW6471 administration. As described in **section 1.7.3** all PPARα ligands have different binding properties to the receptor which lead to differing effects in consequence. Due to our lack of knowledge on the binding properties of GW6471 at

PPARα receptor we can hypothesise whether this may be the case or not, but further investigation into binging properties and consequential effects of GW6471 at PPARα would allow for this. On closer inspection of the food intake 0-5 hours post-injection shows initial reduction in food intake to the same reduction between all treatments in the knockout mice, indicating a very likely similarity of effect between all treatments also. We know OEA and fenofibrate do not cause malaise and GW6471 has previously shown to increase activity when administered alone, so the question lies whether all three compounds have similar affinities for and are acting at another receptor targets to cause this or are they causing a regulation of endogenous modulators of this effect.

Fenofibrate has shown a similar profile to that of GW6471 in both wild-type and knockout mice. It has been more effective in inducing satiety than observed in previous experiments and OEA, using C57bl6 mice, but the effects are less than GW6471.

GW6471 significantly reduced activity in wild-type mice at 24 hours, which could be a result of GW6471 administration. Due to the lack of literature on the use of GW6471 *in vivo*, it is difficult to say if this is the case, but data from GW6471 in knockout mice suggest effects of GW6471 on activity to be PPARα mediated. Activity levels over the 24 hour period are lower in PPARα$^{-/-}$ mice than wild-type, suggesting PPARα receptor mechanism pathway to contribute to activity.

Our previous data suggest compounds to not affect locomotor activity levels, but it may be that PPARα receptors may contribute to activity levels at times of *de novo* synthesis and activation of PPARα (for example, with endogenous OEA).

The trend of reduced VO_2 with GW6471 throughout the 24 hours post-injection in wild-type mice may further support the possibility of malaise evoked by this compound and the malaise may also be accountable for both a reduction in activity and food intake. This effect is not seen in the knockout animals suggesting it is PPARα mediated.

Both GW6471 and fenofibrate show a transient reduction in VO_2, lasting up to 2 hours, which has been observed in previous experiments with fenofibrate, using C57bl6 mice, and comparison with data from knockout mice suggest a PPARα mediated pathway. A reduction in respiratory quotient is associated with increased oxygen consumption, but over the 24 hours we see GW6471 to have a trend towards the lowest oxygen consumption in wild-type mice, hence we would expect a an increase in respiratory quotient, in fact we see a highly significant decrease ($P<0.001$). This suggests a specific effect of GW6471 and the mechanism through which it exerts this effect is unknown. Decreased activity would influence the respiratory quotient more towards oxidation of carbohydrates (RQ=1) or higher, but results suggest increased fat oxidation relative to carbohydrates. We know PPARα transcriptional effects increase fat oxidation, yet changes in RQ toward fat oxidation (RQ=0.7) was not observed in previous experiments in this chapter in C57bl6 mice at 24 hours post administration using GW6471 or fenofibrate, so unsure the mechanism by which this response is created remains obscure. Previous investigations suggested tonic PPARα activation, now with a lack of PPARα receptor the whole body may compensate by enhancing its own fat oxidation as a change to basal metabolic rates, which may explain the reduced RQ with all treatments including vehicle in the knockout animals, but does not explain similar RQ levels in the wild-types.

Overall, it has been difficult, with a reduced effect of OEA observed in the controls, to compare with the knockout animals to determine and further characterize the effects of OEA on satiety mediated through the PPARα receptor mechanism, but these results further profile the unknown effects of PPARα antagonist use *in vivo*.

4.8 Discussion

This chapter provides good evidence of the use of effective doses of all OEA, fenofibrate and GW6471 *in vivo*. There were limitations in the interpretation of data from knockout animal models (**section 4.7**), where we did not see responses previously observed in wild-type mice, providing difficulty in the interpretation and comparison of effects to the PPARα$^{-/-}$ mice. It may also be questioned if the results observed in the PPAR$^{-/-}$ group are true of such effects of this receptor knockout. The only reason they would not be is due to the development of unknown compensatory mechanisms during the study or incorrect genotyping of the animals as a result of human error, but we feel the latter not to be the case. It is not clear why the same sex, age and strain wild-type mice did not produce similar effects to all OEA, fenofibrate and GW6471 as previously observed, but as previously mentioned, this may be a dose selection fault, where the dose of OEA administered is not optimal to its regulating effects on food intake via PPARα. It would have been interesting to determine the expression levels of PPARα receptor in the gut in this group of animals compared to a previous set of mice used where we did see the regulatory effects on food intake. Lower levels of PPARα expression may well explain for the lack of effects observed, but as to what may have caused this to occur in such a subset group of mice only remains unclear. It is clear this experiment would be required to be repeated for a full understanding of the effects of each compound in this study. A better strategy would be to use mice in which PPARα gene disruption was under conditional influences, so that the gene is only disrupted as an adult, rather than from embryo.

OEA has clearly presented a hypophagic response *in vivo* yet its effects are seen to be rapid, yet transient. Identification of possible additive pathways on OEA's effects is very interesting and of some therapeutic use, as these transient effects of OEA could possibly be potentiated through other receptor mechanism, and made to last longer. Yet this would require further *in vivo* investigation. Isolation of each individual possible additive pathway involving OEA in this hypophagic response is required to identify whether pathways could be exploited to use OEA as an anorexiant agent. As it stands alone, it could not be used as an acute treatment to reduce feeding, but we have not investigated chronic *in vivo* effects of OEA, which may provide alternative advantages.

Fenofibrate, as other drugs in the fibrate class, which are known PPARα agonists have been reported not to induce hypophagia at PPARα as potently as OEA, due to weaker binding affinities at the receptor, yet our data clearly show stronger effects of fenofibrate on the reduction of food intake compared to OEA. Further investigation would be required to determine how much of this effect is mediated by other mechanisms, which remain to be identified. GW6471 displayed the involvement of tonic PPARα receptor activation, adding to its regulation of hypophagic responses by OEA. It also showed clear effects on the reduction of food intake for up to the 24 hours measured – displaying a stronger profile as an anorectic agent compared to both OEA and fenofibrate.

Now GW6471 has been successfully employed systemically *in vivo*, further studies will aim to provide additional information on its hypophagic responses and mechanisms. As yet, there is no effect of either compound individually or in unison to exploit as a clinical drug for the treatment of feeding disorders. Overall, therefore, the role of PPARα in

responses to fenofibrate and GW6471 is not clarified by the use of these knockout animals.

Chapter 5: GENERAL DISCUSSION

5.1 FAAH and MAGL inhibition

The use of FAAH inhibitors has potential over the use of synthetic CB receptor agonists, as FAAH inhibitors create actions, primarily, but not solely through CB_1 receptors. One interpretation of their lack of unwanted effects is that, by increasing the endogenous tone of CB_1 receptor partial agonists, they evoke less of a tetrad response compared to synthetic full agonists. As a result of CB_1 receptor activation, there will be the significant therapeutic effects of analgesia together with the potential for hypothermia, but without locomotor deficits, catatonia or any psychoactive CNS effects. In contrast, the selective MAGL inhibitor recently reported by Cravatt's group , JZL184 displayed the tetrad complete with unwanted CNS mediated psychotropic effects (Long et al., 2009).

The use of naturally derived cannabinoids has led to the development of the drug Sativex, which is equiratios of CBD and THC. Its use in the treatment of spasticity in MS (Baker and Pryce, 2003) appears to be devoid of psychotropic effects, as it is found to 'under perform' at CB_1 receptors. CB_1 receptor effects from its ligands are dose-dependant, therefore it is not entirely true that drugs acting at CB_1 receptors are not useful due to the resulting CNS mediated effects, as this is avoided when applying specifically low doses. Whether synthetic drugs can be designed to have the same avoidance of CNS mediated effects at CB_1 receptor is unknown, but clearly the application of purified cannabinoids or the modulation of eCBs and its system are highly favourable when targeting CB_1 receptors, for the treatment of various pathological states.

A full understanding of the eCB system is still ongoing, and many clinical implications of the use of naturally derived CB receptor partial agonists, namely the cannabinoids, as therapeutics exist. It has recently been reported that there is an up-regulation of CB_2 receptor expression in response to neuropathic pain and inflammation in neurodegenerative diseases, such as Huntington's disease and MS (Pertwee, 2008). Due to upregulation of such receptors, agonists at CB_2 receptors unavoidably produce more effec. As CB_2 receptor up-regulation is a direct result of the disease pathology, this provides a clear indication that they have an important role in the regulation of the disease, indicating a future potential target for inhibitors of eCB metabolism.

With the presence of over 60 cannabinoid compounds found in the cannabis plant, we are provided with many differing effects of every compound still to investigate as potential therapeutics. The use of enzyme inhibitors can potentially be very beneficial, as FAAH and MAGL inhibitors act to increase the endogenous tone of eCBs or preserve exogenously administered cannabinoids to potentiate their effect and make it more long lasting by delaying its degradation (which we know to occur rapidly due to the *de novo* control of the eCB system). Such benefits could potentially be tissue specific if given orally, in our case, we would act to increase levels of eCBLs in the upper GI tract to induce satiety and at the same time avoid unwanted interaction with the CB receptors.

FAAH inhibitors may prove a much better target compared to MAGL inhibitors, as FAAH is known to have many substrates, so inhibitors will cause an increase in many eCBs, whereas MAGL only has one main substrate, 2-AG. 2-AG is already present in the brain (Richardson et al., 2007) and in peripheral tissues as seen in **chapter 4**. Hence,

through inhibition of MAGL you would create an even higher level of 2-AG in certain tissues, which may produce a compensatory effect, causing stimulation of other hydrolysing enzymes to metabolise the overload or excess 2-AG. This provides a further problem of the inability to achieve therapeutically beneficial levels of 2-AG *in vivo*, especially in certain tissues. Because FAAH substrates also act at nuclear receptors, such as PPARs, transmitter-gated channels, such as TRPV1, and GPCRS, including CB, GPR119 and possibly GPR55, the range of effects seen with FAAH inhibition could be enormous. The beneficial effects seen in vivo are likely to be a summation of modest effects at each of these targets, in contrast to the 'focused' effect of MAGL inhibition.

5.2 OEA and feeding behaviour

Our results show OEA to cause hypophagic responses in mice, which supports findings in literature, where rats have been used to identify the effects of OEA on feeding behaviours (Fu et al., 2003). Findings in **chapter 4** indicate a possible involvement of other receptor mediated responses and these are hypothesised to be GPR119 or $TRPV_1$. The effects of OEA at these receptors is characterised using their respective animal knockout models (Wang et al., 2005) (Godlewski, 2009). Genetic tools are not ideal to isolate single mechanism pathways due to possible unknown compensatory effects. Alternatively, it would be better to determine OEA's effects on each mechanism using individual receptor antagonists – thus not disrupting the animals natural mechanisms in a chronic fashion. It would also be favourable to use dual administration of antagonists, where two or more receptors may potentially be involved in regulating one effect or response, to isolate a single pathway. Here, the physiological effects of the use of antagonists at their receptors would have to be accounted for. In our study, this proves to be difficult as there is no selective antagonist for GPR119 and no *in vivo* use of a $TRPV_1$ selective antagonist. Another way towards isolation of mechanism pathways is the use of tissue specific knockout models, this would aid further investigation of specific receptors in specific tissue locations, without causing systemic compensatory effects.

Our results on the effects of OEA on food intake are confusing, as they indicate the involvement of unknown mechanisms, yet it has been determined that responses are a direct action of OEA and not a result of the 'entourage effect'. This is now well supported in literature, with the growth of knowledge, since the hypothesis of the

entourage effect, of the individual roles of both AEA and OEA. It cannot be said the entourage effect does not play a role in other areas of investigation, but it is good to determine that effects of OEA on feeding behaviours is independent of that theory.

A limitation in the investigation of OEA's effects *in vivo* is its rapid response and metabolism. There is no way of determining intracellular or extracellular levels so rapidly to determine whether OEA gets into cells to activate such receptors (for example the nuclear receptor PPARα). Even though our quantification method takes into account the whole tissue, we do expect that it does get into cells due to very large increases (30-fold) seen in tissues of the ileum and duodenum in **chapter 4.**

References

Ahern GP. 2003. Activation of TRPV1 by the satiety factor oleoylethanolamide. J Biol Chem 278(33):30429-30434.

Ahn K, McKinney MK, Cravatt BF. 2008. Enzymatic Pathways That Regulate Endocannabinoid Signaling in the Nervous System. Chemical Reviews 108(5):1687-1707.

Alonso-Ferrero ME, Paniagua MA, Mostany R, Pilar-Cuellar F, Diez-Alarcia R, Pazos A, Fernandez-Lopez A. 2006. Cannabinoid system in the budgerigar brain. Brain Res 1087(1):105-113.

Arévalo-Martín Á, García-Ovejero D, Gómez O, Rubio-Araiz A, Navarro-Galve B, Guaza C, Molina-Holgado E, Molina-Holgado E. 2008. CB₂ cannabinoid receptors as an emerging target for demyelinating diseases: from neuroimmune interactions to cell replacement strategies. British Journal of Pharmacology 153(2):216-225.

Baker D, Pryce G. 2003. The therapeutic potential of cannabis in multiple sclerosis. Expert Opin Investig Drugs 12(4):561-567.

Baker D, Pryce G, Croxford JL, Brown P, Pertwee RG, Huffman JW, Layward L. 2000. Cannabinoids control spasticity and tremor in a multiple sclerosis model. Nature 404(6773):84-87.

Baker D, Pryce G, Croxford JL, Brown P, Pertwee RG, Makriyannis A, Khanolkar A, Layward L, Fezza F, Bisogno T, Di Marzo V. 2001. Endocannabinoids control spasticity in a multiple sclerosis model. FASEB J 15(2):300-302.

Bari M, Spagnuolo P, Fezza F, Oddi S, Pasquariello N, Finazzi-Agro A, Maccarrone M. 2006. Effect of Lipid Rafts on Cb2 Receptor Signaling and 2-Arachidonoyl-Glycerol Metabolism in Human Immune Cells. J Immunol 177(8):4971-4980.

Bayewitch M, Avidor-Reiss T, Levy R, Barg J, Mechoulam R, Vogel Z. 1995. The peripheral cannabinoid receptor: adenylate cyclase inhibition and G protein coupling. FEBS Lett 375(1-2):143-147.

Beatrice M, Gabriella M, Francesca G, Oliana C. 2006. Endocannabinoid system in Xenopus laevis development: CB1 receptor dynamics. FEBS Letters 580(8):1941-1945.

Begg M, Baydoun A, Parsons ME, Molleman A. 2001. Signal transduction of cannabinoid CB1 receptors in a smooth muscle cell line. The Journal of Physiology 531(1):95-104.

Beltramo M, Piomelli D. 2000. Carrier-mediated transport and enzymatic hydrolysis of the endogenous cannabinoid 2-arachidonylglycerol. Neuroreport 11(6):1231-1235.

Bisogno T, De Petrocellis L, Di Marzo V. 2002. Fatty acid amide hydrolase, an enzyme with many bioactive substrates. Possible therapeutic implications. Curr Pharm Des 8(7):533-547.

Bisogno T, Hanus L, De Petrocellis L, Tchilibon S, Ponde DE, Brandi I, Moriello AS, Davis JB, Mechoulam R, Di Marzo V. 2001. Molecular targets for cannabidiol and its synthetic analogues: effect on vanilloid VR1 receptors and on the cellular

uptake and enzymatic hydrolysis of anandamide. Br J Pharmacol 134(4):845-852.
Blankman JL, Simon GM, Cravatt BF. 2007. A comprehensive profile of brain enzymes that hydrolyze the endocannabinoid 2-arachidonoylglycerol. Chem Biol 14(12):1347-1356.
Boger DL, Sato H, Lerner AE, Hedrick MP, Fecik RA, Miyauchi H, Wilkie GD, Austin BJ, Patricelli MP, Cravatt BF. 2000. Exceptionally potent inhibitors of fatty acid amide hydrolase: the enzyme responsible for degradation of endogenous oleamide and anandamide. Proc Natl Acad Sci U S A 97(10):5044-5049.
Boldrup L, Wilson SJ, Barbier AJ, Fowler CJ. 2004. A simple stopped assay for fatty acid amide hydrolase avoiding the use of a chloroform extraction phase. J Biochem Biophys Methods 60(2):171-177.
Bouaboula M, Desnoyer N, Carayon P, Combes T, Casellas P. 1999. Gi protein modulation induced by a selective inverse agonist for the peripheral cannabinoid receptor CB2: implication for intracellular signalization cross-regulation. Mol Pharmacol 55(3):473-480.
Bouaboula M, Perrachon S, Milligan L, Canat X, Rinaldi-Carmona M, Portier M, Barth F, Calandra B, Pecceu F, Lupker J, Maffrand JP, Le Fur G, Casellas P. 1997. A selective inverse agonist for central cannabinoid receptor inhibits mitogen-activated protein kinase activation stimulated by insulin or insulin-like growth factor 1. Evidence for a new model of receptor/ligand interactions. J Biol Chem 272(35):22330-22339.
Brengdahl J, Fowler CJ. 2006. A novel assay for monoacylglycerol hydrolysis suitable for high-throughput screening. Anal Biochem 359(1):40-44.
Brown SM, Wager-Miller J, Mackie K. 2002. Cloning and molecular characterization of the rat CB2 cannabinoid receptor. Biochim Biophys Acta 1576(3):255-264.
Burkey TH, Quock RM, Consroe P, Ehlert FJ, Hosohata Y, Roeske WR, Yamamura HI. 1997. Relative efficacies of cannabinoid CB1 receptor agonists in the mouse brain. Eur J Pharmacol 336(2-3):295-298.
Cabral GA, Harmon KN, Carlisle SJ. 2001. Cannabinoid-mediated inhibition of inducible nitric oxide production by rat microglial cells: evidence for CB1 receptor participation. Adv Exp Med Biol 493:207-214.
Cabral GA, Raborn ES, Griffin L, Dennis J, Marciano-Cabral F. 2008. CB2 receptors in the brain: role in central immune function. Br J Pharmacol 153(2):240-251.
Calignano A, Persico P, Mancuso F, Sorrentino L. 1993. Endogenous nitric oxide modulates morphine-induced changes in locomotion and food intake in mice. Eur J Pharmacol 231(3):415-419.
Carayon P, Marchand J, Dussossoy D, Derocq JM, Jbilo O, Bord A, Bouaboula M, Galiegue S, Mondiere P, Penarier G, Fur GL, Defrance T, Casellas P. 1998. Modulation and functional involvement of CB2 peripheral cannabinoid receptors during B-cell differentiation. Blood 92(10):3605-3615.
Carlisle SJ, Marciano-Cabral F, Staab A, Ludwick C, Cabral GA. 2002. Differential expression of the CB2 cannabinoid receptor by rodent macrophages and macrophage-like cells in relation to cell activation. International Immunopharmacology 2(1):69-82.
Carta G, Nava F, Gessa GL. 1998. Inhibition of hippocampal acetylcholine release after acute and repeated Delta9-tetrahydrocannabinol in rats. Brain Res 809(1):1-4.

Chu ZL, Jones RM, He H, Carroll C, Gutierrez V, Lucman A, Moloney M, Gao H, Mondala H, Bagnol D, Unett D, Liang Y, Demarest K, Semple G, Behan DP, Leonard J. 2007. A role for beta-cell-expressed G protein-coupled receptor 119 in glycemic control by enhancing glucose-dependent insulin release. Endocrinology 148(6):2601-2609.

Cravatt BF, Demarest K, Patricelli MP, Bracey MH, Giang DK, Martin BR, Lichtman AH. 2001. Supersensitivity to anandamide and enhanced endogenous cannabinoid signaling in mice lacking fatty acid amide hydrolase. Proc Natl Acad Sci U S A 98(16):9371-9376.

Cravatt BF, Lichtman AH. 2002. The enzymatic inactivation of the fatty acid amide class of signaling lipids. Chem Phys Lipids 121(1-2):135-148.

Cravatt BF, Lichtman AH. 2003. Fatty acid amide hydrolase: an emerging therapeutic target in the endocannabinoid system. Current Opinion in Chemical Biology 7(4):469-475.

Cravatt BF, Simon GM, Yates JR, 3rd. 2007. The biological impact of mass-spectrometry-based proteomics. Nature 450(7172):991-1000.

De Bank PA, Kendall DA, Alexander SP. 2005. A spectrophotometric assay for fatty acid amide hydrolase suitable for high-throughput screening. Biochem Pharmacol 69(8):1187-1193.

de Lago E, Petrosino S, Valenti M, Morera E, Ortega-Gutierrez S, Fernandez-Ruiz J, Di Marzo V. 2005. Effect of repeated systemic administration of selective inhibitors of endocannabinoid inactivation on rat brain endocannabinoid levels. Biochem Pharmacol 70(3):446-452.

De Petrocellis L, Cascio MG, Di Marzo V. 2004. The endocannabinoid system: a general view and latest additions. Br J Pharmacol 141(5):765-774.

Desarnaud F, Cadas H, Piomelli D. 1995. Anandamide amidohydrolase activity in rat brain microsomes. Identification and partial characterization. J Biol Chem 270(11):6030-6035.

Deutsch DG, Chin SA. 1993. Enzymatic synthesis and degradation of anandamide, a cannabinoid receptor agonist. Biochem Pharmacol 46(5):791-796.

Devane WA, Axelrod J. 1994. Enzymatic synthesis of anandamide, an endogenous ligand for the cannabinoid receptor, by brain membranes. Proc Natl Acad Sci U S A 91(14):6698-6701.

Devane WA, Dysarz FA, 3rd, Johnson MR, Melvin LS, Howlett AC. 1988. Determination and characterization of a cannabinoid receptor in rat brain. Mol Pharmacol 34(5):605-613.

Di Marzo V, Melck D, Bisogno T, De Petrocellis L. 1998. Endocannabinoids: endogenous cannabinoid receptor ligands with neuromodulatory action. Trends in Neurosciences 21(12):521-528.

Dinh TP, Carpenter D, Leslie FM, Freund TF, Katona I, Sensi SL, Kathuria S, Piomelli D. 2002. Brain monoglyceride lipase participating in endocannabinoid inactivation. Proc Natl Acad Sci U S A 99(16):10819-10824.

Elphick MR. 2002. Evolution of Cannabinoid Receptors in Vertebrates: Identification of a CB2 Gene in the Puffer Fish Fugu rubripes. Biol Bull 202(2):104-107.

Felder CC, Joyce KE, Briley EM, Mansouri J, Mackie K, Blond O, Lai Y, Ma AL, Mitchell RL. 1995. Comparison of the pharmacology and signal transduction of

the human cannabinoid CB1 and CB2 receptors. Mol Pharmacol 48(3):443-450.
Folch J, Lees M, Sloane Stanley GH. 1957. A simple method for the isolation and purification of total lipides from animal tissues. J Biol Chem 226(1):497-509.
Fowler CJ. 2004. Oleamide: a member of the endocannabinoid family? Br J Pharmacol 141(2):195-196.
Fowler CJ, Holt S, Nilsson O, Jonsson KO, Tiger G, Jacobsson SO. 2005. The endocannabinoid signaling system: pharmacological and therapeutic aspects. Pharmacol Biochem Behav 81(2):248-262.
Fowler CJ, Holt S, Tiger G. 2003. Acidic nonsteroidal anti-inflammatory drugs inhibit rat brain fatty acid amide hydrolase in a pH-dependent manner. J Enzyme Inhib Med Chem 18(1):55-58.
Fowler CJ, Tiger G, Stenstrom A. 1997. Ibuprofen Inhibits Rat Brain Deamidation of Anandamide at Pharmacologically Relevant Concentrations. Mode of Inhibition and Structure-Activity Relationship. J Pharmacol Exp Ther 283(2):729-734.
Fredrikson G, Tornqvist H, Belfrage P. 1986. Hormone-sensitive lipase and monoacylglycerol lipase are both required for complete degradation of adipocyte triacylglycerol. Biochim Biophys Acta 876(2):288-293.
Fu J, Astarita G, Gaetani S, Kim J, Cravatt BF, Mackie K, Piomelli D. 2007. Food intake regulates oleoylethanolamide formation and degradation in the proximal small intestine. J Biol Chem 282(2):1518-1528.
Fu J, Gaetani S, Oveisi F, Lo Verme J, Serrano A, Rodriguez De Fonseca F, Rosengarth A, Luecke H, Di Giacomo B, Tarzia G, Piomelli D. 2003. Oleylethanolamide regulates feeding and body weight through activation of the nuclear receptor PPAR-alpha. Nature 425(6953):90-93.
Fu J, Oveisi F, Gaetani S, Lin E, Piomelli D. 2005. Oleoylethanolamide, an endogenous PPAR-alpha agonist, lowers body weight and hyperlipidemia in obese rats. Neuropharmacology 48(8):1147-1153.
Gaetani S, Oveisi F, Piomelli D. 2003. Modulation of meal pattern in the rat by the anorexic lipid mediator oleoylethanolamide. Neuropsychopharmacology 28(7):1311-1316.
Galiegue S, Mary S, Marchand J, Dussossoy D, Carriere D, Carayon P, Bouaboula M, Shire D, Le Fur G, Casellas P. 1995. Expression of central and peripheral cannabinoid receptors in human immune tissues and leukocyte subpopulations. Eur J Biochem 232(1):54-61.
Gaoni Y MR. 1964. Isolation, structure and partial synthesis of an active constituent of hashish. . Journal of the American Chemical Society(86):1646-1647.
Ghafouri N, Tiger G, Razdan RK, Mahadevan A, Pertwee RG, Martin BR, Fowler CJ. 2004. Inhibition of monoacylglycerol lipase and fatty acid amide hydrolase by analogues of 2-arachidonoylglycerol. Br J Pharmacol 143(6):774-784.
Glass M, Dragunow M, Faull RL. 1997. Cannabinoid receptors in the human brain: a detailed anatomical and quantitative autoradiographic study in the fetal, neonatal and adult human brain. Neuroscience 77(2):299-318.
Glass M, Felder CC. 1997. Concurrent stimulation of cannabinoid CB1 and dopamine D2 receptors augments cAMP accumulation in striatal neurons: evidence for a Gs linkage to the CB1 receptor. J Neurosci 17(14):5327-5333.
Griffin G, Fernando SR, Ross RA, McKay NG, Ashford ML, Shire D, Huffman JW, Yu

S, Lainton JA, Pertwee RG. 1997. Evidence for the presence of CB2-like cannabinoid receptors on peripheral nerve terminals. Eur J Pharmacol 339(1):53-61.

Griffin G, Tao Q, Abood ME. 2000. Cloning and Pharmacological Characterization of the Rat CB2 Cannabinoid Receptor. J Pharmacol Exp Ther 292(3):886-894.

Guzman M, Lo Verme J, Fu J, Oveisi F, Blazquez C, Piomelli D. 2004. Oleoylethanolamide stimulates lipolysis by activating the nuclear receptor peroxisome proliferator-activated receptor alpha (PPAR-alpha). J Biol Chem 279(27):27849-27854.

Hillard CJ, Manna S, Greenberg MJ, DiCamelli R, Ross RA, Stevenson LA, Murphy V, Pertwee RG, Campbell WB. 1999. Synthesis and characterization of potent and selective agonists of the neuronal cannabinoid receptor (CB1). J Pharmacol Exp Ther 289(3):1427-1433.

Ho BY, Zhao J. 1996. Determination of the cannabinoid receptors in mouse × rat hybridoma NG108-15 cells and rat GH4C 1 cells. Neuroscience Letters 212(2):123-126.

Hohmann AG, Suplita RL, 2nd. 2006. Endocannabinoid mechanisms of pain modulation. AAPS J 8(4):E693-708.

Howlett AC. 1995. Pharmacology of cannabinoid receptors. Annu Rev Pharmacol Toxicol 35:607-634.

Izzo AA, Borrelli F, Capasso R, Di Marzo V, Mechoulam R. 2009. Non-psychotropic plant cannabinoids: new therapeutic opportunities from an ancient herb. Trends in Pharmacological Sciences 30(10):515-527.

Johnson JG, Cohen P, Pine DS, Klein DF, Kasen S, Brook JS. 2000. Association between cigarette smoking and anxiety disorders during adolescence and early adulthood. JAMA 284(18):2348-2351.

Kathuria S, Gaetani S, Fegley D, Valino F, Duranti A, Tontini A, Mor M, Tarzia G, Rana GL, Calignano A, Giustino A, Tattoli M, Palmery M, Cuomo V, Piomelli D. 2003. Modulation of anxiety through blockade of anandamide hydrolysis. Nat Med 9(1):76-81.

Labar G, Bauvois C, Muccioli GG, Wouters J, Lambert DM. 2007. Disulfiram is an inhibitor of human purified monoacylglycerol lipase, the enzyme regulating 2-arachidonoylglycerol signaling. Chembiochem 8(11):1293-1297.

Lan H, Vassileva G, Corona A, Liu L, Baker H, Golovko A, Abbondanzo S, Hu W, Yang S, Ning Y, Del Vecchio R, Poulet F, Laverty M, Gustafson E, Hedrick J, Kowalski T. 2009. GPR119 Is Required For Physiological Regulation of Glucagon-Like Peptide-1 Secretion but Not for Metabolic Homeostasis. J Endocrinol:JOE-08-0453.

Lang W, Qin C, Hill WA, Lin S, Khanolkar AD, Makriyannis A. 1996. High-performance liquid chromatographic determination of anandamide amidase activity in rat brain microsomes. Anal Biochem 238(1):40-45.

Lauffer L, Iakoubov R, Brubaker PL. 2008. GPR119: "Double-Dipping" for Better Glycemic Control. Endocrinology 149(5):2035-2037.

Leweke FM, Giuffrida A, Wurster U, Emrich HM, Piomelli D. 1999. Elevated endogenous cannabinoids in schizophrenia. Neuroreport 10(8):1665-1669.

Lichtman AH, Cravatt BF. 2005. Food for thought: endocannabinoid modulation of

lipogenesis. The Journal of Clinical Investigation 115(5):1130-1133.
Lichtman AH, Leung D, Shelton CC, Saghatelian A, Hardouin C, Boger DL, Cravatt BF. 2004. Reversible Inhibitors of Fatty Acid Amide Hydrolase That Promote Analgesia: Evidence for an Unprecedented Combination of Potency and Selectivity. J Pharmacol Exp Ther 311(2):441-448.
Lichtman AH, Varvel SA, Martin BR. 2002. Endocannabinoids in cognition and dependence. Prostaglandins Leukot Essent Fatty Acids 66(2-3):269-285.
Lo Verme J, Gaetani S, Fu J, Oveisi F, Burton K, Piomelli D. 2005. Regulation of food intake by oleoylethanolamide. Cell Mol Life Sci 62(6):708-716.
Long JZ, Li W, Booker L, Burston JJ, Kinsey SG, Schlosburg JE, Pavon FJ, Serrano AM, Selley DE, Parsons LH, Lichtman AH, Cravatt BF. 2009. Selective blockade of 2-arachidonoylglycerol hydrolysis produces cannabinoid behavioral effects. Nat Chem Biol 5(1):37-44.
Maccarrone M, Bari M, Agro AF. 1999. A sensitive and specific radiochromatographic assay of fatty acid amide hydrolase activity. Anal Biochem 267(2):314-318.
Mackie K. 2005. Distribution of cannabinoid receptors in the central and peripheral nervous system. Handb Exp Pharmacol(168):299-325.
Mackie K, Lai Y, Westenbroek R, Mitchell R. 1995. Cannabinoids activate an inwardly rectifying potassium conductance and inhibit Q-type calcium currents in AtT20 cells transfected with rat brain cannabinoid receptor. J Neurosci 15(10):6552-6561.
Mackie K, Stella N. 2006. Cannabinoid receptors and endocannabinoids: evidence for new players. AAPS J 8(2):E298-306.
Makara JK, Mor M, Fegley D, Szabo SI, Kathuria S, Astarita G, Duranti A, Tontini A, Tarzia G, Rivara S, Freund TF, Piomelli D. 2005. Selective inhibition of 2-AG hydrolysis enhances endocannabinoid signaling in hippocampus. Nat Neurosci 8(9):1139-1141.
Marcelis van der S, Anna Maria P, Mauro M, Willem FN, Giacinto B, Gerrit AV, Alessandro Finazzi A, Johannes FGV. 1997. The effect of hydroxylation of linoleoyl amides on their cannabinomimetic properties. FEBS Letters 415(3):313-316.
Matsuda LA. 1997. Molecular aspects of cannabinoid receptors. Crit Rev Neurobiol 11(2-3):143-166.
Matsuda LA, Lolait SJ, Brownstein MJ, Young AC, Bonner TI. 1990. Structure of a cannabinoid receptor and functional expression of the cloned cDNA. Nature 346(6284):561-564.
Matsuda S, Kanemitsu N, Nakamura A, Mimura Y, Ueda N, Kurahashi Y, Yamamoto S. 1997. Metabolism of anandamide, an endogenous cannabinoid receptor ligand, in porcine ocular tissues. Exp Eye Res 64(5):707-711.
Mechoulam R, Ben-Shabat S, Hanus L, Ligumsky M, Kaminski NE, Schatz AR, Gopher A, Almog S, Martin BR, Compton DR, et al. 1995. Identification of an endogenous 2-monoglyceride, present in canine gut, that binds to cannabinoid receptors. Biochem Pharmacol 50(1):83-90.
Mechoulam R, Fride E, Ben-Shabat S, Meiri U, Horowitz M. 1998. Carbachol, an acetylcholine receptor agonist, enhances production in rat aorta of 2-arachidonoyl glycerol, a hypotensive endocannabinoid. Eur J Pharmacol 362(1):R1-3.

Mechoulam R, Fride E, Hanus L, Sheskin T, Bisogno T, Di Marzo V, Bayewitch M, Vogel Z. 1997. Anandamide may mediate sleep induction. Nature 389(6646):25-26.

Movahed P, Jonsson BA, Birnir B, Wingstrand JA, Jorgensen TD, Ermund A, Sterner O, Zygmunt PM, Hogestatt ED. 2005. Endogenous unsaturated C18 N-acylethanolamines are vanilloid receptor (TRPV1) agonists. J Biol Chem 280(46):38496-38504.

Muccioli GG, Stella N. 2008. An optimized GC-MS method detects nanomolar amounts of anandamide in mouse brain. Anal Biochem 373(2):220-228.

Munro S, Thomas KL, Abu-Shaar M. 1993. Molecular characterization of a peripheral receptor for cannabinoids. Nature 365(6441):61-65.

Omeir RL, Chin S, Hong Y, Ahern DG, Deutsch DG. 1995. Arachidonoyl ethanolamide-[1,2-14C] as a substrate for anandamide amidase. Life Sci 56(23-24):1999-2005.

Onaivi ES, Carpio O, Ishiguro H, Schanz N, Uhl GR, Benno R. 2008. Behavioral Effects of CB2 Cannabinoid Receptor Activation and Its Influence on Food and Alcohol Consumption. Annals of the New York Academy of Sciences 1139(Drug Addiction: Research Frontiers and Treatment Advances):426-433.

Overton HA, Babbs AJ, Doel SM, Fyfe MCT, Gardner LS, Griffin G, Jackson HC, Procter MJ, Rasamison CM, Tang-Christensen M, Widdowson PS, Williams GM, Reynet C. 2006. Deorphanization of a G protein-coupled receptor for oleoylethanolamide and its use in the discovery of small-molecule hypophagic agents. Cell Metabolism 3(3):167-175.

Overton HA, Fyfe MC, Reynet C. 2008. GPR119, a novel G protein-coupled receptor target for the treatment of type 2 diabetes and obesity. Br J Pharmacol 153 Suppl 1:S76-81.

Pagotto U, Vicennati V, Pasquali R. 2005. The endocannabinoid system and the treatment of obesity. Ann Med 37(4):270-275.

Paria BC, Deutsch DD, Dey SK. 1996. The uterus is a potential site for anandamide synthesis and hydrolysis: differential profiles of anandamide synthase and hydrolase activities in the mouse uterus during the periimplantation period. Mol Reprod Dev 45(2):183-192.

Patterson JE, Ollmann IR, Cravatt BF, Boger DL, Wong CH, Lerner RA. 1996. Inhibition of Oleamide Hydrolase Catalyzed Hydrolysis of the Endogenous Sleep-Inducing Lipid cis-9-Octadecenamide. Journal of the American Chemical Society 118(25):5938-5945.

Pertwee RG. 1997. Pharmacology of cannabinoid CB1 and CB2 receptors. Pharmacol Ther 74(2):129-180.

Pertwee RG. 2001. Cannabinoid receptors and pain. Prog Neurobiol 63(5):569-611.

Pertwee RG. 2008. The diverse CB1 and CB2 receptor pharmacology of three plant cannabinoids: delta9-tetrahydrocannabinol, cannabidiol and delta9-tetrahydrocannabivarin. Br J Pharmacol 153(2):199-215.

Pertwee RG, Ross RA. 2002. Cannabinoid receptors and their ligands. Prostaglandins Leukot Essent Fatty Acids 66(2-3):101-121.

Piomelli D. 2003. The molecular logic of endocannabinoid signalling. Nat Rev Neurosci 4(11):873-884.

Piomelli D, Tarzia G, Duranti A, Tontini A, Mor M, Compton TR, Dasse O, Monaghan

EP, Parrott JA, Putman D. 2006. Pharmacological profile of the selective FAAH inhibitor KDS-4103 (URB597). CNS Drug Rev 12(1):21-38.

Proulx K, Cota D, Castaneda TR, Tschop MH, D'Alessio DA, Tso P, Woods SC, Seeley RJ. 2005. Mechanisms of oleoylethanolamide-induced changes in feeding behavior and motor activity. Am J Physiol Regul Integr Comp Physiol 289(3):R729-737.

Qin C, Lin S, Lang W, Goutopoulos A, Pavlopoulos S, Mauri F, Makriyannis A. 1998. Determination of anandamide amidase activity using ultraviolet-active amine derivatives and reverse-phase high-performance liquid chromatography. Anal Biochem 261(1):8-15.

Ramarao MK, Murphy EA, Shen MW, Wang Y, Bushell KN, Huang N, Pan N, Williams C, Clark JD. 2005. A fluorescence-based assay for fatty acid amide hydrolase compatible with high-throughput screening. Anal Biochem 343(1):143-151.

Rao GK, Zhang W, Kaminski NE. 2004. Cannabinoid receptor-mediated regulation of intracellular calcium by {Delta}9-tetrahydrocannabinol in resting T cells. J Leukoc Biol 75(5):884-892.

Repetto M, Lopez-Artiguez M, Martinez D. 1976. Separation of cannabinoids. Bull Narc 28(4):69-74.

Richardson D, Ortori CA, Chapman V, Kendall DA, Barrett DA. 2007. Quantitative profiling of endocannabinoids and related compounds in rat brain using liquid chromatography-tandem electrospray ionization mass spectrometry. Anal Biochem 360(2):216-226.

Rodriguez de Fonseca F, Navarro M, Gomez R, Escuredo L, Nava F, Fu J, Murillo-Rodriguez E, Giuffrida A, LoVerme J, Gaetani S, Kathuria S, Gall C, Piomelli D. 2001. An anorexic lipid mediator regulated by feeding. Nature 414(6860):209-212.

Saario SM, Savinainen JR, Laitinen JT, Jarvinen T, Niemi R. 2004. Monoglyceride lipase-like enzymatic activity is responsible for hydrolysis of 2-arachidonoylglycerol in rat cerebellar membranes. Biochem Pharmacol 67(7):1381-1387.

Sakurada T, Noma A. 1981. Subcellular localization and some properties of monoacylglycerol lipase in rat adipocytes. J Biochem 90(5):1413-1419.

Schlicker E, Timm J, Zentner J, Gothert M. 1997. Cannabinoid CB1 receptor-mediated inhibition of noradrenaline release in the human and guinea-pig hippocampus. Naunyn Schmiedebergs Arch Pharmacol 356(5):583-589.

Schwartz GJ, Fu J, Astarita G, Li X, Gaetani S, Campolongo P, Cuomo V, Piomelli D. 2008. The lipid messenger OEA links dietary fat intake to satiety. Cell Metab 8(4):281-288.

Shen M, Piser TM, Seybold VS, Thayer SA. 1996. Cannabinoid receptor agonists inhibit glutamatergic synaptic transmission in rat hippocampal cultures. J Neurosci 16(14):4322-4334.

Shire D, Calandra B, Rinaldi-Carmona M, Oustric D, Pessegue B, Bonnin-Cabanne O, Le Fur G, Caput D, Ferrara P. 1996. Molecular cloning, expression and function of the murine CB2 peripheral cannabinoid receptor. Biochim Biophys Acta 1307(2):132-136.

Silvestri R, Ligresti A, Regina GL, Piscitelli F, Gatti V, Brizzi A, Pasquini S, Lavecchia

A, Allarà M, Fantini N, Carai MAM, Novellino E, Colombo G, Marzo VD, Corelli F. 2009. Synthesis, cannabinoid receptor affinity, molecular modeling studies and in vivo pharmacological evaluation of new substituted 1-aryl-5-(1H-pyrrol-1-yl)-1H-pyrazole-3-carboxamides. 2. Effect of the 3-carboxamide substituent on the affinity and selectivity profile. Bioorganic & Medicinal Chemistry 17(15):5549-5564.

Sipe JC, Arbour N, Gerber A, Beutler E. 2005a. Reduced endocannabinoid immune modulation by a common cannabinoid 2 (CB2) receptor gene polymorphism: possible risk for autoimmune disorders. J Leukoc Biol 78(1):231-238.

Sipe JC, Waalen J, Gerber A, Beutler E. 2005b. Overweight and obesity associated with a missense polymorphism in fatty acid amide hydrolase (FAAH). Int J Obes (Lond) 29(7):755-759.

Soderstrom K, Johnson F. 2001. Zebra Finch CB1 Cannabinoid Receptor: Pharmacology and in Vivo and in Vitro Effects of Activation. J Pharmacol Exp Ther 297(1):189-197.

Soderstrom K, Leid M, Moore FL, Murray TF. 2000. Behaviroal, pharmacological, and molecular characterization of an amphibian cannabinoid receptor. J Neurochem 75(1):413-423.

Soga T, Ohishi T, Matsui T, Saito T, Matsumoto M, Takasaki J, Matsumoto S, Kamohara M, Hiyama H, Yoshida S, Momose K, Ueda Y, Matsushime H, Kobori M, Furuichi K. 2005. Lysophosphatidylcholine enhances glucose-dependent insulin secretion via an orphan G-protein-coupled receptor. Biochem Biophys Res Commun 326(4):744-751.

Somma-Delpero C, Valette A, Lepetit-Thevenin J, Nobili O, Boyer J, Verine A. 1995. Purification and properties of a monoacylglycerol lipase in human erythrocytes. Biochem J 312 (Pt 2):519-525.

Song C, Howlett AC. 1995. Rat brain cannabinoid receptors are N-linked glycosylated proteins. Life Sci 56(23-24):1983-1989.

Stella N, Piomelli D. 2001. Receptor-dependent formation of endogenous cannabinoids in cortical neurons. Eur J Pharmacol 425(3):189-196.

Stincic TL, Hyson RL. 2008. Localization of CB1 cannabinoid receptor mRNA in the brain of the chick (Gallus domesticus). Brain Research 1245:61-73.

Sugiura T, Kishimoto S, Oka S, Gokoh M. 2006. Biochemistry, pharmacology and physiology of 2-arachidonoylglycerol, an endogenous cannabinoid receptor ligand. Prog Lipid Res 45(5):405-446.

Sun Y, Alexander SP, Garle MJ, Gibson CL, Hewitt K, Murphy SP, Kendall DA, Bennett AJ. 2007. Cannabinoid activation of PPAR alpha; a novel neuroprotective mechanism. Br J Pharmacol 152(5):734-743.

Sun Y, Alexander SP, Kendall DA, Bennett AJ. 2006. Cannabinoids and PPARalpha signalling. Biochemical Society transactions 34(Pt 6):1095-1097.

Tarik Ugura MB, Bernhard Kisa, Norbert Scherbaumb. 2008. Psychosis Following Anti-Obesity Treatment with Rimonabant. Obesity Facts: The European Journal of Obesity 1(2):103-105

Thabuis C, Tissot-Favre D, Bezelgues JB, Martin JC, Cruz-Hernandez C, Dionisi F, Destaillats F. 2008. Biological functions and metabolism of oleoylethanolamide. Lipids 43(10):887-894.

Thornton-Jones ZD, Vickers SP, Clifton PG. 2005. The cannabinoid CB1 receptor antagonist SR141716A reduces appetitive and consummatory responses for food. Psychopharmacology (Berl) 179(2):452-460.

Thors L, Belghiti M, Fowler CJ. 2008. Inhibition of fatty acid amide hydrolase by kaempferol and related naturally occurring flavonoids. Br J Pharmacol 155(2):244-252.

Thumser AEA, Buckland AG, Wilton DC. 1998. Monoacylglycerol binding to human serum albumin: Evidence that monooleoylglycerol binds at the dansylsarcosine site. J Lipid Res 39(5):1033-1038.

Turo JN, Mick GS, Barbara H, Peter JT, Bart JM, Derek H. 2007. Sativex successfully treats neuropathic pain characterised by allodynia: A randomised, double-blind, placebo-controlled clinical trial. Pain 133(1):210-220.

Twitchell W, Brown S, Mackie K. 1997. Cannabinoids inhibit N- and P/Q-type calcium channels in cultured rat hippocampal neurons. J Neurophysiol 78(1):43-50.

Van Sickle MD, Duncan M, Kingsley PJ, Mouihate A, Urbani P, Mackie K, Stella N, Makriyannis A, Piomelli D, Davison JS, Marnett LJ, Di Marzo V, Pittman QJ, Patel KD, Sharkey KA. 2005. Identification and functional characterization of brainstem cannabinoid CB2 receptors. Science 310(5746):329-332.

Vane JR. 1971. Inhibition of prostaglandin synthesis as a mechanism of action for aspirin-like drugs. Nat New Biol 231(25):232-235.

Wade MR, Tzavara ET, Nomikos GG. 2004. Cannabinoids reduce cAMP levels in the striatum of freely moving rats: an in vivo microdialysis study. Brain Research 1005(1-2):117-123.

Wang X, Miyares RL, Ahern GP. 2005. Oleoylethanolamide excites vagal sensory neurones, induces visceral pain and reduces short-term food intake in mice via capsaicin receptor TRPV1. J Physiol 564(Pt 2):541-547.

Yamaguchi F, Macrae AD, Brenner S. 1996. Molecular cloning of two cannabinoid type 1-like receptor genes from the puffer fish Fugu rubripes. Genomics 35(3):603-605.

Zhang J-H, Chung TDY, Oldenburg KR. 1999. A Simple Statistical Parameter for Use in Evaluation and Validation of High Throughput Screening Assays. J Biomol Screen 4(2):67-73.